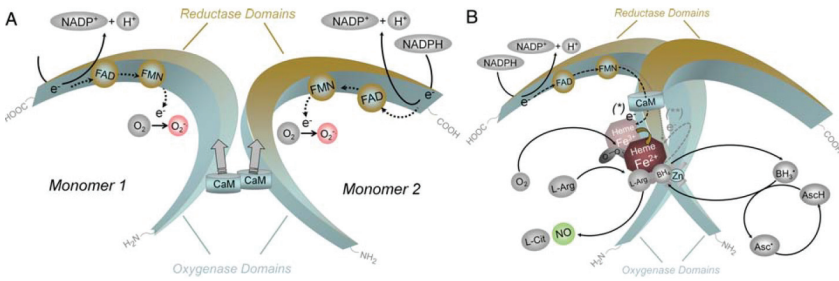


**EVALUATING THE
MICROCIRCULATION
IN EARLY PHASE
CLINICAL TRIALS:
NOVEL METHODOLOGIES
AND INTERVENTIONS**

S.J.W. VAN KRAAIJ

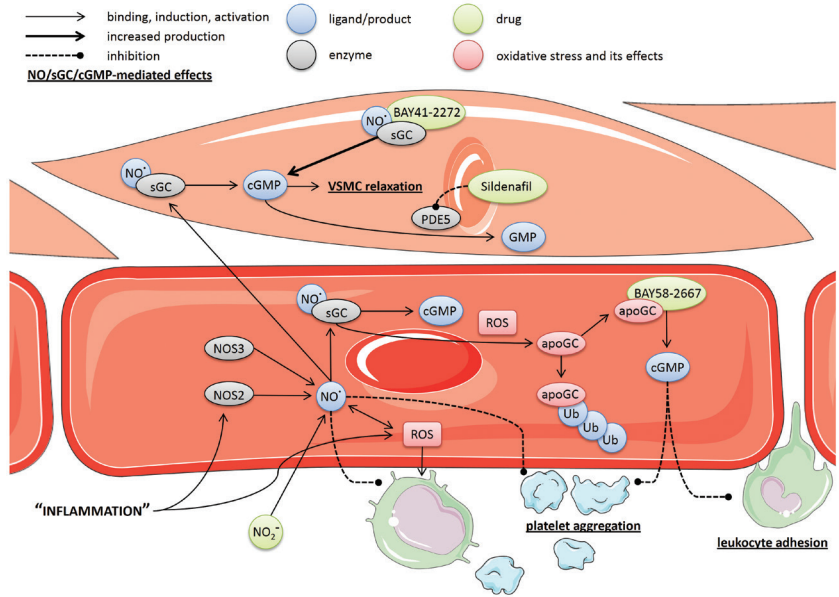
CH.1 / F.1 NOS form and function. A: two uncoupled NOS monomers. B: NOS in dimeric form.



ASCH = ascorbic acid;
 BH4 = tetrahydrobiopterin;
 CAM = calmodulin;
 FAD = flavin adenine dinucleotide; FM = flavin mononucleotide;
 L-ARG = L-arginine;
 L-CIT = L-citrulline;
 NADP = nicotinamide adenine dinucleotide phosphate;
 NO = nitric oxide. (Adapted from Förstermann et al.⁸)

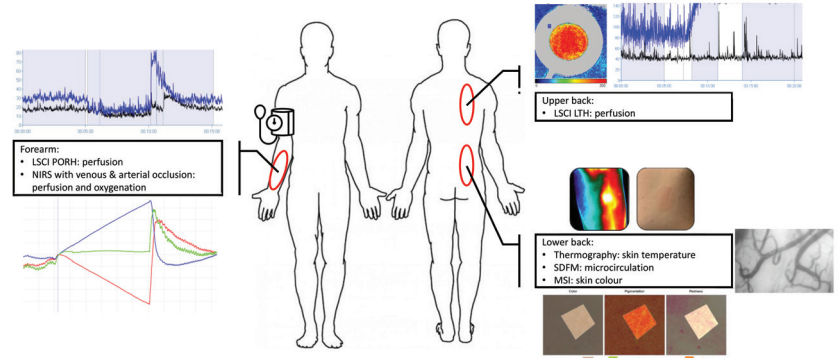
EVALUATING THE MICROCIRCULATION IN EARLY PHASE CLINICAL TRIALS:
 NOVEL METHODOLOGIES AND INTERVENTIONS

CH.1 / F.2 The effects of NO, SGC and cGMP in endothelium and vascular smooth muscle.



APOGC = heme-free guanylyl cyclase; CGMP = cyclic guanosine monophosphate;
 NO = nitric oxide;
 NO2 = nitrogen dioxide;
 NOS = nitric oxide synthase;
 PDE = phosphodiesterase;
 ROS = reactive oxygen species; SGC = soluble guanylyl cyclase;
 UB = ubiquitin;
 VSMC = vascular smooth muscle cell. (Adapted from Vandendriessche et al.¹⁶)

CH.4 / F.1 Overview of measurements performed during study conduct and their locations.



LSCI=laser speckle contrast imaging; LTH=local thermal hyperemia; MSI=multispectral imaging; NIRS=near infrared spectroscopy; PORH=post-occlusive reactive hyperemia; SDFM=side-stream dark field microscopy.

EVALUATING THE
MICROCIRCULATION
IN EARLY PHASE
CLINICAL TRIALS:
NOVEL METHODOLOGIES
AND INTERVENTIONS

Proefschrift

ter verkrijging van
de graad van doctor aan de Universiteit Leiden,
op gezag van de rector magnificus, prof. dr.ir. H. Bijl,
volgens het besluit van college voor promoties
te verdedigen op woensdag 6 maart 2024
klokke 13:45 uur

door
Sebastiaan J.W. van Kraaij
geboren te Nijmegen
in 1994

DESIGN Caroline de Lint, Den Haag (caro@delint.nl)

COVER Fonteinmarmer in blauw (Rijksmuseum, Anoniem, 1700-1850)

The publication of this thesis was financially supported by the foundation
Centre for Human Drug Research (CHDR), Leiden, the Netherlands.

PROMOTOR
prof.dr. J. Burggraaf

CO-PROMOTORES
dr. M. Moerland
dr. P. Gal

LEDEN PROMOTIECOMMISSIE
prof.dr. A.J. van Zonneveld
S.E. le Devedec MSc
Dr J. Versmissen
prof.dr. J.I. Rotmans

CHAPTER I	7
INTRODUCTION	
CHAPTER II	21
MICROVASCULAR EFFECTS OF A MIXED MEAL TOLERANCE TEST: A MODEL VALIDATION STUDY	
CHAPTER III	41
IDENTIFICATION OF PERIPHERAL VASCULAR FUNCTION MEASURES AND CIRCULATING BIOMARKERS OF MITOCHONDRIAL FUNCTION IN PATIENTS WITH MITOCHONDRIAL DISEASE.	
CHAPTER IV	65
A PHASE 1 RANDOMIZED, OPEN-LABEL CLINICAL TRIAL TO EVALUATE THE EFFECT OF A FAR-INFRARED EMITTING PATCH ON LOCAL SKIN PERFUSION, MICROCIRCULATION, AND OXYGENATION.	
CHAPTER V	83
FIRST-IN-HUMAN TRIAL TO ASSESS SAFETY, TOLERABILITY, PHARMACOKINETICS AND PHARMACODYNAMICS OF ZAGOCIGUAT (CY6463), A CNS-PENETRANT SOLUBLE GUANYLYL CYCLASE STIMULATOR.	
CHAPTER VI	109
RANDOMIZED PLACEBO-CONTROLLED CROSSOVER STUDY TO ASSESS TOLERABILITY AND PHARMACODYNAMICS OF ZAGOCIGUAT, A SOLUBLE GUANYLYL CYCLASE STIMULATOR, IN HEALTHY ELDERLY.	
CHAPTER VII	133
EFFECTS OF THE PHOSPHODIESTERASE 2 INHIBITOR BI 474121 ON CENTRAL NERVOUS SYSTEM CYCLIC GUANOSINE MONOPHOSPHATE CONCENTRATIONS: TRANSLATIONAL STUDIES	
CHAPTER VIII	153
GENERAL DISCUSSION	
NEDERLANDSE SAMENVATTING	169
LIST OF PUBLICATIONS	179
CURRICULUM VITAE	181
LIST OF ABBREVIATIONS	182
ACKNOWLEDGEMENTS	184

CHAPTER I
INTRODUCTION

VASCULAR FUNCTION AND ENDOTHELIAL DYSFUNCTION

The theme of this thesis is an appraisal of the use of existing and emerging methodologies to gain information on the status of the vascular system in humans. The vascular system is a vital component of the functioning of virtually every organ system of the human body. Central to the physiology of this vascular system is the endothelium, a single layer of cells lining the interior of all blood vessels. Endothelial cells are involved in the regulation of many crucial processes, most importantly the regulation of vascular tone, but also hemostasis and inflammatory processes. Endothelial dysfunction is a precursor in the development of atherosclerosis and is correlated with various cardiovascular risk factors as well as adverse cardiovascular outcomes.¹ Endothelial dysfunction can be summarized in this context as a disbalance between endothelial-derived relaxing factors, such as bradykinin and prostacyclin, and endothelial-derived contracting factors, such as endothelin-1 and angiotensin II, but most crucially nitric oxide (NO).²⁻³ Although endothelial-derived may be a misnomer, as cell types other than endothelial cells contribute to blood and perivascular concentrations of these factors,⁴⁻⁵ endothelial cells are the main source of vascular NO under normal physiological circumstances.⁶ NO is a crucial molecule for the functioning of the endothelium, but also fulfills other important roles in a host of physiological processes.

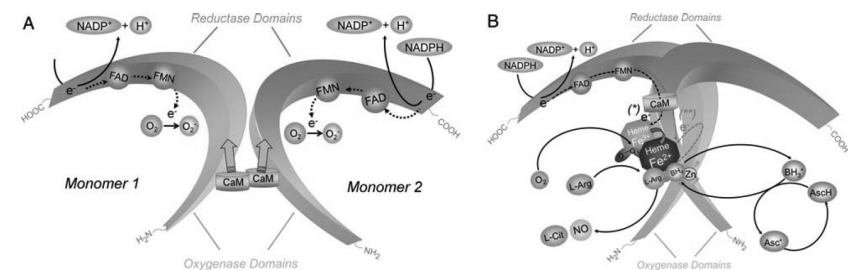
This chapter will first highlight some of the pivotal mechanistic pathways in which NO is involved, then explore therapeutic interventions targeting these pathways, and lastly identify possible imaging strategies to measure the pharmacodynamic effect of interventions on NO bioavailability, some of which will be investigated in this thesis.

NITRIC OXIDE: A PIVOTAL MOLECULE

NO is a highly diffusible, gaseous molecule with an extremely short half-life of 0.05 to 1 second in blood,⁷ which exerts its effects through nitration and nitrosation of proteins and molecules such as glutathione and fatty acids, superoxide scavenging, cytochrome c oxidase, but most importantly the NO-soluble guanylyl cyclase (sGC)-cyclic guanosine monophosphate (cGMP) signaling system. Under physiological circumstances, NO is produced by nitric oxide synthases (NOS) from L-arginine, using reduced nicotinamide adenine dinucleotide phosphate (NADPH) and oxygen as co-substrates (Figure 1).⁸ Cofactors involved in the function of all NOS isoforms are tetrahydrobiopterin (BH₄), flavin adenine dinucleotide (FAD) and flavin mononucleotide (FMN), while calmodulin acts as a catalysator. Within NOS proteins, electrons are transferred from NADPH through

FAD and FMN to L-arginine, oxidizing this substrate and producing L-citrulline and NO. This electron transfer and the binding of BH₄, which are necessary for the function of the enzyme, are only possible when NOS is in its dimeric state, which requires the presence of heme. In their monomeric (uncoupled) state NOS are incapable of binding L-arginine, instead transferring the electron to O₂ to produce superoxide (O₂^{-•}), a reactive oxygen species (ROS).⁸ In endothelial tissue, NO is produced by the endothelial isoform of NOS (eNOS or NOS3), while in various other tissues such as neurons and peripheral mononuclear blood cells, NO is produced by neuronal NOS (nNOS or NOS1) and inducible NOS (iNOS or NOS2), respectively. eNOS and nNOS are dependent on the presence of Ca²⁺ activated calmodulin to form dimers,⁹ whereas iNOS is calcium independent.¹⁰ Activity of eNOS in endothelial cells is thus increased significantly by raised intracellular Ca²⁺ levels, in addition to other physiological signals, such as shear stress,¹¹ bradykinin,¹² and insulin.¹³

FIGURE 1 NOS form and function. **A:** two uncoupled NOS monomers. **B:** NOS in dimeric form.

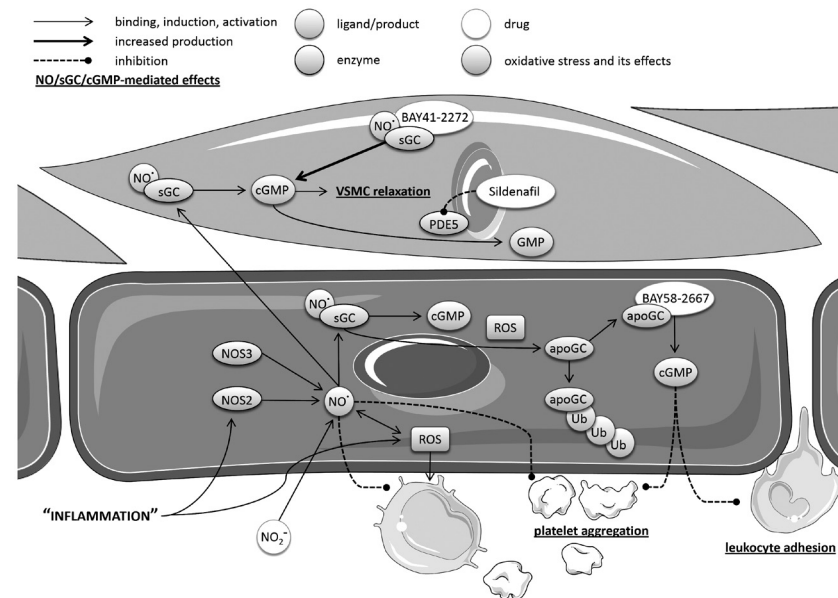


ASCH = ascorbic acid; BH₄ = tetrahydrobiopterin; CAM = calmodulin; FAD = flavin adenine dinucleotide; FM = flavin mononucleotide; L-ARG = L-arginine; L-CIT = L-citrulline; NADP = nicotinamide adenine dinucleotide phosphate; NO = nitric oxide. (Adapted from Förstermann et al.⁸) (see inside front cover for image in fullcolor)

Nitric oxide performs several functions depending on its location. In the endothelium, NO activates sGC in the smooth muscle cells surrounding the endothelial wall to convert guanosine triphosphate to cGMP. sGC is an enzyme consisting of two subunits, one of which contains a heme-NO-oxygen binding domain (HNOX). Physiological activation of sGC by NO is dependent on heme being present in its reduced state, allowing binding of NO and production of cGMP.¹⁴ Some pharmacological compounds targeting NO signaling circumvent this requirement by activating sGC even when the HNOX site is oxidized.¹⁵ When produced by sGC, cGMP

targets cGMP-gated cation channels, phosphodiesterases (PDEs) and protein kinase G I and II in vascular smooth muscle, causing vasodilation, but also reduction of platelet aggregation, leukocyte adhesion, and vascular smooth muscle cell proliferation, illustrating the role of NO in the pathophysiology of inflammation and atherosclerosis (Figure 2).¹⁶ Through this pathway, NO exerts protective effects on cardiovascular disease and associated disorders.¹⁷

FIGURE 2 The effects of NO, sGC and cGMP in endothelium and vascular smooth muscle.



APOGC = heme-free guanylyl cyclase; CGMP = cyclic guanosine monophosphate; NO = nitric oxide; NO₂ = nitrogen dioxide; NOS = nitric oxide synthase; PDE = phosphodiesterase; ROS = reactive oxygen species; sGC = soluble guanylyl cyclase; Ub = ubiquitin; VSMC = vascular smooth muscle cell. (Adapted from Vandendriessche et al.¹⁹) (see inside front cover for image in fullcolor)

iNOS, deriving its name both from being inducible by pathogenic triggers and being independent of Ca²⁺ levels,¹⁸ is expressed in response to inflammatory stimuli in a wide array of cell types, including microglia, astrocytes, hepatocytes, macrophages, Kupffer's cells, and chondrocytes.^{19–21} iNOS exerts immunomodulatory effects and is involved in defence against pathogens.²² When activated, iNOS generates NO in large quantities, contributing to protection against

micro-organisms and exhibiting anti-tumoral effects.²³ However, in case of excessive NO production, ROS are formed, which may result in deleterious effects such as DNA and mitochondrial damage.²⁴ Medical conditions characterized by such a heightened inflammatory response include endotoxemia, psoriasis, colitis, arthritis, and end-stage renal disease. These conditions are associated with increased whole body NO production due to increased expression of iNOS.^{24–26}

Last, nNOS or NOS1 is mainly localized in dendritic spines of specific neurons,²⁷ but also present in cardiac, skeletal, and smooth muscle.^{28–30} NO produced in and around neurons by nNOS, eNOS and iNOS³¹ modulates neurovascular coupling,³² long-term synaptic potentiation,³³ neurogenesis,³⁴ vascular permeability³⁵ and by extension neuronal function and higher-level cognitive functions such as learning and memory.^{34–36} Dysfunction of neuronal NO signaling is implicated in central nervous system disorders as varied as neurodegenerative disease,³⁷ chronic depression,³⁸ multiple sclerosis,³⁹ and stroke.⁴⁰ For example, NOS activity and expression is lower in patients with Alzheimer's disease compared to healthy controls⁴¹ and associated with cognitive decline,⁴² while decreased cGMP levels in the brain are associated with memory impairment,⁴³ supporting the pivotal role for NO in cognitive function. Inhibitors of NOS reduce learning and cause amnesia in preclinical animal models,^{44–45} but their exact role in memory is controversial.^{46–48} Modulation of NO signaling by targeting nNOS in the brain has been extensively researched in the clinic, with until now ambiguous results.⁴⁹

POTENTIAL INTERVENTIONS TARGETING NITRIC OXIDE

Endothelial NO has been the subject of pharmacological research aiming to reduce blood pressure, improve outcomes of cardiovascular disease and, most famously, alleviate erectile dysfunction. NO is also considered an attractive pharmacological target in the central nervous system to improve cognitive function or alleviate cognitive dysfunction, while NO produced by iNOS has been the subject of investigation for treatment of infectious or inflammatory disorders.^{50–51} There are several suitable places for intervention in the NO-sGC-cGMP cascade (Figure 3).⁵² First, increased NO production can be achieved by stimulating NOS activity via NOS isoform coupling. An example of this approach is administration of BH₄, which is approved by the FDA for treatment of phenylketonuria,⁵³ but was also shown to exert beneficial cardiovascular effects through eNOS coupling in animal models.^{54–55} Second, NO enhancers such as AVE9488 can increase NO production by elevating expression of NOS, possibly resulting

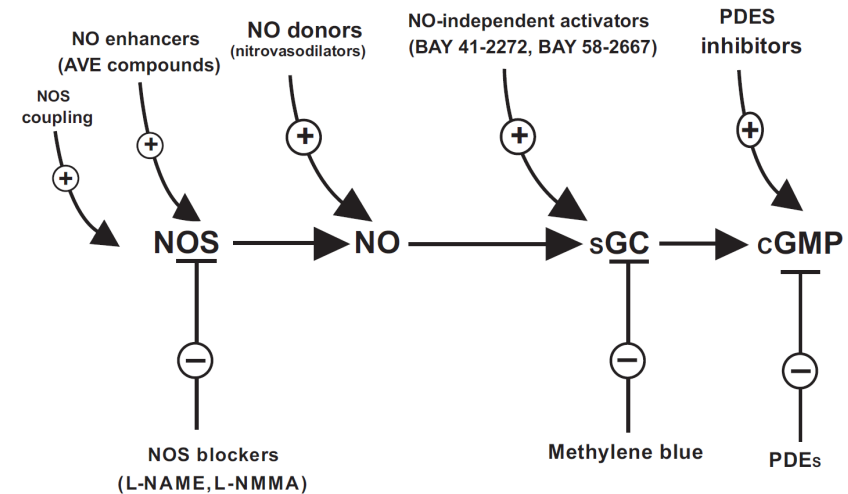
in reduced ischemia-reperfusion injury⁵⁶ and improved cardiac remodeling after infarction.⁵⁷ Third, NO donors can directly increase NO or NO-related molecules and enhance sGC-cGMP signaling independently of endogenous NO production. Nitroglycerin, which induces vasodilation of coronary arteries and relieves anginal chest pain,⁵⁸ is probably the best-known example of this approach. NO donors have also produced beneficial effects in animal models of stroke⁴⁰ and show promise in human clinical trials for treatment of acute stroke,⁵⁹ stroke-like episodes in the context of mitochondrial disorders,⁶⁰ and ischemia-reperfusion injury.⁶¹ Fourth, some drugs aim to either activate or stimulate sGC to produce cGMP.⁶² Activation of sGC can increase production of cGMP regardless of the redox status of the enzyme or presence of heme. This strategy has however been proven risky due to the high potential for hypotensive adverse events and unfavorable pharmacokinetic and pharmacodynamic characteristics of compounds activating sGC, as illustrated by the effects of the experimental drugs cinaciguat and ataciguat.^{63–65} Alternatively, drugs can stimulate sGC in its reduced state, acting independently of, or synergistically with, NO. Examples of this mechanism include riociguat, an NO-independent sGC-stimulator approved for treatment of pulmonary hypertension,⁶⁶ and zagociguat, a novel drug that stimulates sGC both NO-dependently and NO-independently in order to potentially treat cognitive dysfunction. Finally, the NO-sGC-cGMP axis can be affected by inhibiting PDE-mediated breakdown of cGMP. The most widely known PDE inhibitor is sildenafil, which targets the PDE5 family of the enzyme to alleviate erectile dysfunction.⁶⁷ Drugs that target other families of PDE are used in treatment of, or are in development for, a wide array of indications, including heart failure, asthma,⁶⁸ chronic obstructive pulmonary disease,⁶⁹ mitochondrial disorders,⁷⁰ and cognitive dysfunction caused by Alzheimer's disease⁷¹ or schizophrenia.^{72–73}

DEVELOPMENT OF TREATMENTS TARGETING NITRIC OXIDE

Early phase development of pharmacological treatments targeting the NO-sGC-cGMP chain is hampered by the fact that NO itself is difficult to measure due to its short half-life and low (sub-nanomolar) concentrations.⁷⁴ Most *in vivo* assessments have poor sensitivity and high variability, interference of ROS with assays, or other drawbacks.^{75–76} Measurements of products derived from NO such as nitrogen dioxide, peroxynitrite, nitrite or nitrate are similarly limited by a short half-life and high reactivity of their targets,⁷⁷ while measurements of NO precursors such as arginine do not necessarily reflect *in vivo* NO production.⁷⁸ Moreover, due to the complex interactions present in the NO system, no single concentration

measurement of related molecules directly translates to NO bioavailability or effects of NO on a cellular or tissue level.^{76–77,79} As a result there is a gap in knowledge in how to measure the efficacy of NO-modulating drugs. This is particularly true for studies in healthy volunteers, a population most commonly participating in early phase clinical trials.

FIGURE 3 Therapeutic targets in the NO-sGC-cGMP pathway.



CGMP=cyclic guanosine monophosphate; NO=nitric oxide; NOS=nitric oxide synthase; PDE=phosphodiesterase; L-NAME=L-Nitro-Arginine Methyl Ester; L-NMMA=NG-Monomethyl-L-Arginine; sGC=soluble guanylyl cyclase. (Adapted from Evora et al.)⁵²

IMAGING METHODS TO MEASURE NITRIC OXIDE IN VIVO

One way to circumvent the issues associated with blood-based biomarkers to assess NO bioavailability and the resulting endothelial function *in vivo* is to use imaging endpoints. The advantages of this approach are non-invasiveness and ability to measure the effects of NO in the most important target organ: the vascular bed. Various imaging modalities have been used, or are in development for, assessment of NO bioavailability and endothelial (dys)function, including doppler flowmetry, often combined with flow mediated dilation (FMD),^{80–81} laser speckle contrast imaging (LSCI),⁸² passive leg movement (PLM) ultrasonography,⁸³ peripheral arterial tonometry (PAT),⁸⁴ and magnetic resonance imaging.⁸⁵ Some methods, such as FMD and PLM, assess macrovascular reactivity by

measuring vasodilation and/or increases in flow velocity in response to a stimulus. In the case of FMD, this stimulus is most often shear stress induced by occlusion and reperfusion of the upper arm, during which changes in the diameter of the brachial artery are measured. Alternatively, PLM aims to measure increases in blood flow velocity in the femoral artery induced by passively moving the lower leg. LSCI and PAT mainly assess perfusion in the microcirculation, LSCI by deriving the flow of red blood cells in the skin from changes in laser reflection, and PAT by assessing changes in finger blood volume through plethysmography. Given this variety in assessments, a combination of imaging techniques can provide information from a range of vessel types. Further emphasizing the need for integration of different techniques is that each imaging modality has different drawbacks, including variability between individuals and operators, cost of equipment and training, subject burden, and a necessity to combine the imaging modality with physiological challenges to induce tissue responses. Hence, at the Centre for Human Drug Research, where all studies described in this thesis were conducted, a battery of tests containing a variety of imaging modalities was developed to evaluate vascular function, with an emphasis on microcirculation as a proxy for NO bioavailability. This test battery could theoretically fill the gap between proximal endpoints measured in the blood and tissue-level effects of NO. The implemented imaging methods included LSCI with occlusion-reperfusion and local thermal heating challenges, PLM, near infrared spectroscopy (NIRS) combined with venous and arterial vessel occlusion challenges, sidestream dark field imaging (SDFM) of sublingual and skin vasculature, and reduced nicotinamide adenine dinucleotide (NADH) skin fluorescence imaging.

LSCI is an imaging procedure that uses changes in laser speckle pattern reflection of the skin to assess local blood flow changes. When combined with occlusion-reperfusion and heating challenges, LSCI can measure the response of vasculature to physiological stimuli and thus assess endothelial function.⁸⁶⁻⁸⁷ Similarly, PLM is an imaging method in which changes in blood flow in the femoral artery are measured in response to movement of the lower leg to evaluate vasodilatory capacity of vessels in the leg, again providing a measure of NO bioavailability.⁸⁸ NIRS can be used to quantify the oxygenation of tissues by measuring relative and total concentrations of oxygenated and deoxygenated hemoglobin. When combined with occlusion challenges, NIRS provides information on oxygen consumption and blood flow.⁸⁹⁻⁹⁰ SDFM measures the density and flow of small vessels through a portable microscope that emits light in a wavelength absorbed by hemoglobin. This allows visualization of vessels and red

blood cells in real time. Vascular SDFM is typically performed sublingually since the oral mucosa allows penetration of the light necessary to image the underlying blood vessels, which are superficially located.⁹¹⁻⁹² Last, flow mediated skin fluorescence measurements (FMSF) of NADH can measure vascular function by quantifying the level of NADH fluorescence in the skin before and after an occlusion-reperfusion cycle.⁹³ FMSF also provides partial measurement of NAD⁺/NADH ratio and thereby information on cellular redox status,⁹⁴ which is of particular interest given the close interaction of NO with ROS and the dependence of NO production and NO function on reduced sites in the NOS and sGC enzymes.

AIMS AND OUTLINE OF THIS THESIS

The aim of this thesis was to explore the value of non-invasive imaging to assess the functional status of the vasculature. The goals of the studies described in this thesis were to 1) investigate if imaging can be used to reliably evaluate NO-dependent processes, 2) assess whether effects of physiological challenges or interventions on those processes were detectable and finally, 3) explore if early-phase clinical trials evaluating NO-mediated effects can become more informative when these techniques are utilized. First, in **Chapter II**, imaging modalities are employed in healthy volunteers undergoing a mixed-meal metabolic challenge to assess inter- and intraindividual variability of the imaging methods and their potential to detect effects of a challenge. **Chapter III** describes a study exploring if vascular imaging can differentiate between disordered NO function in patients with mitochondrial disease, a population with known elevated reactive oxygen species and lower NO bioavailability, and normal NO function in matched healthy volunteers. In **Chapter IV** the performance of a medical device intended to improve endothelial function and microcirculation in the skin was tested in healthy volunteers through imaging of the skin. The second half of this thesis describes two different approaches to target the NO-sGC-cGMP axis in the brain. In **Chapter V and VI** sGC stimulation was explored in a first-in-human and subsequent proof-of-concept trial with an sGC stimulator that reaches the cerebrospinal fluid. **Chapter VII** describes the effects of a central nervous system penetrant PDE2 inhibitor on cGMP levels in the cerebrospinal fluid. Finally, in **Chapter VIII**, the reliability of imaging modalities in assessment of endothelial function and NO bioavailability, and their value in measuring effects of challenges or potential treatments are discussed. This chapter includes recommendations for the inclusion of imaging-based endpoints to assess pharmacodynamic effects of drugs or therapies targeting the NO system in future clinical trials.

REFERENCES

- 1 Bonetti, P. O.; Lerman, L. O.; Lerman, A., Endothelial Dysfunction: A Marker of Atherosclerotic Risk. *Arteriosclerosis, Thrombosis, and Vascular Biology* **2003**, *23* (2), 168-175.
- 2 Gimbrone, M. A., Jr.; Garcia-Cardena, G., Endothelial Cell Dysfunction and the Pathobiology of Atherosclerosis. *Circ Res* **2016**, *118* (4), 620-36.
- 3 Förstermann, U., Nitric oxide and oxidative stress in vascular disease. *Pflügers Archiv : European journal of physiology* **2010**, *459* (6), 923-39.
- 4 Chen, K.; Pittman, R. N.; Popel, A. S., Nitric oxide in the vasculature: where does it come from and where does it go? A quantitative perspective. *Antioxid Redox Signal* **2008**, *10* (7), 1185-98.
- 5 Khimji, A.-K.; Rockey, D. C., Endothelin-Biology and disease. *Cellular Signalling* **2010**, *22* (11), 1615-1625.
- 6 Moncada, S.; Higgs, E. A., Nitric oxide and the vascular endothelium. *Handbook of experimental pharmacology* **2006**, (176 Pt 1), 213-54.
- 7 Kelm, M., Nitric oxide metabolism and breakdown. *Biochimica et Biophysica Acta (BBA) - Bioenergetics* **1999**, *1411* (2), 273-289.
- 8 Förstermann, U.; Sessa, W. C., Nitric oxide synthases: regulation and function. *European Heart Journal* **2011**, *33* (7), 829-837.
- 9 Fleming, I.; Bauersachs, J.; Busse, R., Calcium-dependent and calcium-independent activation of the endothelial NO synthase. *Journal of vascular research* **1997**, *34* (3), 165-74.
- 10 Lee, S. J.; Stull, J. T., Calmodulin-dependent regulation of inducible and neuronal nitric-oxide synthase. *The Journal of biological chemistry* **1998**, *273* (42), 27430-7.
- 11 Davis, M. E.; Grumbach, I. M.; Fukai, T.; Cutchins, A.; Harrison, D. G., Shear stress regulates endothelial nitric-oxide synthase promoter activity through nuclear factor kappaB binding. *The Journal of biological chemistry* **2004**, *279* (1), 163-8.
- 12 Su, J. B., Role of Bradykinin in the Regulation of Endothelial Nitric Oxide Synthase Expression by Cardiovascular Drugs. *Current pharmaceutical design* **2017**, *23* (40), 6215-6222.
- 13 Steinberg, H. O.; Brechtel, G.; Johnson, A.; Fineberg, N.; Baron, A. D., Insulin-mediated skeletal muscle vasodilation is nitric oxide dependent. A novel action of insulin to increase nitric oxide release. *The Journal of Clinical Investigation* **1994**, *94* (3), 1172-1179.
- 14 Montfort, W. R.; Wales, J. A.; Weichsel, A., Structure and Activation of Soluble Guanylyl Cyclase, the Nitric Oxide Sensor. *Antioxid Redox Signal* **2017**, *26* (3), 107-121.
- 15 Evgenov, O. V.; Pacher, P.; Schmidt, P. M.; Haskó, G.; Schmidt, H. H.; Stasch, J. P., NO-independent stimulators and activators of soluble guanylate cyclase: discovery and therapeutic potential. *Nature reviews. Drug discovery* **2006**, *5* (9), 755-68.
- 16 Vandendriessche, B.; Rogge, E.; Goossens, V.; Vandenaabeele, P.; Stasch, J.-P.; Brouckaert, P.; Cauwels, A., The Soluble Guanylate Cyclase Activator BAY 58-2667 Protects against Morbidity and Mortality in Endotoxic Shock by Recoupling Organ Systems. *PLoS one* **2013**, *8*, e72155.
- 17 Farah, C.; Michel, L. Y. M.; Balligand, J.-L., Nitric oxide signalling in cardiovascular health and disease. *Nature Reviews Cardiology* **2018**, *15* (5), 292-316.
- 18 Wong, J. M.; Billiar, T. R., Regulation and Function of Inducible Nitric Oxide Synthase during Sepsis and Acute Inflammation. In *Advances in Pharmacology*, Ignarro, L.; Murad, F., Eds. Academic Press: 1995; Vol. 34. pp 155-170.
- 19 Sierra, A.; Navascués, J.; Cuadros, M. A.; Calvente, R.; Martín-Oliva, D.; Ferrer-Martín, R. M.; Martín-Estebané, M.; Carrasco, M. C.; Marín-Teva, J. L., Expression of inducible nitric oxide synthase (iNOS) in microglia of the developing quail retina. *PLoS One* **2014**, *9* (8), e106048.
- 20 Govers, R.; Oess, S., To NO or not to NO: 'where?' is the question. *Histology and histopathology* **2004**, *19* (2), 585-605.
- 21 Ahmad, N.; Ansari, M. Y.; Haqqi, T. M., Role of iNOS in osteoarthritis: Pathological and therapeutic aspects. *Journal of cellular physiology* **2020**, *235* (10), 6366-6376.
- 22 Fang, F. C., Perspectives series: host/pathogen interactions. Mechanisms of nitric oxide-related antimicrobial activity. *The Journal of Clinical Investigation* **1997**, *99* (12), 2818-2825.
- 23 Kleinert, H.; Schwarz, P. M.; Förstermann, U., Regulation of the Expression of Inducible Nitric Oxide Synthase. **2003**, *384* (10-11), 1343-1364.
- 24 Kleinert, H.; Forstermann, U., Inducible Nitric Oxide Synthase. In *xPharm: The Comprehensive Pharmacology Reference*, Enna, S. J.; Bylund, D. B., Eds. Elsevier: New York, 2007; pp 1-12.
- 25 Jalan, R.; Olde Damink, S. W. M.; ter Steege, J. C.; Redhead, D. N.; Lee, A.; Hayes, P. C.; Deutz, N. E. P., Acute endotoxemia following transjugular intrahepatic stent-shunt insertion is associated with systemic and cerebral vasodilatation with increased whole body nitric oxide production in critically ill cirrhotic patients. *Journal of Hepatology* **2011**, *54* (2), 265-271.
- 26 Lau, T.; Owen, W.; Yu, Y. M.; Noviski, N.; Lyons, J.; Zurakowski, D.; Tsay, R.; Ajami, A.; Young, V. R.; Castillo, L., Arginine, citrulline, and nitric oxide metabolism in end-stage renal disease patients. *The Journal of Clinical Investigation* **2000**, *105* (9), 1217-1225.
- 27 Caviedes, A.; Varas-Godoy, M.; Lafourcade, C.; Sandoval, S.; Bravo-Alegria, J.; Kaehne, T.; Massmann, A.; Figueroa, J. P.; Nualart, F.; Wyneken, U., Endothelial Nitric Oxide Synthase Is Present in Dendritic Spines of Neurons in Primary Cultures. *Frontiers in Cellular Neuroscience* **2017**, *11*.
- 28 Rothe, F.; Langnaese, K.; Wolf, G., New aspects of the location of neuronal nitric oxide synthase in the skeletal muscle: A light and electron microscopic study. *Nitric Oxide* **2005**, *13* (1), 21-35.
- 29 Schwarz, P. M.; Kleinert, H.; Förstermann, U., Potential Functional Significance of Brain-Type and Muscle-Type Nitric Oxide Synthase I Expressed in Adventitia and Media of Rat Aorta. *Arteriosclerosis, Thrombosis, and Vascular Biology* **1999**, *19* (11), 2584-2590.
- 30 Santizo, R.; Baughman, V. L.; Pelligrino, D. A., Relative contributions from neuronal and endothelial nitric oxide synthases to regional cerebral blood flow changes during forebrain ischemia in rats. *Neuroreport* **2000**, *11* (7).
- 31 Steinert, J. R.; Chernova, T.; Forsythe, I. D., Nitric oxide signaling in brain function, dysfunction, and dementia. *The Neuroscientist : a review journal bringing neurobiology, neurology and psychiatry* **2010**, *16* (4), 435-52.
- 32 Lourenço, C. F.; Laranjinha, J., Nitric Oxide Pathways in Neurovascular Coupling Under Normal and Stress Conditions in the Brain: Strategies to Rescue Aberrant Coupling and Improve Cerebral Blood Flow. *Frontiers in Physiology* **2021**, *12*.
- 33 Malen, P. L.; Chapman, P. F., Nitric oxide facilitates long-term potentiation, but not long-term depression. *J Neurosci* **1997**, *17* (7), 2645-51.
- 34 Zhou, L.; Zhu, D. Y., Neuronal nitric oxide synthase: structure, subcellular localization, regulation, and clinical implications. *Nitric Oxide* **2009**, *20* (4), 223-30.
- 35 Draijer, R.; Atsma, D. E.; van der Laarse, A.; van Hinsbergh, V. W., cGMP and nitric oxide modulate thrombin-induced endothelial permeability. Regulation via different pathways in human aortic and umbilical vein endothelial cells. *Circ Res* **1995**, *76* (2), 199-208.
- 36 Zhuo, M.; Hu, Y.; Schultz, C.; Kandel, E. R.; Hawkins, R. D., Role of guanylyl cyclase and cGMP-dependent protein kinase in long-term potentiation. *Nature* **1994**, *368* (6472), 635-9.
- 37 Ben Aissa, M.; Lee, S. H.; Bennett, B. M.; Thatcher, G. R., Targeting NO/cGMP Signaling in the CNS for Neurodegeneration and Alzheimer's Disease. *Current medicinal chemistry* **2016**, *23* (24), 2770-2788.
- 38 Zhou, Q. G.; Hu, Y.; Hua, Y.; Hu, M.; Luo, C. X.; Han, X.; Zhu, X. J.; Wang, B.; Xu, J. S.; Zhu, D. Y., Neuronal nitric oxide synthase contributes to chronic stress-induced depression by suppressing hippocampal neurogenesis. *Journal of neurochemistry* **2007**, *103* (5), 1843-54.
- 39 Smith, K. J.; Lassmann, H., The role of nitric oxide in multiple sclerosis. *The Lancet. Neurology* **2002**, *1* (4), 232-41.
- 40 Willmot, M.; Gray, L.; Gibson, C.; Murphy, S.; Bath, P. M., A systematic review of nitric oxide donors and L-arginine in experimental stroke; effects on infarct size and cerebral blood flow. *Nitric Oxide* **2005**, *12* (3), 141-9.
- 41 Liu, P.; Fleete, M. S.; Jing, Y.; Collie, N. D.; Curtis, M. A.; Waldvogel, H. J.; Faull, R. L. M.; Abraham, W. C.; Zhang, H., Altered arginine metabolism in Alzheimer's disease brains. *Neurobiol Aging* **2014**, *35* (9), 1992-2003.
- 42 Ugarte, A.; Gil-Bea, F.; García-Barroso, C.; Cedazo-Minguez, A.; Ramírez, M. J.; Franco, R.; García-Osta, A.; Oyarzabal, J.; Cuadrado-Tejedor, M., Decreased levels of guanosine 3', 5'-monophosphate (cGMP) in cerebrospinal fluid (CSF) are associated with cognitive decline and amyloid pathology in Alzheimer's disease. *Neuropathology and applied neurobiology* **2015**, *41* (4), 471-82.
- 43 Hesse, R.; Lausser, L.; Gummert, P.; Schmid, F.; Wahler, A.; Schnack, C.; Kroker, K. S.; Otto, M.; Tumani, H.; Kestler, H. A.; Rosenbrock, H.; von Arnim, C. A., Reduced cGMP levels in CSF of AD patients correlate with severity of dementia and current depression. *Alzheimer's research & therapy* **2017**, *9* (1), 17.
- 44 Baratti, C. M.; Kopf, S. R., A Nitric Oxide Synthase Inhibitor Impairs Memory Storage in Mice. *Neurobiology of Learning and Memory* **1996**, *65* (3), 197-201.
- 45 Estall, L. B.; Grant, S. J.; Cicala, G. A., Inhibition of Nitric Oxide (NO) production selectively impairs learning and memory in the rat. *Pharmacology Biochemistry and Behavior* **1993**, *46* (4), 959-962.
- 46 Boultaidakis, A.; Georgiadou, G.; Pitsikas, N., Effects of the nitric oxide synthase inhibitor L-NAME on different memory components as assessed in the object recognition task in the rat. *Behavioural Brain Research* **2010**, *207* (1), 208-214.
- 47 Bannerman, D. M.; Chapman, P. F.; Kelly, P. A.; Butcher, S. P.; Morris, R. G., Inhibition of nitric oxide synthase does not impair spatial learning. *The Journal of Neuroscience* **1994**, *14* (12), 7404.
- 48 Du, W.; Weiss, H.; Harvey, J. A., Associative learning is enhanced by selective neuronal nitric oxide synthase inhibitors and retarded by a nitric oxide donor in the rabbit. *Psychopharmacology (Berl)* **2000**, *150* (3), 264-271.
- 49 Maccallini, C.; Amoroso, R., Targeting neuronal nitric oxide synthase as a valuable strategy for the therapy of neurological disorders. *Neural regeneration research* **2016**, *11* (11), 1731-1734.
- 50 Heemskerk, S.; Masereeuw, R.; Russel, F. G. M.; Pickkers, P., Selective iNOS inhibition for the treatment of sepsis-induced acute kidney injury. *Nature Reviews Nephrology* **2009**, *5* (11), 629-640.

- 51 Zamora, R.; Vodovotz, Y.; Billiar, T. R., Inducible Nitric Oxide Synthase and Inflammatory Diseases. *Molecular Medicine* **2000**, *6* (5), 347-373.
- 52 Evora, P. R.; Evora, P. M.; Celotto, A. C.; Rodrigues, A. J.; Joviliano, E. E., Cardiovascular therapeutic targets on the NO-sGC-cGMP signaling pathway: a critical overview. *Current drug targets* **2012**, *13* (9), 1207-14.
- 53 Qu, J.; Yang, T.; Wang, E.; Li, M.; Chen, C.; Ma, L.; Zhou, Y.; Cui, Y., Efficacy and safety of saporin dihydrochloride in patients with phenylketonuria: A meta-analysis of randomized controlled trials. *British Journal of Clinical Pharmacology* **2019**, *85* (5), 893-899.
- 54 Dikalova, A.; Aschner, J. L.; Kaplowitz, M. R.; Summar, M.; Fike, C. D., Tetrahydrobiopterin oral therapy recouples eNOS and ameliorates chronic hypoxia-induced pulmonary hypertension in newborn pigs. *American Journal of Physiology-Lung Cellular and Molecular Physiology* **2016**, *311* (4), L743-L753.
- 55 Engineer, A.; Lim, Y. J.; Lu, X.; Kim, M. Y.; Norozi, K.; Feng, Q., Sapropterin reduces coronary artery malformation in offspring of pregestational diabetes mice. *Nitric Oxide* **2020**, *94*, 9-18.
- 56 Frantz, S.; Adamek, A.; Fraccarollo, D.; Tillmanns, J.; Widder, J. D.; Dienesch, C.; Schäfer, A.; Podolskaya, A.; Held, M.; Ruetten, H.; Ertl, G.; Bauersachs, J., The eNOS enhancer AVE 9488: a novel cardioprotectant against ischemia reperfusion injury. *Basic Research in Cardiology* **2009**, *104* (6), 773-779.
- 57 Fraccarollo, D.; Widder, J. D.; Galuppo, P.; Thum, T.; Tsikas, D.; Hoffmann, M.; Ruetten, H.; Ertl, G.; Bauersachs, J., Improvement in Left Ventricular Remodeling by the Endothelial Nitric Oxide Synthase Enhancer AVE9488 After Experimental Myocardial Infarction. *Circulation* **2008**, *118* (8), 818-827.
- 58 Kim, K. H.; Kerndt, C. C.; Adnan, G.; Schaller, D. J., Nitroglycerin. In *StatPearls*, StatPearls Publishing: Treasure Island (FL), 2023.
- 59 Bath, P. M.; Krishnan, K.; Appleton, J. P., Nitric oxide donors (nitrites), L-arginine, or nitric oxide synthase inhibitors for acute stroke. *The Cochrane database of systematic reviews* **2017**, *4* (4), Cd003098.
- 60 Avula, S.; Parikh, S.; Demarest, S.; Kurz, J.; Gropman, A., Treatment of mitochondrial disorders. *Current treatment options in neurology* **2014**, *16* (6), 292.
- 61 Roberts, B. W.; Mitchell, J.; Kilgannon, J. H.; Chansky, M. E.; Trzeciak, S., Nitric Oxide Donor Agents for the Treatment of Ischemia/Reperfusion Injury in Human Subjects: A Systematic Review. *Shock* **2013**, *39* (3), 292.
- 62 Elgert, C.; Rühle, A.; Sandner, P.; Behrends, S., A novel soluble guanylyl cyclase activator, BR 11257, acts as a non-stabilising partial agonist of sGC. *Biochemical Pharmacology* **2019**, *163*, 142-153.
- 63 Hahn, M. G.; Lampe, T.; El Sheikh, S.; Griebenow, N.; Woltering, E.; Schlemmer, K.-H.; Dietz, L.; Gerisch, M.; Wunder, F.; Becker-Pelster, E.-M.; Mondritzki, T.; Tinel, H.; Knorr, A.; Kern, A.; Lang, D.; Hueser, J.; Schomber, T.; Benardeau, A.; Eitner, F.; Truebel, H.; Mittendorf, J.; Kumar, V.; van den Akker, F.; Schaefer, M.; Geiss, V.; Sandner, P.; Stasch, J.-P., Discovery of the Soluble Guanylate Cyclase Activator Runcaciguat (BAY 1101042). *Journal of Medicinal Chemistry* **2021**, *64* (9), 5323-5344.
- 64 Erdmann, E.; Semigran, M. J.; Nieminen, M. S.; Gheorghide, M.; Agrawal, R.; Mitrovic, V.; Mebazaa, A., Cinaciguat, a soluble guanylate cyclase activator, unloads the heart but also causes hypotension in acute decompensated heart failure. *European Heart Journal* **2013**, *34* (1), 57-67.
- 65 Sandner, P.; Zimmer, D. P.; Milne, G. T.; Follmann, M.; Hobbs, A.; Stasch, J.-P., Soluble Guanylate Cyclase Stimulators and Activators. In *Reactive Oxygen Species: Network Pharmacology and Therapeutic Applications*, Schmidt, H. H. W.; Ghezzi, P.; Cuadrado, A., Eds. Springer International Publishing: Cham, 2021; pp 355-394.
- 66 Conole, D.; Scott, L. J., Riociguat: First Global Approval. *Drugs* **2013**, *73* (17), 1967-1975.
- 67 Huang, S. A.; Lie, J. D., Phosphodiesterase-5 (PDE5) Inhibitors In the Management of Erectile Dysfunction. *P & T: a peer-reviewed journal for formulary management* **2013**, *38* (7), 407-19.
- 68 Matera, M. G.; Ora, J.; Cavalli, F.; Rogliani, P.; Cazzola, M., New Avenues for Phosphodiesterase Inhibitors in Asthma. *Journal of experimental pharmacology* **2021**, *13*, 291-302.
- 69 Chong, J.; Leung, B.; Poole, P., Phosphodiesterase 4 inhibitors for chronic obstructive pulmonary disease. *The Cochrane database of systematic reviews* **2017**, *9* (9), Cd002309.
- 70 Corum, D. G.; Jenkins, D. P.; Heslop, J. A.; Tallent, L. M.; Beeson, G. C.; Barth, J. L.; Schnellmann, R. G.; Muise-Helmericks, R. C., PDE5 inhibition rescues mitochondrial dysfunction and angiogenic responses induced by Akt3 inhibition by promotion of PRC expression. *The Journal of biological chemistry* **2020**, *295* (52), 18091-18104.
- 71 Sanders, O.; Rajagopal, L., Phosphodiesterase Inhibitors for Alzheimer's Disease: A Systematic Review of Clinical Trials and Epidemiology with a Mechanistic Rationale. *Journal of Alzheimer's disease reports* **2020**, *4* (1), 185-215.
- 72 Menniti, F. S.; Chappie, T. A.; Schmidt, C. J., PDE10A Inhibitors—Clinical Failure or Window Into Antipsychotic Drug Action? *Frontiers in Neuroscience* **2021**, *14*.
- 73 Snyder, G. L.; Vanover, K. E., PDE Inhibitors for the Treatment of Schizophrenia. In *Phosphodiesterases: CNS Functions and Diseases*, Zhang, H.-T.; Xu, Y.; O'Donnell, J. M., Eds. Springer International Publishing: Cham, 2017; pp 385-409.
- 74 Piknova, B.; Park, J. W.; Cassel, K. S.; Gilliard, C. N.; Schechter, A. N., Measuring Nitrite and Nitrate, Metabolites in the Nitric Oxide Pathway, in *Biological Materials using the Chemiluminescence Method. J Vis Exp* **2016**, (118).
- 75 Goshi, E.; Zhou, G.; He, Q., Nitric oxide detection methods in vitro and in vivo. *Medical gas research* **2019**, *9* (4), 192-207.
- 76 Siervo, M.; Stephan, B. C. M.; Feilisch, M.; Bluck, L. J. C., Measurement of in vivo nitric oxide synthesis in humans using stable isotopic methods: a systematic review. *Free Radical Biology and Medicine* **2011**, *51* (4), 795-804.
- 77 Möller, M. N.; Rios, N.; Trujillo, M.; Radi, R.; Denicola, A.; Alvarez, B., Detection and quantification of nitric oxide-derived oxidants in biological systems. *Journal of Biological Chemistry* **2019**, *294* (40), 14776-14802.
- 78 Alvares, T. S.; Conte-Junior, C. A.; Silva, J. T.; Paschoalin, V. M. F., Acute L-Arginine supplementation does not increase nitric oxide production in healthy subjects. *Nutrition & Metabolism* **2012**, *9* (1), 54.
- 79 Lauer, T.; Kleinbongard, P.; Kelm, M., Indexes of NO Bioavailability in Human Blood. *Physiology* **2002**, *17* (6), 251-255.
- 80 Stewart, J. M.; Taneja, I.; Goligorsky, M. S.; Medow, M. S., Noninvasive measure of microvascular nitric oxide function in humans using very low-frequency cutaneous laser Doppler flow spectra. *Microcirculation* **2007**, *14* (3), 169-80.
- 81 Thijssen, D. H. J.; Bruno, R. M.; van Mil, A. C. C. M.; Holder, S. M.; Fatta, F.; Greyling, A.; Zock, P. L.; Taddei, S.; Deanfield, J. E.; Luscher, T.; Green, D. J.; Ghiadoni, L., Expert consensus and evidence-based recommendations for the assessment of flow-mediated dilation in humans. *European Heart Journal* **2019**, *40* (30), 2534-2547.
- 82 Cordovil, I.; Huguenin, G.; Rosa, G.; Bello, A.; Kohler, O.; de Moraes, R.; Tibirica, E., Evaluation of systemic microvascular endothelial function using laser speckle contrast imaging. *Microvasc Res* **2012**, *83* (3), 376-9.
- 83 Groot, H. J.; Trinity, J. D.; Layec, G.; Rossman, M. J.; Ives, S. J.; Morgan, D. E.; Bledsoe, A.; Richardson, R. S., The role of nitric oxide in passive leg movement-induced vasodilatation with age: insight from alterations in femoral perfusion pressure. *J Physiol* **2015**, *593* (17), 3917-28.
- 84 Matheus, A. S. M.; da Matta, M. d. F. B.; Clemente, E. L. S.; Rodrigues, M. d. L. G.; Valença, D. C. T.; Gomes, M. B., Sensibility and specificity of laser speckle contrast imaging according to Endo-PAT index in type 1 diabetes. *Microvascular Research* **2018**, *117*, 10-15.
- 85 Sharma, R.; Seo, J.-W.; Kwon, S., In Vivo Imaging of Nitric Oxide by Magnetic Resonance Imaging Techniques. *Journal of Nanomaterials* **2014**, *2014*, 523646.
- 86 Bezemer, R.; Klijn, E.; Khalilzada, M.; Lima, A.; Heger, M.; van Bommel, J.; Ince, C., Validation of near-infrared laser speckle imaging for assessing microvascular (re)perfusion. *Microvasc Res* **2010**, *79* (2), 139-43.
- 87 Iredahl, F.; Lofberg, A.; Sjöberg, F.; Farnebo, S.; Tesselaar, E., Non-Invasive Measurement of Skin Microvascular Response during Pharmacological and Physiological Provocations. *PLoS One* **2015**, *10* (8), e0133760.
- 88 Mortensen, S. P.; Askew, C. D.; Walker, M.; Nyberg, M.; Hellsten, Y., The hyperaemic response to passive leg movement is dependent on nitric oxide: a new tool to evaluate endothelial nitric oxide function. *J Physiol* **2012**, *590* (17), 4391-400.
- 89 Dennis, J. J.; Wiggins, C. C.; Smith, J. R.; Isautier, J. M. J.; Johnson, B. D.; Joyner, M. J.; Cross, T. J., Measurement of muscle blood flow and O₂ uptake via near-infrared spectroscopy using a novel occlusion protocol. *Scientific Reports* **2021**, *11* (1), 918.
- 90 Lucero, A. A.; Addae, G.; Lawrence, W.; Neway, B.; Credeur, D. P.; Faulkner, J.; Rowlands, D.; Stoner, L., Reliability of muscle blood flow and oxygen consumption response from exercise using near-infrared spectroscopy. *Exp Physiol* **2018**, *103* (1), 90-100.
- 91 Scorcella, C.; Damiani, E.; Domizi, R.; Pierantozzi, S.; Tondi, S.; Carsetti, A.; Ciucani, S.; Monaldi, V.; Rogani, M.; Marini, B.; Adrario, E.; Romano, R.; Ince, C.; Boerma, E. C.; Donati, A., MicroDAIMON Study: Microcirculatory DAILY MONitoring in critically ill patients: a prospective observational study. *Ann Intensive Care* **2018**, *8* (1), 64.
- 92 Treu, C. M.; Lupi, O.; Bottino, D. A.; Bouskela, E., Sidestream dark field imaging: the evolution of real-time visualization of cutaneous microcirculation and its potential application in dermatology. *Archives of dermatological research* **2011**, *303* (2), 69-78.
- 93 Katarzynska, J.; Cholewinski, T.; Sieron, L.; Marcinek, A.; Gebicki, J., Flowmotion Monitored by Flow Mediated Skin Fluorescence (FMSF): A Tool for Characterization of Microcirculatory Status. *Frontiers in Physiology* **2020**, *11*.
- 94 Marcinek, A.; Katarzynska, J.; Sieron, L.; Skokowski, R.; Zielinski, J.; Gebicki, J., Non-Invasive Assessment of Vascular Circulation Based on Flow Mediated Skin Fluorescence (FMSF) *Biology* [Online], 2023.

CHAPTER II

MICROVASCULAR EFFECTS OF A MIXED MEAL TOLERANCE TEST: A MODEL VALIDATION STUDY

Sebastiaan JW van Kraaij, MD,^{1,2} Boukje C Eveleens Maarse, MD,^{1,2}
Femke PM Hoevenaars, PhD,³ Ines Warnke, MSc,⁴ Marieke L de Kam, MSc,¹
Matthijs Moerland, PhD,^{1,2} Pim Gal, PhD.^{1,2}

1: Centre for Human Drug Research, Leiden, NL

2: Leiden University Medical Centre, Leiden, NL

3: TNO, Netherlands Organisation for Applied Scientific Research, Leiden, NL

4: DSM-firmenich, Aiseraugst, SU

Abstract

INTRODUCTION

Endothelial dysfunction is a pathophysiological change preceding many cardiovascular events. Measuring improvements of endothelial function is challenging when function is already optimal, which may be remediated using a physiological challenge. This study aimed to determine whether imaging assessments can detect microvascular effects of a mixed meal tolerance test (MMTT).

METHODS

Twenty healthy volunteers (age ≥ 45 and ≤ 70 years) underwent two MMTTs at the beginning (Day 1) and end (Day 84) of a twelve-week period. Imaging methods included laser speckle contrast imaging (LSCI) combined with post-occlusive reactive hyperaemia (PORH) and local thermal hyperaemia (LTH) challenges, passive leg movement ultrasonography (PLM), and side-stream dark field microscopy (SDFM). Measurements were conducted pre-MMTT and at 5 timepoints post-MMTT for PLM and SDFM and 3 timepoints post-MMTT for PORH and LTH.

RESULTS

No consistent effects of the MMTT were detected on LSCI LTH, PLM and SDFM endpoints. LSCI PORH maximum perfusion was significantly suppressed 46, 136 and 300 min post-MMTT administration on Day 1, while rest perfusion decreased significantly 46 and 136 min post-MMTT on Day 1. However, when repeated on Day 84, PORH endpoints were not significantly affected by the MMTT.

CONCLUSION

SDFM, PLM and LSCI LTH endpoints displayed high intra-subject variability and did not detect consistent effects of MMTT. LSCI PORH endpoints had low intra-subject variability and were affected by the MMTT on Day 1, but not on Day 84. Further standardization of methods or more robust challenges to affect vascular endpoints may be needed.

Introduction

The vascular endothelium plays a central role in maintaining homeostasis in the cardiovascular system. Endothelial cells regulate vascular tone, promote restoration of damaged vessels, inhibit excessive coagulation and aid inflammatory and immunological responses.¹ Dysfunction of the endothelium is characterized by a reduction in nitric oxide (NO) bioavailability. The lack of vasodilatory effects of NO and thereby a relative overabundance of endothelial constrictive factors, hampers the function of the endothelium. This dysfunctional state is regarded as a risk factor for and cause of cardiovascular disease.² Endothelial dysfunction is correlated to traditional cardiovascular risk factors such as smoking, dyslipidaemia and hypertension and associated with worse outcomes in cardiovascular disease.³⁻⁵ Endothelial dysfunction is also associated with metabolic disturbances in the form of insulin resistance and diabetes mellitus type 2,⁶ and evidence mounts that endothelial cells are actively involved in metabolic homeostasis.⁷ Proposed mechanisms for endothelial dysfunction in metabolic disturbance include increased oxidative stress and inflammation, increased exposure to advanced glycation end-products and lipotoxicity.⁶⁻⁷

In healthy humans, endothelial function is assumed to be optimal and hence improvement by intervention unlikely, complicating the detection of treatment effects on endothelial function. However, this normal physiological balance can be disturbed by a metabolic challenge, such as a mixed meal tolerance test (MMTT), also termed 'PhenFlex' test.⁸⁻⁹ This MMTT can induce metabolic disturbance in the form of hyperlipidemia¹⁰ and hyperglycemia,¹¹ affecting endothelial function through several pathways.¹²⁻¹⁴ Although evidence of induction of endothelial dysfunction by a glucose load is mixed, with evidence for deterioration of endothelial function after an oral glucose load,¹⁵⁻¹⁶ but improvement after intravenously induced hyperglycemia,¹⁷ meals with high fat content consistently attenuate endothelial function in healthy volunteers.¹⁸⁻¹⁹ The response to MMTT is usually only evaluated using blood-based biomarkers or the flow mediated dilation (FMD) technique,²⁰ which measures the NO-dependent vasodilatory response of the endothelium to shear stress, and is known to decrease after ingestion of meals.²¹

The addition of other imaging assessments besides FMD may provide additional information on pathways involved in endothelial (dys)function, such as axon reflexes, cyclo-oxygenase function, and vascular angiogenesis, as well as different vascular beds. The additional methods investigated in this study

include laser-speckle contrast imaging (LSCI) combined with local thermal hyperaemia (LTH) and post-occlusive reactive hyperaemia (PORH) challenges, passive leg movement (PLM) ultrasonography and side-stream dark field microscopy (SDFM). These techniques capture various physiological pathways involved in endothelial function. Different phases of the response to LTH capture both NO-dependent vasodilation,²²⁻²³ as well as the role of the role of axon reflexes.²⁴ The increase in femoral artery flow during PLM as measured with doppler ultrasonography is 80-90% NO-dependent,²⁵⁻²⁷ while changes in PORH response follow different physiological pathways, with involvement of cyclo-oxygenase derived prostanoids, sensory nerves and endothelial-derived hyperpolarizing factors.²⁸ The imaging techniques also assess different vessel sizes, as LSCI measures skin microcirculation up to approximately 700 µm depth,²⁹ PLM measures large (femoral) artery blood flow, and SDFM measures density and blood flow in the sublingual microcirculation, thereby deriving a measure of vessel growth and patency. The combination of these different techniques can therefore provide mechanistic insights in endothelial function on several levels. In combination with a challenge that can induce a change in endothelial function, the spectrum of endothelial physiology and effects of intervention on it can then be measured.

In this validation study, the variability and ability to detect of an MMTT of the aforementioned imaging methods were investigated in order to examine their usefulness in the assessment of endothelial function. The investigated imaging techniques could then potentially be used in the assessment of investigational medical products aimed at reducing or preventing endothelial dysfunction, e.g., cardiovascular risk management drugs.

Methods

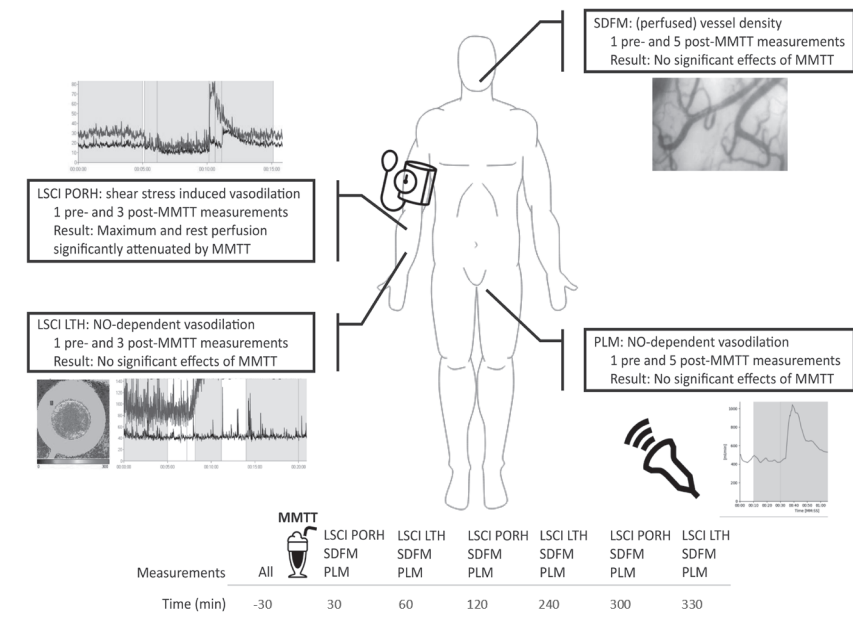
This study was conducted at Centre for Human Drug Research (CHDR) in accordance with the principles of the Declaration of Helsinki, the International Council on Harmonisation Good Clinical Practice and ethical principles as referenced in EU Directive 2001/20/EC and was approved by an independent ethics committee (BEBO, Assen) prior to study execution. The study was performed as a sub-study investigating the effects of specific dietary fibres on gut microbiome and resilience.⁸ (Manuscript in preparation, CHDR, Leiden, The Netherlands) All participants signed an Informed Consent Form before any study-related procedures were conducted. The trial was registered in the Dutch clinical trial registry toetsingonline.nl (NL71723.056.19) and at clinicaltrials.gov (NCT04829396).

STUDY DESIGN

Twenty participants were planned to be included in the study, which was a sub-study of a larger study of 64 participants investigating treatment effects of dietary fibre intervention. Participants underwent an MMTT during an ambulatory visit at the start of the study to identify treatment-naïve responses to MMTT in the assessed endpoints. Then, as part of the overarching study, participants received 13 g of a dietary fibre mixture or matching placebo once daily for 12 weeks, randomized in a 1:1 ratio. At the end of the 12-week treatment period, an MMTT was administered during an ambulatory visit to the study centre, i.e., on Day 84.

Pre-MMTT on Day 1 and Day 84, all endothelial measurements were conducted to establish a baseline. Post-MMTT, endothelial measurements were repeated following the schedule depicted in Table 1 and Figure 1. A complete list of endpoints analysed per imaging technique is provided in Supplemental Table S1.

FIGURE 1 Overview of employed imaging techniques and timepoints of assessments pre- and post-MMTT administration.



LSCI=laser speckle contrast imaging; LTH=local thermal hyperaemia; min=minutes; MMTT=mixed meal tolerance test; NO=nitric oxide; PLM=passive leg movement; PORH=post occlusive reactive hyperaemia; SDFM=side-stream dark field microscopy. (see inside back cover for image in fullcolor)

TABLE 1 Schedule of imaging assessments and pharmacodynamic blood sampling before and after mixed meal tolerance test (zero point) on Day 1 and Day 84.

	-30 min	30 min	60 min	120 min	240 min	300 min	330 min
LSCI LTH	X		X		X		X
LSCI PORH	X	X		X		X	
PLM	X	X	X	X	X		X
SDFM	X	X	X	X	X		X

LSCI=laser speckle contrast imaging; LTH=local thermal hyperemia PLM=passive leg movement; PORH=post-occlusive reactive hyperemia; SDFM=side-stream dark field microscopy.

STUDY POPULATION

Adult (age ≥ 45 and ≤ 70 years) male and female participants were eligible for inclusion if no clinically significant abnormal findings were obtained during a medical screening, which included medical history, physical examination, 12-lead ECG, alcohol breathalyzer, and clinical laboratory tests (i.e., serum chemistry, haematology, coagulation, urine drug screen, and urinalysis). Participants using any type of medication or dietary supplements in the 7 days before study start, with the exception of paracetamol up to 4 g/day and ibuprofen up to 1 g/day, or history of use of antibiotics, antacids, laxatives, statins, anti-diarrheal, immunomodulatory or antidiabetic medication < 3 months before the start of study were excluded, as well as participants with documented food allergies, a history of multiple severe drug allergies and participants with a vegan, macrobiotic or a medically prescribed diet.

SAMPLE SIZE JUSTIFICATION

The endothelial functional testing was exploratory in nature and therefore no formal power calculation was performed, although small sample sizes, e.g. 10-20, are generally accepted in early phase clinical trials employing explorative pharmacodynamic endpoints.³⁰

MIXED-MEAL TOLERANCE TEST (MMTT)

During the ambulatory visits, an MMTT was performed in the morning after participants fasted for at least 10 h. The MMTT consisted of 500mL mixed-meal challenge drink, composed as described in literature (produced by 'Instituut voor Landbouw- Visserij- en Voedingsonderzoek, Eenheid Technologie & Voeding, Food Pilot', Melle, Belgium).⁹ MMTT challenge drinks were stored in a refrigerator with restricted access at 2-8 °C until dispensing and were to be completely consumed by participants within 5 min of dispensing.²⁰

STUDY ASSESSMENTS

LASER SPECKLE CONTRAST IMAGING (LSCI)

LSCI is a technique used to determine superficial blood flux in the skin by comparing changes in speckle contrast, creating a measure of movement of red blood cells expressed in arbitrary units.³¹ Cutaneous microcirculation was assessed through LSCI using a dedicated laser speckle imager (PeriScan PSI system, Perimed, Järfälla, Sweden). The characteristics of LSCI measurements have been discussed in the literature³²⁻³⁴ and were described in the clinical study protocol. All LSCI imaging was conducted on the same arm for each subject throughout the study.

LOCAL THERMAL HEATING

After fixation of the arm in a sand cushion, a round heating probe 1 cm in diameter (moor VMS-HEAT, Moor Instruments, Axminster, United Kingdom) was placed on the forearm and filled with lukewarm water. Basal cutaneous perfusion was measured through this probe from a distance of approximately 15 cm for 5 min, after which the probe was heated to 43 °C and skin perfusion response to heating as measured by LSCI was assessed for 20 min. After the measurement, the region of interest was defined as inside the inner circumference of the heating probe, and 3 time periods of interest were defined: start of measurement-300 s = basal perfusion period, 420 s-500 s = maximum perfusion period and 780 s-end of measurement = plateau perfusion period.

POST-OCCLUSIVE REACTIVE HYPERAEMIA (PORH)

A blood pressure cuff was placed around the upper arm, after which forearm cutaneous perfusion was measured in an area of 10 by 4 cm from a distance of approximately 15 cm. After 5 min of measurement, the blood pressure cuff was inflated to > 50 mmHg above systolic blood pressure for 5 min and subsequently released, recording respectively 5-min basal, 5-min occlusion and 5-min post-occlusion cutaneous perfusion data as measured with LSCI. After the measurement, the region of interest was defined as the entire measured area and 4 time periods of interest were defined: start of measurement - 300 s = basal perfusion period, 300 s - 600 s = occlusion perfusion period, 600 s - 630 s = maximum perfusion period, and 630 s-end of measurement = post-occlusive rest perfusion period.

SINGLE PASSIVE LEG MOVEMENT (PLM)

Single PLM is a technique for assessing vasodilation in the lower leg in response to movement of the lower leg. The diameter of the common femoral artery was measured using ultrasonography while the leg was stretched in a horizontal position. With continuous doppler flowmetry, videos were obtained of the velocity of blood flow through the femoral artery for 30 s as a baseline measurement. Then, the leg was bent and stretched 90 degrees to induce lower limb vasodilation. The doppler flowmetry continued for 180 s after movement. Custom automatic video analysis software (Van Stein & Groentjes, Leiden, The Netherlands) extracted time averaged maximum velocity of blood flow for every heart cycle in the measurement. Blood flow volume in mL/min was then calculated with the formula:

$$\text{Flow} = \pi r^2 \times v \times 60$$

in which r is the femoral artery radius in cm and v flow velocity in cm/s. Time periods of interest were defined as start of measurement – 30 s = baseline flow, 30 s–60 s = peak blood flow and 60 s–end of measurement = rest blood flow.

SIDE-STREAM DARK FIELD MICROSCOPY (SDFM)

The SDFM technique uses light in a wavelength absorbed by red blood cells penetrating 0.5 mm into the imaged tissues, allowing for visualisation of red blood cells and vessels in the surface layer of that tissue as black opacities.^{35–36} Sublingual microvascular function was assessed by SDFM imaging with a hand-held microcirculation scanner (MicroScan, MicroVision Medical, Amsterdam, The Netherlands). At each timepoint, five 300-frame videos with a framerate of 60 Hz were obtained of the sublingual vasculature and the following parameters were calculated using AVA5 software (MicroVision Medical, Amsterdam, The Netherlands): number of vessel crossings, DeBacker density, number of small vessel crossings, small vessel DeBacker density, perfused number of vessel crossings, perfused DeBacker density, perfused number of small vessel crossings, perfused small vessel DeBacker density, consensus proportion perfused vessels (PPV) and consensus PPV for small vessels.

STATISTICAL ANALYSIS

All statistical analyses were performed according to a statistical analysis plan written prior to database lock. All safety and statistical programming was conducted with SAS 9.4 for Windows (SAS Institute Inc., Cary, NC, USA). Continuous

demographic variables (e.g., age, height, weight, BMI) were summarized by descriptive statistics (n, mean, SD, median, Min, Max). Qualitative demographic characteristics (sex, race/ethnicity) were summarized by counts and percentages.

The analysis population for MMTT response tests on Day 1 was defined as all participants who received the MMTT and had at least one post-baseline assessment of the analyzed parameter. On Day 84, only subjects treated with placebo were included in the analysis population. All repeatedly measured endothelial parameters were summarized (n, mean, SD, SEM, median, minimum, and maximum values) by treatment and time, with treatment 'none' representing measurements before the start of intervention, i.e., all Day 1 measurements. Least squares means (LSMs) of the change from baseline (CFB), with baseline defined as the first pre-MMTT imaging assessment, and 95% confidence intervals (CI) were calculated using a linear mixed model for the 'placebo' and 'none' treatment groups for each timepoint. Intrasubject variability was assessed by calculating the coefficient of variation (CV%) between Day 1 and Day 84 measurements for placebo subjects who received both MMTTs.

Results

PARTICIPANT DISPOSITION

A total of 21 participants were enrolled in the endothelial assessment sub-study, one more than originally planned due to drop-out of one participant after the first MMTT on Day 1 due to antibiotic use. Hence, 21 participants were included in the analysis of treatment-naïve effects of MMTT on Day 1. Ten participants were treated with placebo for 12 weeks and included in the analysis of intra-subject variability.

Baseline characteristics of the study population are shown in Table 2. No clear differences between participants assigned to placebo versus all participants were identified, hence group characteristics on Day 1 and 84 were comparable.

TABLE 2 Baseline characteristics of study participants on Day 1 and 84 before MMTT administration.

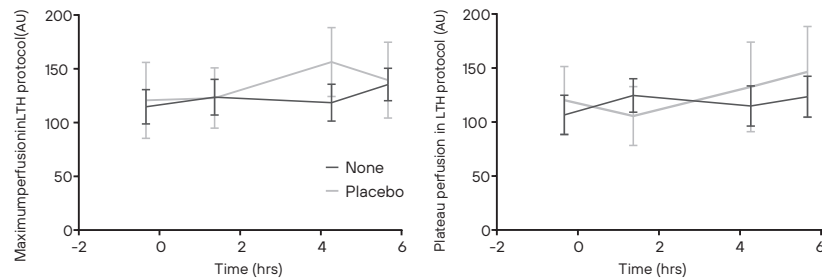
Parameter [Unit]	Day 84 (n=10)	Day 1 (All) (n=21)
Sex [% male]	73	67
Age [Years] mean ±SD	62.9±4.6	59.4±5.9
Body weight [kg] mean ±SD	85.6±8.8	87.4±11.1

(Continuation Table 2)

Parameter [Unit]	Day 84 (n=10)	Day 1 (All) (n=21)
Body mass index [kg/m ²] mean ±SD	27.4±1.9	27.7±1.5
Systolic BP [mmHg] mean ±SD	133.1±21.2	129.5±17.1
Diastolic BP [mmHg] mean ±SD	76.9±9.5	74.8±8.1
Heart rate [bpm] mean ±SD	66.3±9.8	67.0±9.6
Hip circumference [cm] mean ±SD	104.7±10.3	105.3±7.8
Waist circumference [cm] mean ±SD	98.3±9.9	97.3±9.4

BP=blood pressure; MMTT=mixed meal tolerance test; SD=standard deviation.

FIGURE 2 Mean (SD) of maximum and plateau perfusion in LSCI LTH protocol before and after MMTT on Day 1 (treatment = none) and Day 84 (placebo only).



MMTT was administered at time (hrs)=0. AU=arbitrary units; LTH=local thermal hyperaemia; LSCI=laser speckle contrast imaging; MMTT=mixed meal tolerance test; SD=standard deviation.

TABLE 3 LSMs CFB with 95% CI of maximum perfusion and plateau perfusion during LTH protocol on study Day 1 and 84.

Treatment	Time post-MMTT (h:mm)	LSM CFB	95% CI	
			Lower	Upper
Maximum perfusion				
None (Day 1)	1:22	9.564	-5.755	24.884
	4:16	4.375	-10.944	19.695
	5:40	21.125	5.805	36.444
Placebo (Day 84)	1:22	9.698	-14.464	33.860
	4:16	40.581	17.290	63.871
	5:40	23.998	0.707	47.288
Plateau perfusion				
None (Day 1)	1:22	16.460	0.821	32.099
	4:16	6.907	-8.732	22.546
	5:40	15.264	-0.375	30.903
Placebo (Day 84)	1:22	-4.214	-29.055	20.628

(Continuation Table 3)

Treatment	Time post-MMTT (h:mm)	LSM CFB	95% CI	
			Lower	Upper
	4:16	17.087	-6.635	40.809
	5:40	33.707	9.984	57.429

Statistically significant changes ($p<0.05$) from pre-MMTT values bolded. CFB=change from baseline; CI=confidence interval; LSM=least squares means; MMTT=mixed meal tolerance test.

LASER SPECKLE CONTRAST IMAGING

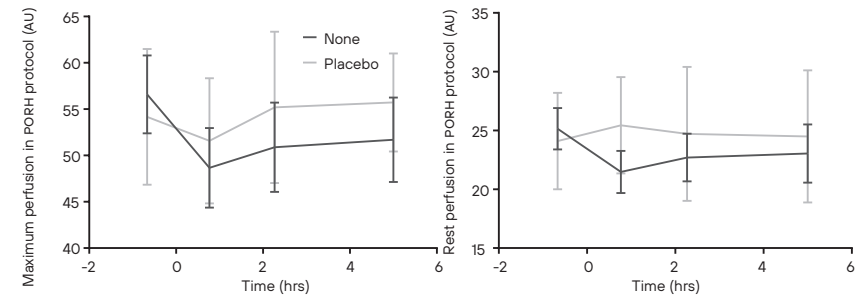
LOCAL THERMAL HYPERAEMIA

Maximum and plateau perfusion during LSCI LTH protocol before and after performance of MMTT are shown in Figure 2. No consistent statistically significant changes after MMTT administration occurred (Table 3). The intrasubject CV% for maximum and plateau perfusion were 26.58% and 23.61%, respectively.

POST OCCLUSIVE REACTIVE HYPERAEMIA

Results of the PORH endpoints maximum perfusion and rest perfusion before and after MMTT administration on Day 1 and 84 are shown in Figure 3 and Table 3.

FIGURE 3 Mean (SD) of maximum and rest perfusion in LSCI PORH protocol before and after MMTT on Day 1 (treatment = none) and Day 84 (placebo only).



MMTT was administered at time (hrs)=0. AU=arbitrary units; LSCI=laser speckle contrast imaging; MMTT=mixed meal tolerance test; PORH=post occlusive reactive hyperemia; SD=standard deviation.

Maximum perfusion after PORH decreased significantly 46, 136 and 300 min post-MMTT administration in all participants on Day 1 (LSMS CFB -8.328, 95% confidence interval (CI): -11.378, -5.278, -5.983, 95% CI: -9.033, -2.934 and -5.052, 95% CI: -8.102, -2.002, respectively). On Day 84, maximum perfusion after PORH

did not decrease significantly. The intrasubject CV% for maximum perfusion was 6.86%. Rest perfusion during PORH also decreased significantly 46 and 136 min post-MMTT in all participants on Day 1 (LSMS CFBS -3.775, 95% CI: -6.028, -1.523 and -2.546, 95% CI: -4.798, -0.293, respectively). On Day 84, this decrease was not significant, similar to the findings for maximum perfusion. The intrasubject CV% for rest perfusion was 9.11%.

TABLE 4 LSMS CFB with 95% CI of maximum perfusion and rest perfusion during PORH protocol on study Day 1 and 84.

Treatment	Time post-MMTT (h:mm)	LSM CFB	95% CI	
			Lower	Upper
Maximum perfusion				
None (Day 1)	0:46	-8.328	-11.378	-5.278
	2:16	-5.983	-9.033	-2.934
	5:00	-5.052	-8.102	-2.002
Placebo (Day 84)	0:46	-3.888	-8.751	0.976
	2:16	-0.538	-5.208	4.132
	5:00	-0.587	-5.257	4.084
Rest perfusion				
None (Day 1)	0:46	-3.775	-6.028	-1.523
	2:16	-2.546	-4.798	-0.293
	5:00	-2.185	-4.438	0.068
Placebo (Day 84)	0:46	-1.265	-4.560	2.030
	2:16	-0.871	-4.097	2.355
	5:00	-1.039	-4.265	2.187

Statistically significant changes ($p < 0.05$) from pre-MMTT values **bolded**. CFB=change from baseline; CI=confidence interval; LSM=least squares means; MMTT=mixed meal tolerance test.

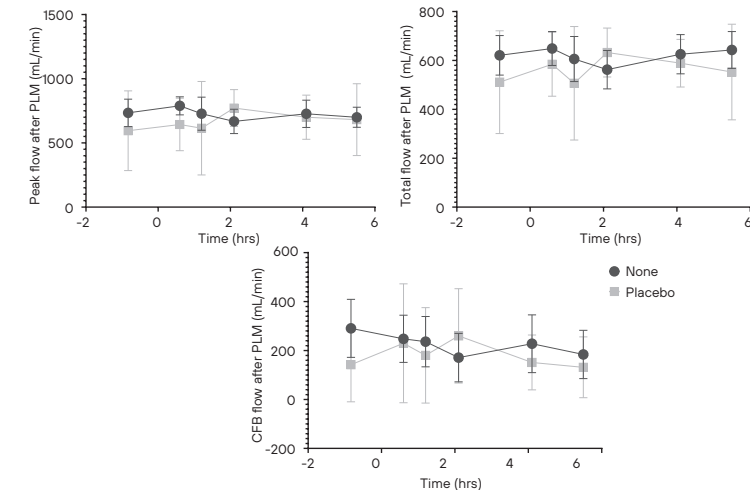
SINGLE PASSIVE LEG MOVEMENT

The results of PLM testing pre- and post-MMTT are shown in Figure 4. No consistent statistically significant changes after MMTT administration occurred on Day 1 (Supplementary Table S2). The intrasubject CV% was 18.06% for peak, 17.01% for total and 40.12% for CFB flow.

SIDE-STREAM DARK FIELD MICROSCOPY

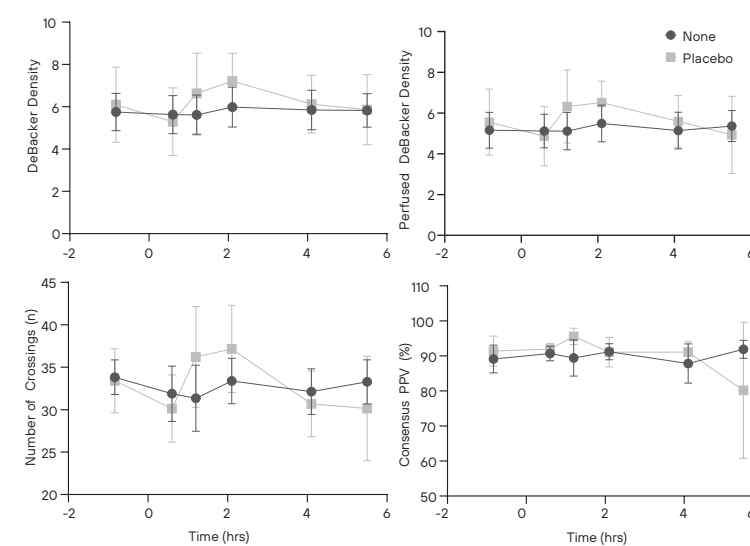
SDFM parameters before and after administration of MMTT on Day 1 and 84 are shown in Figure 5. No consistent statistically significant changes after MMTT administration occurred on Day 1. Intrasubject CV% was 20.09%, 21.53%, 14.00% and 5.55% for DeBacker density, perfused DeBacker density, number of crossings and consensus PPV, respectively.

FIGURE 4 Mean (SD) of peak, total and CFB flow in the femoral artery after PLM, before and after MMTT on Day 1 and Day 84 (placebo only).



MMTT was administered at time (hrs) = 0. CFB = change from baseline; MMTT = mixed meal tolerance test; PLM = passive leg movement; SD = standard deviation.

FIGURE 5 Mean (SD) of DeBacker density (A), perfused DeBacker density (B), number of crossings (C) and Consensus PPV (D) before and after MMTT on Day 1 and 84 (placebo only).



MMTT was administered at time (hrs) = 0. MMTT = mixed meal tolerance test; PPV = proportion perfused vessels; SD = standard deviation.

Discussion

This study assessed the variability of several imaging techniques and whether these techniques could detect changes in endothelial function caused by a MMTT. In addition, the variability of MMTT-induced changes over time was evaluated. Overall, LSCI combined with PORH had the lowest intrasubject CV% with 6.86% and 9.11% for peak and rest perfusion, respectively, which is slightly lower than the CV% for FMD measured in previous studies ($9.9 \pm 8.4\%$).³⁷ This indicates that the LSCI PORH protocol has comparable or better technical reproducibility. LSCI combined with LTH, PLM and most SDFM parameters showed high intra-subject variability with CV% ranging from 14.00% to 40.12%. SDFM PPV showed little intrasubject variability, possibly since the percentage of perfused vessels in healthy volunteers is almost always close to 100%.

LSCI PORH was the only assessed imaging modality that detected significant decreases in endpoints after MMTT administration on Day 1, likely due to its low intra-subject variability. This may have been caused by a reduction of endothelial function through induction of low-grade inflammation and oxidative stress.^{16,38-40} PORH is a relatively broad measure of vascular function, as it can be influenced by a range of factors including a high-salt diet,⁴¹ cyclo-oxygenase inhibition,⁴² nitric oxide inhibition⁴³ and neuronal blockade,⁴⁴ although evidence is mixed.^{28,45} PORH therefore may reflect overall (micro)vascular function and ability of the endothelium to respond to stimuli, in particular shear stress,⁴⁶ without pointing to specific pathways involved in vasodilation. Maximum and rest perfusion during and after PORH were significantly reduced after administration of a mixed meal on Day 1, but not on Day 84, potentially due to the smaller sample size ($n=10$) on study Day 84 and the limited magnitude of the detected effects. This is supported by the fact that response curves on Day 1 and Day 84 show similar patterns.

The effects of meals on vascular function as assessed with FMD have been well characterized. FMD decreases after ingestion of both mixed meals and a glucose challenge, and this effect is modulated by BMI, sex and importantly cardiometabolic disease status. Assessment of post-prandial FMD has therefore been suggested as a method of identifying individuals at risk for cardiometabolic disease.²¹ FMD and LSCI PORH measure similar physiological processes since both employ an occlusion-reperfusion challenge. However, in this study, LSCI PORH achieved better technical reproducibility than FMD based on literature. Moreover, the LSCI PORH technique does not suffer from the drawbacks

associated with FMD, such as technical complexity and high operator-dependence.⁴⁷ Finally, while FMD measures larger arteries, LSCI PORH is limited to assessment of superficial skin microcirculation. This vascular bed can be differently affected by various challenges, such as the MMTT. The imaging techniques may therefore complement each other. It is however advisable to include larger sample sizes than employed in this study for the assessment of effects of LSCI PORH, since the effect of the MMTT on occlusion-reperfusion did not rise to statistical significance on Day 84.

The other measures of vascular function, i.e., LSCI combined with LTH, PLM, and SDFM showed high variability and no clear response to the mixed meal test in this study. The intrasubject CV% for PLM and LSCI LTH in this study were comparable to those found in earlier studies, while those for SDFM were substantially higher.⁴⁸⁻⁵⁰ The high intrasubject CV% combined with the small sample size of this study may have increased the chance for type II error for these techniques, limiting the ability of these imaging methods to detect effects of the MMTT. Moreover, for SDFM, the time period of the assessments performed post-MMTT may have been too short to allow assessment of long-term effects of a glucose and fat load on angiogenesis. Alternatively, vascular function as measured with PLM, SDFM or LSCI LTH might not be affected to a large enough extent by the MMTT to be detected in a study with the current sample size. Although the MMTT may not have been robust enough to modulate NO-dependent vasodilation as measured with PLM and LTH or angiogenesis as measured with SDFM acutely,⁵¹⁻⁵² meal effects were detected by the more sensitive LSCI PORH technique, but not consistently. Therefore, employing a challenge known to significantly and acutely affect microcirculation and endothelial function, such as lipopolysaccharide infusion,⁵³ may be advisable when examining effects of pharmacological interventions using the less sensitive SDFM, PLM or LSCI LTH modalities. Combining these techniques with hyper- or euglycemic and hyper- or euinsulinemic clamps⁵⁴ to isolate specific physiological mechanisms⁵⁵ may also create opportunities to detect metabolic effects on the vasculature more precisely.

LIMITATIONS

This study was part of a larger study aiming to assess the effects of a 12-week fibre intervention on MMTT response and gut microbiome. Hence, the study design was not optimized for the objectives described in this sub-study. Specifically, no control group undergoing assessments without MMTT administration was included, limiting the statistical possibilities to determine effects of the challenge

on the assessed parameters, as changes post-MMTT administration could be due to diurnal or random variation. Since the effects of the MMTT on occlusion-reperfusion were not consistent across the study period, the likelihood that factors other than MMTT mediated the effects measured on Day 1 increases. Alternatively, the lack of significant effects on occlusion-reperfusion on Day 84 could be explained by the reduction of sample size and hence statistical power, since participants receiving active treatment in the overarching study were excluded from Day 84 analysis. Another limitation of the present study is that the calculation of intrasubject variability was based on repeated measurements in the placebo group over a 12-week period of time and might therefore have been influenced by the placebo intervention. Finally, this study did not include FMD or blood-based biomarkers in its design, limiting the possibilities to benchmark the measured effects against findings in the literature.

CONCLUSION

Significant effects of MMTT administration on occlusion-reperfusion response were identified in this study. However, these effects were not consistent over the 3-month study period, possibly due to a smaller sample size at the 3-month time-point. Occlusion-reperfusion as assessed with LSCI showed excellent reproducibility. Other assessed imaging modalities showed high variability and did not detect effects of the MMTT.

SUPPORTING INFORMATION

Additional supporting information may be found in the online version of the article at the publisher's website.



Table S1



Table S2

REFERENCES

- Daiber, A.; Steven, S.; Weber, A.; Shuvaev, V. V.; Muzykantov, V. R.; Laher, I.; Li, H.; Lamas, S.; Münzel, T., Targeting vascular (endothelial) dysfunction. *British journal of pharmacology* **2017**, *174* (12), 1591-1619.
- Gimbrone, M. A., Jr.; Garcia-Cardena, G., Endothelial Cell Dysfunction and the Pathobiology of Atherosclerosis. *Circ Res* **2016**, *118* (4), 620-36.
- Bonetti, P. O.; Lerman, L. O.; Lerman, A., Endothelial Dysfunction: A Marker of Atherosclerotic Risk. *Arteriosclerosis, Thrombosis, and Vascular Biology* **2003**, *23* (2), 168-175.
- Higashi, Y.; Noma, K.; Yoshizumi, M.; Kihara, Y., Endothelial function and oxidative stress in cardiovascular diseases. *Circulation journal : official journal of the Japanese Circulation Society* **2009**, *73* (3), 411-8.
- Constans, J.; Conri, C., Circulating markers of endothelial function in cardiovascular disease. *Clin Chim Acta* **2006**, *368* (1-2), 33-47.
- Polovina, M. M.; Potpara, T. S., Endothelial Dysfunction in Metabolic and Vascular Disorders. *Postgraduate Medicine* **2014**, *126* (2), 38-53.
- Pi, X.; Xie, L.; Patterson, C., Emerging Roles of Vascular Endothelium in Metabolic Homeostasis. *Circ Res* **2018**, *123* (4), 477-494.
- van den Broek, T. J.; Bakker, G. C. M.; Rubingh, C. M.; Bijlsma, S.; Stroeve, J. H. M.; van Ommen, B.; van Erk, M. J.; Wopereis, S., Ranges of phenotypic flexibility in healthy subjects. *Genes Nutr* **2017**, *12*, 32.
- Wopereis, S.; Stroeve, J. H. M.; Stafleu, A.; Bakker, G. C. M.; Burggraaf, J.; van Erk, M. J.; Pellis, L.; Boessen, R.; Kardinaal, A. A. F.; van Ommen, B., Multi-parameter comparison of a standardized mixed meal tolerance test in healthy and type 2 diabetic subjects: the PhenFlex challenge. *Genes Nutr* **2017**, *12*, 21.
- Neumann, H. F.; Egert, S., Impact of Meal Fatty Acid Composition on Postprandial Lipemia in Metabolically Healthy Adults and Individuals with Cardiovascular Disease Risk Factors: A Systematic Review. *Adv Nutr* **2022**, *13* (1), 193-207.
- Al Balwi, R.; Al Madani, W.; Al Ghamdi, A., Efficacy of insulin dosing algorithms for high-fat high-protein mixed meals to control postprandial glycemic excursions in people living with type 1 diabetes: A systematic review and meta-analysis. *Pediatric diabetes* **2022**, *23* (8), 1635-1646.
- Williams, S. B.; Goldfine, A. B.; Timimi, F. K.; Ting, H. H.; Roddy, M. A.; Simonson, D. C.; Creager, M. A., Acute hyperglycemia attenuates endothelium-dependent vasodilation in humans in vivo. *Circulation* **1998**, *97* (17), 1695-701.
- Meza, C. A.; La Favor, J. D.; Kim, D. H.; Hickner, R. C., Endothelial Dysfunction: Is There a Hyperglycemia-Induced Imbalance of NOX and NOS? *Int J Mol Sci* **2019**, *20* (15).
- Kim, J. A.; Montagnani, M.; Chandrasekran, S.; Quon, M. J., Role of lipotoxicity in endothelial dysfunction. *Heart failure clinics* **2012**, *8* (4), 589-607.
- Major-Pedersen, A.; Ihlemann, N.; Hermann, T. S.; Christiansen, B.; Dominguez, H.; Kveiborg, B.; Nielsen, D. B.; Svendsen, O. L.; Køber, L.; Torp-Pedersen, C., Effects of oral glucose load on endothelial function and on insulin and glucose fluctuations in healthy individuals. *Exp Diabetes Res* **2008**, *2008*, 672021.
- Weiss, E. P.; Arif, H.; Villareal, D. T.; Marzetti, E.; Holloszy, J. O., Endothelial function after high-sugar-food ingestion improves with endurance exercise performed on the previous day. *Am J Clin Nutr* **2008**, *88* (1), 51-7.
- Horton, W. B.; Jahn, L. A.; Hartline, L. M.; Aylor, K. W.; Patrie, J. T.; Barrett, E. J., Acute hyperglycaemia enhances both vascular endothelial function and cardiac and skeletal muscle microvascular function in healthy humans. *J Physiol* **2022**, *600* (4), 949-962.
- Fewkes, J. J.; Kellow, N. J.; Cowan, S. F.; Williamson, G.; Dordevic, A. L., A single, high-fat meal adversely affects postprandial endothelial function: a systematic review and meta-analysis. *The American Journal of Clinical Nutrition* **2022**, *116* (3), 699-729.
- Steer, P.; Sarabi, D. M.; Karlström, B.; Basu, S.; Berne, C.; Vessby, B.; Lind, L., The effect of a mixed meal on endothelium-dependent vasodilation is dependent on fat content in healthy humans. *Clin Sci (Lond)* **2003**, *105* (1), 81-7.
- Hoevenaars, F. P. M.; Esser, D.; Schutte, S.; Priebe, M. G.; Vonk, R. J.; van den Brink, W. J.; van der Kamp, J.-W.; Stroeve, J. H. M.; Afman, L. A.; Wopereis, S., Whole Grain Wheat Consumption Affects Postprandial Inflammatory Response in a Randomized Controlled Trial in Overweight and Obese Adults with Mild Hypercholesterolemia in the Graandios Study. *The Journal of Nutrition* **2019**.
- Thom, N. J.; Early, A. R.; Hunt, B. E.; Harris, R. A.; Herring, M. P., Eating and arterial endothelial function: a meta-analysis of the acute effects of meal consumption on flow-mediated dilation. *Obesity reviews : an official journal of the International Association for the Study of Obesity* **2016**, *17* (11), 1080-1090.
- Brunt, V. E.; Minson, C. T., KCa channels and epoxyeicosatrienoic acids: major contributors to thermal hyperaemia in human skin. *J Physiol* **2012**, *590* (15), 3523-34.
- Cracowski, J. L.; Roustit, M., Current Methods to Assess Human Cutaneous Blood Flow: An Updated Focus on Laser-Based-Techniques. *Microcirculation* **2016**, *23* (5), 337-44.
- Minson, C. T., Thermal provocation to evaluate microvascular reactivity in human skin. *J Appl Physiol (1985)* **2010**, *109* (4), 1239-46.

- 25 Mortensen, S. P.; Askew, C. D.; Walker, M.; Nyberg, M.; Hellsten, Y., The hyperaemic response to passive leg movement is dependent on nitric oxide: a new tool to evaluate endothelial nitric oxide function. *J Physiol* **2012**, *590* (17), 4391-400.
- 26 Trinity, J. D.; Groot, H. J.; Layec, G.; Rossman, M. J.; Ives, S. J.; Runnels, S.; Gmelch, B.; Bledsoe, A.; Richardson, R. S., Nitric oxide and passive limb movement: a new approach to assess vascular function. *J Physiol* **2012**, *590* (6), 1413-25.
- 27 Groot, H. J.; Trinity, J. D.; Layec, G.; Rossman, M. J.; Ives, S. J.; Morgan, D. E.; Bledsoe, A.; Richardson, R. S., The role of nitric oxide in passive leg movement-induced vasodilatation with age: insight from alterations in femoral perfusion pressure. *J Physiol* **2015**, *593* (17), 3917-28.
- 28 Hellmann, M.; Gaillard-Bigot, F.; Roustit, M.; Cracowski, J. L., Prostanoids are not involved in postocclusive reactive hyperaemia in human skin. *Fundam Clin Pharmacol* **2015**, *29* (5), 510-6.
- 29 Davis, M. A.; Kazmi, S. M.; Dunn, A. K., Imaging depth and multiple scattering in laser speckle contrast imaging. *Journal of biomedical optics* **2014**, *19* (8), 086001.
- 30 Rubinstein, L. V.; Steinberg, S. M.; Kummar, S.; Kinders, R.; Parchment, R. E.; Murgo, A. J.; Tomaszewski, J. E.; Doroshow, J. H., The statistics of phase o trials. *Statistics in medicine* **2010**, *29* (10), 1072-6.
- 31 Bezemer, R.; Klijn, E.; Khalilzada, M.; Lima, A.; Heger, M.; van Bommel, J.; Ince, C., Validation of near-infrared laser speckle imaging for assessing microvascular (re)perfusion. *Microvasc Res* **2010**, *79* (2), 139-43.
- 32 Heeman, W.; Steenbergen, W.; van Dam, G.; Boerma, E. C., Clinical applications of laser speckle contrast imaging: a review. *Journal of biomedical optics* **2019**, *24* (8), 1-11.
- 33 Cracowski, J. L.; Roustit, M., Local Thermal Hyperemia as a Tool to Investigate Human Skin Microcirculation. *Microcirculation* **2010**, *17* (2), 79-80.
- 34 Roustit, M.; Cracowski, J. L., Non-invasive Assessment of Skin Microvascular Function in Humans: An Insight Into Methods. *Microcirculation* **2012**, *19* (1), 47-64.
- 35 Rovas, A.; Seidel, L. M.; Vink, H.; Pohlkötter, T.; Pavenstadt, H.; Ertmer, C.; Hessler, M.; Kumpers, P., Association of sublingual microcirculation parameters and endothelial glycocalyx dimensions in resuscitated sepsis. *Crit Care* **2019**, *23* (1), 260.
- 36 Lee, D. H.; Dane, M. J.; van den Berg, B. M.; Boels, M. G.; van Teeffelen, J. W.; de Mutsert, R.; den Heijer, M.; Rosendaal, F. R.; van der Vlag, J.; van Zonneveld, A. J.; Vink, H.; Rabelink, T. J.; group, N. E. O. s., Deeper penetration of erythrocytes into the endothelial glycocalyx is associated with impaired microvascular perfusion. *PLoS One* **2014**, *9* (5), e96477.
- 37 Ghiadoni, L.; Faita, F.; Salvetti, M.; Cordiano, C.; Biggi, A.; Puato, M.; Di Monaco, A.; De Sisti, L.; Volpe, M.; Ambrosio, G.; Gemignani, V.; Muiesan, M. L.; Taddei, S.; Lanza, G. A.; Cosentino, F., Assessment of flow-mediated dilation reproducibility: a nationwide multicenter study. *Journal of hypertension* **2012**, *30* (7), 1399-405.
- 38 Lee, I. K.; Kim, H. S.; Bae, J. H., Endothelial dysfunction: its relationship with acute hyperglycaemia and hyperlipidemia. *International journal of clinical practice. Supplement* **2002**, (129), 59-64.
- 39 Aljada, A.; Mohanty, P.; Ghanim, H.; Abdo, T.; Tripathy, D.; Chaudhuri, A.; Dandona, P., Increase in intranuclear nuclear factor kappaB and decrease in inhibitor kappaB in mononuclear cells after a mixed meal: evidence for a proinflammatory effect. *Am J Clin Nutr* **2004**, *79* (4), 682-90.
- 40 Emerson, S. R.; Sciarrillo, C. M.; Kurti, S. P.; Emerson, E. M.; Rosenkranz, S. K., High-Fat Meal-Induced Changes in Markers of Inflammation and Angiogenesis in Healthy Adults Who Differ by Age and Physical Activity Level. *Current Developments in Nutrition* **2018**, *3* (1).
- 41 Cavka, A.; Cosic, A.; Jukic, I.; Jelakovic, B.; Lombard, J. H.; Phillips, S. A.; Seric, V.; Mihaljevic, I.; Drenjancevic, I., The role of cyclo-oxygenase-1 in high-salt diet-induced microvascular dysfunction in humans. *J Physiol* **2015**, *593* (24), 5313-24.
- 42 Medow, M.; Taneja, I.; Stewart, J., Cyclooxygenase and nitric oxide synthase dependence of cutaneous reactive hyperemia in humans. *American journal of physiology. Heart and circulatory physiology* **2007**, *293*, H425-32.
- 43 Dakak, N.; Husain, S.; Mulcahy, D.; Andrews, N. P.; Panza, J. A.; Waclawiw, M.; Schenke, W.; Quyyumi, A. A., Contribution of Nitric Oxide to Reactive Hyperemia. *Hypertension* **1998**, *32* (1), 9-15.
- 44 McGarr, G. W.; Cheung, S. S., Effects of sensory nerve blockade on cutaneous microvascular responses to ischemia-reperfusion injury. *Microvascular Research* **2022**, *144*, 104422.
- 45 Wong, B. J.; Wilkins, B. W.; Holowatz, L. A.; Minson, C. T., Nitric oxide synthase inhibition does not alter the reactive hyperemic response in the cutaneous circulation. *Journal of Applied Physiology* **2003**, *95* (2), 504-510.
- 46 Balasubramanian, G.; Chockalingam, N.; Naemi, R., A systematic evaluation of cutaneous microcirculation in the foot using post-occlusive reactive hyperemia. *Microcirculation* **2021**, *28* (5), e12692.
- 47 Thijssen, D. H.; Black, M. A.; Pyke, K. E.; Padilla, J.; Atkinson, G.; Harris, R. A.; Parker, B.; Widlansky, M. E.; Tschakovsky, M. E.; Green, D. J., Assessment of flow-mediated dilation in humans: a methodological and physiological guideline. *Am J Physiol Heart Circ Physiol* **2011**, *300* (1), H2-12.
- 48 Groot, H. J.; Broxterman, R. M.; Gifford, J. R.; Garten, R. S.; Rossman, M. J.; Jarrett, C. L.; Kwon, O. S.; Hydren, J. R.; Richardson, R. S., Reliability of the passive leg movement assessment of vascular function in men. *Exp Physiol* **2022**, *107* (5), 541-552.
- 49 Roustit, M.; Millet, C.; Blaise, S.; Dufournet, B.; Cracowski, J. L., Excellent reproducibility of laser speckle contrast imaging to assess skin microvascular reactivity. *Microvasc Res* **2010**, *80* (3), 505-11.
- 50 Gu, Y.-M.; Wang, S.; Zhang, L.; Liu, Y.-P.; Thijs, L.; Petit, T.; Zhang, Z.; Wei, F.-F.; Kang, Y.-Y.; Huang, Q.-F.; Sheng, C.-S.; Struijker-Boudier, H. A. J.; Kuznetsova, T.; Verhamme, P.; Li, Y.; Staessen, J. A., Characteristics and Determinants of the Sublingual Microcirculation in Populations of Different Ethnicity. *Hypertension* **2015**, *65* (5), 993-1001.
- 51 Okon, E. B.; Chung, A. W.; Zhang, H.; Laher, I.; van Breemen, C., Hyperglycemia and hyperlipidemia are associated with endothelial dysfunction during the development of type 2 diabetes. *Canadian journal of physiology and pharmacology* **2007**, *85* (5), 562-7.
- 52 Bakker, W.; Eringa, E. C.; Sipkema, P.; van Hinsbergh, V. W. M., Endothelial dysfunction and diabetes: roles of hyperglycemia, impaired insulin signaling and obesity. *Cell and Tissue Research* **2009**, *335* (1), 165-189.
- 53 Dillingh, M. R.; van Poelgeest, E. P.; Malone, K. E.; Kemper, E. M.; Stroes, E. S. G.; Moerland, M.; Burggraaf, J., Characterization of inflammation and immune cell modulation induced by low-dose LPS administration to healthy volunteers. *Journal of Inflammation* **2014**, *11* (1), 28.
- 54 Perkins, J. M.; Joy, N. G.; Tate, D. B.; Davis, S. N., Acute effects of hyperinsulinemia and hyperglycemia on vascular inflammatory biomarkers and endothelial function in overweight and obese humans. *American Journal of Physiology-Endocrinology and Metabolism* **2015**, *309* (2), E168-E176.
- 55 Scherrer, U.; Randin, D.; Vollenweider, P.; Vollenweider, L.; Nicod, P., Nitric oxide release accounts for insulin's vascular effects in humans. *The Journal of Clinical Investigation* **1994**, *94* (6), 2511-2515.

CHAPTER III

IDENTIFICATION OF PERIPHERAL VASCULAR FUNCTION MEASURES AND CIRCULATING BIOMARKERS OF MITOCHONDRIAL FUNCTION IN PATIENTS WITH MITOCHONDRIAL DISEASE

Sebastiaan JW van Kraaij, MD,^{1,2} Diana R Pereira, MsC,¹ Bastiaan Smal, BsC,¹
Luciana Summo, PhD,³ Anne Konkel, PhD,³ Janine Lossie, PhD,³ Andreas Busjahn, PhD,⁴
Tom N Grammatopoulos, PhD,⁵ Erica Klaassen, MsC,¹ Robert Fischer, PhD,³
Wolf-Hagen Schunck, PhD,^{3,6} Pim Gal, MD, PhD,^{1,2} Matthijs Moerland, PhD^{1,2}

1: Centre for Human Drug Research, Leiden, NL

2: Leiden University Medical Centre, Leiden, NL

3: OMEICOS Therapeutics GmbH, Berlin, D

4: HealthTwiSt GmbH, Berlin, D

5: BioEnergetics LLC, Boston, MA, USA

6: Max Delbrück Center for Molecular Medicine
in the Helmholtz Association, Berlin, D

Study highlights

WHAT IS THE CURRENT KNOWLEDGE ON THE TOPIC?

Mitochondrial disorders cause significant disease burden, and staging and evaluation of mitochondrial disease relies mainly on clinical evaluation and invasive procedures.

Development of treatments for mitochondrial disease is likewise burdened by a lack of non-invasive evaluable endpoints in early phase research, in addition to the large variability between different mitochondrial diseases, between patients with the same mitochondrial mutation and between different tissues in a single patient, resulting in few evidence-based treatments available.

WHAT QUESTION DID THIS STUDY ADDRESS?

Whether a combination of circulating biochemical markers, *ex vivo* cellular assays and imaging techniques can differentiate between patients with mitochondrial disease and healthy volunteers.

WHAT DOES THIS STUDY ADD TO OUR KNOWLEDGE?

Several imaging techniques and serum biomarkers can distinguish individuals with mitochondrial disease from healthy volunteers.

Ex vivo cellular assays are less reliable in distinguishing individuals with mitochondrial disease from healthy volunteers, possibly due to tissue heterogeneity in mutational load causing cells collected from blood to be less affected by disease than end organs such as the heart.

HOW MIGHT THIS CHANGE CLINICAL PHARMACOLOGY OR TRANSLATIONAL SCIENCE?

This study confirms the need for an integral approach to the development of treatments for mitochondrial disorders, including endpoints at various tissue levels, e.g. blood, skin, muscle and blood vessels

Abstract

The development of pharmacological therapies for mitochondrial diseases is hampered by the lack of tissue-level and circulating biomarkers reflecting effects of compounds on endothelial and mitochondrial function. This phase-0 study aimed to identify biomarkers differentiating between patients with mitochondrial disease and healthy volunteers.

In this cross-sectional case-control study, 8 participants with mitochondrial disease and 8 healthy volunteers (HVS) matched on age, sex and body mass index underwent study assessments consisting of blood collection for evaluation of plasma and serum biomarkers, mitochondrial function in peripheral blood mononuclear cells (PBMCS) and an array of imaging methods for assessment of (micro)circulation.

Plasma biomarkers GDF-15, IL-6, NT-PROBNP and CTNI were significantly elevated in patients compared to HVs, as were several clinical chemistry and hematology markers. No differences between groups were found for mitochondrial membrane potential, mitochondrial reactive oxygen production, oxygen consumption rate or extracellular acidification rate in PBMCS. Imaging revealed significantly higher nicotinamide-adenine-dinucleotide-hydrogen content in skin as well as reduced passive leg movement-induced hyperaemia in patients.

This study confirmed results of earlier studies regarding plasma biomarkers in mitochondrial disease and identified several imaging techniques that could detect functional differences on tissue level between participants with mitochondrial disease and HVS. However, assays of mitochondrial function in PBMCS did not show differences between participants with mitochondrial disease and HVS, possibly reflecting compensatory mechanisms and heterogeneity in mutational load. In future clinical trials, using a mix of imaging and blood-based biomarkers may be advisable, as well as combining these with an *in vivo* challenge to disturb homeostasis.

Introduction

Mitochondrial disorders are a group of diseases caused by defects in the mitochondrial oxidative phosphorylation chain and presenting with a variety of phenotypes. The most common mutation in mitochondrial DNA causing mitochondrial dysfunction is m.3243A>G, also known as the mitochondrial encephalopathy, lactic acidosis, and stroke like episodes (MELAS) mutation,¹ which causes a combined defect of the oxidative phosphorylation chain proteins encoded in mitochondrial DNA.² The resulting disorders due to mitochondrial dysfunction in these individuals include MELAS, maternally inherited diabetes deafness, hypertrophic cardiomyopathy, macular dystrophy, focal segmental glomerulosclerosis, and myoclonic epilepsy with ragged-red fibers.

Defects in mitochondrial function lead to a disturbance in cellular redox balance and increase in cellular oxidative stress.³ This results in, among other effects, cardiovascular disease, and in particular endothelial dysfunction.⁴ Assessment of functional status in individuals with mitochondrial disease can be done through questionnaires or evaluation of clinical symptoms, or by *in vitro* assays of mitochondrial function,⁵ although these have limitations such as high inter-tissue variability, necessitating invasive procedures to acquire affected tissues.⁶ Mitochondrial mutation load, for example, was found to be correlated with functional status in muscle tissue, but not in blood.⁷ Other limitations of *in vitro* functional assays are high inter-laboratory variability, a low margin between individuals with mitochondrial disease and healthy controls, and the inability to differentiate between primary mitochondrial dysfunction (e.g., due to a mutation in mitochondrial DNA) and mitochondrial dysfunction due to other factors (e.g., sedentary lifestyle).⁶

Recently, the Centre for Human Drug Research has developed and validated a test array for non-invasive evaluation of metabolic and endothelial function *in vivo* in different tissues. This test battery includes the flow-mediated skin fluorescence technique, which measures nicotinamide-adenine-dinucleotide hydrogen (NADH) fluorescence in the skin and can be used to assess cellular metabolic status and response to ischemia, near-infrared spectroscopy which can be used to measure skin and muscle tissue oxygenation and has been used previously to evaluate mitochondrial oxidative capacity *in vivo*,⁸ laser speckle contrast imaging, which when combined with reactive hyperaemia and thermal hyperaemia challenges can measure microvascular reactivity in the skin, passive leg movement, used to measure nitric oxide-mediated large vessel vasodilation, and sidestream dark field microscopy, to assess sublingual vascular density and perfusion status.

In addition, the Centre for Human Drug Research developed novel cell-based techniques capable of assessing mitochondrial status. These include assessments of mitochondrial reactive oxygen species and mitochondrial membrane potential. Reactive oxygen species are important regulators of physiological cell signalling, and excessive mitochondrial reactive oxygen species production can induce mitochondrial damage and may have a role in the pathogenesis of mitochondrial disorders,⁹ while mitochondrial membrane potential is an essential energy storage component for oxidative phosphorylation and ATP production.¹⁰ These cell-based biomarkers can be combined with serum or plasma biomarkers such as GDF-15, an established systemic biomarker of mitochondrial disease and integrated stress response,¹¹ to assess mitochondrial function on multiple physiological levels.

In current clinical practice, there are limited treatments available for patients with mitochondrial disease. Treatments include administering of arginine and citrulline as nitric oxide-donors to improve endothelial function¹² and thereby possibly prevent or treat MELAS-related stroke,¹³ exercise to improve mitochondrial function, and administration of vitamins and supplements such as coenzyme Q10, creatine, L-carnitine, dichloroacetate, dimethylglycine, α -lipoic acid, and B-vitamins, although evidence of clinical efficacy of these treatments is very limited and mixed.¹⁴ Moreover, the measures used to evaluate clinical effects in these trials are variable and not all proven to correlate with functional status of patients.

A phase 0 clinical study was performed to identify biomarkers differentiating between healthy volunteers and patients with mitochondrial disease, based on the aforementioned set of imaging and cellular techniques, supported by circulating biochemical biomarkers of inflammation and myocardial damage. Ultimately, these biomarkers could be used as early clinical endpoints in future phase 1B/phase 2A clinical pharmacology studies in patients with mitochondrial disease.

Materials & methods

This study was conducted at the Centre for Human Drug Research (Leiden, The Netherlands), in accordance with the principles of the Declaration of Helsinki, the International Conference on Harmonisation Good Clinical Practice and ethical principles as referenced in EU Directive 2001/20/EC. The protocol was approved by the Medical Research Ethics Committee of the BEBO foundation (Assen, The Netherlands).

The trial was prospectively registered in [toetsingonline.nl](https://www.toetsingonline.nl) (CHDR2111, NL77982.056.21, ABR number 79322).

PARTICIPANTS

Eight participants with mitochondrial disease, with a confirmed m.3243A>G mutation in genetic testing and a Newcastle Mitochondrial Disease Scale score ≥ 11 , and eight healthy matched volunteers (HVS), all aged between 18 and 75 years and with body mass index between 18 and 30 kg/m², were recruited at Radboud University Medical Center, Nijmegen, the Netherlands. For participants with mitochondrial disease, only individuals with current cardiomyopathy defined as evidence of left ventricular hypertrophy, reduced systolic function or strain or electrocardiographic abnormalities consistent with cardiac involvement of mitochondrial disease were included. HVS were included if no clinically significant abnormal findings were obtained on medical history, physical examination, hematological laboratory tests or drug and alcohol screening. Pregnant women were excluded from participation, as were participants who received treatment with metformin, cytostatic medication, soluble guanylyl cyclase stimulators or activators, or nitrate agents less than 3 months before study day 1. HVS were matched to participants with mitochondrial disease on sex, age (+/- 5 years), and body mass index (+/- 3 kg/m²).

STUDY DESIGN

This was a translational phase-0, non-interventional, cross-sectional case-control study in which all participants with mitochondrial disease and healthy participants underwent all study assessments once. Participants received no investigational treatment.

STUDY ASSESSMENTS

SAFETY

Safety evaluation included assessment of adverse events and concomitant medication use and measurement of vital signs.

PLASMA AND SERUM BIOMARKERS

Venous blood was collected in K2EDTA tubes for assessment of hematology and glycated hemoglobin (HBA1C), SST Gel and Clot activator tubes for assessment of clinical chemistry and Sodium Fluoride tubes for assessment of glucose at the Clinical Chemistry Laboratory of Leiden University Medical Center (Leiden, The Netherlands). Additional venous blood was collected in K2EDTA tubes for as-

essment of plasma biomarkers growth/differentiation factor 15 (GDF-15; ELISA, Quantikine ELISA Human GDF-15, R&D Systems), pentraxin 3 (PTX 3; ELISA, Quantikine ELISA human Pentraxin 3/TGS-4, R&D Systems), interleukin 6 (IL-6; ECLIA, Proinflammatory Panel 1 (human) Kit, Meso Scale Discovery), N-terminal pro-hormone of brain natriuretic peptide (NT-PROBNP; ECLIA, Elecsys PROBNP II, Roche Diagnostics), cardiac troponin I (CTNI; CLEIA, Lumipulse® G hs Troponin I, Fujirebio) and high sensitivity C-reactive protein (hsCRP; Immunoturbidimetric Test Kit, CRP4, Roche Diagnostics) at MLM Medical Labs GmbH (Mönchengladbach, Germany). All blood collection was performed in fasted state after an overnight fast.

MITOCHONDRIAL FUNCTIONAL ASSAYS

Mitochondrial function was evaluated in fresh peripheral blood mononuclear cells (PBMCs). Venous blood was collected in Cell Preparation tubes containing sodium-heparin (Becton Dickinson, San Jose, A, USA). Blood was centrifuged at 1800x g for 30 minutes and PBMCs were collected by pouring supernatant into a polypropylene tube. PBMCs were assessed by flow cytometry ($\sim 2 \times 10^5$ cells/well) and by plate reader (2.5×10^5 cells/well).

Mitochondrial reactive oxygen species were quantified by MitoSOX™ Red (Molecular Probes, Invitrogen). PBMCs were incubated with MitoSOX™ at 5 μ M for 15 minutes at 37 °C in a humidified atmosphere with 5% CO₂. Mitochondrial mass was assessed by incubation of PBMCs with 25 nM MitoTracker™ Green FM (Molecular Probes, Invitrogen) for 45 minutes at 37 °C in a humidified atmosphere with 5% CO₂. PBMCs were stained with CD14 and CD3 markers for monocyte and T-cell discrimination, respectively. Propidium iodide was used to assess PBMCs viability. After staining, PBMCs were washed twice with phosphate buffer saline and analyzed by flow cytometry (MACSQuant16, Miltenyi Biotec). For flow cytometry data, to ensure proper gate setting, a minimum of 100,000 events (viable leukocytes) were collected. Gating strategy plots can be found in supplementary figures S2 and S3.

In addition, mitochondrial membrane potential was assessed by tetraethylbenzimidazolylcarbocyanine iodide (JC-1) staining (JC-1 kit fluorometric, Abcam). PBMCs were incubated with 0.5 μ M of JC-1. A positive control for membrane depolarization was included by incubation of PBMCs with FCCP at 100 μ M. Incubations were done for 30 minutes at 37 °C in a humidified atmosphere with 5% CO₂. Technical duplicates were produced for all mitochondrial membrane potential measurements. A Varioskan Lux plate reader (ThermoFisher) equipped with fluorescence filters was used to measure JC-1

fluorometric signals using excitation filter= 475 ±20 nm and emission filters: 530 ±15 nm and 590 ±17.5 nm. Data was collected using SkanIt software for microplate readers RE version 4.1.0.43. Mitochondrial membrane potential was calculated as presented in Equation 1:

$$\text{MMP} = \frac{\text{red aggregates}_{\text{condition}} / \text{green aggregates}_{\text{condition}}}{\text{red aggregates}_{\text{CCCP or FCCP}} / \text{green monomers}_{\text{CCCP or FCCP}}}$$

Bioenergetic profiles of freshly thawed and subsequently cultured PBMCs were evaluated using the Seahorse XF96 platform, measuring oxygen consumption rate at baseline and after oligomycin, FCCP and antimycin A treatment to evaluate mitochondrial function and extracellular acidification rate at baseline and after oligomycin treatment to assess glycolytic capacity (Bioenergetics LLC).

IMAGING ASSESSMENTS

Measurements were conducted in temperature-controlled rooms (20-24 °C) at the Centre for Human Drug Research. Study assessments conducted included flow-mediated skin fluorescence, near-infrared spectroscopy, laser speckle contrast imaging, passive leg movement and sidestream dark field microscopy.

Flow-mediated skin fluorescence is a technique used to measure mitochondrial function *in vivo* based on measuring the intensity of NADH fluorescence in skin tissue on the forearm during a challenge consisting of occluding and then releasing arterial flow. Flow-mediated skin fluorescence was used to assess cellular metabolic status by measuring NADH fluorescence during the various stages of the intervention, and vascular responses were assessed by analysing vasomotion using Fourier transformation. Flow-mediated skin fluorescence was measured using the purpose-built Angionica AngioExpert device (Angionica, Łódź, Poland).

Near-infrared spectroscopy is used to measure fractions of oxygenated and deoxygenated hemoglobin in tissues up to 3-4 cm deep with a spectroscopic device placed on the skin (Artinis Portamon, Artinis Medical Systems, Elst, the Netherlands). Near-infrared spectroscopy was conducted on the forearms of participants and combined with an arterial and venous occlusion challenge, in which blood flow is temporarily occluded with a blood pressure cuff inflated above systolic pressure (arterial occlusion) and diastolic pressure (venous occlusion). In combination with the arterial and venous occlusion, near-infrared spectroscopy allowed the quantification of tissue oxygen consumption, blood flow and vascular response to influx of blood in the arm.¹⁵

Laser speckle contrast imaging is a non-invasive imaging method that uses changes in the speckle pattern reflected when illuminating an imaged object with laser light (Pericam PSI NR system, Perimed, Järfälla, Sweden). Changes in the reflected pattern signify any movement on or inside the imaged object, which when imaging still human tissue reflects the flow of blood cells, which can be used to derive an estimation of blood flow in the imaged tissue. Laser speckle contrast imaging was performed in combination with post-occlusive reactive hyperaemia, where blood flow was temporarily occluded with a blood pressure cuff placed around the upper arm and then released. The subsequent increase in flow was used as a measure of vascular reactivity to shear stress caused by the sudden influx of blood into the arm.¹⁶ Laser speckle contrast imaging was also combined with the local thermal hyperaemia challenge, in which skin is heated to approximately 43 °C while continuously measuring blood flow, allowing the assessment of axon- and nitric oxide-dependent vasodilation.¹⁷

Passive leg movement-induced hyperaemia is a physiological response in the common femoral artery to passive movement of the lower leg. Passive movement of the lower leg induces peripheral vasodilation, which then induces an increase in arterial blood flow, quantifiable by measuring the flow speed through the common femoral artery with ultrasonography (Sparq Ultrasound System, Philips Medical Systems, Best, The Netherlands). Passive leg movement-induced hyperaemia is mediated mainly by nitric oxide release in endothelial cells, which makes it a reliable investigation to assess nitric oxide bioavailability.¹⁸

Sidestream dark field microscopy is a technique used to visualize blood vessels *in vivo* using light in a wavelength absorbed by red blood cells emitted by a microscope (MicroScan, MicroVision Medical, Amsterdam, the Netherlands). Sidestream dark field microscopy assessments were conducted on the mucous membranes of the mouth, which allow penetration of the light and visualisation of the underlying blood vessels. Analysed sidestream dark field microscopy parameters included the number of vessel crossings on an imaginary grid, De Backer density of vessels and the proportion of perfused vessels in the field of view.¹⁹

STATISTICAL ANALYSIS

All parameters were summarized by participant group and listed with mean, SD, CV, median, minimum, and maximum. Differences between parameters of all assessments were compared between HVS and participants with mitochondrial

disease. Parameters were assessed for normality and log-transformed if necessary to facilitate analysis. Log-transformed endpoints were back-transformed after analysis where results could be interpreted as percentage difference.

For imaging assessments, group differences were assessed using a mixed model analysis of covariance with time and group as fixed factor and subject as random factor. Results were reported with the estimated difference, 95% confidence interval, least square mean (LSM) estimates and the p-value. Graphs of the LSM estimates by participant group were presented with 95% confidence intervals as error bars.

For biomarkers and mitochondrial function assessments differences in continuous variables between groups were assessed using non-parametric tests, i.e., Wilcoxon rank-sum and Kruskal-Wallis, and categorical data were analysed with cross-tables by Fisher's exact test. Data from the Seahorse assessment were analysed with a student's t-test or a two-way analysis of variance with a Dunnett's multiple comparison test using GraphPad Prism 7.00.

Results

CLINICAL AND DEMOGRAPHIC CHARACTERISTICS OF STUDY PARTICIPANTS

A total of 18 participants were screened, 9 in the participants with mitochondrial disease group and 9 in the HV group. An overview of the flow of participants in the study is shown in Figure S1.

An overview of characteristics and demographics for the participants is provided in Table S1. Participants were all white (100%), and predominantly female (HV 57% vs MitoD 63%). Temperature and ethnicity did not differ significantly between study groups. No clinically significant medical history or concomitant medication was noted in the HV group. In the mitochondrial disease group, 7/8 participants had a history of diabetes mellitus, treated with long- and short-acting insulin in 5/8 participants and with sulfonylureas in 2/8 participants, in 1 participant combined with dipeptidyl peptidase 4 inhibition. Other notable medical history included hearing loss in 7/8 participants as well as vision loss in 3/8 participants, myocardial infarction in 2/8 participants and cardiac arrhythmia and kidney insufficiency, the latter in one different participant each. All participants were prescribed an angiotensin-converting enzyme inhibitor or angiotensin II receptor blocker for their documented cardiomyopathy, in 1 participant combined with neprilysin inhibition. Six out of 8 participants used β -blockers and

3/8 loop diuretics. Two participants used acetylsalicylic acid and a platelet aggregation inhibitor for coronary artery disease. Other notable medication use was pancreatic enzymes for chronic pancreatitis in 1 participant and a vitamin K antagonist for prevention of vascular events in another participant.

SAFETY DATA

No safety evaluation was planned for this study, since participants did not receive a study intervention. However, adverse events were collected. No participants experienced adverse events during the study.

BIOMARKERS AND MITOCHONDRIAL FUNCTIONAL ASSAYS

CLINICAL CHEMISTRY, HEMATOLOGY, AND ADDITIONAL PLASMA BIOMARKERS

Results of clinical chemistry, hematology and additional plasma biomarkers are summarized in Table 1. Significant clinical chemistry differences between participants with mitochondrial disease and HVs were seen in medians of glucose, LDH, sodium and HBA1C. Significant median differences between MitoD patients and HVS were also seen for lymphocyte count and monocyte count. Evaluation of additional plasma biomarkers revealed significant median differences for GDF-15, IL-6, NT-PROBNP and CTNI, and a trend towards higher hsCRP in participants with mitochondrial disease versus HVS.

TABLE 1 Comparison between HV and MitoD participants for clinical chemistry, haematology and biomarker parameters.

Parameter [Unit]	HV (median, 95% CI)	MitoD (median, 95% CI)	p-value HV vs. MitoD
Glucose [mmol/L]	5.20 (4.90 / 5.30)	8.8 (6.3 / 11.2)	0.002
Creatine Kinase [U/L]	75 (64 / 150)	220 (109 / 355)	0.054
Lactate dehydrogenase [U/L]	165 (152 / 245)	250 (187 / 288)	0.037
Sodium [mmol/L]	142 (141 / 142)	135 (130 / 138)	0.001
Triglycerides [mmol/L]	1.14 (0.89 / 1.64)	2.04 (1.24 / 3.63)	0.072
Blood Urea [mmol/L]	5.00 (4.70 / 7.10)	8.15 (6.70 / 8.95)	0.054
Uric Acid [mmol/L]	0.270 (0.250 / 0.320)	0.335 (0.280 / 0.500)	0.063
HBA1C [mmol/mol HB]	35.1 (32.4 / 36.0)	60.5 (57.5 / 69.7)	0.001
Basophil Count [$10^9/L$]	0.0400 (0.0300 / 0.0800)	0.0350 (0.0300 / 0.0551)	0.637
Eosinophil Count [$10^9/L$]	0.140 (0.060 / 0.230)	0.180 (0.120 / 0.220)	0.601
Lymphocyte Count [$10^9/L$]	1.58 (1.38 / 1.67)	1.94 (1.84 / 2.12)	0.009
Monocyte Count [$10^9/L$]	0.490 (0.410 / 0.540)	0.675 (0.560 / 0.790)	0.004

(Continuation Table 1)

Parameter [Unit]	HV (median, 95% CI)	MitoD (median, 95% CI)	p-value HV vs. MitoD
Neutrophil Count [10 ⁹ /L]	4.09 (3.00 / 4.69)	3.84 (3.63 / 5.75)	0.955
Platelet Count [10 ⁹ /L]	227 (209 / 336)	204 (192 / 292)	0.463
GDF-15 [pg/mL]	470 (393 / 728)	2141 (1755 / 3927)	0.001
PTX-3 [ng/mL]	0.318 (0.156 / 0.608)	0.340 (0.156 / 0.484)	0.720
IL-6 [pg/mL]	0.200 (0.200 / 0.600)	0.90 (0.40 / 2.10)	0.026
NT-PROBNP [pg/mL]	60.0 (38.0 / 79.0)	680 (94 / 2262)	0.021
CTNI [pg/mL]	23.1 (19.3 / 25.8)	152 (53 / 497)	0.001
hsCRP [mg/L]	0.60 (0.30 / 2.10)	1.55 (1.10 / 3.15)	0.056

CI=confidence interval, CTNI=cardiac troponin I, GDF-15=growth/differentiation factor 15, HBA1C=glycated hemoglobin, hsCRP=high sensitivity C-reactive protein, HV=healthy volunteers, IL-6=interleukin-6, MitoD=mitochondrial disease patients, MIN=minimum, MAX=maximum, N=number of subjects, NT-PROBNP=N-terminal prohormone of brain natriuretic peptide. p-value based on Wilcoxon-test, * for 3 subjects with values < BLOQ the value 0.1565 was taken (½ of BLOQ), ** for 4 subjects with values < BLOQ the value 0.2 was taken (½ of BLOQ). P-values <0.05 bolded.

MITOCHONDRIAL REACTIVE OXYGEN SPECIES PRODUCTION, MITOCHONDRIAL MASS AND MITOCHONDRIAL MEMBRANE POTENTIAL

Results of flow cytometry analyses are summarised in Table 2. No significant differences between participants with mitochondrial disease and HVS were observed in mitochondrial reactive oxygen species production or mitochondrial membrane potential.

TABLE 2 Comparison between HV and MitoD participants for MTRoS and MMP parameters.

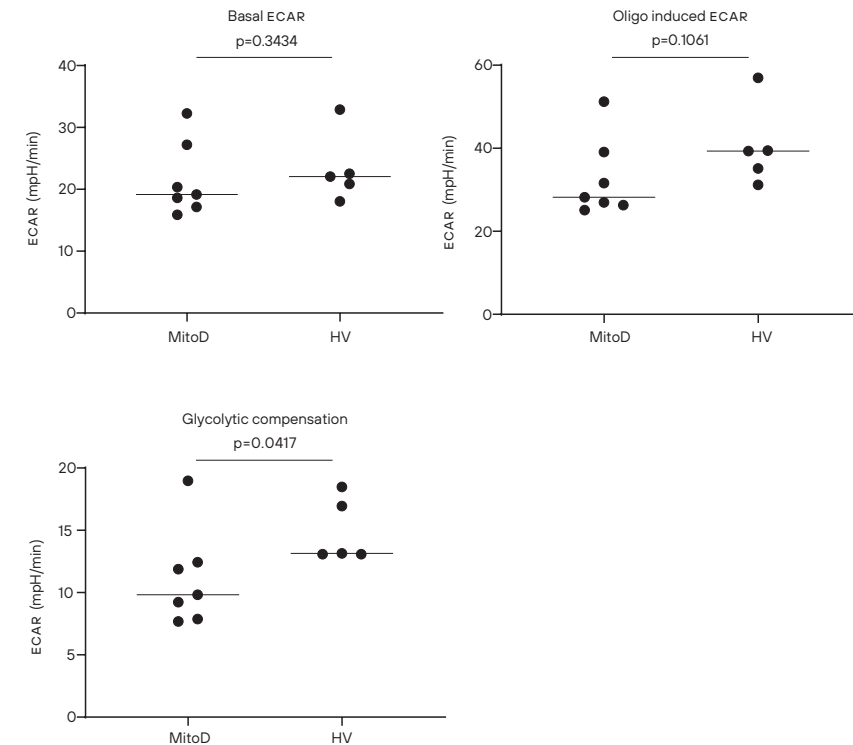
Measure of Mitochondrial Function	HV (median, 95% CI)	MitoD (median, 95% CI)	p-value HV vs MitoD
MitoSOX monocytes	1.01 (0.83 / 1.19)	0.85 (0.78 / 1.10)	0.4634
MitoTracker monocytes	6.1 (4.1 / 14.3)	15.4 (4.7 / 32.4)	0.1206
MitoSOX/MitoTracker Ratio (monocytes)	0.152 (0.095 / 0.241)	0.073 (0.026 / 0.156)	0.0721
MitoSOX T cells	0.280 (0.270 / 0.300)	0.280 (0.250 / 0.330)	1.0000
MitoTracker T cells	2.35 (1.61 / 4.55)	5.7 (2.0 / 11.9)	0.0721
MitoSOX/MitoTracker Ratio (T cells)	0.119 (0.071 / 0.161)	0.056 (0.029 / 0.145)	0.0939
JC-1, Aggregates/ Monomers Ratio	4.84 (1.61 / 6.02)	5.34 (4.54 / 6.12)	0.2319

HV=healthy volunteers; JC-1=tetraethylbenzimidazolylcarbocyanine iodide; MitoD=mitochondrial disease patients; N=number of subjects; MMP=mitochondrial membrane potential; MTRoS=mitochondrial reactive oxygen species; NA=not applicable; min=minimum; max=maximum; CI=confidence interval; p-value based on Wilcoxon-test with adjustment. P-values <0.05 bolded.

MITOCHONDRIAL BIOENERGETIC PROFILES

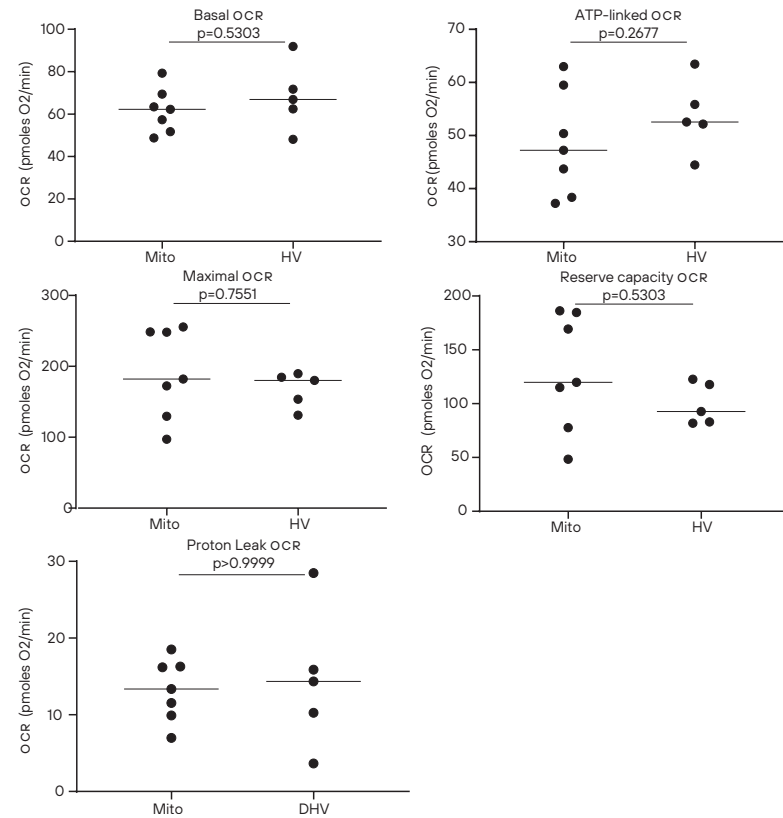
One participant with mitochondrial disease and 1 HV were excluded from Seahorse analysis due to insufficient cells, 1 HV due to insufficient quality of cells and 1 participant with mitochondrial disease due to a positive tetrahydrocannabinol drug screening. There were no statistically significant differences between HVS and participants with mitochondrial disease detected in any oxygen consumption rate or extracellular acidification rate parameter except for a lower glycolytic compensation in participants with mitochondrial disease when compared to HVS (p = 0.0417) (Figure 1 and 2).

FIGURE 1 Extracellular acidification rate and glycolytic compensation, individual datapoints with medians.



ECAR=extracellular acidification rate; HVs=healthy volunteers; MitoD=mitochondrial disease.

FIGURE 2 Oxygen consumption rate, individual datapoints with medians.



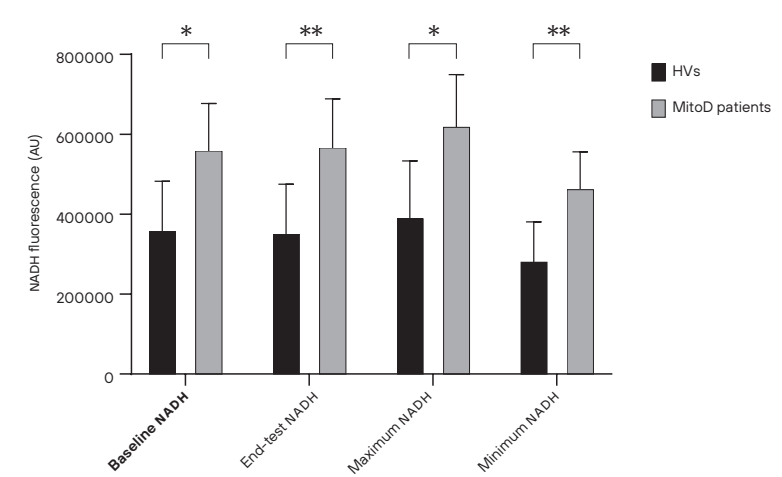
ATP=adenosine triphosphate; HVS=healthy volunteers; MitoD=mitochondrial disease; OCR=oxygen consumption rate.

IMAGING ASSESSMENTS

FLOW-MEDIATED SKIN FLUORESCENCE

Assessment of skin NADH content showed a baseline NADH (LSM difference -201771, 95% CI: -352349, -51193), end-test NADH (LSM difference -214942, 95% CI: -367462, -62423), maximum NADH (LSM difference -229504, 95% CI: -400052, 59555) and minimum (LSM difference -180800, 95% CI: -298856, -62743) were all significantly higher in participants with mitochondrial disease when compared to HVS, as shown in Figure 3. No other statistically significant differences were found in flow-mediated skin fluorescence parameters.

FIGURE 3 NADH fluorescence during FMSF, means with 95% CI.



* indicates significance $p < 0.05$; ** indicates significance $p < 0.01$. AU=arbitrary units; FMSF=flow-mediated skin fluorescence; HVS=healthy volunteers; MitoD=mitochondrial disease; NADH=nicotinamide adenine dinucleotide hydrogen.

NEAR-INFRARED SPECTROSCOPY

Assessment of skin and muscle oxy- and deoxygenated haemoglobin did not show statistically significant differences between HVS and participants with mitochondrial disease in muscle oxygen consumption, muscle blood flow, hyperaemic response speed or hyperaemic response duration as assessed with near-infrared spectroscopy.

LASER SPECKLE CONTRAST IMAGING

The results from laser speckle contrast imaging measurements are summarised in Table 3. No statistically significant differences between HVS and participants with mitochondrial disease were seen in basal, maximal or plateau flow (including change from baseline for maximal and plateau flow) during local thermal hyperaemia challenge, although all observed dermal blood flows were lower in participants with mitochondrial disease, specifically local thermal hyperaemia-induced plateau blood flow. Similarly, no statistically significant differences in basal, maximal, or mean flow (including change from baseline for maximal flow) during post-occlusive reactive hyperaemia challenges were found.

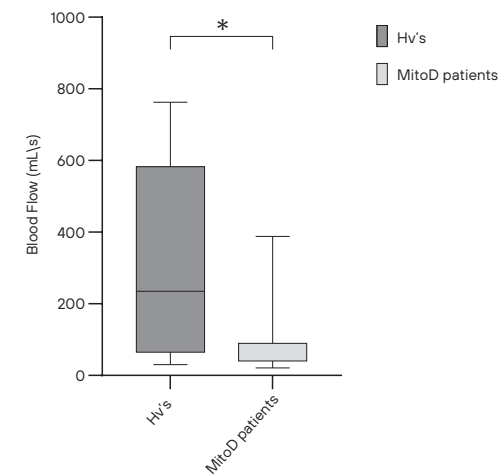
TABLE 3 Comparison between HV and MitoD participants for LSCI parameters.

Parameter [Unit]	P-value	HV (LSM)	MitoD (LSM)	LSM difference	95% CI	
					Lower	Upper
LSCI LTH Basal Flow [AU]	0.4605	102.394	94.877	7.517	-13.634	28.668
LSCI LTH Maximal Flow [AU]	0.2165	177.339	156.152	21.187	-13.809	56.182
LSCI LTH Maximal Flow CFB [AU]	0.2626	74.945	61.276	13.669	-11.361	38.700
LSCI LTH Plateau Flow [AU]	0.1212	191.409	161.578	29.831	-8.875	68.537
LSCI LTH Plateau Flow CFB [AU]	0.1431	89.015	66.701	22.314	-8.462	53.090
LSCI PORH Basal Flow [AU]	0.2635	33.921	30.096	3.826	-3.193	10.845
LSCI PORH Maximal Flow [AU]	0.2521	70.020	60.258	9.762	-7.708	27.232
LSCI PORH Maximal Flow CFB [AU]	0.4299	36.099	30.162	5.937	-9.662	21.535
LSCI PORH Mean Flow [AU]	0.3605	12.640	10.990	1.650	-2.078	5.378
LSCI PORH Rest Flow [AU]	0.7304	37.664	36.308	1.356	-6.876	9.588

AU=arbitrary units; CI=confidence interval; HV=healthy volunteers; LSM=least squares mean(s); LSCI=laser speckle contrast imaging; LTH=local thermal hyperaemia; MitoD=mitochondrial disease patients; PORH=post occlusive reactive hyperaemia. P-values <0.05 bolded.

PASSIVE LEG MOVEMENT

Flow increase after passive leg movement was significantly higher in HVS when compared to participants with mitochondrial disease (LSM difference: 224.05, 95% CI: 12.34, 435.76), as shown in Figure 4.

FIGURE 4 Femoral artery blood flow CFB after PLM, means with 95% CI.

* indicates significance $p < 0.05$. CFB=change from baseline; HVS=healthy volunteers; MitoD=mitochondrial disease; PLM=passive leg movement.

SIDESTREAM DARK FIELD MICROSCOPY

De Backer density, a measure of vessel density, was significantly higher HVS when compared to participants with mitochondrial disease (LSM difference 0.94, 95% CI: 0.015, 1.87), as was the number of crossings (LSM difference 9.5, 95% CI: 0.1, 18.9), which is a related parameter. There were no other statistically significant differences between groups in other sidestream dark field microscopy parameters.

Discussion

In this phase-0, observational, translational, and mechanistic study, biomarkers and imaging methods were evaluated for their ability to distinguish between mitochondrial disease participants with a confirmed m.3243A>G mutation and healthy participants matched on sex, age and body mass index. Significant differences in clinical chemistry, hematology and markers of inflammation and myocardial damage were identified, unsurprising given the clinical status of the participants with mitochondrial disease, all of whom were diagnosed with diabetes

mellitus and cardiomyopathy. This study also confirmed earlier results showing GDF-15 as a biomarker specific for mitochondrial disease.¹¹

No significant differences between study groups were seen in experiments evaluating mitochondrial reactive oxygen species production or mitochondrial membrane potential in fresh PBMCS, and only one significant difference, a lower glycolytic compensation in participants with mitochondrial disease, was found when assessing oxygen consumption rate and extracellular acidification rate in freshly thawed PBMCS. Higher mitochondrial reactive oxygen species production, reduced oxygen consumption rate and impaired glycolysis in PBMCS has been shown in patients with heart failure,²⁰ chronic kidney disease,²¹ and other patient groups,²²⁻²³ although literature is relatively scarce and heterogenous, and many studies are conducted in cells other than PBMCS. Mitochondrial function has also previously been evaluated in specific, but heterogenous mitochondrial disease patient populations in small samples, and in various cell or tissue types.¹¹ In a study of children with various defects of the oxidative phosphorylation chain, mitochondrial membrane potential and ATP production was found lower in lymphocytes of affected participants compared to controls.²⁴ For patients with the specific m.3243A>G mutation, higher mitochondrial reactive oxygen species production, lower ATP production, and lower mitochondrial membrane potential in PBMCS was shown in 2 previous studies,²⁵⁻²⁶ and higher mitochondrial reactive oxygen species production and lower mitochondrial membrane potential and ATP production was also shown in m.3243A>G mutated fibroblasts,²⁷ and in endothelial cells created from induced pluripotent stem cells derived from an individual with high m.3243A>G mutational load.²⁸ Lower mitochondrial oxygen consumption rate has been found in both human myoblasts²⁹ and induced pluripotent stem cells with the m.3243A>G mutation.³⁰ This study did not replicate the findings regarding mitochondrial membrane potential and mitochondrial reactive oxygen species production seen in previous studies. This might reflect a small sample size with intra-individual variability, especially in the heterogeneous group of participants with mitochondrial disease, or a higher metabolic flexibility of PBMCS compared to other tissues affected in individuals with the m.3243A>G mutation.³¹

This is the first study to evaluate an array of imaging methods for evaluation of metabolic and endothelial function in individuals with the m.3243A>G mutation, although the methods employed in this study have been studied previously in diverse study populations, such as patients with cardiovascular disease,

diabetes mellitus, chronic kidney disease, chronic obstructive pulmonary disease, and critical illness.^{17,32-34}

NADH fluorescence was significantly elevated in skin of participants with the m.3243A>G mutation compared to HVS. Due to dysfunction of mitochondrial complex I of the mitochondrial OXPHOS chain and decrease in activity of NADH reductive pathways in these patients,³⁵⁻³⁶ NADH/NAD⁺ ratio and consequently cellular reductive stress will increase, leading to downstream metabolic changes in these patients and contributing to the disease phenotypes associated with this mutation. NAD⁺ metabolism and NADH/NAD⁺ ratio have previously been the target of interventions aiming to treat mitochondrial disorders,³⁷⁻³⁸ but these have not been proven efficacious in human trials. The flow-mediated skin fluorescence method likely detected the higher NADH levels associated with the pathophysiology of mitochondrial dysfunction in peripheral tissue (skin), suggesting that there is a difference in the effects of the genetic defect in peripheral tissue compared to PBMCS, in which no differences in mitochondrial function were detected.

Hypoxia sensitivity as measured with flow-mediated skin fluorescence and resting muscle tissue oxygen consumption as measured with near-infrared spectroscopy did not differ significantly between participants with mitochondrial disease and HVS, possibly due to the compensatory mechanisms in the former during rest, e.g., hyperoxygenation of muscle,³⁹ which might be revealed by applying blood volume corrections in future studies.⁴⁰

Microvascular reactivity to passive leg movement of the lower leg was significantly lower in participants with mitochondrial disease compared to HVS, probably reflecting the higher oxidative stress in the former⁴¹ causing reduced nitric oxide bioavailability. This is supported by a trend towards lower local thermal hyperaemia-induced dermal blood flow in participants with mitochondrial disease versus HVS, another indicator of nitric oxide bioavailability.¹⁷ Last, significantly lower sublingual vessel density was observed in participants with mitochondrial disease versus HVS. This contradicts earlier findings of higher capillary growth induced by poor oxygen utilization in muscles affected by mitochondrial dysfunction,⁴² but in this study vessel density was measured in non-muscular tissue which may be affected more by reduced angiogenic capacity of endothelial cells due to mitochondrial dysfunction.⁴³

In this study, mitochondrial functional assays conducted on PBMCS did not distinguish between individuals with mitochondrial disease and healthy volunteers, while several imaging methods testing skin metabolic status

(flow mediated skin fluorescence) or general vascular function (passive leg movement, laser speckle contrast imaging, sidestream darkfield microscopy) detected differences. This likely reflects the heterogeneity of mutational load within individuals with mitochondrial disease, with some tissues with a higher mutational load than others,⁴⁴ as well as compensatory mechanisms, e.g., metabolic flexibility, in PBMCS.⁴⁵ In addition, the process of purifying selection, by which PBMCS expressing high mutational loads of the pathogenic mitochondrial DNA are filtered out during production or targeted for removal after entering the bloodstream,⁴⁶ thereby resulting in PBMCS with low mutational loads predominating in the bloodstream and therefore in the blood samples taken for analysis, may have reduced the likelihood of finding significantly decreased mitochondrial function in PBMCS of individuals with mitochondrial disease compared to PBMCS of healthy volunteers. Moreover, small differences on proximal, cell-level endpoints might coalesce into detectable effects tissue-level endpoints such as imaging and serum biomarkers. In future clinical studies evaluating potential treatments for mitochondrial disease, a mixed approach of cellular, imaging and serum biomarker endpoints may be advisable to fully capture pharmacodynamic effects of the studied compound in different tissues and on different physiological levels. Moreover, since basal cellular assays conducted during homeostasis did not discriminate between participants with mitochondrial disease and HVS in this study, *in vivo* stressors, such as intravenous administration of lipopolysaccharide⁴⁷ or oral administration of statins⁴⁸ may challenge the system and thereby reveal drug effects.

LIMITATIONS

Since the array of circulating biomarkers evaluated in this study was limited, biomarkers that have since been identified by proteomics and metabolomics were not tested in this study.³⁶ This study was further limited by variability in disease severity, comorbidity, medication use, lifestyle, and age in the mitochondrial disease group. Some of the medications used by the participants with mitochondrial disease in this study are known to influence inflammation, oxidative stress and mitochondrial function and may therefore have influenced the outcomes of the assessments of this study.^{49–50} Variation within the mitochondrial disease group was partially compensated for by matching HVS and participants with mitochondrial disease, but due to a small sample size, further stratification in subgroups or other means of controlling for this variation were not possible. However, it is likely that the used medications shifted the

measured parameters towards levels observed in healthy volunteers, reducing the likelihood that observed differences would disappear when controlling for medication use. A limitation of the mitochondrial reactive oxygen species assay specifically is that detection of superoxide only does not reflect the complete spectrum of ROS and its effects. A limitation of the FMSF technique is that only skin NADH content can be measured, hence NADH/NAD⁺ ratio cannot be determined, and only partial evaluation of cellular metabolic state is possible.

CONCLUSION

In this study several biomarkers and imaging assessments were able to distinguish between healthy participants and participants with mitochondrial disease, indicating a potential for use as endpoints in clinical trials investigating treatments for mitochondrial dysfunction in addition to traditional methods of assessment, such as clinical evaluation.³⁵ Further avenues for research on these investigative tools could be to combine the different endpoints with an *in vivo* medicinal challenge affecting mitochondrial function.

SUPPORTING INFORMATION

Additional supporting information may be found in the online version of the article at the publisher's website.



Figure S1



Figure S2



Figure S3



Table S1



Table S2

REFERENCES

- 1 Gorman, G. S.; Schaefer, A. M.; Ng, Y.; Gomez, N.; Blakely, E. L.; Alston, C. L.; Feeney, C.; Horvath, R.; Yu-Wai-Man, P.; Chinnery, P. F.; Taylor, R. W.; Turnbull, D. M.; McFarland, R., Prevalence of nuclear and mitochondrial DNA mutations related to adult mitochondrial disease. *Annals of neurology* **2015**, *77* (5), 753-9.
- 2 de Laat, P.; Koene, S.; van den Heuvel, L. P. W. J.; Rodenburg, R. J. T.; Janssen, M. C. H.; Smeitink, J. A. M., Clinical features and heteroplasmy in blood, urine and saliva in 34 Dutch families carrying the m.3243A > G mutation. *Journal of Inherited Metabolic Disease* **2012**, *35* (6), 1059-1069.
- 3 Peoples, J. N.; Saraf, A.; Ghazal, N.; Pham, T. T.; Kwong, J. Q., Mitochondrial dysfunction and oxidative stress in heart disease. *Experimental & Molecular Medicine* **2019**, *51* (12), 1-13.
- 4 Davidson, S. M.; Duchon, M. R., Endothelial Mitochondria. *Circulation Research* **2007**, *100* (8), 1128-1141.
- 5 Pesta, D.; Gnaiger, E., High-Resolution Respirometry: OXPHOS Protocols for Human Cells and Permeabilized Fibers from Small Biopsies of Human Muscle. In *Mitochondrial Bioenergetics: Methods and Protocols*, Palmeira, C. M.; Moreno, A. J., Eds. Humana Press: Totowa, NJ, 2012; pp 25-58.
- 6 Parikh, S.; Goldstein, A.; Koenig, M. K.; Scaglia, F.; Enns, G. M.; Saneto, R.; Anselm, I.; Cohen, B. H.; Falk, M. J.; Greene, C.; Gropman, A. L.; Haas, R.; Hirano, M.; Morgan, P.; Sims, K.; Tarnopolsky, M.; Van Hove, J. L.; Wolfe, L.; DiMauro, S., Diagnosis and management of mitochondrial disease: a consensus statement from the Mitochondrial Medicine Society. *Genetics in medicine : official journal of the American College of Medical Genetics* **2015**, *17* (9), 689-701.
- 7 Mehrazin, M.; Shanske, S.; Kaufmann, P.; Wei, Y.; Coku, J.; Engelstad, K.; Naini, A.; De Vivo, D. C.; DiMauro, S., Longitudinal changes of mtDNA A3243G mutation load and level of functioning in MELAS. *American Journal of Medical Genetics Part A* **2009**, *149A* (4), 584-587.
- 8 Willingham, T. B.; McCully, K. K., In Vivo Assessment of Mitochondrial Dysfunction in Clinical Populations Using Near-Infrared Spectroscopy. *Frontiers in Physiology* **2017**, *8*, 689.
- 9 Sena, L. A.; Chandel, N. S., Physiological roles of mitochondrial reactive oxygen species. *Molecular cell* **2012**, *48* (2), 158-67.
- 10 Gorman, G. S.; Chinnery, P. F.; DiMauro, S.; Hirano, M.; Koga, Y.; McFarland, R.; Suomalainen, A.; Thorburn, D. R.; Zeviani, M.; Turnbull, D. M., Mitochondrial diseases. *Nature reviews. Disease primers* **2016**, *2*, 16080.
- 11 Hubens, W. H. G.; Vallbona-Garcia, A.; de Coo, I. F. M.; van Tienen, F. H. J.; Webers, C. A. B.; Smeets, H. J. M.; Gorgels, T. G. M. F., Blood biomarkers for assessment of mitochondrial dysfunction: An expert review. *Mitochondrion* **2022**, *62*, 187-204.
- 12 Gambardella, J.; Khondkar, W.; Morelli, M. B.; Wang, X.; Santulli, G.; Trimarco, V., Arginine and Endothelial Function. *Biomedicines* **2020**, *8* (8), 277.
- 13 El-Hattab, A. W.; Hsu, J. W.; Emrick, L. T.; Wong, L.-J. C.; Craigen, W. J.; Jahoor, F.; Scaglia, F., Restoration of impaired nitric oxide production in MELAS syndrome with citrulline and arginine supplementation. *Molecular genetics and metabolism* **2012**, *105* (4), 607-614.
- 14 Kerr, D. S., Review of clinical trials for mitochondrial disorders: 1997-2012. *Neurotherapeutics : the journal of the American Society for Experimental NeuroTherapeutics* **2013**, *10* (2), 307-19.
- 15 Dennis, J. J.; Wiggins, C. C.; Smith, J. R.; Isautier, J. M. J.; Johnson, B. D.; Joyner, M. J.; Cross, T. J., Measurement of muscle blood flow and O2 uptake via near-infrared spectroscopy using a novel occlusion protocol. *Scientific Reports* **2021**, *11* (1), 918.
- 16 Vuilleumier, P.; Decosterd, D.; Maillard, M.; Burnier, M.; Hayoz, D., Postischemic forearm skin reactive hyperemia is related to cardiovascular risk factors in a healthy female population. *Journal of hypertension* **2002**, *20* (9), 1753-7.
- 17 Cracowski, J. L.; Roustit, M., Local Thermal Hyperemia as a Tool to Investigate Human Skin Microcirculation. *Microcirculation* **2010**, *17* (2), 79-80.
- 18 Groot, H. J.; Trinity, J. D.; Layec, G.; Rossman, M. J.; Ives, S. J.; Morgan, D. E.; Bledsoe, A.; Richardson, R. S., The role of nitric oxide in passive leg movement-induced vasodilatation with age: insight from alterations in femoral perfusion pressure. *J Physiol* **2015**, *593* (17), 3917-28.
- 19 Treu, C. M.; Lupi, O.; Bottino, D. A.; Bouskela, E., Sidestream dark field imaging: the evolution of real-time visualization of cutaneous microcirculation and its potential application in dermatology. *Archives of dermatological research* **2011**, *303* (2), 69-78.
- 20 Zegelbone, P. M.; BAYBAYON-GRANDGEORGE, A.; Stauffer, B.; Sucharov, C.; Miyamoto, S.; Garcia, A. M., Abstract 8963: Mitochondrial Dysfunction in Peripheral Blood Mononuclear Cells is Associated With Heart Failure in Patients With Single Ventricle Congenital Heart Disease. *Circulation* **2021**, *144* (Suppl_1), A8963-A8963.
- 21 Altintas, M. M.; DiBartolo, S.; Tadros, L.; Samelko, B.; Wasse, H., Metabolic Changes in Peripheral Blood Mononuclear Cells Isolated From Patients With End Stage Renal Disease. *Front Endocrinol (Lausanne)* **2021**, *12*, 629239.
- 22 Ederlé, C.; Charles, A.-L.; Khayath, N.; Poirot, A.; Meyer, A.; Clere-Jehl, R.; Andres, E.; De Blay, F.; Geny, B., Mitochondrial Function in Peripheral Blood Mononuclear Cells (PBMC) Is Enhanced, Together with Increased Reactive Oxygen Species, in Severe Asthmatic Patients in Exacerbation. *Journal of Clinical Medicine* **2019**, *8* (10), 1613.
- 23 Lee, H.-T.; Lin, C.-S.; Pan, S.-C.; Wu, T.-H.; Lee, C.-S.; Chang, D.-M.; Tsai, C.-Y.; Wei, Y.-H., Alterations of oxygen consumption and extracellular acidification rates by glutamine in PBMCs of SLE patients. *Mitochondrion* **2019**, *44*, 65-74.
- 24 Pecina, P.; Houštková, H.; Mráček, T.; Pecinová, A.; Nůšková, H.; Tesařová, M.; Hansíková, H.; Janota, J.; Zeman, J.; Houštek, J., Noninvasive diagnostics of mitochondrial disorders in isolated lymphocytes with high resolution respirometry. *BBA Clinical* **2014**, *2*, 62-71.
- 25 Geng, X.; Zhang, Y.; Yan, J.; Chu, C.; Gao, F.; Jiang, Z.; Zhang, X.; Chen, Y.; Wei, X.; Feng, Y.; Lu, H.; Wang, C.; Zeng, F.; Jia, W., Mitochondrial DNA mutation m.3243A>G is associated with altered mitochondrial function in peripheral blood mononuclear cells, with heteroplasmy levels and with clinical phenotypes. *Diabetic Medicine* **2019**, *36* (6), 776-783.
- 26 Jiang, Z.; Zhang, Y.; Yan, J.; Li, F.; Geng, X.; Lu, H.; Wei, X.; Feng, Y.; Wang, C.; Jia, W., De Novo Mutation of m.3243A>G together with m.16093T>C Associated with Metaphical Clinical Features in a Pedigree with MIDD Syndrome. *Journal of Diabetes Research* **2019**, *2019*, 5184647.
- 27 Shepherd, R. K.; Checcarelli, N.; Naini, A.; De Vivo, D. C.; DiMauro, S.; Sue, C. M., Measurement of ATP production in mitochondrial disorders. *J Inherit Metab Dis* **2006**, *29* (1), 86-91.
- 28 Pek, N. M. Q.; Phua, Q. H.; Ho, B. X.; Pang, J. K. S.; Hor, J.-H.; An, O.; Yang, H. H.; Yu, Y.; Fan, Y.; Ng, S.-Y.; Soh, B.-S., Mitochondrial 3243A>G mutation confers pro-atherogenic and pro-inflammatory properties in MELAS IPS derived endothelial cells. *Cell Death & Disease* **2019**, *10* (11), 802.
- 29 Motlagh Scholle, L.; Schieffers, H.; Al-Robaity, S.; Thaele, A.; Dehghani, F.; Lehmann Urban, D.; Zierz, S., The Effect of Resveratrol on Mitochondrial Function in Myoblasts of Patients with the Common m.3243A>G Mutation. *Biomolecules* **2020**, *10* (8), 1103.
- 30 Klein Gunnewiek, T. M.; Van Hugte, E. J. H.; Frega, M.; Guardia, G. S.; Foreman, K.; Panneman, D.; Mossink, B.; Linda, K.; Keller, J. M.; Schubert, D.; Cassiman, D.; Rodenburg, R.; Vidal Folch, N.; Oglesbee, D.; Perales-Clemente, E.; Nelson, T. J.; Morava, E.; Nadif Kasri, N.; Kozicz, T., m.3243A > G-Induced Mitochondrial Dysfunction Impairs Human Neuronal Development and Reduces Neuronal Network Activity and Synchronicity. *Cell Reports* **2020**, *31* (3), 107538.
- 31 Mancuso, M.; Orsucci, D.; Angelini, C.; Bertini, E.; Carelli, V.; Comi, G. P.; Donati, A.; Minetti, C.; Moggio, M.; Mongini, T.; Servidei, S.; Tonin, P.; Toscano, A.; Uziel, G.; Bruno, C.; Ienco, E. C.; Filosto, M.; Lamperti, C.; Catteruccia, M.; Moroni, I.; Musumeci, O.; Pegoraro, E.; Ronchi, D.; Santorelli, F. M.; Sauchelli, D.; Scarpelli, M.; Sciacco, M.; Valentino, M. L.; Vercelli, L.; Zeviani, M.; Siciliano, G., The m.3243A>G mitochondrial DNA mutation and related phenotypes. A matter of gender? *Journal of neurology* **2014**, *261* (3), 504-10.
- 32 Ives, S. J.; Layec, G.; Hart, C. R.; Trinity, J. D.; Gifford, J. R.; Garten, R. S.; Witman, M. A. H.; Sorensen, J. R.; Richardson, R. S., Passive leg movement in chronic obstructive pulmonary disease: evidence of locomotor muscle vascular dysfunction. *J Appl Physiol* (1985) **2020**, *128* (5), 1402-1411.
- 33 Katulka, E. K.; Hirt, A. E.; Kirkman, D. L.; Edwards, D. G.; Witman, M. A. H., Altered vascular function in chronic kidney disease: evidence from passive leg movement. *Physiol Rep* **2019**, *7* (8), e14075.
- 34 Souza, E. G.; De Lorenzo, A.; Huguenin, G.; Oliveira, G. M.; Tibirica, E., Impairment of systemic microvascular endothelial and smooth muscle function in individuals with early-onset coronary artery disease: studies with laser speckle contrast imaging. *Coron Artery Dis* **2014**, *25* (1), 23-8.
- 35 Fujii, T.; Nozaki, F.; Saito, K.; Hayashi, A.; Nishigaki, Y.; Murayama, K.; Tanaka, M.; Koga, Y.; Hiejima, I.; Kumada, T., Efficacy of pyruvate therapy in patients with mitochondrial disease: a semi-quantitative clinical evaluation study. *Molecular genetics and metabolism* **2014**, *112* (2), 133-8.
- 36 Sharma, R.; Reinstadler, B.; Engelstad, K.; Skinner, O. S.; Stackowitz, E.; Haller, R. G.; Clish, C. B.; Pierce, K.; Walker, M. A.; Fryer, R.; Oglesbee, D.; Mao, X.; Shungu, D. C.; Khatri, A.; Hirano, M.; De Vivo, D. C.; Mootha, V. K., Circulating markers of NADH-reductive stress correlate with mitochondrial disease severity. *J Clin Invest* **2021**, *131* (2), e136055.
- 37 Lee, C. F.; Caudal, A.; Abell, L.; Nagana Gowda, G. A.; Tian, R., Targeting NAD+ Metabolism as Interventions for Mitochondrial Disease. *Scientific Reports* **2019**, *9* (1), 3073.
- 38 Khan, N. A.; Auranen, M.; Paetau, I.; Pirinen, E.; Euro, L.; Forsström, S.; Pasila, L.; Velagapudi, V.; Carroll, C. J.; Auwerx, J.; Suomalainen, A., Effective treatment of mitochondrial myopathy by nicotinamide riboside, a vitamin B3. *EMBO molecular medicine* **2014**, *6* (6), 721-31.
- 39 Chance, B.; Bank, W., Genetic disease of mitochondrial function evaluated by NMR and NIR spectroscopy of skeletal tissue. *Biochimica et Biophysica Acta (BBA) - Molecular Basis of Disease* **1995**, *1271* (1), 7-14.
- 40 Ryan, T. E.; Erickson, M. L.; Brizendine, J. T.; Young, H.-J.; McCully, K. K., Noninvasive evaluation of skeletal muscle mitochondrial capacity with near-infrared spectroscopy: correcting for blood volume changes. *Journal of Applied Physiology* **2012**, *113* (2), 175-183.

- 41 Hayashi, G.; Cortopassi, G., Oxidative stress in inherited mitochondrial diseases. *Free Radical Biology and Medicine* **2015**, *88*, 10-17.
- 42 Taivassalo, T.; Ayyad, K.; Haller, R. G., Increased capillaries in mitochondrial myopathy: implications for the regulation of oxygen delivery. *Brain : a journal of neurology* **2012**, *135* (Pt 1), 53-61.
- 43 Yu, B.-B.; Zhi, H.; Zhang, X.-Y.; Liang, J.-W.; He, J.; Su, C.; Xia, W.-H.; Zhang, G.-X.; Tao, J., Mitochondrial dysfunction-mediated decline in angiogenic capacity of endothelial progenitor cells is associated with capillary rarefaction in patients with hypertension via downregulation of CXCR4/JAK2/SIRT5 signaling. *eBioMedicine* **2019**, *42*, 64-75.
- 44 Grady, J. P.; Pickett, S. J.; Ng, Y. S.; Alston, C. L.; Blakely, E. L.; Hardy, S. A.; Feeney, C. L.; Bright, A. A.; Schaefer, A. M.; Gorman, G. S.; McNally, R. J.; Taylor, R. W.; Turnbull, D. M.; McFarland, R., mtDNA heteroplasmy level and copy number indicate disease burden in m.3243A>G mitochondrial disease. *EMBO molecular medicine* **2018**, *10* (6), e8262.
- 45 Zeng, Y.; David, J.; Rémond, D.; Dardevet, D.; Savary-Auzeloux, I.; Polakof, S., Peripheral Blood Mononuclear Cell Metabolism Acutely Adapted to Postprandial Transition and Mainly Reflected Metabolic Adipose Tissue Adaptations to a High-Fat Diet in Minipigs. *Nutrients* **2018**, *10* (11), 1816.
- 46 Walker, M. A.; Lareau, C. A.; Ludwig, L. S.; Karaa, A.; Sankaran, V. G.; Regev, A.; Mootha, V. K., Purifying Selection against Pathogenic Mitochondrial DNA in Human T Cells. *The New England journal of medicine* **2020**, *383* (16), 1556-1563.
- 47 van Poelgeest, E. P.; Dillingh, M. R.; de Kam, M.; Malone, K. E.; Kemper, M.; Stroes, E. S. G.; Burggraaf, J.; Moerland, M., Characterization of immune cell, endothelial, and renal responses upon experimental human endotoxemia. *J Pharmacol Toxicol Methods* **2018**, *89*, 39-46.
- 48 van Diemen, M. P. J.; Berends, C. L.; Akram, N.; Wezel, J.; Teeuwisse, W. M.; Mik, B. G.; Kan, H. E.; Webb, A.; Beenakker, J. W. M.; Groeneveld, G. J., Validation of a pharmacological model for mitochondrial dysfunction in healthy subjects using simvastatin: A randomized placebo-controlled proof-of-pharmacology study. *Eur J Pharmacol* **2017**, *815*, 290-297.
- 49 Rizzo, M. R.; Barbieri, M.; Marfella, R.; Paolisso, G., Reduction of oxidative stress and inflammation by blunting daily acute glucose fluctuations in patients with type 2 diabetes: role of dipeptidyl peptidase-IV inhibition. *Diabetes care* **2012**, *35* (10), 2076-82.
- 50 Yang, J.; Guo, Q.; Feng, X.; Liu, Y.; Zhou, Y., Mitochondrial Dysfunction in Cardiovascular Diseases: Potential Targets for Treatment. *Frontiers in cell and developmental biology* **2022**, *10*, 841523.

CHAPTER IV

A PHASE 1 RANDOMIZED, OPEN-LABEL CLINICAL TRIAL TO EVALUATE THE EFFECT OF A FAR-INFRARED EMITTING PATCH ON LOCAL SKIN PERFUSION, MICROCIRCULATION, AND OXYGENATION

Sebastian JW van Kraaij, MD,^{1,2} Michael R Hamblin, PhD,³ Gisele Pickering, MD, PhD,⁴
Bill Giannokopoulos, PharmMBA,⁵ Hayet Kechemir, MD,⁶ Moritz Heinz, MSc,⁶
Iva Igracki-Turudic, MD,⁷ Yalçın Yavuz, MSc,¹ Robert Rissmann, PhD,^{1,8} Pim Gal, MD, PhD^{1,2}

1: Centre for Human Drug Research, Leiden, NL

2: Leiden University Medical Centre, Leiden, NL

3: Laser Research Centre, Faculty of Health Science,
University of Johannesburg, Johannesburg, SA

4: Clinical Investigation Center CIC Inserm 1405;
University Hospital Clermont-Ferrand, Clermont-Ferrand, FR

5: Sanofi, CHC Science Hub, Athens, GR

6: Sanofi, Research & Development, Chilly-Mazarin, FR

7: Sanofi, CHC Science Hub, Frankfurt, D

8: Leiden Academic Centre for Drug Research, Leiden, NL

Abstract

Far-infrared radiation (FIR) has been investigated for reduction of pain and improvement of dermal blood flow. The FIRTECH patch is a medical device designed to re-emit FIR radiated by the body. This phase 1 study was conducted to evaluate the local effects of the FIRTECH patch on local skin perfusion, microcirculation, and oxygenation. This prospective, randomized, open-label, parallel designed study admitted 20 healthy participants to a medical research facility for treatment for 31 hours on three anatomical locations. During treatment, imaging assessments consisting of laser speckle contrast imaging (LSCI), near-infrared spectroscopy (NIRS), side-stream dark-field microscopy (SDFM), multispectral imaging (MSI), and thermography were conducted regularly on patch-treated skin and contralateral non-treated skin. The primary endpoint was baseline perfusion increase during treatment on the upper back. Secondary endpoints included change in baseline perfusion, oxygen consumption and temperature of treated versus untreated areas. The primary endpoint was not statistically significantly different between treated and non-treated areas. The secondary endpoints baseline perfusion on the forearm (least square means [LSMs] difference 2.63 PU, 95% CI: 0.97, 4.28), oxygen consumption (LSMs difference: 0.42 arbitrary units [AU], 95% CI: 0.04, 0.81) and skin temperature (LSMs difference 0.35 °C, 95% CI: 0.16, 0.6) were statistically significantly higher in treated areas. Adverse events observed during the study were mild and transient. The vascular response to the FIRTECH patch was short-lived suggesting a non-thermal vasodilatory effect of the patch. The FIRTECH patch was well tolerated, with mild and transient adverse events observed during the study. These results support the therapeutic potential of FIR in future investigations.

Introduction

Far infrared radiation (FIR) is radiation in the electromagnetic spectrum ranging between 3000 nm to 100 µm. This type of radiation has been the subject of investigation for its therapeutic benefits when delivered through various powered or non-powered modalities such as FIR-emitting bioceramics and belts, lamps and saunas.¹ Clinical and preclinical evidence point to FIR therapy exerting beneficial effects on cardiovascular and endothelial function by improving vascular endothelial function, increasing endothelial nitric oxide synthase activity and by increasing exercise tolerance,^{2,3} and it has been also found to have therapeutic benefits in acute and chronic pain conditions such as musculoskeletal pain.⁴⁻⁷ The mechanism of action of FIR is not yet fully known but vascular effects of FIR may be mediated through an increase in nitric oxide (NO) bioavailability and reduction in oxidative stress,⁸⁻¹¹ and improvement of mitochondrial function by FIR has also been shown *ex vivo*.^{12,13} Some effects of FIR may be due to heat associated with the absorption of the radiation, however FIR is known to induce the nuclear translocation of promyelocytic leukemia zinc finger protein in the cells, which affects microcirculation independently from thermal effects. Few studies have highlighted a significant and quickened wound healing process upon exposure to non-thermal FIR therapies that do not heat the skin but still seem to have therapeutic benefits.¹

The FIRTECH patch^o is a non-medicated thin medical device containing titanium dioxide dispersed in an adhesive layer. The FIRTECH patch is designed to absorb emitted body heat and re-emit this energy in the form of FIR. This mode of delivery of FIR is hypothesized to not heat the skin while exerting beneficial effects on local skin microcirculation, oxygenation, and mitochondrial function. Since studies with other FIR-emitting therapeutic modalities have shown promise in treatment of pain,^{5,6,14,15} the intended mode of action of the FIRTECH patch is to alleviate acute pain across various parts of the body such as joints, tendons, bones, and muscles (articular and musculoskeletal pain) by improving local microcirculation. Preclinical testing of the FIRTECH patch conducted in rabbits and guinea pigs showed the device to be safe and non-irritating. The present first-on-human clinical study aimed to elucidate the possible mechanisms of action of FIR re-emitted by the FIRTECH patch by evaluating the local effects of this patch on local perfusion, skin temperature and tissue oxygen consumption.

Methods

This study was conducted at a medical research facility in accordance with the principles of the Declaration of Helsinki, the International Conference on Harmonisation Good Clinical Practice, and ethical principles as referenced in EU Directive 2001/20/EC. The protocol was submitted and approved in accordance with European Union Medical Device Regulation, article 82. All volunteers provided written informed consent prior to any study-related activity. The trial was prospectively registered in [toetsingonline.nl](https://www.toetsingonline.nl) (NL77899.100.21, ABR number 77899).

SUBJECTS

Adult (age ≥ 18 and < 55 years) male and female participants were included if no clinically significant abnormal findings were found in the medical history, physical examination, 12-lead electrocardiogram (ECG), alcohol breathalyser, and clinical laboratory tests (i.e., serum chemistry, haematology, coagulation, urine drug screen, and urinalysis). Pregnant and nursing women were excluded from participation, as well as subjects using any type of medication (exception paracetamol/acetaminophen up to 4g/day) and subjects with body modifications or impediments for imaging on the locations where treatment with the study patch was planned.

STUDY DESIGN

This was a prospective, randomized, open-label, parallel designed study in which contralateral non-treated areas served as control for treated areas in the same subject. One cohort of 20 subjects received treatment with 3 FIRTECH patches for 31 hours, one located on the inner surface of the lower forearm on glabrous skin, one vertically placed on the lower back, and one vertically placed on the upper back. Subjects were body-site randomized to receive the FIRTECH patch (target treatment group) placed on either the left or right side of the body, and the same area on the opposite side of the body was used as control. Study assessments were performed through a 1x1cm 'window' cut in the patch which was folded up for assessing underlying skin and attached to the skin in between measurements.

STUDY ASSESSMENTS

SAFETY

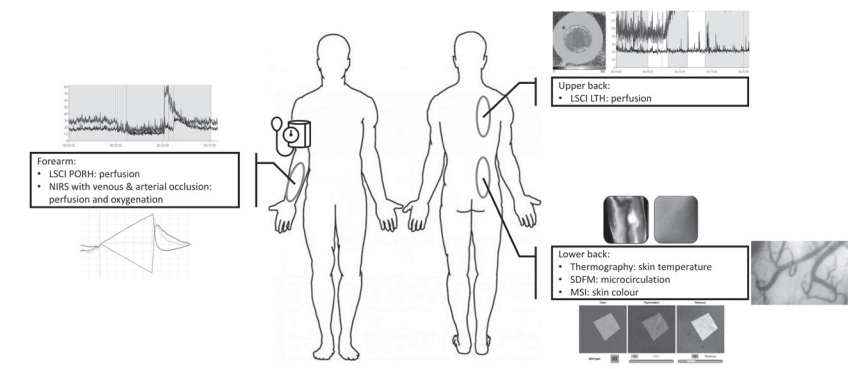
Safety assessments included monitoring of adverse events and concomitant medication use and measurement of vital signs. Adverse events were coded

using Medical Dictionary for Regulatory Activities (MedDRA) version 24.0 (March 2021). Vital signs were measured before treatment administration and at 1 h, 2 h, 4 h, 6 h, 8 h, 24 h, 27 h and 30 h after treatment administration.

PHARMACODYNAMIC ASSESSMENTS

Imaging assessments of local skin microcirculation were conducted at regular intervals on treated and contralateral non-treated sites, before treatment administration and at 1 h, 2 h, 4 h, 6 h, 8 h, 24 h, 27 h and 30 h after start of treatment. Imaging assessments were conducted on several locations with patches placed, as shown in Figure 1. Measurements were conducted in temperature-controlled rooms (20–24 °C) at the medical research facility. Study assessments conducted to evaluate microvascular function were laser speckle contrast imaging (LSCI), side-stream dark-field microscopy (SDFM), near-infrared spectroscopy (NIRS) multispectral imaging (MSI) and thermography.

FIGURE 1 Overview of measurements performed during study conduct and their locations.



LSCI=laser speckle contrast imaging; LTH=local thermal hyperemia; MSI=multispectral imaging; NIRS=near infrared spectroscopy; PORH=post-occlusive reactive hyperemia; SDFM=side-stream dark field microscopy. (see inside front cover for image in fullcolor)

LSCI is a non-invasive imaging method that uses changes in the speckle pattern reflection when illuminating an imaged object with laser light. Changes in the speckle pattern signify movement on or inside the imaged object. When imaging human tissue, the movement of blood cells causes changes in the speckle pattern which can be used to derive an estimation of blood flow in the imaged tissue.¹⁶ LSCI imaging was performed as a baseline measurement of blood flow

in treated and non-treated areas as well as in combination with two challenges (temporary occlusion and local hyperthermia) to assess microvascular responses in the imaged area. Post-occlusive reactive hyperaemia (PORH) was assessed in treated and non-treated areas on the arm. During this procedure, blood flow was temporarily occluded with a blood pressure cuff placed around the upper arm and then released. The subsequent increase in flow can be used as a measure of vascular reactivity to shear stress caused by the sudden influx of blood into the arm.¹⁷⁻¹⁹ Additionally, LSCI was combined with the local thermal hyperaemia (LTH) challenge, in which skin is heated to approximately 43 °C while continuously measuring blood flow. The skin blood flow response to heating can be used to assess neuronal and nitric-oxide dependent vascular reactivity.²⁰⁻²²

SDFM is a technique used to visualize blood vessels *in vivo* using light with a wavelength absorbed by red blood cells. Assessment of blood vessels in the skin was done after removing the top layer of the epidermis through tape stripping to allow penetration of light up to 0.5mm into the skin. SDFM imaging provided information on blood vessel density and perfusion.²³

NIRS was used to measure fractions of oxygenated and deoxygenated haemoglobin in treated and non-treated areas on the arm up to 3-4 cm deep. In combination with a venous and arterial occlusion challenge, NIRS allowed the quantification of tissue oxygen consumption, blood flow and vascular response to influx of blood in the arm.^{24,25}

MSI was used to measure skin colour and erythema. Colour was defined in the CIELAB colour space $L^*a^*b^*$, in which L^* represent lightness, a^* represents the green-red colour axis and b^* represents the blue-yellow axis. Lastly, thermography was used to assess changes in skin temperature on treated and non-treated sites.

STATISTICAL ANALYSIS

All statistical analyses were conducted according to a statistical analysis plan written before unblinding of the database.

SAFETY DATA

All subjects who received ≥ 1 FIRTECH patch treatment were included in the safety analyses. Treatment emergent adverse events (TEAEs) were summarised, and percentages calculated by treatment, System Organ Class, preferred term, severity, and study drug relatedness. Vital signs were summarised similarly, and number and percentage of out-of-range values calculated by treatment and

time point. Treatment exposure was calculated in minutes using patch application as start time and patch removal as end time and summarised with mean, standard deviation (SD), minimum, maximum and median treatment duration.

PHARMACODYNAMIC DATA

All subjects who received ≥ 1 FIRTECH patch treatment and underwent at least 1 physiological assessment after patch administration were included in the pharmacodynamic analyses. All repeatedly measured pharmacodynamic (PD) endpoints were summarized (n, mean, SD, standard error of mean [SEM], median, MIN and MAX values) by treatment and time. To establish whether significant treatment effects could be detected on the repeatedly measured pharmacodynamic endpoints, each endpoint was analysed with a mixed model analysis of covariance (ANCOVA) with treatment, time, treatment side and treatment by time as fixed factors, subject, subject by treatment and subject by time as random factors and the baseline measurement as covariate. Three contrasts were made in the model, namely patch versus no-patch over two days and at Day 1 only and at Day 2 only. Adjustment for multiple testing was done by using the following procedure:

- The p-value associated with the second primary endpoints (LSCI: absolute blood flow measurements during post occlusive reactive hyperemia challenges over two days) was interpreted in a confirmatory way only if the first primary endpoint (LSCI: absolute blood flow measurements during local thermal hyperemia challenges over two days) was statistically significant.
- The p-values associated with the main secondary endpoint (NIRS) were interpreted in a confirmatory way only if the primary objective was met and if the preceding endpoint as defined in the statistical analysis plan was met.
- The multiplicity of other secondary endpoints was handled using Benjamini-Hochberg controlling procedure in False Discovery Rate (FDR) approach, assuming FDR=10%, in case the primary and main secondary endpoint were met.

Results

SUBJECT DISPOSITION

A total of 20 subjects received the study treatment and completed the study period and follow-up, 10 treated on the right side of the body and 10 on the left. The median (min, max) of study treatment exposure was 1874.5 minutes on the left side (1863, 1886 minutes) and 1875 minutes on the right side (1819, 1886 minutes).

One subject lost one treatment patch on the back during the night from Study Day 1 to Day 2. A new patch was applied upon arrival of the subject on the study site on Study Day 2. Since the subject was without patch for a maximum of 8 hours, treatment exposure was at least 25/33 hours or 75% for this subject.

BASELINE CHARACTERISTICS

Baseline characteristics of treatment groups are presented in Table 1. All participants were healthy male (70%) or female (30%) volunteers of predominantly white ethnicity (80%).

TABLE 1 Baseline subject characteristics.

	Mean (SD)	Median	MIN	MAX
Age (years)	25.2 (7.3)	24	18	49
Height (cm)	180.48 (7.77)	181.3	163.0	194.5
Weight (kg)	73.64 (7.83)	76.28	54.20	85.45
BMI (kg/m ²)	22.64 (2.57)	22.5	18.4	28.9

BMI=body mass index; MAX=maximum; MIN=minimum; SD=standard deviation.

SAFETY DATA

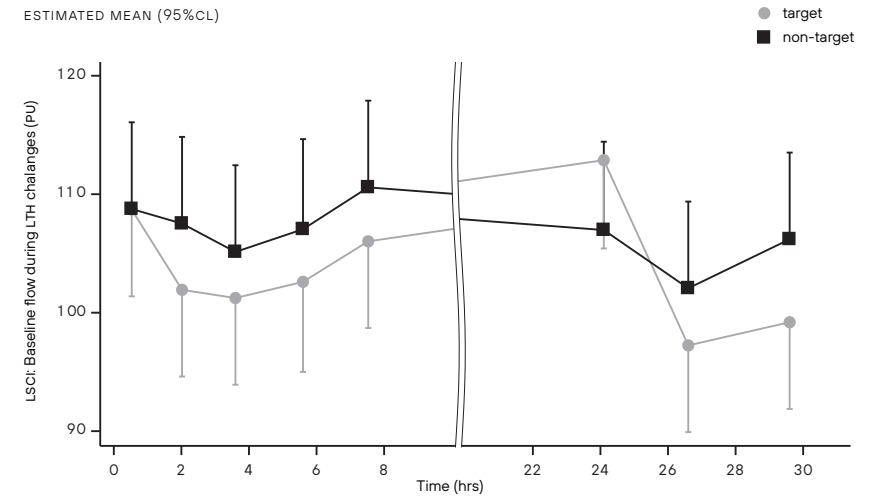
Data from 20 subjects were used for safety evaluation. No serious adverse events nor treatment discontinuations occurred. Observed TEAEs were mild, transient, and unlikely to be related to study treatment except one possibly related adverse event with MedDRA v24.0 preferred term 'eczema', which resolved spontaneously within one day. Vital signs evaluation showed no notable out-of-range values or changes during study treatment.

PHARMACODYNAMIC ANALYSES

LSCI

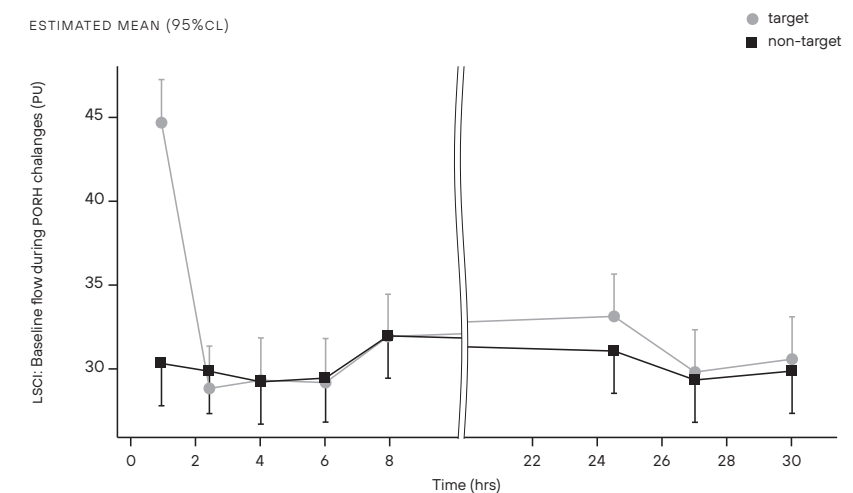
Baseline blood flow on the upper back measured with LSCI before initiating LTH was not statistically different between treated and non-treated areas (least squares means [LSMs] difference: -3.06 perfusion units (PU), 95% CI: -6.55, 0.44) (Figure 2). Due to the application of the hierarchical procedure, p-values of all other endpoints were interpreted exploratively. Due to the effects of the LTH technique, baseline flow was already increased before start of LTH challenges when compared to PORH measurements. Plateau and peak flow during heating was higher in the non-treated areas compared to the treated areas (LSMs: -4.02 vs -14.18 PU, LSMs difference -10.16 PU, 95% CI: -15.72, -4.59).

FIGURE 2 LSMs of absolute baseline blood flow before LTH challenges, measured using LSCI.



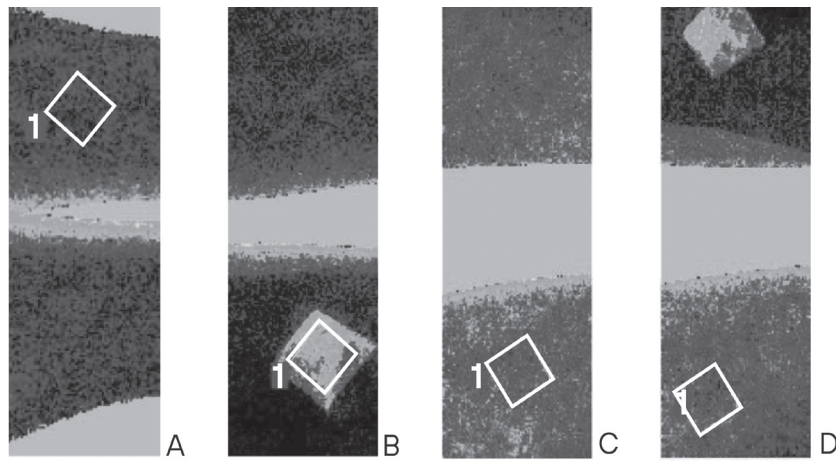
Differences between treated and non-treated areas LSMs were not statistically significant. CI=confidence interval; HRS=hours; LSCI=laser speckle contrast imaging; LSMs=least squares means; LTH=local thermal hyperemia; PU=perfusion units.

FIGURE 3 LSMs of absolute baseline blood flow before PORH challenges, measured using LSCI.



Increase in flow was observed higher in treated areas vs non-treated areas. CI=confidence interval; HRS=hours; LSCI=laser speckle contrast imaging; LSMs=least squares means; PORH=post-occlusive reactive hyperemia; PU=perfusion units.

FIGURE 4 Representative LSCI images of baseline flow before and after patch application for subject 4 (A, B) and 6 (C, D).



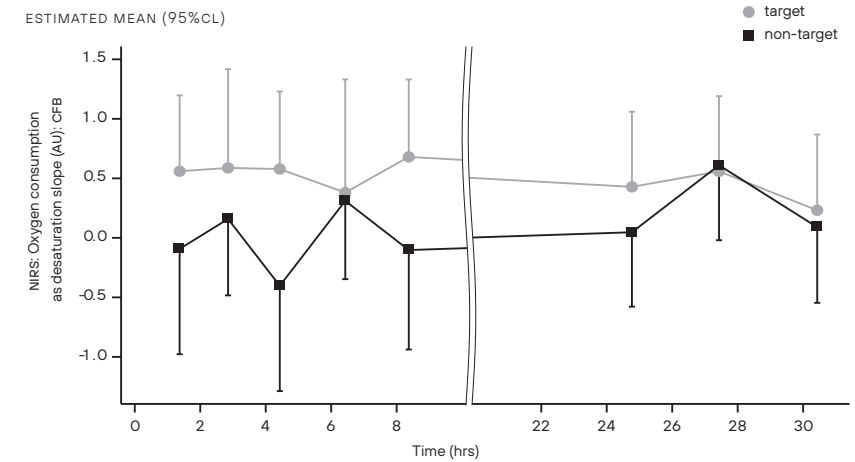
The window in the patch through which measurements were performed is shown in picture B and D (area marked with '1' in picture B). LSCI=laser speckle contrast imaging. (see inside back cover for image in fullcolor)

Baseline blood flow on the forearm measured before initiating PORH was overall higher in treated areas when compared to non-treated areas (LSMs difference: 2.05 PU, 95% CI: 0.54, 3.56) (Figure 3), owing to an approximately 50% higher perfusion in the treated areas (44.62 PU, SD: 17.31) versus non-treated areas (30.33 PU, SD: 5.12) at the first measurement post treatment administration, i.e., 30 minutes after starting treatment. Figure 4 shows an example of increased blood flow underneath the patch in two subjects. Peak blood flow after PORH was not significantly different between treated and non-treated areas (LSMs: 6.61 vs 5.66 PU, LSMs difference: 0.94 PU, 95% CI: -1.42, 3.30).

NIRS

Oxygen consumption was higher in treated areas on the forearm when compared to non-treated areas (LSMs difference 0.42 AU, 95% CI: 0.04, 0.81) (Figure 5). Other evaluated NIRS endpoints, including blood flow, duration of PORH and percent increase in blood flow after arterial occlusion did not differ significantly between treated and non-treated areas.

FIGURE 5 LSMs of CFB in oxygen consumption, measured with NIRS as desaturation slope during arterial occlusion.



Increase in oxygen consumption was observed higher in treated areas vs non-treated areas on Day 1. This difference was not significant on Day 2. AU=arbitrary units; CFB=change from baseline; CI=confidence interval; HRS=hours; LSMs=least squares means; NIRS=near infrared spectroscopy.

SDFM

There were no clinically or statistically significant effects of the patch on SDFM readouts on the lower back.

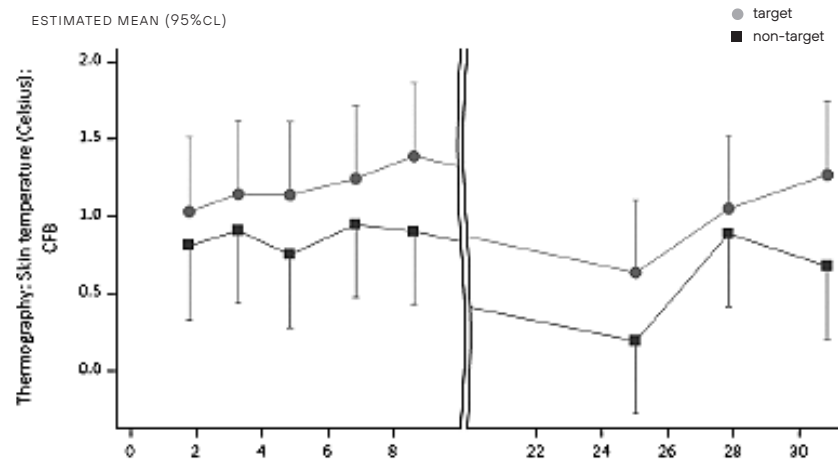
MSI

There were no clinically relevant differences between treated and non-treated areas as measured with MSI on the lower back. Specifically, no statistically significant differences in redness (LSMs difference 0.01, 95% CI: -0.27, 0.28) or haemoglobin content (LSMs difference -0.32, 95% CI: -1.13, 0.49) of the skin were found.

THERMOGRAPHY

Skin temperature was higher in treated areas on the lower back compared to non-treated areas (LSMs: +1.11 °C vs +0.76 °C, LSMs difference 0.35 °C, 95% CI: 0.15, 0.56) (Figure 6).

FIGURE 6 LSMs of CFB of absolute skin temperature in Celsius measured using thermography.



Temperature increased in both treated and non-treated sides, but numerically more in treated areas. CFB = change from baseline; CI = confidence interval; HRS = hours; LSMs = least squares means; SD = standard deviation.

Discussion

In the present first-on-human study, FIRTECH patch application was associated with a local increase in dermal blood flow, increased oxygen consumption and increased skin temperature, although the primary endpoint was not met. Dermal blood flow improved approximately 30 minutes post administration of treatment and returned to baseline after 2 hours, while oxygen consumption and skin temperature in treated areas remained elevated during the entire patch administration. In addition, the FIRTECH patch showed an excellent safety and tolerability profile. The FIRTECH patch thus has the potential to non-invasively modulate local microvascular function.

Previous literature has already reported the positive effects of FIR on the microvasculature, believed to be primarily mediated by the induction of local nitric oxide synthase expression and stimulation of this enzyme^{9,26,27} increasing local NO bioavailability and thereby local vasodilation. However, NO also exerts other beneficial effects, including anti-inflammatory and anti-analgesic. It is noteworthy that the vascular response that was observed in this study was generally

short-lived as opposed to the longer-lasting increase in skin temperature, suggesting a non-thermal effect of the FIRTECH patch immediately post application. Hypothetically, the short-lived nature of the effect might be caused by the induction of buffering mechanisms in the skin. In this case, local NO production is still increased, and non-vascular beneficial effects might extend beyond the vascular effects. This is supported by the observation that the NO-dependent plateau flow during LTH showed a decrease over time in treated areas, possibly owing to the increased local NO production creating a ceiling for the increase of blood flow by heating.

Increased resting oxygen consumption as measured with NIRS2^{8,29} on the forearm was observed in this study throughout the patch application duration. To date, evidence of the effects of FIR on oxygen consumption have been mixed, with some studies showing reduced oxygen uptake during exercise and others showing increases or no changes in oxygen consumption or concentration.^{30–33} *In vitro* and *in vivo* evidence however points towards FIR promoting mitochondrial function, thereby possibly leading to increased aerobic metabolism and oxygen consumption.^{12,13,34,35} The findings in this study indicate that the FIRTECH patch can increase oxygen consumption, hypothetically through increasing mitochondrial activity. Notably, results from the LSCI analysis showed a hypothetical lasting increase in NO availability, which is associated with decreased mitochondrial respiration.³⁶ The FIR effect increasing mitochondrial respiration was apparently greater than the possible negative effect on NO.

In our study, we also observed an effect of the FIRTECH patch on the local skin temperature. Potentially, this is caused by the FIR being reflected onto the skin, or the prevention of heat loss from the underlying skin by the fabric of the patch itself. This temperature increase possibly contributes to the measured increase in oxygen consumption, as well as an increase in blood flow.³⁷ Whether increasing the local skin temperature has beneficial effects on pain perception is not known, as this may be dependent on pain type.

For logistical reasons as well as to reduce subject burden, the imaging assessments in this study were performed on different locations, i.e., forearm, upper and lower back. Although measurements were compared to the same location on the other side of the body, it is possible that characteristics of skin on the various measurement sites influenced the ability of the imaging techniques to detect effects of the FIRTECH patch. However, epidermal thickness is comparable on the volar forearm and back,³⁸ as are stratum corneum thickness and skin roughness,³⁹ indicating comparability of skin characteristics. This

increases the likelihood that the observed differences are due to intra-individual variation, or that distinct physiological aspects of microcirculation were assessed by the employed imaging techniques and differed between the measurement sites.

Both improved blood flow⁴⁰ as well as improved mitochondrial function⁴¹ could be promising mechanisms in the treatment of various types of pain such as acute musculoskeletal pain since both mitochondrial dysfunction and reduced blood flow have been implicated in the development of various pain syndromes.⁴²⁻⁴⁴ Previous studies with infrared (IR) therapy have shown promise for its application in relieving a variety of pain conditions,^{6,15,45-47} and the present study further supports the physiological effects of treatment with FIR which could potentially be used in the treatment of pain.

STUDY LIMITATIONS

In this study, treatment with the FIRTECH patch was not compared to a placebo or mock patch, thereby introducing the possibility of a placebo effect as well as unblinding. However, the used assessments provide objective information on blood circulation and oxygenation on a microscopic level and are therefore not likely to have been affected by placebo effects. Since all materials re-emit IR to various degrees, the effects of the FIRTECH patch may not be limited to the ceramic particles, but also a result of the other components of the patch. Since it is not possible to manufacture a patch that is entirely IR inert, comparison to non-treated sites can be considered the most objective evaluation of IR effects.

CONCLUSION

The present study shows that the FIRTECH patch is a safe treatment with beneficial effects on both skin microcirculation and oxygen consumption which warrant further investigation of its efficacy.

REFERENCES

- 1 Vatansever F, Hamblin MR. Far infrared radiation (FIR): its biological effects and medical applications. *Photonics & Lasers in Medicine*. Nov 1 2012;4:255-266. doi:10.1515/plm-2012-0034
- 2 Sobajima M, Nozawa T, Ihori H, et al. Repeated sauna therapy improves myocardial perfusion in patients with chronically occluded coronary artery-related ischemia. *Int J Cardiol*. Jul 15 2013;167(1):237-43. doi:10.1016/j.ijcard.2011.12.064
- 3 Ohori T, Nozawa T, Ihori H, et al. Effect of repeated sauna treatment on exercise tolerance and endothelial function in patients with chronic heart failure. *The American journal of cardiology*. Jan 1 2012;109(1):100-4. doi:10.1016/j.amjcard.2011.08.014
- 4 Bagnato G, Miceli G, Atteritano M, Marino N, Bagnato G. Far infrared emitting plaster in knee osteoarthritis: a single blinded, randomised clinical trial. *Reumatismo*. 2012;64 6:388-94.
- 5 Ricci M, Micheloni GM, Perusi F, Corbo VR, Vecchini E, Magnan B. Use of a non-medicated plaster in shoulder tendinopathies. *Acta bio-medica : Atenei Parmensis*. Apr 15 2016;87 Suppl 1:90-4.
- 6 Lai YT, Chan HL, Lin SH, et al. Far-infrared ray patches relieve pain and improve skin sensitivity in myofascial pain syndrome: A double-blind randomized controlled study. *Complementary therapies in medicine*. Dec 2017;35:127-132. doi:10.1016/j.ctim.2017.10.007
- 7 Kyselovic J, Masarik J, Kechemir H, Koscova E, Turudic, II, Hamblin MR. Physical properties and biological effects of ceramic materials emitting infrared radiation for pain, muscular activity, and musculoskeletal conditions. *Photodermatology, photoimmunology & photomedicine*. May 5 2022;doi:10.1111/phpp.12799
- 8 Ikeda Y, Biro S, Kamogawa Y, et al. Repeated sauna therapy increases arterial endothelial nitric oxide synthase expression and nitric oxide production in cardiomyopathic hamsters. *Circulation journal : official journal of the Japanese Circulation Society*. Jun 2005;69(6):722-9. doi:10.1253/circj.69.722
- 9 Park JH, Lee S, Cho DH, Park YM, Kang DH, Jo I. Far-infrared radiation acutely increases nitric oxide production by increasing Ca(2+) mobilization and Ca(2+)/calmodulin-dependent protein kinase II-mediated phosphorylation of endothelial nitric oxide synthase at serine 1179. *Biochem Biophys Res Commun*. Jul 12 2013;436(4):601-6. doi:10.1016/j.bbrc.2013.06.003
- 10 Shui S, Wang X, Chiang JY, Zheng L. Far-infrared therapy for cardiovascular, autoimmune, and other chronic health problems: A systematic review. *Experimental biology and medicine (Maywood, NJ)*. Oct 2015;240(10):1257-65. doi:10.1177/1535370215573391
- 11 Masuda A, Miyata M, Kihara T, Minagoe S, Tei C. Repeated sauna therapy reduces urinary 8-epi-prostaglandin F(2alpha). *Japanese heart journal*. Mar 2004;45(2):297-303. doi:10.1536/jhj.45.297
- 12 Chang J-C, Wu S-L, Hoel F, et al. Far-infrared radiation protects viability in a cell model of Spinocerebellar Ataxia by preventing polyQ protein accumulation and improving mitochondrial function. *Scientific Reports*. 2016/07/29 2016;6(1):30436. doi:10.1038/srep30436
- 13 Seo Y, Kim YW, Lee D, et al. Far-infrared rays enhance mitochondrial biogenesis and GLUT3 expression under low glucose conditions in rat skeletal muscle cells. *The Korean journal of physiology & pharmacology : official journal of the Korean Physiological Society and the Korean Society of Pharmacology*. Mar 1 2021;25(2):167-175. doi:10.4196/kjpp.2021.25.2.167
- 14 Choi SJ, Cho EH, Jo HM, et al. Clinical utility of far-infrared therapy for improvement of vascular access blood flow and pain control in hemodialysis patients. *Kidney Res Clin Pract*. 2016;35(1):35-41. doi:10.1016/j.krcp.2015.12.001
- 15 Gur A, Cosut A, Sarac AJ, Cevik R, Nas K, Uyar A. Efficacy of different therapy regimes of low-power laser in painful osteoarthritis of the knee: a double-blind and randomized-controlled trial. *Lasers in surgery and medicine*. 2003;33(5):330-8. doi:10.1002/lsm.10236
- 16 Heeman W, Steenbergen W, van Dam G, Boerma EC. Clinical applications of laser speckle contrast imaging: a review. *Journal of biomedical optics*. Aug 2019;24(8):1-11. doi:10.1117/1.jbo.24.8.080901
- 17 Vuilleumier P, Decosterd D, Maillard M, Burnier M, Hayoz D. Postischemic forearm skin reactive hyperemia is related to cardiovascular risk factors in a healthy female population. *Journal of hypertension*. Sep 2002;20(9):1753-7. doi:10.1097/00004872-200209000-00018
- 18 Lorenzo S, Minson CT. Human cutaneous reactive hyperaemia: role of BKCa channels and sensory nerves. *J Physiol*. Nov 15 2007;585(Pt 1):295-303. doi:10.1113/jphysiol.2007.143867
- 19 Tee GBY, Rasool AHG, Halim AS, Rahman ARA. Dependence of human forearm skin postocclusive reactive hyperemia on occlusion time. *Journal of Pharmacological and Toxicological Methods*. 2004/07/01/ 2004;50(1):73-78. doi:https://doi.org/10.1016/j.vascn.2004.02.002
- 20 Kellogg DL, Jr. In vivo mechanisms of cutaneous vasodilation and vasoconstriction in humans during thermoregulatory challenges. *J Appl Physiol (1985)*. May 2006;100(5):1709-18. doi:10.1152/jappphysiol.01071.2005
- 21 Avery MR, Voegeli D, Byrne CD, Simpson DM, Clough GF. Age and cigarette smoking are independently associated with the

- cutaneous vascular response to local warming. *Microcirculation*. Nov 2009;16(8):725-34. doi:10.3109/10739680903199194
- 22 Cracowski JL, Roustit M. Local Thermal Hyperemia as a Tool to Investigate Human Skin Microcirculation. *Microcirculation*. 2010;17(2):79-80. doi:https://doi.org/10.1111/j.1549-8719.2009.00018.x
- 23 Treu CM, Lupi O, Bottino DA, Bouskela E. Sidestream dark field imaging: the evolution of real-time visualization of cutaneous microcirculation and its potential application in dermatology. *Archives of dermatological research*. Mar 2011;303(2):69-78. doi:10.1007/s00403-010-1087-7
- 24 Creteur J, Neves AP, Vincent J-L. Near-infrared spectroscopy technique to evaluate the effects of red blood cell transfusion on tissue oxygenation. *Critical Care*. 2009;11(30) 2009;13(5):S11. doi:10.1186/cc8009
- 25 Dennis JJ, Wiggins CC, Smith JR, et al. Measurement of muscle blood flow and O₂ uptake via near-infrared spectroscopy using a novel occlusion protocol. *Scientific Reports*. 2021/01/13 2021;11(1):918. doi:10.1038/s41598-020-79741-w
- 26 Hsu YH, Chen YC, Chen TH, et al. Far-infrared therapy induces the nuclear translocation of PLZF which inhibits VEGF-induced proliferation in human umbilical vein endothelial cells. *PLoS One*. 2012;7(1):e30674. doi:10.1371/journal.pone.0030674
- 27 Leung T-K, Lin Y-S, Chen Y-C, et al. Immunomodulatory effects of far-infrared ray irradiation via increasing calmodulin and nitric oxide production in raw 264.7 Macrophages. *Biomedical Engineering: Applications, Basis and Communications*. 2009/10/01 2009;21(05):317-323. doi:10.4015/S1016237209001404
- 28 Malagoni AM, Felisatti M, Mandini S, et al. Resting Muscle Oxygen Consumption by Near-Infrared Spectroscopy in Peripheral Arterial Disease: A Parameter to be Considered in a Clinical Setting? *Angiology*. 2010/08/01 2010;61(6):530-536. doi:10.1177/0003319710362975
- 29 Kao W-L, Sun C-W. Gender-Related Effect in Oxygenation Dynamics by Using Far-Infrared Intervention with Near-Infrared Spectroscopy Measurement: A Gender Differences Controlled Trial. *PLoS one*. 2015;10(11):e0135166-e0135166. doi:10.1371/journal.pone.0135166
- 30 Bontemps B, Gruet M, Vercruyssen F, Louis J. Utilisation of far infrared-emitting garments for optimising performance and recovery in sport: Real potential or new fad? A systematic review. *PLoS one*. 2021;16(5):e0251282-e0251282. doi:10.1371/journal.pone.0251282
- 31 Worobets JT, Skolnik ER, Stefanyshyn DJ. Apparel with Far Infrared Radiation for Decreasing an Athlete's Oxygen Consumption during Submaximal Exercise. *Research Journal of Textile and Apparel*. 2015;19(3):52-57. doi:10.1108/RJTA-19-03-2015-0007
- 32 Leung TK, Kuo CH, Lee CM, Kan NW, Hou CW. Physiological effects of bioceramic material: harvard step, resting metabolic rate and treadmill running assessments. *The Chinese journal of physiology*. Dec 31 2013;56(6):334-40. doi:10.4077/cjp.2013.bab132
- 33 Chuang KH, Chuang ML, Sia SK, Sun CW. Oxygenation dynamics of sepsis patients undergoing far-infrared intervention based on near-infrared spectroscopy. *Journal of biophotonics*. Mar 2017;10(3):360-366. doi:10.1002/jbio.201600147
- 34 Lagerwaard B, Nieuwenhuizen AG, de Boer VCJ, Keijer J. In vivo assessment of mitochondrial capacity using NIRS in locomotor muscles of young and elderly males with similar physical activity levels. *GeroScience*. Feb 2020;42(1):299-310. doi:10.1007/s11357-019-00145-4
- 35 Hsu Y-H, Chen Y-W, Cheng C-Y, Lee S-L, Chiu T-H, Chen C-H. Detecting the limits of the biological effects of far-infrared radiation on epithelial cells. *Scientific Reports*. 2019/08/12 2019;9(1):11586. doi:10.1038/s41598-019-48187-0
- 36 Moncada S, Erusalimsky JD. Does nitric oxide modulate mitochondrial energy generation and apoptosis? *Nature Reviews Molecular Cell Biology*. 2002/03/01 2002;3(3):214-220. doi:10.1038/nrm762
- 37 Brooks GA, Hittelman KJ, Faulkner JA, Beyer RE. Temperature, skeletal muscle mitochondrial functions, and oxygen debt. *American Journal of Physiology-Legacy Content*. 1971/04/01 1971;220(4):1053-1059. doi:10.1152/ajplegacy.1971.220.4.1053
- 38 Lintzeri DA, Karimian N, Blume-Peytavi U, Kottner J. Epidermal thickness in healthy humans: a systematic review and meta-analysis. *Journal of the European Academy of Dermatology and Venereology*. 2022;36(8):1191-200.
- 39 Maiti R, Duan M, Danby SG, Lewis R, Matcher SJ, Carré MJ. Morphological parametric mapping of 21 skin sites throughout the body using optical coherence tomography. *Journal of the Mechanical Behavior of Biomedical Materials*. 2020;102:103501.
- 40 Gordon R, Bloxham S. A Systematic Review of the Effects of Exercise and Physical Activity on Non-Specific Chronic Low Back Pain. *Healthcare (Basel, Switzerland)*. Apr 25 2016;4(2)doi:10.3390/healthcare4020022
- 41 Sui BD, Xu TQ, Liu JW, et al. Understanding the role of mitochondria in the pathogenesis of chronic pain. *Postgraduate medical journal*. Dec 2013;89(1058):709-14. doi:10.1136/postgradmedj-2012-131068
- 42 Meeus M, Nijs J, Hermans L, Goubert D, Calders P. The role of mitochondrial dysfunctions due to oxidative and nitrosative stress in the chronic pain or chronic fatigue syndromes and fibromyalgia patients: peripheral and central mechanisms as therapeutic targets? *Expert Opinion on Therapeutic Targets*. 2013/09/01 2013;17(9):1081-1089. doi:10.1517/14728222.2013.818657
- 43 Katz DL, Greene L, Ali A, Faridi Z. The pain of fibromyalgia syndrome is due to muscle hypoperfusion induced by regional vasomotor dysregulation. *Med Hypotheses*. 2007;69(3):517-25. doi:10.1016/j.mehy.2005.10.037
- 44 Flatters SJL. Chapter Five - The Contribution of Mitochondria to Sensory Processing and Pain. In: Price TJ, Dussor G, eds. *Progress in Molecular Biology and Translational Science*. Academic Press; 2015:119-146.
- 45 Gale GD, Rothbart PJ, Li Y. Infrared therapy for chronic low back pain: a randomized, controlled trial. *Pain research & management*. Autumn 2006;11(3):193-6. doi:10.1155/2006/876920
- 46 Ervolino F, Gazze R. Far infrared wavelength treatment for low back pain: Evaluation of a non-invasive device. *Work (Reading, Mass)*. 2015;53(1):157-62. doi:10.3233/wor-152152
- 47 Ke YM, Ou MC, Ho CK, Lin YS, Liu HY, Chang WA. Effects of somatothermal far-infrared ray on primary dysmenorrhea: a pilot study. *Evidence-based complementary and alternative medicine : eCAM*. 2012;2012:240314. doi:10.1155/2012/240314

CHAPTER V

FIRST-IN-HUMAN TRIAL TO ASSESS SAFETY, TOLERABILITY, PHARMACOKINETICS AND PHARMACODYNAMICS OF ZAGOCIGUAT (CY6463), A CNS-PENETRANT SOLUBLE GUANYLYL CYCLASE STIMULATOR

Sebastiaan JW van Kraaij, MD,^{1,2} Pim Gal, MD, PhD,^{1,2} Laura GJM Borghans, PhD,¹
Erica S Klaassen, MSc,¹ Francis Dijkstra, MD,^{1,2} Christopher Winrow, PhD,³
Chad Glasser, PharmD,³ Geert Jan Groeneveld, MD, PhD.^{1,2}

1: Centre for Human Drug Research, Leiden, NL

2: Leiden University Medical Centre, Leiden, NL

3: Cycleron Therapeutics, Cambridge, MA, USA.

Study highlights

WHAT IS THE CURRENT KNOWLEDGE ON THE TOPIC?

The NO-sGC-cGMP system is involved with memory formation and learning and has been a target for treatment of neurodegenerative disease in previous clinical trials. sGC stimulators can elevate cGMP concentrations in an NO-dependent manner. To our knowledge, no sGC stimulators have been shown to penetrate the central nervous system in humans thus far.

WHAT QUESTION DID THIS STUDY ADDRESS?

The present study investigated safety, PK and PD of zagociguat, a novel sGC stimulator.

WHAT DOES THIS STUDY ADD TO OUR KNOWLEDGE?

Single doses of zagociguat up to 50 mg and multiple doses up to 15 mg QD for 14 days were well tolerated with no safety signals, with dose-proportionally increasing exposure levels. Zagociguat showed pharmacodynamic effects on blood pressure consistent with the mechanism of action and effects of other sGC stimulators. Zagociguat penetrated the CSF compartment with a mean CSF/free plasma concentration ratio of 0.43.

HOW MIGHT THIS CHANGE CLINICAL PHARMACOLOGY OR TRANSLATIONAL SCIENCE?

Zagociguat is the first sGC stimulator shown to reach the cerebrospinal fluid compartment in humans, supporting its development as a compound for treating CNS diseases in which NO-sGC-cGMP is implicated.

Abstract

Soluble guanylyl cyclase (sGC) and its product, cyclic guanosine monophosphate play a role in learning and memory formation. Zagociguat (CY6463) is a novel stimulator of sGC being developed for the treatment of neurodegenerative disease. Single zagociguat doses of 0.3, 1, 3, 10, 20, 30 and 50 mg were administered once to healthy participants in a single-ascending-dose phase; then zagociguat 2, 5, 10 and 15 mg was administered QD for 14 days in a multiple-ascending-dose phase; and finally, zagociguat 10 mg was administered once in both fed and fasted state in a food-interaction phase. Safety of zagociguat was evaluated by monitoring treatment-emergent adverse events, suicide risk, vital signs, electrocardiography, and laboratory tests. Pharmacokinetics of zagociguat were assessed through blood, urine, and cerebrospinal fluid (CSF) sampling. Pharmacodynamic effects of zagociguat were evaluated with central nervous system (CNS) tests and pharmaco-electroencephalography. Zagociguat was well tolerated across all doses evaluated. Zagociguat exposures increased in a dose-proportional manner. Median T_{max} ranged from 0.8 h to 5 h and mean $T_{1/2}$ from 52.8 h to 67.1 h. CNS penetration of the compound was confirmed by CSF sampling. Zagociguat induced up to 6.1 mmHg reduction in mean systolic and up to 7.5 mmHg reduction in mean diastolic blood pressure. No consistent pharmacodynamic effects on neurocognitive function were observed. Zagociguat was well tolerated, CNS-penetrant and demonstrated pharmacodynamic activity consistent with other sGC stimulators. The results of this study support further development of zagociguat.

Introduction

A range of physiological processes are controlled by nitric oxide-soluble guanylyl cyclase-cyclic guanosine monophosphate (NO-sGC-cGMP) signaling.¹⁻³ In this pathway, NO, produced by nitric oxide synthases (NOS), activates sGC to produce cGMP, which produces various downstream effects.⁴ In the brain, the NO-sGC-cGMP pathway plays a central role in learning and memory through induction and expression of long-term potentiation, a form of synaptic plasticity that is pivotal in memory and learning,⁵ and numerous *in vitro* and *in vivo* preclinical studies confirm the role of this pathway in cognitive functioning.⁶⁻⁹ Dysfunction of the NO-sGC-cGMP pathway is implicated in neurodegenerative and other diseases and has been associated with a range of disruptive processes including increased inflammation, endothelial dysfunction, and dysregulation of cerebral blood flow.¹⁰⁻¹¹ In patients with Alzheimer's disease (AD), NOS activity and expression are decreased compared to healthy controls,¹² and decreased cGMP levels correlate with memory impairment.¹³⁻¹⁴ In addition, targeting the NO-sGC-cGMP axis via inhibition of degradation of cGMP by phosphodiesterases has shown therapeutic potential in the treatment of AD by improving markers of cognition.¹⁵⁻¹⁷ This evidence suggests that modulation of the NO-sGC-cGMP pathway is a promising approach for treatment of neurodegenerative diseases.^{4,18-20}

One therapeutic approach to increase NO-sGC-cGMP signalling in the brain is to stimulate sGC.²¹⁻²³ Preclinical studies with the CNS-penetrant sGC stimulator zagociguat (CY6463, 8-(2-fluorobenzyl)-6-(3-(trifluoromethyl)-1H-1,2,4-triazol-5-yl)imidazo[1,2-a]pyrazine)²⁴ showed that this compound can act as a positive allosteric modulator to stimulate cGMP production *in vitro* in an NO-dependent and concentration-responsive manner. *In vivo* experiments showed increases in cGMP concentrations in the CSF of treated rodents, confirming CNS penetration of the compound, as well as increased gamma band power as measured with quantitative electro-encephalography (QEEG), a characteristic that is associated with increased attention and focus.^{23,25} Additionally, in an *in vivo* rat model of cognitive impairment caused by administration of a non-competitive N-methyl-D-aspartate (NMDA) receptor antagonist, 0.1 mg/kg and 1 mg/kg zagociguat treatment attenuated deficits in learning and memory.²³ Finally, in a model of aged rats (21 months old) with cognitive impairment in learning as assessed by the Morris water maze, 1 mg/kg and 10 mg/kg zagociguat administration decreased thigmotaxis time compared to placebo, an indication of improved spatial learning. (data on file, CycLERion Therapeutics,

Cambridge, MA, USA) Since no sGC stimulators have been shown to be CNS-penetrant in humans and no sGC stimulators have been approved for treatment of CNS disease, zagociguat may be uniquely positioned for treatment of disorders associated with deficient NO-sGC-cGMP signalling in the brain, such as AD,²⁶ mitochondrial encephalopathy and lactic acidosis,²⁷ and cognitive impairment associated with schizophrenia.

In this study, the safety, pharmacokinetics (PK), and pharmacodynamics (PD) of zagociguat were evaluated in a first-in-human (FIH) trial in single-ascending-dose (SAD), multiple-ascending-dose (MAD), and crossover food-interaction (FI) settings.

Methods

This study was conducted at the Centre for Human Drug Research (Leiden, The Netherlands), in accordance with the principles of the Declaration of Helsinki, the International Council on Harmonisation Good Clinical Practice and ethical principles as referenced in EU Directive 2001/20/EC. The protocol was approved by the Medical Research Ethics Committee of the BEBO foundation (Assen, The Netherlands) and prospectively registered in EudraCT (number 2018-003694-99), toetsingonline.nl (CHDR1844, ABR-number 67677), and clinicaltrials.gov (NCT03856827).

SUBJECTS

Healthy male and female subjects aged ≥ 18 and < 65 years were eligible for inclusion in this FIH trial if no clinically significant abnormal findings were obtained on medical history, physical examination, 12-lead ECG, and laboratory tests (serum chemistry, haematology, coagulation, urine drug screen, and urinalysis). Pregnant and nursing women were excluded from participation, as well as subjects using any medication (exceptions were paracetamol/acetaminophen up to 4g/day, oral contraceptives, and hormone replacement therapy) and subjects with documented allergy or hypersensitivity to inactive compounds of the study drug formulation (tablets).

STUDY DESIGN

The first phase of the study was a double-blind, randomized, placebo-controlled SAD study. Seven cohorts of 8 subjects were planned to evaluate increasing dose levels of zagociguat, randomized in a 6:2 ratio to receive a single, oral dose

of zagociguat or placebo, respectively. Sentinel dosing was performed in all cohorts by randomizing the first 2 subjects to zagociguat or placebo (1 each) and dosing these subjects at least 24 h before the remainder of the cohort. The second phase was a double-blind, randomized, placebo-controlled MAD study with 4 cohorts of 10 subjects to evaluate increasing repeat-dose levels of zagociguat. Each cohort was randomized in a 4:1 ratio to receive once-daily, oral zagociguat or placebo for 14 days. The third phase was an open-label, randomized, 2-period, 2-treatment crossover FI study. Fourteen subjects were planned to receive 2 single doses of zagociguat, 1 in fasted and 1 in fed state. Subjects were randomized 1:1 to a fed-fasted or fasted-fed sequence with a 21-day washout in between. In the fed dosing period, subjects were administered study drug approximately 30 minutes after being served a high-fat meal (i.e., 800–1000 kcal total with approximately 150, 250, and 500 to 600 kcal derived from protein, carbohydrate, and fat, respectively). During the SAD and MAD phases, doses were administered after an overnight fast of at least 10 h. All doses were administered in tablet form.

The sample size for each stage of this phase 1 study was based on usual considerations regarding phase 1 studies of similar design aimed at obtaining initial information on safety, PK and PD effects.

DOSE LEVEL JUSTIFICATION

The 0.3 mg starting dose was based on 1/3 of the human equivalent dose (HED) of the lowest pharmacologically active dose observed in nonclinical QEEG assessments in rats,²³ in line with EMA recommendations. This dose was approximately 100-fold lower than the no-observed-adverse-event-level (NOAEL) HED observed in the 28-day good laboratory practice (GLP) toxicity study in the most sensitive species (rats), which was estimated to be 29 mg/subject/day, assuming a body weight of 60 kg, and was expected to result in 100-fold lower exposure. Subsequent dose levels were determined in dose escalation meetings based on safety, PK, and PD measurements from previous cohorts, using approximately log 0.5 exposure increases. These increases were slightly reduced when approaching the NOAEL, as this was the first exploration of a CNS penetrant compound with a plentiful pharmacological target in the brain. Final dose levels administered in the SAD phase of the study were 0.3 mg, 1 mg, 3 mg, 10 mg, 20 mg, 30 mg, and 50 mg. Although the 50 mg dose was predicted to exceed the NOAEL area under the curve (AUC), but not NOAEL maximum concentration (C_{max}) in the most sensitive species, since zagociguat was well tolerated in humans up to 30 mg, this dose level was added during study conduct.

The 2 mg starting dose for the MAD phase was chosen based on preliminary PK data showing an expected total exposure approximately twice the exposure of the 3 mg SAD cohort and lower than the exposure of the 10 mg SAD cohort, both of which showed no safety signals. Based on preliminary PK data from the SAD phase showing estimated steady state achieved at 11 days and $T_{1/2}$ supporting once daily (QD) dosing, the treatment regimen was set to 14 days QD. Subsequent dose levels were determined based on safety, PK, and PD data from the preceding SAD and MAD cohorts. Final dose levels administered were 2 mg, 5 mg, 10 mg and 15 mg in the MAD phase and 10 mg in the FI phase of the study.

STUDY ASSESSMENTS

SAFETY

Safety assessments during all phases of the study included standard FIH safety assessments, recording of adverse events (AES) and concomitant medication use, measurement of vital signs, electrocardiograms (ECG), physical examinations and safety laboratory tests. Given the potential blood pressure lowering mechanism of action of the compound, measurements of orthostatic blood pressure and continuous ECG monitoring (Holter) were also included in the safety assessments. In addition, since enhancement of NO-sGC-cGMP signalling may influence thrombocyte aggregation,²⁸ IVY bleeding time was monitored, and as the compound has potential CNS effects, the Columbia Suicide Severity Rating Scale was performed to assess any development of suicidality in participating subjects. Measurement of BP was assessed using the following procedure: BP was measured after 5 minutes of supine rest. Then, participants assumed sitting position for ≥ 1 minute and subsequently standing position for 1 to 3 minutes, and BP was measured to assess orthostasis, i.e. a systolic blood pressure (SBP) decrease of at least 20 mmHg or a diastolic blood pressure (DBP) decrease of at least 10 mmHg within three minutes of standing.²⁹ AES were coded according to the Medical Dictionary for Regulatory Activities version 21.1.

PHARMACOKINETIC ASSESSMENTS

PK sampling was performed prior to study drug administration and at timepoints 15 min, 30 min, 1 h, 2 h, 3 h, 4 h, 5 h, 6 h, 12 h, 24 h, and 48 h post study drug administration in the SAD phase. In the MAD phase, PK samples were collected daily before study drug administrations, and on treatment days 1 and 14 PK samples were collected on the same timepoints as in the SAD phase. In the FI phase, PK samples were obtained around study drug administration at the same timepoints

as in the SAD phase during both treatment periods. Additional PK samples were obtained 7 (\pm 1) and 14 (\pm 1) days post study drug administration in the first crossover period and 5 (\pm 1) and 9 (\pm 1) days post study drug administration in the second crossover period.

Urine was collected for 48 h after drug administration on day 1 in the SAD phase and for 24 h (i.e., 1 dosing interval) on days 1 and 14 in the MAD phase. A single CSF sample was obtained 3 h after drug administration on day 7 in cohort 3 (10 mg) of the MAD phase.

Quantification of zagociguat in plasma (in potassium ethylenediaminetetraacetic acid), urine, and CSF was conducted using a GLP-validated liquid chromatography with tandem mass spectrometry methods. Zagociguat was extracted using protein precipitation with an internal standard. (MM-501250) High-performance liquid chromatography separation was conducted at 0.7 mL/min through an ACE 50x2.1mm C18 column (Advanced Chromatography Technologies Ltd) using a gradient of 0.1% formic acid in water and in acetonitrile. The compound was detected using an API-5500 (Applied Biosystems/MDS SCIEX, Framingham, Massachusetts) in positive-ion mode, multiple reaction monitoring using parent/product transitions of 367.1/271.0 m/z for zagociguat and 367.1/271.0 m/z for the internal standard. The method for all 3 matrices was validated with a standard curve range of 1.00 to 1000 ng/mL, and linear peak area ratios were assessed with linear regression with $1/x^2$ weighting. Each analytical run included duplicate calibration curves, appropriate blanks, and triplicate quality controls at three concentrations. The inter-run accuracy and precision for plasma were -1.5 to 1.3 and 2.4 to 4.7, respectively, -3.0 to 3.0 and 2.0 to 4.0 for urine, respectively, and the accuracy for CSF was -2.3 to 4.0.

PHARMACODYNAMIC ASSESSMENTS

Vital signs were evaluated as both safety and PD endpoints.³⁰ In the SAD phase, BP and pulse rate were measured before study drug administration and at 30 min, 1 h, 2 h, 4 h, 6 h, 12 h, 24 h, and 48 h after administration, and orthostatic BP was assessed at the same timepoints as well as 24 h and 48 h after study drug administration. In the MAD phase, BP and pulse rate were measured before study drug administration on all treatment days and, on days 1, 2, and 14, were additionally collected 1 h, 2 h, 4 h, 6 h, and 12 h after study drug administration. Orthostatic BP was measured at 24 h and 48 h after the last study drug administration.

The CNS PD tests consisted of pharmaco-electroencephalography (PEEG) and a CNS test battery (NeuroCart®). PEEG was conducted using a 40-channel

recording system under vigilance-controlled conditions for 10 minutes per assessed timepoint employing alternating 64-second periods of eyes open and eyes closed. The CNS test battery included measurements of saccadic eye movement and smooth pursuit eye movements, body sway, adaptive tracking, Visual Verbal Learning test (VVLt), Milner Learning Maze Test (MMT), simple reaction time test, and choice reaction time test. These tests were chosen because they are sensitive to low doses of CNS-active agents.³¹ Eye movements, body sway, and reaction time tests have been used extensively to assess the CNS effects of sleep deprivation,³² alcohol,³³⁻³⁴ and benzodiazepines.³⁵⁻³⁷ Adaptive tracking testing according to Borland and Nicholson³⁸ was conducted to assess zagociguat effects on visuo-motor coordination and vigilance, while MMT was used to assess spatial working memory,³⁹ and VVLt to assess acquisition and consolidation of information, active retrieval from long-term memory, and memory storage using respectively immediate recall, delayed recall, and delayed recognition tasks.⁴⁰⁻⁴² To avoid learning effects during the study, subjects were familiarized with the tests during a training session within 21 days prior to admission to the clinic. In the SAD phase, the CNS assessments including PEEG but excluding VVLt were conducted twice before study drug administration and at 2 h, 4 h, 6 h, 10 h, and 24 h after administration. In the MAD phase, CNS tests including PEEG but excluding VVLt were conducted before study drug administration on day 1 and 14, and at 1 h, 5 h, and 10 h after administration on these days. On day 1, 13 and 15, CNS tests were performed at approximately T_{max} (90 min). VVLt was conducted at 2.5 h (immediate recall) and 3.5 h (delayed recall) after study drug administration in the SAD phase, and at 2 h (immediate recall) and 2.5 h (delayed recall) after study drug administration on day 1 and 14 in the MAD phase.

STATISTICAL ANALYSIS

All statistical analyses were conducted according to a statistical analysis plan written before unblinding of treatment allocation. All safety and statistical programming was conducted using SAS 9.4 for Windows (SAS Institute Inc., Cary, NC, USA), with non-compartmental analysis done using Phoenix WinNonlin version 8.1 (Certara USA, Inc., Princeton, NJ, USA).

ANALYSIS OF SAFETY DATA

All subjects who received ≥ 1 dose of study drug were included in the safety analyses. Treatment-emergent AES (TEAES) were summarized, and percentages

calculated by treatment, system organ class, preferred term, severity, and study drug-relatedness. ECG, safety laboratory results, and vital signs were summarized similarly. The number and percentage of out-of-range values were calculated by treatment and time point.

ANALYSIS OF PK DATA

All subjects who received ≥ 1 dose of zagociguat and had ≥ 1 post dose PK assessment were included in the PK analyses. In the SAD, AUC until last PK sample (AUC_{last}), C_{max} , and time to maximum concentration (T_{max}) were calculated for dose levels 0.3 mg, 1.0 mg, and 3.0 mg. For the subsequent dose levels these parameters plus AUC extrapolated to infinity (AUC_{inf}), total clearance (CL/F), and terminal elimination half-time ($T_{1/2}$) were calculated. The excreted amount of zagociguat, both absolute (AE_{last}) and as a percentage of plasma concentrations ($AE_{last}\%$), as well as renal clearance (CLR) were calculated from urine data. In the MAD phase, the C_{max} , T_{max} , and $T_{1/2}$ were calculated, as well as the AUC during one dosing interval (AUC_T), trough concentration (C_{trough}), peak-to-trough ratio (PTR), and accumulation ratios based on AUCS (R_{AUC}), maximum concentrations (R_{max}), and trough concentrations (R_{trough}). The same urine PK parameters calculated in the SAD were calculated per dosing interval in the MAD. For CSF PK, ratio between plasma and CSF concentration was calculated (R_{CSF}) and corrected for protein binding ($R_{CSF-free}$). In *in vitro* experiments, the mean percentage of protein-bound zagociguat (1 and 10 μM) was 97.27%, 98.47%, 96.71%, 98.69%, and 98.89% in mouse, rat, dog, monkey, and human plasma, respectively, determined using equilibrium dialysis method. (data on file, Cyclerion Therapeutics, Cambridge, MA, USA) Hence, to calculate the ratio between concentration in the CSF and the unbound concentration in plasma, it was assumed that the free zagociguat concentration in human plasma was 1.11% of total zagociguat concentration in plasma. All PK parameters were expressed as geometric means with 95% confidence intervals (CI) and medians with minimum and maximum values.

Dose proportionality was calculated using log transformed AUC_{last} , AUC_{inf} , and C_{max} for the SAD phase and using AUC_T and C_{max} for day 1 and day 14 for the MAD phase. Above PK parameters were fitted to a regression model and resulting slope estimates compared to a pre-specified critical interval of 0.5 to 2.0.⁴³ Steady state analysis was performed by calculating Helmert contrasts between subsequent trough concentrations until the contrast was not statistically significant.⁴⁴ Food effects were assessed by comparing C_{max} , AUC_T, and

AUC_{inf} in the fed and fasted state using an analysis of variance model with food condition, sequence and period as fixed effects and subject within sequence as a random effect.

ANALYSIS OF PD DATA

All repeatedly measured PD parameters were summarized (n, mean, SD, SEM, median, minimum, and maximum values) by treatment and time, while single measured PD variables were only summarized by treatment. Treatment effects on PD variables, pulse rate, and BP were assessed using an analysis of covariance model with fixed factors treatment, time, and treatment by time, random factor subject and the average of the value before drug administration were used as covariates. From these models estimated differences, the least square mean (LSM) estimates, and the p-value were calculated. Differences between zagociguat and placebo for each dose level were calculated both pooled and for each dose level, and for both day 1 and day 14 in the MAD phase.

Results

SUBJECT DISPOSITION

In the SAD phase, 56/56 planned subjects received study drug and completed the study, of which 42 received zagociguat and 14 placebo. In the MAD phase, 40 subjects received at least 1 dose of study drug, of which 32 received zagociguat and 8 placebo. 38 subjects completed the MAD phase; 1 subject dropped out due to non-study related reasons after 1 dose of zagociguat (10 mg), and 1 subject was lost to follow-up after completion of 14-day zagociguat (2 mg) treatment. Study drug (placebo) was discontinued in 1 subject on day 10 due to a liver enzyme elevation. This subject completed study assessments including follow-up as planned. In the FI phase, 13/14 subjects who received study drug completed both treatment periods while 1 subject dropped out after the 1st treatment period due to non-study related reasons.

BASELINE STATISTICS

No remarkable differences in age, height, weight, or BMI were noted between study cohorts in any phases of the study (Table S1). Sex distribution was also similar across the SAD and FI phases but in the MAD phase, the percentage of male subjects in the placebo group was 100% compared to 37.50-75% across the zagociguat groups.

SAFETY DATA

No deaths or other serious AES were observed. Paracetamol was occasionally used as concomitant medication for headache or malaise. Across all study phases, observed TEAES were mild and transient. An overview of TEAES across study phases is provided in Table 1.

TABLE 1 Overview of TEAES across study phases.

SAD Dose level	TEAES, n	Subjects with ≥ 1 TEAE, n (%)	Subjects with ≥ 1 study drug related TEAE, n	Subjects with ≥ 1 SAE, n	Subjects discontinued from study drug due to ≥ 1 TEAE, n
0.3 mg (n=6)	5	2 (33.3%)	2	0	0
1 mg (n=6)	5	2 (33.3%)	1	0	0
3 mg (n=6)	7	3 (50.0%)	2	0	0
10 mg (n=6)	7	2 (33.3%)	2	0	0
20 mg (n=6)	5	3 (50.0%)	2	0	0
30 mg (n=6)	13	5 (83.3%)	5	0	0
50 mg (n=6)	15	5 (83.3%)	3	0	0
Pooled Zagociguat group (n=42)	57	22 (52.4%)	17	0	0
Placebo (n=14)	11	9 (64.3%)	6	0	0
MAD Dose Level					
2 mg (n=8)	17	6 (75%)	6	0	0
5 mg (n=8)	27	8 (100%)	7	0	0
10 mg (n=8)	19	8 (100%)	5	0	0
15 mg (n=8)	18	7 (87.5%)	5	0	0
Pooled Zagociguat group (n=32)	81	29 (90.1%)	23	0	0
Placebo (n=8)	13	7 (87.5%)	6	0	1
FI Sequence					
10mg Fed-Fasted (n=7)	7	5 (35.7%)	1	0	0
10mg Fasted-Fed (n=7)	7	4 (30.8%)	2	0	0

FI=food interaction; MAD=multiple ascending dose; SAD=single ascending dose; SAE=serious adverse event; TEAE=treatment emergent adverse event.

SAD PHASE

The overall incidence of TEAES was lower in the pooled zagociguat group (22/42 subjects, 52.4%) than in the placebo group (9/14 subjects, 64.3%). A greater number of subjects experienced ≥ 1 TEAE in the groups with the higher zagociguat dosages of 30 mg (5/6 subjects, 83.3%) and 50 mg (5/6 subjects, 83.3%) when compared with the 0.3, 1, 3, 10 and 20 mg dose groups (range of 2/6 (33.3%) to 3/6 subjects (50%)). For all zagociguat treated subjects, 8/42 subjects (19.0%)

experienced at least 1 dizziness TEAE, compared to 0 subjects in the placebo group. One orthostatic hypotension TEAE was reported in a subject who received 3 mg zagociguat. Gastro-intestinal (GI)-related TEAES were reported more frequently in zagociguat groups (1/6 subjects, 16.7%, all cohorts except 50 mg, 4/6 subjects, 66.7%) when compared with placebo (1/14 subjects, 7.1%) (Table S2). No clinically relevant abnormalities were seen in safety laboratory tests (including IVY bleeding time), vital signs measurements, and ECG analysis (including safety Holter).

MAD PHASE

Comparable overall percentages of subjects with TEAES were seen across treatment groups and compared with placebo (Table S3). Two subjects in the 2 mg, 5 mg, and 15 mg zagociguat groups and 5 subjects in the 10 mg group experienced GI TEAES, compared to 0 subjects in the placebo group. Postural dizziness was observed in 1 subject who received 5 mg zagociguat. One subject in the 2 mg, 5 mg, and 10 mg zagociguat group each reported a non-postural dizziness TEAE, compared to 0 subjects in the placebo group. No orthostatic hypotension events were reported.

Two subjects experienced mild increases in liver enzymes. For one subject, this manifested after 10 placebo administrations (peak AST 53 U/L [normal range <35 U/L], ALT 97 U/L [normal range <45 U/L], GGT 25 U/L [normal range <55 U/L]). The subject was subsequently withdrawn from dosing. At follow-up, liver enzyme elevation was resolving (AST 34 U/L, ALT 49 U/L, GGT 19 U/L). The second subject developed liver enzyme elevation on day 6 of 2 mg zagociguat QD. Liver enzyme elevation peaked after the last dose of zagociguat (day 16, AST 49 U/L, ALT 92 U/L, GGT 22 U/L). Upon follow-up on day 30, liver enzymes were decreasing (AST 43 U/L, ALT 49 U/L, GGT 23 U/L). Review of all other safety laboratory parameters (including IVY bleeding time), vital signs, and ECG analysis (safety Holter) revealed no other clinically significant changes.

FI PHASE

A comparable number of subjects experienced ≥ 1 TEAE under fasted (n=5/14, 35.7%) and fed conditions (n=4/13, 30.8%) (Table S4). Three subjects had dizziness TEAES: 2 different subjects experienced respectively postural and non-postural dizziness during the fasted condition, while another subject experienced both a non-postural and separate postural dizziness event during the fed condition. No orthostatic hypotension events were recorded.

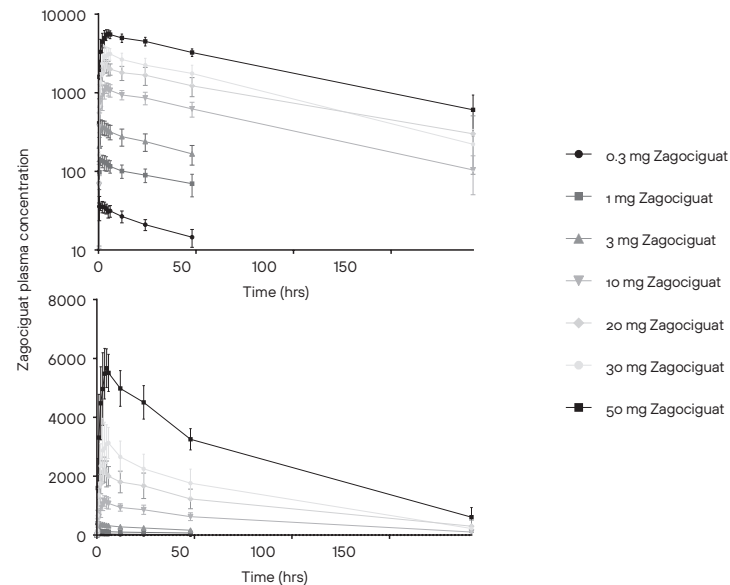
PHARMACOKINETIC ANALYSES

Data from 42 subjects in the SAD phase, 32 subjects in the MAD phase, and 14 subjects in FI phase were included in PK analyses.

SAD PHASE

Mean zagociguat concentrations in plasma up to 192 h post administration in the SAD phase are shown in Figure 1. A summary of PK parameters across cohorts is given in Table 2. Mean terminal $T_{1/2}$ ranged between 57 and 68 hr after single administrations of 10 to 50 mg. Zagociguat was absorbed more rapidly at doses of 0.3 to 3 mg (median T_{max} 0.5 - 2.1 hr) than at doses of 10 to 50 mg (3.5 to 5 hr), and a dose-linear increase in C_{max} and AUC after single doses of 0.3 to 50 mg zagociguat was observed. Zagociguat was detectable in urine from the 10 mg dose level, with a low percentage of dose administered excreted in urine (median 0.01% - 0.02%). Dose linearity analysis using AUC_T and C_{max} indicated dose proportionality (Table S5).

FIGURE 1 Mean (SD) zagociguat concentration in plasma (ng/mL) (top: semi-log scale, bottom: linear scale) on Day 1 during the SAD phase.



First dose is at protocol time=0. Concentrations below limit of quantification (1.00 ng/mL) were set to 0. SAD=single ascending dose; SD=standard deviation.

TABLE 2 Summary of Plasma and CSF PK Parameters of Zagociguat-SAD Phase.

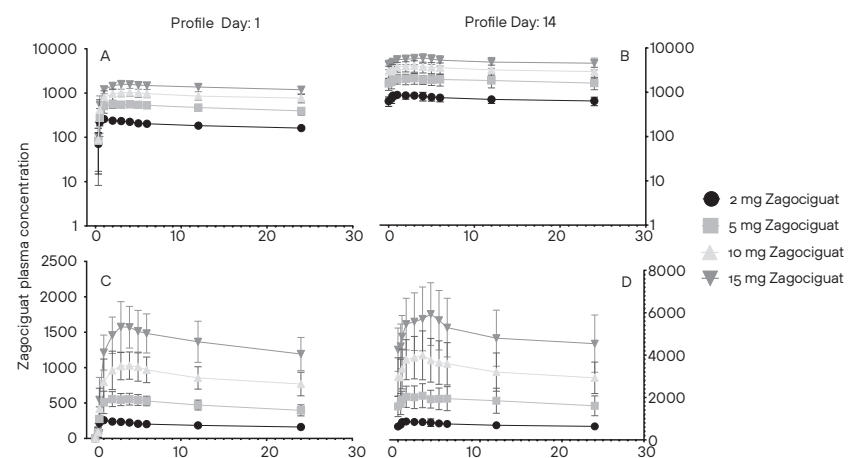
Treatment	Parameter	N	GEOMEAN	95% CI (lower, upper)	Median	MIN	MAX
0.3 mg	C_{max} (ng/mL)	6	39.95	33.55, 47.58	40.45	31.70	50.70
	T_{max} (h)	6			0.8	0.5	4.0
	AUC_{last} (h*ng/mL)	6	1062	885, 1275	1087	844	1291
1 mg	C_{max} (ng/mL)	8	142.46	123.75, 164.00	150.00	114.00	161.00
	T_{max} (h)	8			1.0	0.5	3.0
	AUC_{last} (h*ng/mL)	8	4337	3497, 5377	4456	3264	5456
3 mg	C_{max} (ng/mL)	8	372.93	292.01, 476.27	372.00	285.00	514.00
	T_{max} (h)	8			2.1	0.5	4.0
	AUC_{last} (h*ng/mL)	8	11381	9031, 14342	11220	8785	16427
10 mg	C_{max} (ng/mL)	6	1190.17	999.97, 1416.55	1290.00	889.00	1340.00
	T_{max} (h)	6			3.5	3.0	6.0
	$T_{1/2}$ (h)	3	63.4	29.1, 138.3	64.8	45.8	85.8
	AUC_{inf} (h*ng/mL)	3	92293	55049, 154736	95039	73984	111808
	AUC_{last} (h*ng/mL)	6	57602	37016, 89639	57922	32439	103436
20 mg	C_{max} (ng/mL)	6	2191.70	1783.28, 2693.65	2265.00	1690.00	2730.00
	T_{max} (h)	6			4.0	3.0	4.0
	$T_{1/2}$ (h)	6	67.1	54.44, 82.8	68.0	50.4	88.9
	AUC_{inf} (h*ng/mL)	6	194329	132134, 285800	180286	112219	313840
	AUC_{last} (h*ng/mL)	6	166913	122796, 226878	158060	109973	237435
30 mg	C_{max} (ng/mL)	6	3365.05	2703.22, 4188.91	3650.00	2270.00	3950.00
	T_{max} (h)	6			4.5	3.0	6.0
	$T_{1/2}$ (h)	6	65.7	46.7, 92.4	62.2	42.0	101.8
	AUC_{inf} (h*ng/mL)	6	271998	181509, 407599	288299	171361	492575
	AUC_{last} (h*ng/mL)	6	251099	171612, 367296	273032	156449	425747
50 mg	C_{max} (ng/mL)	6	5727.44	5033.81, 6516.64	5815.00	4820.00	6680.00
	T_{max} (h)	6			5.0	4.0	6.0
	$T_{1/2}$ (h)	6	57.0	46.4, 70.0	57.3	45.5	74.5
	AUC_{inf} (h*ng/mL)	6	478098	412224, 554497	471151	413139	604738
	AUC_{last} (h*ng/mL)	6	424802	374171, 482284	427283	344645	498002

AUC_{inf} =area under concentration-time the curve from time zero to infinity; AUC_{last} =area under the concentration-time curve from time zero to last measurable concentration; CI=confidence interval; C_{max} =maximum concentration, CSF=cerebrospinal fluid; GEOMEAN=geometric mean; N=Number of subjects; MAX=maximum; MIN=minimum; PK=pharmacokinetic; SAD=single ascending dose; SD=standard deviation; $T_{1/2}$ = Apparent terminal phase half-life; T_{max} =time of maximum concentration.

MAD PHASE

Mean zagociguat concentrations in plasma on day 1 and 14 of are shown in Figure 2. A summary of PK parameters across cohorts is given in Table 3. Mean PTR ranged from 1.35 (15 mg cohort, day 14) to 1.62 (2 mg cohort, day 1), indicating $T_{1/2}$ longer than the dosing interval (>24 h), and median observed T_{max} ranged from 1 to 3.5 h. CSF samples showed a mean CSF/free plasma concentration ratio of 0.43. Zagociguat was detectable in urine from the 2 mg dose level onwards, and as in the SAD phase a very low percentage of administered zagociguat was excreted in urine (median 0.00% - 0.04%). Dose linearity analysis using AUC_T and C_{max} indicated dose proportionality both on day 1 and day 14 (Table S6). Steady state analysis showed that for all doses administered, steady state was attained on day 11.

FIGURE 2 Mean (SD) zagociguat concentration in plasma (ng/mL) (A and B: semi-log scale, C and D: linear scale) on Day 1 (A and C) and Day 14 (B and D) during the MAD phase.



First dose is at protocol time=0. Concentrations below limit of quantification (1.00 ng/mL) were set to 0. MAD= multiple ascending dose; SD=standard deviation.

TABLE 3 Summary of Plasma and CSF PK Parameters of Zagociguat-MAD Phase (Days 1 and 14).

Treatment	Parameter	Day	N	GEOMEAN	95% CI (lower, upper)	Median	MIN	MAX
2 mg	C_{max} (ng/mL)	1	8	260.40	243.42, 278.56	268	224	282
		14	8	879.83	771.21, 1003.75	888	704	1170
	T_{max} (h)	1	8			1.0	0.5	2.0
		14	8			1.0	0.5	4.0
	$T_{1/2-eff}$ (h)		8	54.60	43.60, 68.37	54.46	42.63	66.67
	AUC_T (h*ng/mL)	1	8	4500	4209, 4812	4524	4067	5201
		14	8	16895	14508, 19674	16960	12894	23549
	CTROUGH (ng/mL)	1	8	161.13	149.10, 174.13	157.0	147	192
		11	8	587.49	484.50, 712.38	579.0	407	911
		12	8	593.32	491.16, 716.74	584.0	427	911
13		8	616.39	510.84, 743.74	609.5	439	938	
14		8	624.08	524.04, 743.20	631.5	454	914	
PTR	1	8	1.62	1.54, 1.70	1.64	1.47	1.77	
	14	8	1.41	1.34, 1.48	1.40	1.28	1.55	
R_{auc}		8	3.75	3.37, 4.18	3.80	3.09	4.53	
R_{max}		8	3.38	3.09, 3.70	3.32	2.9	4.15	
RTHROUGH		8	3.87	3.40, 4.41	4.06	3.09	4.76	
5 mg	C_{max} (ng/mL)	1	8	601.97	535.60, 676.56	597	464	707
		14	8	2079.08	1661.53, 2601.56	2230	1230	2950
	T_{max} (h)	1	8			2.0	1.0	5.0
		14	8			3.0	0.6	3.0
	$T_{1/2-eff}$ (h)		8	54.60	43.60, 68.37	56.63	32.27	83.04
	AUC_T (h*ng/mL)	1	8	11004	9597, 12517	11488	8329	12874
		14	8	42085	32189, 55024	43934	22299	64599
	CTROUGH (ng/mL)	1	8	389.14	325.85, 464.71	410.5	267	482
		11	8	1478.18	1110.15, 1968.22	1545.0	781	2380
		12	8	1495.10	1143.49, 1954.82	1575.0	785	2260
13		8	1507.11	1125.74, 2017.68	1580.0	740	2290	
14		8	1539.88	1167.04, 2031.84	1635.0	778	2350	
PTR	1	8	1.55	1.39, 1.72	1.50	1.37	2.05	
	14	8	1.35	1.27, 1.43	1.34	1.26	1.58	
R_{auc}		8	3.83	3.17, 4.62	3.93	2.48	5.51	
R_{max}		8	3.45	2.88, 4.15	3.56	2.24	4.89	
RTHROUGH		8	3.98	3.41, 4.59	3.79	2.91	5.33	
10 mg	C_{max} (ng/mL)	1	8	1071.70	903.40, 1271.37	1140	728	1370
		14	7	3911.16	2996.09, 5105.72	4050	2570	5730
	T_{max} (h)	1	8			3.0	2.0	6.0
		14	7			2.2	1.0	3.0
$T_{1/2-eff}$ (h)		7	54.29	42.76, 68.92	54.53	37.32	82.55	

(Continuation Table 3)

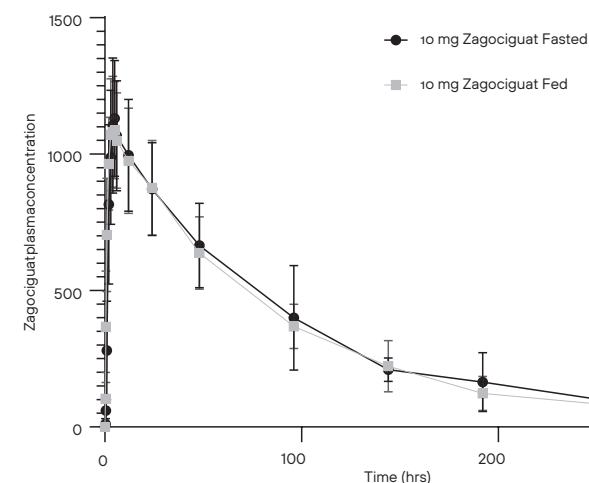
TreatmentParameter	Day	N	GEOMEAN	95% CI (lower, upper)	Median	MIN	MAX
AUC _T (h*ng/mL)	1	8	20065	16847, 23898	21523	12966	25246
	14	7	76786	58939, 100037	82073	49313	107639
CTROUGH (ng/mL)	1	8	751.32	614.64, 918.40	750.5	455	989
	11	7	2763.22	2034.92, 3752.18	3090.0	1650	4170
	12	7	2912.46	2187.20, 3878.23	3240.0	1880	4450
	13	7	2837.85	2095.18, 3843.78	3190.0	1710	4220
	14	7	2847.64	2239.24, 3621.34	2820.0	1980	3910
PTR	1	8	1.35	1.27, 1.43	1.36	1.27	1.67
	14	7	1.37	1.31, 1.44	1.37	1.30	1.47
R _{csf}	7	7	0.005	0.003, 0.006	0.005	0.003	0.007
R _{csf} F _{free}	7	7	0.415	0.307, 0.560	0.437	0.251	0.664
R _{auc}	7	7	3.80	3.10, 4.66	3.8	2.78	5.48
R _{max}	7	7	3.60	2.86, 4.53	3.68	2.62	5.25
RTHROUGH	7	7	3.79	3.17, 4.54	3.56	3.03	5.37
15 mg C _{max} (ng/mL)	1	8	1616.87	1371.50, 1906.14	1530	1190	2270
	14	8	5850.17	4746.81, 7210.00	5805	4420	8420
T _{max} (h)	1	8			3.0	1.0	5.0
	14	8			3.5	1.0	4.0
T _{1/2-eff} (h)	8	8	52.80	44.05, 63.28	51.81	40.69	75.26
AUC _T (h*ng/mL)	1	8	31299	26949, 36350	30092	24204	42871
	14	8	116128	93512, 144213	111532	83912	175583
CTROUGH (ng/mL)	1	8	1173.20	997.97, 1379.19	1165	884	1580
	11	8	4149.25	3342.27, 5151.05	4140	3000	5880
	12	8	4246.79	3480.29, 5182.12	4140	3190	6500
	13	8	4157.21	3434.86, 5031.59	4160	3090	6290
	14	8	4377.90	3446.62, 5560.81	4275	2930	6980
PTR	1	8	1.38	1.30, 1.46	1.37	1.22	1.50
	14	8	1.35	1.20, 1.49	1.33	1.12	1.61
R _{auc}	8	8	3.71	3.18, 4.33	3.64	2.98	5.04
R _{max}	8	8	3.61	3.16, 4.15	3.54	2.95	4.46
RTHROUGH	8	8	3.73	3.17, 4.39	3.81	2.97	4.85

AUC_T=area under the concentration - time curve between consecutive dosing; CI=confidence interval; C_{max}=maximum concentration, CSF=cerebrospinal fluid; C_{trough}=through concentration; GEOMEAN=geometric mean; MAD=multiple ascending dose; PK=pharmacokinetic; PTR=peak-to-trough ratio; R_{AUC}=accumulation ratio calculated from AUC_T at steady state and after a single dose; R_{CSF}=ratio of CSF concentration divided by plasma concentration; R_{CSF free}=ratio of CSF concentration divided by free plasma concentration; R_{max}=accumulation ratio calculated from C_{max} at steady state and after a single dose; R_{trough}=accumulation ratio calculated from C_{trough} at steady state and after a single dose; SD=standard deviation; T_{1/2-eff}=effective half-life based on accumulation; T_{max}=time of maximum concentration.

FI PHASE

No food effects were observed in C_{max} (LSM ratio fed vs fasted 0.99, 95%CI: 0.94, 1.03) or AUC_{inf} (LSM ratio fed vs fasted 0.99, 95%CI: 0.95, 1.04) (Figure 3). For all subjects, zagociguat concentration in plasma was below limit of quantification in pre-dose samples in the second treatment period, indicating a sufficiently long washout period.

FIGURE 3 Mean (SD) zagociguat concentration in plasma (ng/mL) (normal scale) on Day 1 of fed and fasted treatment periods during the FI phase.



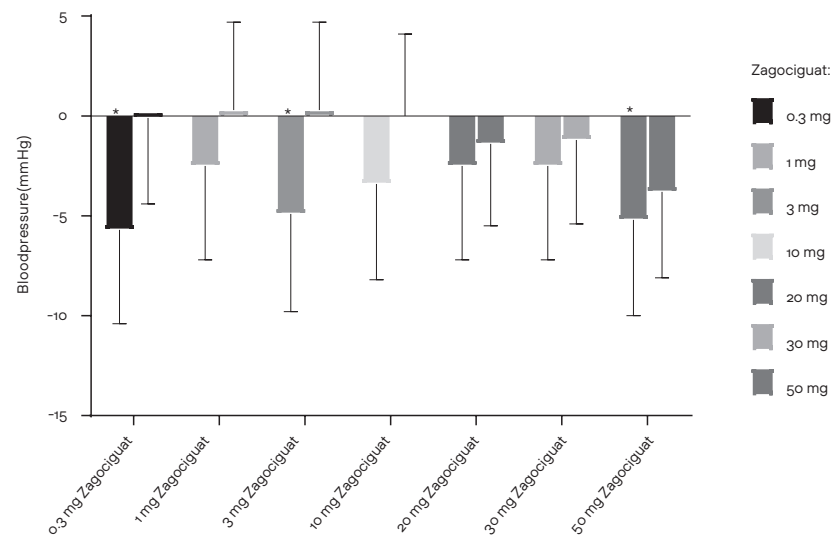
First dose is at protocol time=0. Concentrations below limit of quantification (1.00 ng/mL) were set to 0. FI=food interaction; SD=standard deviation.

PHARMACODYNAMIC ANALYSES

BLOOD PRESSURE

In the SAD phase, decreases in mean SBP over 48 h were observed after 0.3 mg zagociguat (LSMs difference from placebo: -5.7, 95% CI: -10.4, -1.0, p=0.019); 3 mg zagociguat (LSMs difference: -4.9, 95% CI: -9.8, -0.1, p=0.047), and 50 mg zagociguat (LSMs difference: -5.2, 95% CI: -10.0, -0.5, p=0.032). No decreases in SBP in other dose groups were observed, and no decreases in DBP were observed. LSMs of SBP and DBP across treatment groups over the course of the study are presented in Figure 4.

FIGURE 4 SAD phase: SBP (left bar) and DBP (right bar), mean difference in LSMs (SD) over entire treatment period, zagociguat vs placebo.



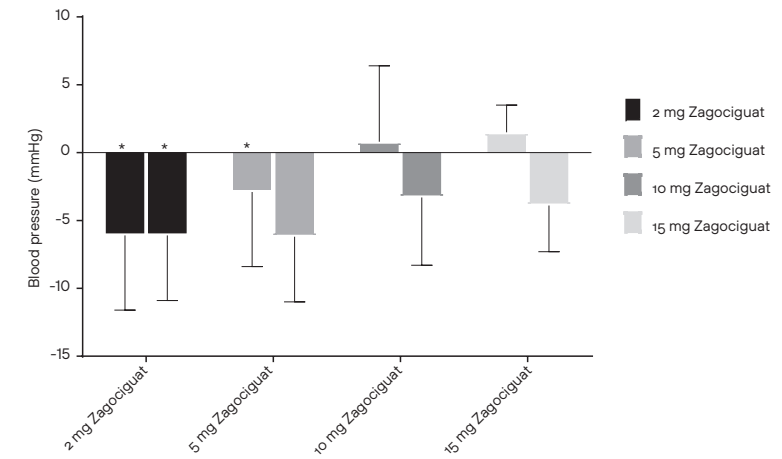
* denotes difference in LSMs of zagociguat vs placebo with $p < 0.05$. DBP=diastolic blood pressure; LSM=least squares mean; SAD=single ascending dose; SBP=systolic blood pressure; SD=standard deviation.

In the MAD phase (Figure 5), over 14 days of 2 mg zagociguat once-daily dosing, compared with placebo, a mean decrease in SBP and DBP was observed (LSMs difference: -6.1 , 95% CI: $-11.6, -0.6$, $p = 0.032$ and LSMs difference: -6.1 , 95% CI: $-10.9, -1.3$, $p = 0.015$; respectively). DBP over 14 days was also lower compared to placebo after 5 mg zagociguat administration (LSMs difference: -6.2 , 95% CI: $-11.0, -1.4$, $p = 0.014$), with a maximum difference from placebo of -7.5 mmHg (95% CI: $-13.0, -2.0$, $p = 0.009$) on Day 14. No decreases in SBP or DBP were observed in the 10 and 15 mg zagociguat groups.

CNS FUNCTION AND PEEG ASSESSMENTS

An overview of analysis results of CNS function and PEEG assessments is provided in Tables S7 and S8. No dose-dependent or consistent statistically significant differences between placebo and zagociguat groups were observed in PEEG or CNS tests in either the SAD or MAD phase.

FIGURE 5 MAD phase: SBP (left bar) and DBP (right bar), overall difference in LSMs (SD), zagociguat vs placebo.



* denotes difference in LSMs of zagociguat vs placebo with $p < 0.05$. DBP=diastolic blood pressure; LSM=least squares mean; MAD=multiple ascending dose; SBP=systolic blood pressure; SD=standard deviation.

Discussion

Zagociguat was well tolerated across all doses evaluated in this study with no safety concerns. A higher proportion of zagociguat-treated subjects reported mild dizziness and GI-related TEAES, which is consistent with AES reported for other sGC stimulators.⁴⁵⁻⁴⁶ Both dizziness and GI-related events can be linked to the mechanism of action of zagociguat, since NO-sGC-cGMP signalling is involved in smooth muscle relaxation in both blood vessels and the GI tract, including the lower esophageal sphincter.⁴⁷ No clinically relevant abnormalities in ECGs, vital signs or safety laboratory assessments were observed. Of note, although enhancement of NO-sGC-cGMP signalling has been shown to inhibit platelet function *in vitro*,²⁸ and serious bleeding events were reported more frequently with riociguat treatment in the phase 3, placebo-controlled clinical trials in pulmonary hypertension,⁴⁸ no increases in bleeding time nor any bleeding events were associated with zagociguat administration in this study. One subject had elevated liver enzymes after 6 administrations of 2 mg zagociguat, but

no other indications of potential drug-induced liver injury were observed at higher dose levels, indicating a low likelihood of drug relatedness of this AE.

Zagociguat exposures increased in a dose-proportional manner following both single and multiple escalating doses. Effective $T_{1/2}$ and terminal elimination $T_{1/2}$ are supportive of QD dosing and suggest steady state will be achieved after 11 days of zagociguat treatment, with moderate drug accumulation over a treatment period of 14 days. Zagociguat can be given with or without food since no food effects were observed in this study. Additionally, CNS penetration of the compound was confirmed by CSF sampling during the MAD phase, with a mean CSF/free plasma concentration ratio of 0.43, comparable to CSF/free plasma ratios in preclinical experiments with dogs (0.45 at 1 h, 0.32 at 2 h, 0.3 at 4 h and 0.28 at 8 h after oral administration of 1 mg/kg zagociguat) and monkeys (geometric mean CSF/free plasma ratio of 0.57 and 0.48 after intravenous and oral administration, respectively). Although sGC stimulators have been shown to penetrate the blood-brain barrier in preclinical studies,⁴⁹ zagociguat is the first confirmed CNS-penetrant sGC stimulator to be in clinical development for the treatment of CNS diseases. Based on the totality of preclinical pharmacology across multiple models (e.g., EEG, NMDA), a CSF steady state concentration of >30 nM was established as the target threshold for pharmacological activity of zagociguat. Simulations based on plasma exposures achieved in the 10 mg and 15 mg MAD cohorts and CSF exposure achieved in the 10 mg MAD cohort predicted CSF exposures above the 30 nM threshold from day 3 of 15 mg zagociguat QD, indicating that the investigated dose range reached theoretical efficacious exposures in the CNS. Effects of zagociguat on BP were observed, which is a documented effect of sGC stimulation through vasodilation induced by smooth muscle relaxation in response to cGMP.⁵⁰ Though this observation was not dose dependent, it suggests that zagociguat engages sGC. Although no consistent or dose dependent PD CNS effects were observed across dose levels using PEEG or the NeuroCart® test battery, we hypothesize that in healthy subjects with normal neurocognitive functioning, sGC stimulation may not measurably improve cognitive function.³¹ Importantly, no negative effects of zagociguat on tests for cognitive function were detected.

LIMITATIONS

The population tested in this study likely had normal neurocognitive function, which may have caused a ceiling effect and prevented the detection of neurocognitive improvement. Additionally, to induce cognitive improvement, as

opposed to reversing impairment as shown in preclinical studies, treatment duration longer than the evaluated 14 days may be needed. A single CSF sample was obtained at a timepoint when steady state was not yet achieved in plasma, limiting the evaluation of PK of zagociguat in CSF. Lastly, cohorts were not balanced with respect to sex, which may have limited the extent to which conclusions can be drawn regarding sex differences in PK or PD effects of zagociguat.

CONCLUSION

Based on this study, zagociguat is a safe and CNS-penetrant sGC stimulator with potential for pharmacological action in neurodegenerative disease. These data support further development of zagociguat.

SUPPORTING INFORMATION

Additional supporting information may be found in the online version of the article at the publisher's website.



Figure S1



Figure S2



Figure S3



Figure S4



Figure S5



Figure S6



Figure S7



Figure S8

REFERENCES

- 1 Tousoulis, D.; Kampoli, A. M.; Tentolouris, C.; Papageorgiou, N.; Stefanadis, C., The role of nitric oxide on endothelial function. *Current vascular pharmacology* **2012**, *10* (1), 4-18.
- 2 Duran, W. N.; Breslin, J. W.; Sanchez, F. A., The NO cascade, eNOS location, and microvascular permeability. *Cardiovasc Res* **2010**, *87* (2), 254-61.
- 3 Förstermann, U.; Sessa, W. C., Nitric oxide synthases: regulation and function. *European heart journal* **2012**, *33* (7), 829-37, 837a-837d.
- 4 Chachlaki, K.; Garthwaite, J.; Prevot, V., The gentle art of saying NO: how nitric oxide gets things done in the hypothalamus. *Nat Rev Endocrinol* **2017**, *13* (9), 521-535.
- 5 Fedele, E.; Ricciarelli, R., Memory Enhancers for Alzheimer's Dementia: Focus on cGMP. *Pharmaceuticals (Basel)* **2021**, *14* (1), 61.
- 6 Piedrafitá, B.; Cauli, O.; Montoliu, C.; Felipo, V., The function of the glutamate-nitric oxide-cGMP pathway in brain in vivo and learning ability decrease in parallel in mature compared with young rats. *Learning & memory (Cold Spring Harbor, N.Y.)* **2007**, *14* (4), 254-8.
- 7 Komsuoglu Celikyurt, I.; Utkan, T.; Ozer, C.; Gacar, N.; Aricioglu, F., Effects of YC-1 on learning and memory functions of aged rats. *Medical science monitor basic research* **2014**, *20*, 130-7.
- 8 Acquarone, E.; Argyrousi, E. K.; van den Berg, M.; Gulisano, W.; Fà, M.; Staniszewski, A.; Calcagno, E.; Zuccarello, E.; D'Adamo, L.; Deng, S. X.; Puzzo, D.; Arancio, O.; Fiorito, J., Synaptic and memory dysfunction induced by tau oligomers is rescued by up-regulation of the nitric oxide cascade. *Molecular neurodegeneration* **2019**, *14* (1), 26.
- 9 Lu, Y. F.; Kandel, E. R.; Hawkins, R. D., Nitric oxide signaling contributes to late-phase LTP and CREB phosphorylation in the hippocampus. *J Neurosci* **1999**, *19* (23), 10250-10261.
- 10 Toth, P.; Tarantini, S.; Csiszar, A.; Ungvari, Z., Functional vascular contributions to cognitive impairment and dementia: mechanisms and consequences of cerebral autoregulatory dysfunction, endothelial impairment, and neurovascular uncoupling in aging. *Am J Physiol Heart Circ Physiol* **2017**, *312* (1), H1-H20.
- 11 Daiber, A.; Steven, S.; Weber, A.; Shuvaev, V. V.; Muzykantov, V. R.; Laher, I.; Li, H.; Lamas, S.; Münzel, T., Targeting vascular (endothelial) dysfunction. *British journal of pharmacology* **2017**, *174* (12), 1591-1619.
- 12 Liu, P.; Fleete, M. S.; Jing, Y.; Collie, N. D.; Curtis, M. A.; Waldvogel, H. J.; Faull, R. L. M.; Abraham, W. C.; Zhang, H., Altered arginine metabolism in Alzheimer's disease brains. *Neurobiol Aging* **2014**, *35* (9), 1992-2003.
- 13 Ugarte, A.; Gil-Bea, F.; García-Barroso, C.; Cedazo-Minguez, Á.; Ramírez, M. J.; Franco, R.; García-Osta, A.; Oyarzabal, J.; Cuadrado-Tejedor, M., Decreased levels of guanosine 3', 5'-monophosphate (cGMP) in cerebrospinal fluid (CSF) are associated with cognitive decline and amyloid pathology in Alzheimer's disease. *Neuropathology and applied neurobiology* **2015**, *41* (4), 471-82.
- 14 Hesse, R.; Lausser, L.; Gummert, P.; Schmid, F.; Wahler, A.; Schnack, C.; Kroker, K. S.; Otto, M.; Tumani, H.; Kestler, H. A.; Rosenbrock, H.; von Arnim, C. A., Reduced cGMP levels in CSF of AD patients correlate with severity of dementia and current depression. *Alzheimer's research & therapy* **2017**, *9* (1), 17.
- 15 Zuccarello, E.; Acquarone, E.; Calcagno, E.; Argyrousi, E. K.; Deng, S.-X.; Landry, D. W.; Arancio, O.; Fiorito, J., Development of novel phosphodiesterase 5 inhibitors for the therapy of Alzheimer's disease. *Biochem Pharmacol* **2020**, *176*, 113818-113818.
- 16 Sanders, O.; Rajagopal, L., Phosphodiesterase Inhibitors for Alzheimer's Disease: A Systematic Review of Clinical Trials and Epidemiology with a Mechanistic Rationale. *Journal of Alzheimer's disease reports* **2020**, *4* (1), 185-215.
- 17 Prickaerts, J.; Heckman, P. R. A.; Blokland, A., Investigational phosphodiesterase inhibitors in phase I and phase II clinical trials for Alzheimer's disease. *Expert opinion on investigational drugs* **2017**, *26* (9), 1033-1048.
- 18 Stephan, B. C. M.; Harrison, S. L.; Keage, H. A. D.; Babateen, A.; Robinson, L.; Siervo, M., Cardiovascular Disease, the Nitric Oxide Pathway and Risk of Cognitive Impairment and Dementia. *Curr Cardiol Rep* **2017**, *19* (9), 87-87.
- 19 Steinert, J. R.; Chernova, T.; Forsythe, I. D., Nitric oxide signaling in brain function, dysfunction, and dementia. *The Neuroscientist : a review journal bringing neurobiology, neurology and psychiatry* **2010**, *16* (4), 435-52.
- 20 Ben Aissa, M.; Lee, S. H.; Bennett, B. M.; Thatcher, G. R., Targeting NO/cGMP Signaling in the CNS for Neurodegeneration and Alzheimer's Disease. *Current medicinal chemistry* **2016**, *23* (24), 2770-2788.
- 21 Evgenov, O. V.; Pacher, P.; Schmidt, P. M.; Haskó, G.; Schmidt, H. H.; Stasch, J. P., NO-independent stimulators and activators of soluble guanylate cyclase: discovery and therapeutic potential. *Nature reviews. Drug discovery* **2006**, *5* (9), 755-68.
- 22 Hollas, M. A.; Ben Aissa, M.; Lee, S. H.; Gordon-Blake, J. M.; Thatcher, G. R. J., Pharmacological manipulation of cGMP and NO/cGMP in CNS drug discovery. *Nitric Oxide* **2019**, *82*, 59-74.
- 23 Correia, S. S.; Iyengar, R. R.; Germano, P.; Tang, K.; Bernier, S. G.; Schwartzkopf, C. D.; Tobin, J.; Lee, T. W. H.; Liu, G.; Jacobson, S.; Carvalho, A.; Rennie, G. R.; Jung, J.; Renhowe, P. A.; Lonie, E.; Winrow, C. J.; Hadcock, J. R.; Jones, J. E.; Currie, M. G., The CNS-Penetrant Soluble Guanylate Cyclase Stimulator CY6463 Reveals its Therapeutic Potential in Neurodegenerative Diseases. *Front Pharmacol* **2021**, *12*, 656561-656561.
- 24 Information, N. C. f. B. PubChem Compound Summary for CID 134304734, Zagociguat. <https://pubchem.ncbi.nlm.nih.gov/compound/Zagociguat> (accessed 23 Jan 2023).
- 25 Başar, E., A review of gamma oscillations in healthy subjects and in cognitive impairment. *International journal of psychophysiology : official journal of the International Organization of Psychophysiology* **2013**, *90* (2), 99-117.
- 26 Zhihui, Q., Modulating nitric oxide signaling in the CNS for Alzheimer's disease therapy. *Future medicinal chemistry* **2013**, *5* (12), 1451-68.
- 27 Sandner, P.; Follmann, M.; Becker-Pelster, E.; Hahn, M. G.; Meier, C.; Freitas, C.; Roessig, L.; Stasch, J.-P., Soluble GC stimulators and activators: Past, present and future. *British journal of pharmacology* **2021**, *n/a* (n/a).
- 28 Reiss, C.; Mindukshev, I.; Bischoff, V.; Subramanian, H.; Kehrer, L.; Friebe, A.; Stasch, J. P.; Gambaryan, S.; Walter, U., The sGC stimulator riociguat inhibits platelet function in washed platelets but not in whole blood. *British journal of pharmacology* **2015**, *172* (21), 5199-210.
- 29 Bradley, J. G.; Davis, K. A., Orthostatic hypotension. *American family physician* **2003**, *68* (12), 2393-8.
- 30 Frey, R.; Mück, W.; Unger, S.; Artmeier-Brandt, U.; Weimann, G.; Wensing, G., Single-Dose Pharmacokinetics, Pharmacodynamics, Tolerability, and Safety of the Soluble Guanylate Cyclase Stimulator BAY 63-2521: An Ascending-Dose Study in Healthy Male Volunteers. *Journal of clinical pharmacology* **2008**, *48* (8), 926-934.
- 31 Groeneveld, G. J.; Hay, J. L.; Van Gerven, J. M., Measuring blood-brain barrier penetration using the NeuroCart, a CNS test battery. *Drug Discov Today Technol* **2016**, *20*, 27-34.
- 32 van Steveninck, A. L.; van Berckel, B. N.; Schoemaker, R. C.; Breimer, D. D.; van Gerven, J. M.; Cohen, A. F., The sensitivity of pharmacodynamic tests for the central nervous system effects of drugs on the effects of sleep deprivation. *Journal of psychopharmacology (Oxford, England)* **1999**, *13* (1), 10-7.
- 33 van Steveninck, A. L.; Gieschke, R.; Schoemaker, H. C.; Pieters, M. S.; Kroon, J. M.; Breimer, D. D.; Cohen, A. F., Pharmacodynamic interactions of diazepam and intravenous alcohol at pseudo steady state. *Psychopharmacology (Berl)* **1993**, *110* (4), 471-8.
- 34 Zoethout, R. W.; Delgado, W. L.; Ippel, A. E.; Dahan, A.; van Gerven, J. M., Functional biomarkers for the acute effects of alcohol on the central nervous system in healthy volunteers. *Br J Clin Pharmacol* **2011**, *71* (3), 331-50.
- 35 van Steveninck, A. L.; Wallnöfer, A. E.; Schoemaker, R. C.; Pieters, M. S.; Danhof, M.; van Gerven, J. M.; Cohen, A. F., A study of the effects of long-term use on individual sensitivity to temazepam and lorazepam in a clinical population. *Br J Clin Pharmacol* **1997**, *44* (3), 267-75.
- 36 Bittencourt, P. R.; Wade, P.; Smith, A. T.; Richens, A., Benzodiazepines impair smooth pursuit eye movements. *Br J Clin Pharmacol* **1983**, *15* (2), 259-62.
- 37 Rijnen, S. J. M.; van der Linden, S. D.; Emons, W. H. M.; Sitskoorn, M. M.; Gehring, K., Test-retest reliability and practice effects of a computerized neuropsychological battery: A solution-oriented approach. *Psychological assessment* **2018**, *30* (12), 1652-1662.
- 38 Borland, R. G.; Nicholson, A. N., Visual motor coordination and dynamic visual acuity. *Br J Clin Pharmacol* **1984**, *18* (Suppl 1), 69s-72s.
- 39 Milner, B., Visually-guided maze learning in man: effects of bilateral hippocampal, bilateral frontal, and unilateral cerebral lesions. *Neuropsychologia* **1965**, *3*, 317-338.
- 40 de Haas, S. L.; Francon, K. L.; Schmitt, J. A.; Cohen, A. F.; Fau, J. B.; Dubruc, C.; van Gerven, J. M., The pharmacokinetic and pharmacodynamic effects of SL65,1498, a GABA-A alpha2,3 selective agonist, in comparison with lorazepam in healthy volunteers. *Journal of psychopharmacology (Oxford, England)* **2009**, *23* (6), 625-32.
- 41 Hart, E. P.; Alvarez-Jimenez, R.; Davidse, E.; Doll, R. J.; Cohen, A. F.; Van Gerven, J. M. A.; Groeneveld, G. J., A Computerized Test Battery to Study Pharmacodynamic Effects on the Central Nervous System of Cholinergic Drugs in Early Phase Drug Development. *J Vis Exp* **2019**, (144).
- 42 Stroop, J. R., Studies of interference in serial verbal reactions. *J Exp Psychol* **1935**, *18* (6), 643-662.
- 43 Hummel, J.; Kendrick, S.; Brindley, C.; French, R., Exploratory assessment of dose proportionality: review of current approaches and proposal for a practical criterion. *Pharmaceutical statistics* **2009**, *8* (1), 38-49.
- 44 Maganti, L.; Panebianco, D. L.; Maes, A. L., Evaluation of methods for estimating time to steady state with examples from phase 1 studies. *AAPS J* **2008**, *10* (1), 141-147.
- 45 Boettcher, M.; Thomas, D.; Mueck, W.; Loewen, S.; Arens, E.; Yoshikawa, K.; Becker, C., Safety, pharmacodynamic, and pharmacokinetic characterization of vericiguat: results from six phase I studies in healthy subjects. *Eur J Clin Pharmacol* **2021**, *77* (4), 527-537.
- 46 Khouri, C.; Lepelley, M.; Roustit, M.; Montastruc, F.; Humbert, M.; Cracowski, J. L., Comparative

- Safety of Drugs Targeting the Nitric Oxide Pathway in Pulmonary Hypertension: A Mixed Approach Combining a Meta-Analysis of Clinical Trials and a Disproportionality Analysis From the World Health Organization Pharmacovigilance Database. *Chest* **2018**, *154* (1), 136-147.
- 47 Groneberg, D.; Voussen, B.; Friebe, A., Integrative Control of Gastrointestinal Motility by Nitric Oxide. *Current medicinal chemistry* **2016**, *23* (24), 2715-2735.
- 48 Bayer AG. Adempas (riociguat) [package insert]. U.S. Food and Drug Administration website. https://www.accessdata.fda.gov/drugsatfda_docs/label/2021/204819s015lbl.pdf. Revised September 2021. Accessed November 15, 2022.
- 49 Correia, S. S.; Liu, G.; Jacobson, S.; Bernier, S. G.; Tobin, J. V.; Schwartzkopf, C. D.; Atwater, E.; Lonie, E.; Rivers, S.; Carvalho, A.; Germano, P.; Tang, K.; Iyengar, R. R.; Currie, M. G.; Hadcock, J. R.; Winrow, C. J.; Jones, J. E., The CNS-penetrant soluble guanylate cyclase stimulator CYR119 attenuates markers of inflammation in the central nervous system. *Journal of neuroinflammation* **2021**, *18* (1), 213.
- 50 Bonderman, D.; Pretsch, I.; Steringer-Mascherbauer, R.; Jansa, P.; Rosenkranz, S.; Tufaro, C.; Bojic, A.; Lam, C. S. P.; Frey, R.; Ochan Kilama, M.; Unger, S.; Roessig, L.; Lang, I. M., Acute hemodynamic effects of riociguat in patients with pulmonary hypertension associated with diastolic heart failure (DILATE-1): a randomized, double-blind, placebo-controlled, single-dose study. *Chest* **2014**, *146* (5), 1274-1285.

CHAPTER VI

RANDOMIZED PLACEBO-CONTROLLED CROSSOVER STUDY TO ASSESS TOLERABILITY AND PHARMACODYNAMICS OF ZAGOCIGUAT, A SOLUBLE GUANYLYL CYCLASE STIMULATOR, IN HEALTHY ELDERLY

Sebastiaan JW van Kraaij, MD,^{1,2} Laura Borghans, PhD,¹ Erica S Klaassen, MSc,¹ Pim Gal, MD, PhD,^{1,2} Jeroen van der Grond, PhD,³ Ken Tripp, MA,⁴ Christopher Winrow, PhD,⁴ Chad Glasser, PharmD,⁴ Geert Jan Groeneveld, MD, PhD.^{1,2}

1: Centre for Human Drug Research, Leiden, NL
 2: Leiden University Medical Centre, Leiden, NL
 3: Dept of Radiology, Leiden University Medical Centre, Leiden, NL
 4: Cycleron Therapeutics, Cambridge, MA, USA

Bullet point summary

WHAT IS ALREADY KNOWN ABOUT THE SUBJECT

- The NO-sGC-cGMP system is involved in memory formation and learning and has been a target for treatment of neurodegenerative disease in previous clinical trials.
- Zagociguat is a blood-brain barrier penetrant sGC stimulator with a favorable safety profile in healthy young participants.
- One of the putative mechanisms of action of sGC stimulators in the treatment of neurodegenerative disease is improvement of cerebral blood flow, which is often impaired in the elderly and patients with neurodegenerative disease.

WHAT THIS STUDY ADDS:

- Pharmacodynamics and safety of zagociguat were investigated in healthy elderly participants, a population likely to have reduced cerebral blood flow.
- Zagociguat 15 mg QD for 15 days was well tolerated in healthy elderly participants and showed pharmacodynamic effects on systemic blood pressure consistent with the mechanism of action and effects of other sGC stimulators.
- Zagociguat did not show consistent pharmacodynamic effects on cerebral blood flow, central nervous system tests, electroencephalography, or various brain metabolites and biomarkers.

Abstract

AIM

Dysfunction of nitric oxide (NO)-soluble guanylyl cyclase (sGC)-cyclic guanosine monophosphate (cGMP) signalling is implicated in the pathophysiology of cognitive impairment. Zagociguat is a central nervous system-(CNS-) penetrant sGC stimulator designed to amplify NO-cGMP signalling in the CNS. This article describes a phase 1B study evaluating the safety and pharmacodynamic effects of zagociguat.

METHODS

In this randomized crossover study, 24 healthy participants ≥ 65 years of age were planned to receive 15 mg zagociguat or placebo once daily for two 15-day periods separated by a 27-day washout. Adverse events, vital signs, electrocardiograms, and laboratory tests were conducted to assess safety. Pharmacokinetics of zagociguat were evaluated in blood and CSF. Pharmacodynamic assessments included evaluation of cerebral blood flow, CNS tests, pharmaco-electroencephalography, passive leg movement, and biomarkers in blood, CSF, and brain.

RESULTS

Twenty-four participants were enrolled; 12 participants completed both treatment periods while the other 12 participants completed only one treatment period. Zagociguat was well tolerated and penetrated the blood-brain barrier, with a CSF/free plasma concentration ratio of 0.45 (SD 0.092) measured 5 hours after the last dose of zagociguat on Day 15. Zagociguat induced modest decreases in blood pressure. No consistent effects of zagociguat on other pharmacodynamic parameters were detected.

CONCLUSION

Zagociguat was well tolerated and induced modest blood pressure reductions consistent with other sGC stimulators. No clear pharmacodynamic effects of zagociguat were detected. Studies in participants with proven reduced cerebral blood flow or CNS function may be an avenue for further evaluation of the compound.

Introduction

The nitric oxide-soluble guanylyl cyclase-cyclic guanosine monophosphate (NO-sGC-cGMP) signalling pathway is involved in the regulation of a wide range of physiological systems, and dysfunction in this pathway is likewise involved in the pathophysiology of numerous disorders, including central nervous system (CNS) disorders. NO-cGMP signalling regulates endothelial cell function and permeability, neurovascular coupling, and the integrity of the blood-brain barrier,¹⁻² and is involved in long-term potentiation, the underlying mechanism of synaptic plasticity and memory formation.³⁻⁴ All of these processes are intimately involved in the pathophysiology of cognitive impairment and dementia.⁵ Since dysfunction of NO-cGMP signalling is also associated with increased oxidative stress, a major pathway of neuronal degradation and cognitive decline,⁶⁻⁷ restoration of NO-cGMP signalling is an attractive target for treatment of diseases involving cognitive dysfunction and aging of the brain.⁸⁻¹¹ Pharmacological interventions have targeted the NO-sGC-cGMP axis for decades through NO donors or precursors,¹²⁻¹⁴ inhibition of cGMP degradation¹⁵ and stimulation or activation of sGC,¹⁶ but CNS-targeted intervention in this system is relatively new.⁴

Zagociguat (CY6463, 8-(2-fluorobenzyl)-6-(3-(trifluoromethyl)-1H-1,2,4-triazol-5-yl)imidazo[1,2-a]pyrazine)¹⁷ is an sGC stimulator with the ability to enter CSF in humans, as shown in preclinical studies¹⁸ and a first-in-human (FIH) study.¹⁹ In this study, zagociguat was present in CSF after 7 days of 10 mg zagociguat administration QD, with a CSF/free plasma concentration ratio of 0.43. The FIH study also indicated a favourable safety and tolerability profile, with mild diastolic and systolic blood pressure (BP) decreases, a known effect of sGC stimulators, indicating peripheral target engagement of the compound.¹⁹⁻²⁰ Zagociguat therefore has potential to be used for treatment of disorders in which impaired NO-cGMP signalling in the CNS is implicated, such as neurodegenerative diseases, schizophrenia, and mitochondrial encephalopathies.²¹⁻²³ Since one facet of the putative mechanism of pharmacological action for sGC stimulation is an increase in cerebral blood flow, this study was conducted to assess the pharmacodynamic (PD) effects and safety of zagociguat in healthy elderly, a population hypothesized to have lower NO bioavailability and consequently lower cerebral blood flow compared to young healthy participants.²⁴

Methods

The study was conducted from January 2020 to May 2020 at the Centre for Human Drug Research (Leiden, The Netherlands), in accordance with the principles of the Declaration of Helsinki, the International Conference on Harmonisation Good Clinical Practice (ICH GCP), and ethical principles as referenced in EU Clinical Trials Directive 2001/20/EC and EU Clinical Trials Regulation No 536/2014. The protocol was approved by the Medical Review and Ethics Committee of the BEBO foundation (Assen, The Netherlands).

The study was prospectively registered in EudraCT (number 2019-003161-18), toetsingonline.nl (CHDR1919, ABR-number 71059), and clinicaltrials.gov (NCT-04240158).

Drug and molecular target nomenclature in this manuscript conforms to the IUPHAR/BPS Guide to Pharmacology nomenclature classification.²⁵

PARTICIPANTS

Men and women aged ≥ 65 years were eligible for inclusion if no clinically significant abnormal findings were obtained on medical history, physical examination, 12-lead ECG, alcohol breathalyser, and clinical laboratory tests (i.e., serum chemistry, haematology, coagulation, urine drug screen, and urinalysis) at screening. Participants using any type of medication (exception paracetamol/acetaminophen up to 4g per day) and participants with documented allergy or hypersensitivity to inactive compounds of the study product were excluded from participation.

DESIGN

A randomized, double-blind, placebo-controlled, multiple-dose, 2-way crossover study design was used. Two cohorts of 12 participants were planned to undergo two 15-day treatment periods separated by a 27-day washout, corresponding to approximately 10 half-lives of the study drug, ensuring no interference of zagociguat administered in treatment period 1 with the evaluation of safety and PD in treatment period 2 for participants randomized to the zagociguat-placebo sequence. This washout period is in line with FDA guidance, which recommends a washout period of at least 5 half-lives in bioequivalence studies, and approximately 10 half-lives to eliminate 99.9% of carry-over effects.²⁶ Treatment consisted of 15 days of 15 mg zagociguat or placebo once daily (QD). On the first day of both treatment periods, baseline PD testing, except functional magnetic

resonance imaging (fMRI), was conducted before zagociguat or placebo ('study drug') administration and on the last day of each treatment period, PD testing was conducted before and after the last study drug administration. Functional MRI was conducted at screening to establish a baseline and at the end of both treatment periods. During the treatment periods, periodic visits for safety tests were scheduled and a final safety follow-up was scheduled approximately 13 days after conclusion of both treatment periods. The primary endpoints of the study were the safety and tolerability of zagociguat in healthy elderly as assessed with the number of treatment emergent adverse events (TEAES) after receiving zagociguat compared to placebo, and the evaluation of the effect of zagociguat on cerebral blood flow (CBF) as assessed with MRI with arterial spin labelling (ASL). All other assessments were exploratory.

DOSE LEVEL JUSTIFICATION

The zagociguat dose level for Cohort 1 was selected based on emerging data from the highest daily dose evaluated in the multiple-ascending-dose stage of the FIH study with zagociguat, i.e., 15 mg. In preclinical studies in rats, desirable PD effects of zagociguat were observed at a C_{max} of 1170 ng/mL, comparable to the C_{max} achieved with 10 and 20 mg single doses of zagociguat in humans in the FIH study.¹⁹ The dose level administered in Cohort 2 remained at 15 mg zagociguat QD, since target exposure levels were reached in Cohort 1 and no safety concerns emerged.

STUDY ASSESSMENTS

SAFETY

Safety assessments to evaluate the first primary endpoint of safety and tolerability of zagociguat in healthy elderly included recording of AES and concomitant medication use, measurement of vital signs including BP, electrocardiograms (ECG), physical examinations and laboratory tests (including clinical chemistry, haematology, coagulation, and urinalysis). BP was automatically measured after 5 minutes of supine rest using a regularly maintained Dash 4000, Dash 3000 or Dynamap V100 device with the cuff placed just above the antecubital fossa. AES were coded according to the Medical Dictionary for Regulatory Activities version 21.1.

PHARMACODYNAMIC AND PHARMACOKINETIC ASSESSMENTS

Since an increase of cGMP production by sGC stimulation could induce vasodilation and possibly increase total or regional CBF,²⁷ fMRI with ASL was conducted

before study start and at steady state, i.e. on Day 15 and Day 57 at approximate T_{max} based on data from the FIH study,¹⁹ to evaluate possible effects of zagociguat on CBF as a second primary endpoint.

In addition, as an exploratory endpoint, vascular reactivity was assessed with fMRI, measuring changes in the blood-oxygen-level-dependent (BOLD) level during and after a visual stimulus. Various brain metabolites and biomarkers were explored using proton magnetic resonance spectroscopy (1H-MRS), including L-alanine, aspartate, creatinine, glucose, glutamine, glutamate, glycerophosphocholine, myo-inositol and N-acetylaspartate (NAA). NAA, glutamine and glutamate are markers of neuronal health,²⁸ shown to improve with zagociguat treatment in preclinical studies in rats,¹⁸ while L-alanine, aspartate, creatinine, glucose, glycerophosphocholine and myo-inositol are abundant brain metabolites that can be altered in the context of neurocognitive disorders.²⁹⁻³¹

Blood samples for analysis of zagociguat pharmacokinetics (PK) were collected before drug administration at the beginning of each treatment period (Day 1 and Day 43), before and 5 h after drug administration at the end of each treatment period (Day 15 and Day 57), and at follow-up (Day 70). Samples for analysis of zagociguat PK, cGMP and NF-L concentrations in CSF were collected through lumbar punctures before study drug administration on Day 1 and 5 h after study drug administration on Day 15 and 57. Blood sampling for exploratory biomarker analysis was performed before the first drug administration (Day 1 and Day 43) and before the last drug administration (Day 15 and 57) in each treatment period. Plasma PK samples were placed on ice until processed and stored upright at -80 °C within 2 hours of collection until shipping. Plasma PD samples were placed on melting ice until processed and stored at -80 °C within 60 minutes after centrifugation until shipping. CSF PK and PD samples were stored at -80 °C within 2 hours and 30 minutes of collection, respectively, until shipping. All samples were shipped on dry ice to the bioanalytical lab (Ardena Bioanalytical Laboratory, Assen, The Netherlands).

Quantification of zagociguat in plasma (in potassium ethylenediaminetetraacetic acid, K2EDTA), and CSF were determined using GLP-validated liquid chromatography with tandem mass spectrometry (LC-MS/MS) methods. Zagociguat was extracted using acetonitrile protein precipitation containing a deuterated internal standard. High-performance liquid chromatography separation was conducted at 0.7 mL/min through a C_{18} analytical column (3.0 μ m particle size, 50 x 2.1mm C_{18} column; (Advanced Chromatography Technologies Ltd). Mobile phase A consisted of 0.1% formic acid in water and mobile phase

B consisted of 0.1% formic acid in acetonitrile. Compound was detected using an API-5500 (Applied Biosystems/MDS SCIEX, Framingham, Massachusetts) in positive-ion mode, multiple reaction monitoring using parent/product transitions of 363.1/267.0 m/z for zagociguat and 367.1/271.0 m/z for the internal standard.

Calibration standards were prepared in either human plasma (K2EDTA) or CSF and analysed in duplicate with each analytical batch. Blank matrix was tested for interference at the retention time and mass transition of the analyte was found to be free of significant interference. The standard curve was linear over the range of 1.00 to 1000 ng/mL using linear regression with $1/x^2$ weighting for both plasma and CSF. Inter-batch precision values ranged from 3.7 to 7.1% for plasma and 7.4 to 9.2% for CSF calibration standards, while accuracy values ranged from 2.0 to 11.0% bias for plasma and 2.1 to 6.0% bias for CSF. The percent extraction recovery for zagociguat from plasma was 107.3% and from CSF was 81.4%. Validation results demonstrated high accuracy ($\leq 11.4\%$ deviation for plasma and $\leq 3.3\%$ for CSF) and high precision ($\leq 6.81\%$ CV for plasma and $\leq 4.5\%$ for CSF) for quality control samples. The lower limit of quantification of zagociguat concentration was 1.00 ng/mL in both plasma and CSF.

Exploratory biomarkers included in plasma analysis were asymmetric and symmetric dimethylarginine (ADMA and SDMA), L-arginine, vascular cell adhesion molecule 1 (VCAM-1) and neurofilament light chains (NF-L).³²⁻³⁴ All plasma and CSF biomarkers were considered exploratory endpoints and the assays determining them were thus considered fit-for-purpose. Isolation of L-Arginine, ADMA and SDMA from human K2EDTA plasma was performed by protein precipitation, followed by derivatisation using benzoylchloride under alkaline conditions. Finally, the concentration of derivatised analytes were measured using an API 5500 LC-MS/MS system. The lower limits of quantification were 15.0 $\mu\text{mol/L}$ and 0.300 $\mu\text{mol/L}$ and the upper limits of quantification were 210 $\mu\text{mol/L}$ and 4.10 $\mu\text{mol/L}$ for L-arginine and ADMA/SDMA respectively. VCAM-1 and NF-L in plasma were determined using respectively the human VCAM-1/CD106 Quantikine enzyme-linked immunosorbent assay (ELISA) kit of R&D Systems (Minneapolis, MN, USA) and the human NF-L High Sensitivity ELISA Kit of Aviva Systems Biology (San Diego, CA, USA). NF-L concentration and cGMP concentration were also assessed in CSF. For determination of NF-L in CSF, the human NF-L ELISA Kit (Colorimetric) of Novus Biologicals (Abingdon, UK) was used, and cGMP CSF concentration was measured using a validated LC-MS/MS system method using an API 5500 LC-MS/MS system.

Pharmaco-electroencephalography (PEEG), including measurement of P300 event-related potential (ERP), as well as a broad CNS test battery (NeuroCart®) were conducted at the start and end of each treatment period. PEEG was conducted using a 40-channel recording system under vigilance-controlled conditions for 10 minutes per assessed timepoint employing alternating 64-second periods of eyes open and eyes closed conditions. P300 ERPs were measured using an active auditory oddball task. During EEG measurements, participants were presented with 500 auditory stimuli at a frequency of 1 Hz and asked to press a response button when identifying a deviant (infrequent) tone. The frequent and infrequent stimuli were 150 ms tones of respectively 500 Hz and 1000 Hz at a sound pressure level of 75 dB, with a 5 ms rise and fall time. The probability for an infrequent stimulus to occur was 0.2. The NeuroCart® test battery included measurement of saccadic and smooth pursuit eye movements, body sway, adaptive tracking, visual verbal learning test (VVLT, immediate recall, delayed recall, and delayed recognition) and N-back test.³⁵ During the course of the study, subjective effects of zagociguat were assessed using visual analogue scales (VAS), from which 3 main factors were calculated: alertness, mood, and calmness.³⁶

Effects of zagociguat on endothelial function were assessed at baseline and at the end of each treatment period using the single passive leg movement (PLM) technique, in which the blood flow increase in the femoral artery in response to leg movement is quantified using Doppler ultrasonography (SparQ Ultrasound System, Philips, Eindhoven, The Netherlands), allowing the measurement of systemic vascular function.³⁷

BENEFIT/RISK ANALYSIS OF STUDY ASSESSMENTS

The study assessments included in the study were considered minimally invasive and burdensome for participants, save for CSF sampling through lumbar puncture. Evaluating concentrations of zagociguat in the CSF was considered important to aid in interpretation of results and to provide more insight into the mechanism of action of zagociguat. Since single lumbar punctures using atraumatic needles carry an approximately 2% risk of post-lumbar puncture headache, which is a self-limiting condition, and the elderly participants included in this study are known to be at an even lower risk for post-lumbar puncture adverse events when compared to young participants,³⁸ the benefits of inclusion of CSF sampling in the study outweighed the risks in the opinion of the investigator. Participants were informed about the potential

adverse effects associated with lumbar puncture through the informed consent form and verbal information from the investigator, and all consented to this procedure.

STATISTICAL ANALYSIS

All statistical analyses were conducted according to a statistical analysis plan written before unblinding of the database.

Due to the COVID-19 pandemic, the trial was prematurely terminated while cohort 2 was in the washout period, and therefore, cohort 2 did not finish the treatment sequence. Main statistical analysis was conducted on all available data, with the period 2 data for cohort 2 considered missing (missing at random).

SAFETY DATA

All participants who received ≥ 1 dose of study drug were included in the safety analyses. TEAES were summarised, and percentages calculated by treatment, system organ class, preferred term, severity, and study drug relatedness. ECG, safety laboratory results and vital signs were summarised similarly, and number and percentage of out-of-range values calculated by treatment and time point.

PHARMACOKINETIC DATA

All participants who received ≥ 1 dose of study drug and had ≥ 1 measurable drug concentration of zagociguat in collected samples were included in PK analysis. Zagociguat plasma (free and total) and CSF concentrations were summarized by time after last dose. If more than 1/3 of the concentrations were BLQ then mean, standard deviation (SD) and percent coefficient of variation (%CV) were not calculated. Individual PK parameters (N, mean, SD, %CV, geometric mean, geometric %CV, median, minimum, and maximum) were also calculated and summarized.

PHARMACODYNAMIC DATA

All participants who received ≥ 1 dose of study drug and had ≥ 1 post-baseline assessment of the analysed parameter were included in PD analysis. All repeatedly measured PD parameters were summarized (N, mean, SD, standard error of the mean, median, minimum, and maximum values) by treatment and time, while single measured PD parameters were summarized by treatment only. Treatment effects on single measured PD parameters were analysed using a mixed analysis

of variance model with treatment and period as fixed effects, subject as a random effect, and the baseline measure as a covariate, if available. Treatment effects on multiple measured PD parameters were analysed using a mixed model analysis of covariance (ANCOVA) with treatment, period, time and treatment by time as fixed effect, subject, subject by treatment and subject by time as random effects, and the average baseline as covariate. For all continuous PD parameters, the change from baseline was calculated by post-dose measurement minus baseline. Treatment effect significance was reported with nominal p-values.

ADDITIONAL SENSITIVITY ANALYSES DUE TO THE COVID-19 PANDEMIC.

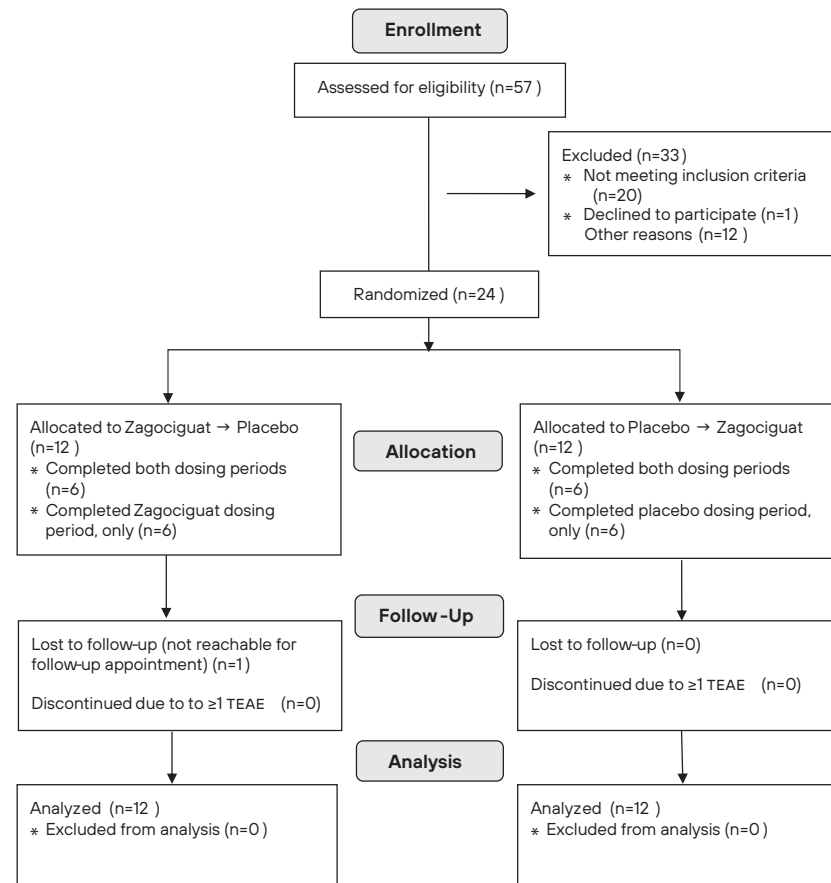
Additional sensitivity analyses were prespecified in the SAP to aid in the interpretation of the results with missing Cohort 2 data. These consisted of reanalysis of the parameters CBF, fMRI BOLD signal, brain metabolites, CSF cGMP and several NeuroCart variables in 2 extra PD population sets, namely a set containing all participants in the PD population who received ≥ 1 dose of study treatment in period 2 (i.e., all cohort 1 participants) and a set of all participants in the PD population only including data from treatment period 1. For the set containing both periods, all PD analyses were performed as defined above. For the analysis of the period 1 data only, single-measured endpoints were analysed using ANCOVA to assess treatment differences with treatment as fixed factor and the baseline, if available, as covariate, and multiple measured endpoints were analysed with a mixed model ANCOVA with treatment, time, and treatment by time as fixed factors, participant as random factor and the average baseline as covariate.

Results

PARTICIPANT DISPOSITION

Twenty-four participants were enrolled in two 12-participant cohorts. Cohort 1 completed both treatment periods. Cohort 2 completed treatment period 1, after which the study was prematurely terminated due to the COVID-19 pandemic, since the target population was determined to be at high risk of infection, and the Dutch Health Inspectorate mandated that all ongoing phase I studies be discontinued due to the COVID-19 pandemic. This resulted in 6 participants completing only zagociguat treatment and 6 participants completing only placebo treatment in Cohort 2. (Figure 1)

FIGURE 1 Trial flow chart (CONSORT diagram).



TEAE=treatment emergent adverse event.

BASELINE CHARACTERISTICS

An overview of baseline characteristics of study participants per completed treatment sequence is given in Table 1. No notable differences in participant age, height, weight, BMI, or sex distribution were observed across different treatment sequences. Overall, among the 24 randomized participants, 41.7% were female and 87.5% had white ethnicity.

TABLE 1 Demographic and baseline data (Safety Population).

Treatment sequence	Age (SD)	Height (SD)	Weight (SD)	BMI (SD)	Sex (male)	Ethnicity (white)
Zagociguat-Placebo (N=6)	69.3±2.7	175.72±10.12	80.18±11.66	25.90±2.77	83.3%	100%
Placebo-Zagociguat (N=6)	70.0±5.2	171.68±13.44	74.38±10.68	25.33±2.41	66.7%	83.3%
Zagociguat only (N=6)	69.2±2.6	170.35±9.33	72.02±10.34	25.32±2.58	50.0%	66.7%
Placebo only (N=6)	71.8±5.0	170.35±15.02	73.67±10.27	26.03±3.78	33.3%	100%

All values presented as means and standard deviation. BMI=body mass index; SD=standard deviation.

SAFETY DATA

An overview of TEAEs by system organ class, preferred term and study drug relatedness is shown in Table 2. Incidence of participants experiencing at least 1 TEAE was comparable between zagociguat and placebo treatment periods. A total of 13 participants (72.2%) receiving zagociguat treatment experienced ≥1 TEAE vs 12 (66.7%) participants receiving placebo treatment. All AEs were mild or moderate and resolved at study follow-up visit. Nine participants (50%) receiving zagociguat experienced TEAEs considered related by the investigator, compared to 8 participants (44.4%) receiving placebo. During both zagociguat and placebo treatment, 7/18 participants (38.9%) reported TEAEs in the nervous system disorders system organ class, with the most common TEAE headache (6/18 (33.3%) of zagociguat treated participants, 7/18 (38.9%) of placebo treated participants). Musculoskeletal TEAEs were reported more often by participants during zagociguat treatment (7/18 participants, 38.9%) than during placebo treatment (2/18 participants, 11.1%), with the most common TEAE musculoskeletal stiffness reported in 5/18 (27.8%) of zagociguat treated participants and 1/18 (5.6%) of placebo treated participants. Similarly, gastrointestinal TEAEs were more often reported during zagociguat treatment (7/18 participants, 38.9% vs 3/18 participants, 16.7%), with 5/18 (27.8%) zagociguat treated participants reporting the most common TEAE dyspepsia, as opposed to 0/18 placebo treated participants. Six participants, 4/18 (22.2%) in the placebo treatment periods and 2/18 (11.1%) in the zagociguat treatment periods reported pain localized to the lumbar puncture site temporally associated with the lumbar puncture procedure, which was coded as traumatic lumbar puncture. No post-lumbar puncture syndrome, defined as postural headache temporally associated with lumbar puncture, occurred in this

study. Most TEAES were mild in severity; moderate TEAES included 1 event of moderate arthralgia and 1 event of moderate erythema due to gout arthritis in the same participant during zagociguat treatment and 1 event of moderate nasopharyngitis and 1 event of headache in the same participant during placebo treatment.

No clinically significant trends in laboratory assessments, vital signs, or ECG results were observed during the study. One participant experienced transient ALT elevation (55, upper limit of normal 34) considered clinically significant and not related to study drug at the end of the washout period and start of zagociguat treatment, which resolved completely by day 7 of zagociguat treatment.

TABLE 2 Summary of number and percentage of participants with TEAES by treatment, SOC, PT and study drug relatedness.

SOC / PT (n, (%))	15 mg Zagociguat (n=18)		Placebo (n=18)	
	Related	Unrelated	Related	Unrelated
Assessment of relatedness				
ALL	9 (50.0)	9 (50.0)	8 (44.4)	8 (44.4)
Ear and labyrinth disorders	0	0	1 (5.6)	0
Tinnitus	0	0	1 (5.6)	0
Eye disorders	0	1 (5.6)	0	0
Dry eye	0	1 (5.6)	0	0
Gastrointestinal disorders	2 (11.1)	5 (27.8)	3 (16.7)	0
Abdominal pain lower	0	1 (5.6)	0	0
Abdominal pain upper	0	0	1 (5.6)	0
Constipation	0	1 (5.6)	0	0
Diarrhoea	0	0	1 (5.6)	0
Dyspepsia	2 (11.1)	3 (16.7)	0	0
Flatulence	0	0	1 (5.6)	0
Nausea	0	0	2 (11.1)	0
Oropharyngeal pain	0	1 (5.6)	0	0
Vomiting	1 (5.6)	0	0	0
General disorders and administration site conditions	1 (5.6)	0	2 (11.1)	0
Fatigue	0	0	2 (11.1)	0
Feeling abnormal	1 (5.6)	0	0	0
Feeling cold	0	0	1 (5.6)	0
Infections and infestations	0	0	1 (5.6)	0
Nasopharyngitis	0	0	1 (5.6)	0
Injury, poisoning and procedural complications	0	2 (11.1)	0	5 (27.8)
Post-traumatic pain	0	0	0	1 (5.6)

(Continuation Table 2)

Traumatic lumbar puncture	0	2 (11.1)	0	4 (22.2)
Investigations	0	0	0	1 (5.6)
Hepatic enzyme increased	0	0	0	1 (5.6)
Musculoskeletal and connective tissue disorders	2 (11.1)	5 (27.8)	1 (5.6)	1 (5.6)
Arthralgia	1 (5.6)	0	0	0
Musculoskeletal stiffness	1 (5.6)	4 (22.2)	1 (5.6)	0
Neck pain	0	1 (5.6)	0	1 (5.6)
Nervous system disorders	7 (38.9)	0	7 (38.9)	0
Dysgeusia	1 (5.6)	0	0	0
Headache	6 (33.3)	0	7 (38.9)	0
Restlessness	1 (5.6)	0	0	0
Somnolence	1 (5.6)	0	0	0
Tremor	0	0	1 (5.6)	0
Reproductive system and breast disorders	1 (5.6)	0	0	0
Erection increased	1 (5.6)	0	0	0
Respiratory, thoracic and mediastinal disorders	0	0	1 (5.6)	3 (16.7)
Dysphonia	0	0	1 (5.6)	1 (5.6)
Nasal congestion	0	0	0	1 (5.6)
Upper respiratory tract infection	0	0	0	1 (5.6)
Skin and subcutaneous tissue disorders	1 (5.6)	0	0	0
Erythema	1 (5.6)	0	0	0

TEAES counted once per subject per period at the closest relationship to treatment. PT=preferred term; TEAE=treatment emergent adverse event; SOC=system organ class.

PHARMACODYNAMIC DATA

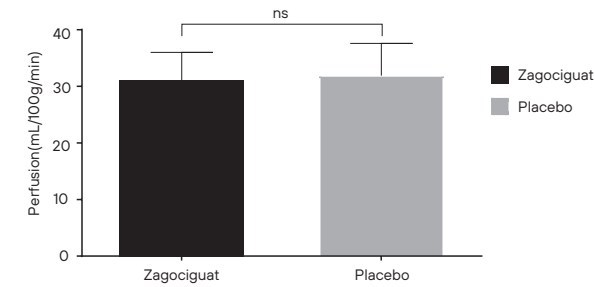
MAGNETIC RESONANCE IMAGING & VASCULAR ASSESSMENTS

A complete overview of analysed ASL parameters is given in Table 3. No effect of zagociguat on total CBF as measured with ASL was observed when compared to placebo (-0.77, 95% CI: -2.95, 1.41; p=0.458), Figure 2. In both placebo- and zagociguat-treated groups, total CBF increased post-treatment when compared to baseline measurement. Similarly, no regional differences in CBF were detected. Sensitivity analyses of CBF as described above did not reveal any treatment effects. A summary of other PD parameters is provided in Table S1. No differences between placebo and zagociguat treatment periods were observed in 1H-MRS measured brain metabolite concentrations. Assessment of vascular reactivity with fMRI BOLD and endothelial function with PLM similarly did not reveal differences between treatment groups.

TABLE 3 Summary of CBF findings.

Parameter	Contrasts (95% CI) p-value	LS MEANS	
		Zagociguat	Placebo
Total grey matter perfusion (mL/100g/min)	-0.7703 (-2.9510, 1.4104) p=0.4581	31.128	31.898
Frontal grey matter perfusion (mL/100g/min)	-0.5400 (-3.0964, 2.0164) p=0.6548	34.361	34.901
Parietal grey matter perfusion (mL/100g/min)	-0.7625 (-3.2828, 1.7579) p=0.5230	36.210	36.972
Temporal grey matter perfusion (mL/100g/min)	-0.7027 (-2.5588, 1.1534) p=0.4249	30.416	31.118
Occipital grey matter perfusion (mL/100g/min)	-0.8252 (-3.1148, 1.4645) p=0.4480	30.559	31.384
Left thalamus perfusion (mL/100g/min)	-0.5119 (-3.7823, 2.7585) p=0.7417	30.972	31.483
Right thalamus perfusion (mL/100g/min)	-1.0674 (-4.0803, 1.9456) p=0.4583	30.148	31.215
Left caudate perfusion (mL/100g/min)	-1.3872 (-3.9915, 1.2171) p=0.2758	24.975	26.362
Right caudate perfusion (mL/100g/min)	-0.8074 (-3.3250, 1.7102) p=0.5009	23.964	24.771
Left putamen perfusion (mL/100g/min)	-1.1016 (-3.6334, 1.4303) p=0.3666	28.207	29.308
Right putamen perfusion (mL/100g/min)	-1.2874 (-3.5702, 0.9954) p=0.2446	27.108	28.395
Left pallidum perfusion (mL/100g/min)	-2.0787 (-5.0386, 0.8811) p=0.1565	23.440	25.519
Right pallidum perfusion (mL/100g/min)	-1.8248 (-4.3177, 0.6681) p=0.1391	21.355	23.180
Left hippocampus perfusion (mL/100g/min)	-0.7842 (-3.1497, 1.5813) p=0.4869	27.190	27.974
Right hippocampus perfusion (mL/100g/min)	-0.8045 (-3.3933, 1.7843) p=0.5143	26.176	26.981
Left amygdala perfusion (mL/100g/min)	0.0215 (-2.3963, 2.4393) p=0.9851	25.645	25.623
Right amygdala perfusion (mL/100g/min)	-1.7198 (-4.0821, 0.6425) p=0.1406	23.106	24.825
Left accumbens perfusion (mL/100g/min)	-0.2618 (-3.8948, 3.3712) p=0.8796	36.031	36.292
Right accumbens perfusion (mL/100g/min)	-1.6074 (-6.0087, 2.7939) p=0.4457	35.178	36.786

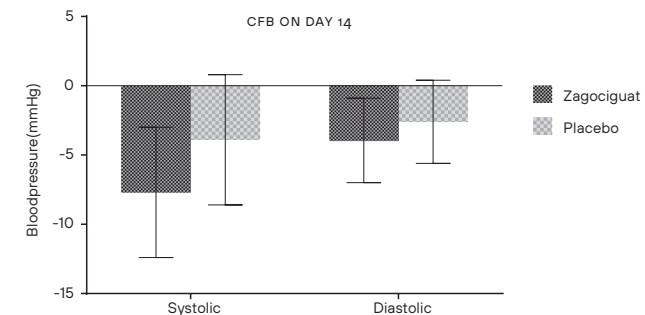
CBF=cerebral blood flow; CI=confidence interval; LS=least squares.

FIGURE 2 LSMs of total cerebral blood flow during treatment periods.

Cerebral blood flow did not differ significantly between zagociguat and placebo treated groups ($p=0.458$). LSM=least squares means; NS=not significant.

SYSTEMIC BLOOD PRESSURE

Zagociguat induced mild decreases in systolic BP (-5.7 mmHg, 95% CI: -10.1, -1.4; $p=0.0143$) and diastolic BP (-3.2 mmHg, 95% CI: -6.3, -0.1; $p=0.0438$), sustained throughout treatment with zagociguat, as illustrated in Figure 3.

FIGURE 3 CFB (LSM with 95% CI) in diastolic and systolic BP on treatment day 14.

Over the whole treatment period, systolic ($p=0.0143$) and diastolic ($p=0.0438$) BP decreased more in zagociguat treated participants when compared to placebo. BP=blood pressure; CI=confidence interval; CFB=change from baseline; LSM=least squares means.

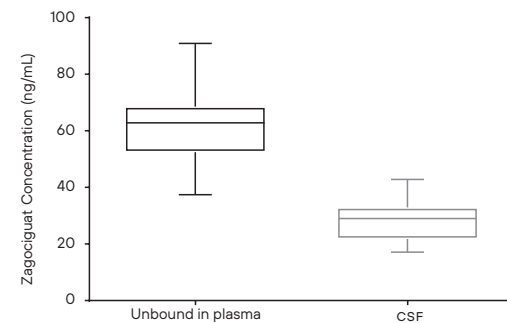
ELECTROENCEPHALOGRAPHY (EEG) AND NEUROCARD CNS TEST BATTERY

A complete overview of EEG and CNS test analyses is given in Table S2. Analysis of spectral EEG parameters at individual bipolar channels near the midline (Fz-Cz, Pz-O1, and Pz-O2) and of P300 at Pz did not show any differences between zagociguat and placebo treatment. A decrease of 0.030 ($p=0.0038$) in the ratio (correct-incorrect/total) for One-Back in the N-back test was observed with zagociguat treatment vs placebo (95% CI: -0.049, -0.011). Prespecified exploratory analysis of saccadic reaction time showed a decrease of 0.0066 seconds (95% CI: -0.0119, -0.0013; $p=0.0216$) with zagociguat treatment when compared to placebo. No other notable differences were observed between zagociguat vs placebo treatment in NeuroCart® results in either primary analysis or sensitivity analyses.

PHARMACOKINETIC DATA

A summary of CSF and plasma zagociguat concentrations is provided in Table S3. Plasma zagociguat concentrations were highest at Day 15 post dose (median: 5665.00 ng/mL, min: 3370.00 ng/mL, max: 8190.00 ng/mL). Mean ratio between CSF zagociguat concentration and free plasma zagociguat concentration on Day 15 was 0.45 (SD 0.092) (Figure 4).

FIGURE 4 Box plot of zagociguat concentration unbound in plasma and in CSF on treatment day 15.



CSF=cerebrospinal fluid.

Discussion

Zagociguat was well tolerated in healthy elderly and shown to penetrate the blood-brain barrier, with concentrations of zagociguat in the CSF of approximately half that free in plasma. Peripheral target engagement was shown with decreases in systolic and diastolic BP. Zagociguat did not affect CBF as measured using ASL but some possible CNS effects of zagociguat were observed in NeuroCart® parameters, namely a reduction of correct/incorrect ratio in the N-back test and an improvement in saccadic reaction time.

The effects of CNS-penetrant sGC stimulators have been studied in various rodent models and have been shown to increase cerebral blood flow, improve cognitive performance, increase long-term potentiation, and reduce markers of inflammation.^{18,39} However, in this study in healthy elderly, no meaningful alterations in CBF or concentrations of brain metabolites such as L-alanine, aspartate, creatinine, glucose, glutamine, glutamate, glycerophosphocholine, myo-inositol and N-acetylaspartate were detected. CBF increased in both placebo and zagociguat groups over the course of the treatment periods. There could be several explanations for this, such as the extensive amount of neurological testing conducted before fMRI on the last treatment day inducing increased cerebral blood flow, the presence of a placebo effect, or changes in participant behaviour or lifestyle, e.g., physical activity, due to participation in the study.⁴⁰

In the NeuroCart® assessments, effects on correct/incorrect ratio in the N-back test and saccadic reaction time were observed; no other consistent treatment effects on NeuroCart® tests were observed. Since no correction for multiple testing was performed, these observed effects could be the result of type 1 error. The NeuroCart® assessments measure cerebral functions that may already be near-optimal in healthy elderly, reducing the likelihood of zagociguat improving performance on these tests or detecting small changes in underlying processes.³⁵ Alternatively, the administered dose or duration of dosing might not be sufficient to induce treatment effects in healthy humans, although the C_{max} values reached during the study did induce beneficial cognitive effects in some rat models. Importantly zagociguat did not show impairment in this healthy elderly population.

Headache, musculoskeletal stiffness, and dyspepsia were the most reported AES in this study, with gastrointestinal and musculoskeletal TEAES more frequently reported under zagociguat treatment. Gastrointestinal TEAES could be attributed to the relaxing effect of sGC stimulation on the smooth muscle cells

of the intestinal tract,⁴¹⁻⁴² and have been described in studies with other sGC stimulators, both in healthy participants and patients.⁴³⁻⁴⁵ Musculoskeletal pain and headache are common TEAES in all early phase clinical studies although in prior studies evaluating sGC stimulators, an increased incidence of headache has been observed.^{43,46} The vasodilatory effects of sGC stimulation has the potential to contribute to the occurrence of headaches.²⁰ However, any association between zagociguat and headaches in this study is limited given the small sample size and the balanced occurrence of headache between treatments. NO-cGMP signalling has also been implicated in both anti- and pro-nociceptive signalling in preclinical studies, further expanding the possible pathways for development of the observed TEAES.⁴⁷⁻⁵⁰

LIMITATIONS

Due to the COVID-19 pandemic, the study was prematurely halted and not all participants completed their treatment sequence, reducing the power to achieve statistical significance in the measured endpoints and possibly affecting the validity of the results since selection bias in the distribution of participants who completed the whole study versus only one treatment period cannot be ruled out, although no differences in baseline characteristics were found. Moreover, results of sensitivity analyses did not change the results, and a parallel design with 18 participants per group is still an accepted sample size for phase 1B studies. It is therefore unlikely that this lack of power significantly impacted the conclusions derived from this study. Additionally, the study population was chosen based on literature evidence of reduced CBF in this population. However, reduced CBF or neurocognitive dysfunction was not part of the participant selection criteria,²⁴ possibly resulting in some participants having optimal CBF and cognitive function, limiting the ability to detect treatment effects. In addition, 15-day QD administration of study treatment might not have been sufficient to induce increases in cerebral blood flow or changes in other PD parameters. Finally, the population who received at least 1 dose of zagociguat was predominantly male (50.0-83.3%), while the participants who received placebo only due to the early termination of the study were predominantly female (33.3%). Although no clear sex-differences are known for the mechanism of action of zagociguat,⁵¹ differences in symptom presentation between male and female participants may hypothetically have influenced the interpretation of the safety results.

CONCLUSION

The sGC stimulator zagociguat was demonstrated to be safe, tolerable, CNS-penetrant, and potentially CNS active with 15 days of once-daily treatment in healthy elderly participants. However, no definitive PD effect of the compound in the CNS was established. Further study in participants with proven reduced CBF and cognitive dysfunction, for example in patient populations, may be an avenue to further investigate the effects of the compound.

SUPPORTING INFORMATION

Additional supporting information may be found in the online version of the article at the publisher's website.



Table S1



Table S2



Table S3

REFERENCES

- 1 Surapisitchat, J.; Jeon, K. I.; Yan, C.; Beavo, J. A., Differential regulation of endothelial cell permeability by cGMP via phosphodiesterases 2 and 3. *Circ Res* 2007, 101 (8), 811-8.
- 2 Draijer, R.; Atsma, D. E.; van der Laarse, A.; van Hinsbergh, V. W., cGMP and nitric oxide modulate thrombin-induced endothelial permeability. Regulation via different pathways in human aortic and umbilical vein endothelial cells. *Circ Res* 1995, 76 (2), 199-208.
- 3 Zhuo, M.; Hu, Y.; Schultz, C.; Kandel, E. R.; Hawkins, R. D., Role of guanylyl cyclase and cGMP-dependent protein kinase in long-term potentiation. *Nature* 1994, 368 (6472), 635-9.
- 4 Hollas, M. A.; Ben Aissa, M.; Lee, S. H.; Gordon-Blake, J. M.; Thatcher, G. R. J., Pharmacological manipulation of cGMP and NO/cGMP in CNS drug discovery. *Nitric Oxide* 2019, 82, 59-74.
- 5 Iadecola, C.; Duering, M.; Hachinski, V.; Joutel, A.; Pendlebury, S. T.; Schneider, J. A.; Dichgans, M., Vascular Cognitive Impairment and Dementia: JACC Scientific Expert Panel. *Journal of the American College of Cardiology* 2019, 73 (25), 3326-3344.
- 6 Cahill-Smith, S.; Li, J. M., Oxidative stress, redox signalling and endothelial dysfunction in ageing-related neurodegenerative diseases: a role of NADPH oxidase 2. *Br J Clin Pharmacol* 2014, 78 (3), 441-53.
- 7 Förstermann, U.; Xia, N.; Li, H., Roles of Vascular Oxidative Stress and Nitric Oxide in the Pathogenesis of Atherosclerosis. *Circ Res* 2017, 120 (4), 713-735.
- 8 Kandlur, A.; Satyamoorthy, K.; Gangadharan, G., Oxidative Stress in Cognitive and Epigenetic Aging: A Retrospective Glance. *Frontiers in Molecular Neuroscience* 2020, 13.
- 9 Berr, C.; Balansard, B.; Arnaud, J.; Roussel, A.-M.; Alperovitch, A.; Group, E. S., Cognitive Decline Is Associated with Systemic Oxidative Stress: The EVA Study. *Journal of the American Geriatrics Society* 2000, 48 (10), 1285-1291.
- 10 Luca, M.; Luca, A.; Calandra, C., The Role of Oxidative Damage in the Pathogenesis and Progression of Alzheimer's Disease and Vascular Dementia. *Oxidative medicine and cellular longevity* 2015, 2015, 504678-504678.
- 11 Sandner, P.; Follmann, M.; Becker-Pelster, E.; Hahn, M. G.; Meier, C.; Freitas, C.; Roessig, L.; Stasch, J. P., Soluble GC stimulators and activators: Past, present and future. *British journal of pharmacology* 2021.
- 12 Willmot, M.; Gray, L.; Gibson, C.; Murphy, S.; Bath, P. M., A systematic review of nitric oxide donors and L-arginine in experimental stroke; effects on infarct size and cerebral blood flow. *Nitric Oxide* 2005, 12 (3), 141-9.
- 13 El-Hattab, A. W.; Emrick, L. T.; Craigen, W. J.; Scaglia, F., Citrulline and arginine utility in treating nitric oxide deficiency in mitochondrial disorders. *Molecular genetics and metabolism* 2012, 107 (3), 247-52.
- 14 Feelisch, M., The use of nitric oxide donors in pharmacological studies. *Naunyn-Schmiedeberg's archives of pharmacology* 1998, 358 (1), 113-122.
- 15 Padda, I. S.; Tripp, J., Phosphodiesterase inhibitors. *StatPearls [Internet]* 2020.
- 16 Evgenov, O. V.; Pacher, P.; Schmidt, P. M.; Haskó, G.; Schmidt, H. H.; Stasch, J. P., NO-independent stimulators and activators of soluble guanylate cyclase: discovery and therapeutic potential. *Nature reviews. Drug discovery* 2006, 5 (9), 755-68.
- 17 Information, N. C. f. B. PubChem Compound Summary for CID 134304734, Zagogicuat. <https://pubchem.ncbi.nlm.nih.gov/compound/Zagogicuat> (accessed 23 Jan 2023).
- 18 Correia, S. S.; Iyengar, R. R.; Germano, P.; Tang, K.; Bernier, S. G.; Schwartzkopf, C. D.; Tobin, J.; Lee, T. W. H.; Liu, G.; Jacobson, S.; Carvalho, A.; Rennie, G. R.; Jung, J.; Renhowe, P. A.; Lonie, E.; Winrow, C. J.; Hadcock, J. R.; Jones, J. E.; Currie, M. G., The CNS-Penetrant Soluble Guanylate Cyclase Stimulator CY6463 Reveals its Therapeutic Potential in Neurodegenerative Diseases. *Front Pharmacol* 2021, 12, 656561-656561.
- 19 van Kraaij, S. J. W.; Gal, P.; Borghans, L.; Klaassen, E. S.; Dijkstra, F.; Winrow, C.; Glasser, C.; Groeneveld, G. J., First-in-human trial to assess safety, tolerability, pharmacokinetics, and pharmacodynamics of zagogicuat (CY6463), a CNS-penetrant soluble guanylyl cyclase stimulator. *Clin Transl Sci* 2023.
- 20 Buys, E.; Sips, P., New insights into the role of soluble guanylate cyclase in blood pressure regulation. *Current opinion in nephrology and hypertension* 2014, 23 (2), 135-42.
- 21 Ben Aissa, M.; Lee, S. H.; Bennett, B. M.; Thatcher, G. R., Targeting NO/cGMP Signaling in the CNS for Neurodegeneration and Alzheimer's Disease. *Current medicinal chemistry* 2016, 23 (24), 2770-2788.
- 22 Hallak, J. E.; Maia-de-Oliveira, J. P.; Abrau, J.; Evora, P. R.; Zuardi, A. W.; Crippa, J. A.; Belmonte-de-Abreu, P.; Baker, G. B.; Dursun, S. M., Rapid improvement of acute schizophrenia symptoms after intravenous sodium nitroprusside: a randomized, double-blind, placebo-controlled trial. *JAMA psychiatry* 2013, 70 (7), 668-76.
- 23 El-Hattab, A. W.; Emrick, L. T.; Hsu, J. W.; Chanprasert, S.; Almannai, M.; Craigen, W. J.; Jahoor, F.; Scaglia, F., Impaired nitric oxide production in children with MELAS syndrome and the effect of arginine and citrulline supplementation. *Molecular genetics and metabolism* 2016, 117 (4), 407-12.
- 24 Venturelli, M.; Pedrinolla, A.; Boscolo Galazzo, I.; Fonte, C.; Smania, N.; Tamburin, S.; Muti, E.; Crispoltoni, L.; Stabile, A.; Pistilli, A.; Rende, M.; Pizzini, F. B.; Schena, F., Impact of Nitric Oxide Bioavailability on the Progressive Cerebral and Peripheral Circulatory Impairments During Aging and Alzheimer's Disease. *Front Physiol* 2018, 9, 169.
- 25 Alexander, S. P.; Kelly, E.; Marrion, N. V.; Peters, J. A.; Faccenda, E.; Harding, S. D.; Pawson, A. J.; Sharman, J. L.; Southan, C.; Buneman, O. P.; Cidlowski, J. A.; Christopoulos, A.; Davenport, A. P.; Fabbro, D.; Spedding, M.; Striessnig, J.; Davies, J. A., THE CONCISE GUIDE TO PHARMACOLOGY 2017/18: Overview. *British journal of pharmacology* 2017, 174 Suppl 1 (Suppl Suppl 1), S1-s16.
- 26 Lawrence, X. Y.; Li, B. V., *FDA bioequivalence standards*. Springer: 2014; Vol. 13.
- 27 Carter, K. J.; Ward, A. T.; Kellawan, J. M.; Eldridge, M. W.; Al-Subu, A.; Walker, B. J.; Lee, J. W.; Wieben, O.; Schrage, W. G., Nitric oxide synthase inhibition in healthy adults reduces regional and total cerebral macrovascular blood flow and microvascular perfusion. *J Physiol* 2021, 599 (22), 4973-4989.
- 28 Clementi, V.; Tonon, C.; Lodi, R.; Malucelli, E.; Barbiroli, B.; Iotti, S., Assessment of glutamate and glutamine contribution to in vivo N-acetylaspartate quantification in human brain by (1)H-magnetic resonance spectroscopy. *Magnetic resonance in medicine* 2005, 54 (6), 1333-9.
- 29 Haris, M.; Cai, K.; Singh, A.; Hariharan, H.; Reddy, R., In vivo mapping of brain myo-inositol. *NeuroImage* 2011, 54 (3), 2079-85.
- 30 Walter, A.; Korth, U.; Hilgert, M.; Hartmann, J.; Weichel, O.; Hilgert, M.; Fassbender, K.; Schmitt, A.; Klein, J., Glycerophosphocholine is elevated in cerebrospinal fluid of Alzheimer patients. *Neurobiol Aging* 2004, 25 (10), 1299-303.
- 31 Mullins, R.; Reiter, D.; Kapogiannis, D., Magnetic resonance spectroscopy reveals abnormalities of glucose metabolism in the Alzheimer's brain. *Annals of clinical and translational neurology* 2018, 5 (3), 262-272.
- 32 Böger, R. H., Asymmetric dimethylarginine, an endogenous inhibitor of nitric oxide synthase, explains the 'L-arginine paradox' and acts as a novel cardiovascular risk factor. *J Nutr* 2004, 134 (10 Suppl), 2842S-2847S; discussion 2853S.
- 33 Nossaman, B.; Kadowitz, P., Stimulators of Soluble Guanylyl Cyclase: Future Clinical Indications. *The Ochsner journal* 2013, 13, 147-56.
- 34 Gaetani, L.; Blennow, K.; Calabresi, P.; Di Filippo, M.; Parnetti, L.; Zetterberg, H., Neurofilament light chain as a biomarker in neurological disorders. *Journal of neurology, neurosurgery, and psychiatry* 2019, 90 (8), 870-881.
- 35 Groeneveld, G. J.; Hay, J. L.; Van Gerven, J. M., Measuring blood-brain barrier penetration using the NeuroCart, a CNS test battery. *Drug Discov Today Technol* 2016, 20, 27-34.
- 36 Bond, A.; Lader, M., The use of analogue scales in rating subjective feelings. *British Journal of Medical Psychology* 1974, 47 (3), 211-218.
- 37 Gifford, J. R.; Richardson, R. S., CORP: Ultrasound assessment of vascular function with the passive leg movement technique. *J Appl Physiol (1985)* 2017, 123 (6), 1708-1720.
- 38 Peskind, E. R.; Riekse, R.; Quinn, J. F.; Kaye, J.; Clark, C. M.; Farlow, M. R.; Decarli, C.; Chabal, C.; Vavrek, D.; Raskind, M. A.; Galasko, D., Safety and acceptability of the research lumbar puncture. *Alzheimer disease and associated disorders* 2005, 19 (4), 220-5.
- 39 Correia, S. S.; Liu, G.; Jacobson, S.; Bernier, S. G.; Tobin, J. V.; Schwartzkopf, C. D.; Atwater, E.; Lonie, E.; Rivers, S.; Carvalho, A.; Germano, P.; Tang, K.; Iyengar, R. R.; Currie, M. G.; Hadcock, J. R.; Winrow, C. J.; Jones, J. E., The CNS-penetrant soluble guanylate cyclase stimulator CYR119 attenuates markers of inflammation in the central nervous system. *Journal of neuroinflammation* 2021, 18 (1), 213.
- 40 Clement, P.; Mutsaerts, H.-J.; Václavů, L.; Gharib, E.; Pizzini, F. B.; Smits, M.; Acou, M.; Jovicich, J.; Vanninen, R.; Kononen, M.; Wiest, R.; Rostrup, E.; Bastos-Leite, A. J.; Larsson, E.-M.; Achten, E., Variability of physiological brain perfusion in healthy subjects – A systematic review of modifiers. Considerations for multi-center ASL studies. *Journal of Cerebral Blood Flow & Metabolism* 2017, 38 (9), 1418-1437.
- 41 Cosyns, S. M.; Huyghe, L.; Thoonen, R.; Stasch, J. P.; Brouckaert, P.; Lefebvre, R. A., Influence of cinaciguat on gastrointestinal motility in apo-sGC mice. *Neurogastroenterology and motility : the official journal of the European Gastrointestinal Motility Society* 2014, 26 (11), 1573-85.
- 42 Jun, C. H.; Lee, T. S.; Sohn, U. D., NO/cyclic GMP pathway mediates the relaxation of feline lower oesophageal sphincter. *Autonomic and Autacoid Pharmacology* 2003, 23 (3), 159-166.
- 43 Boettcher, M.; Thomas, D.; Mueck, W.; Loewen, S.; Arens, E.; Yoshikawa, K.; Becker, C., Safety, pharmacodynamic, and pharmacokinetic characterization of vericiguat: results from six phase I studies in healthy subjects. *Eur J Clin Pharmacol* 2021, 77 (4), 527-537.
- 44 Ghofrani, H.-A.; Gomez Sanchez, M.-A.; Humbert, M.; Pittrow, D.; Simonneau, G.; Gall, H.; Grünig, E.; Klose, H.; Halank, M.; Langleben, D.; Snijder, R. J.; Escribano Subias, P.; Mielniczuk, L. M.; Lange, T. J.; Vachiéry, J.-L.; Wirtz, H.; Helmersen, D. S.; Tsangaris, I.; Barberá, J. A.; Pepke-Zaba, J.; Boonstra, A.; Rosenkranz, S.; Ulrich, S.; Steringer-Mascherbauer, R.; Delcroix, M.; Jansa, P.; Šimková, I.; Giannakoulas, G.; Klotsche, J.; Williams, E.; Meier, C.; Hoepfer, M.

M.; Caneva, J.; Tuhay, G.; Diez, M.; Talavera, M. L.; Acosta, A.; Vulcano, N.; Bosio, M.; Maldonado, L.; Deleo, S.; Melatini, L.; Keogh, A.; Kotlyar, E.; Feenstra, J.; Dwyer, N.; Adams, H.; Stevens, W.; Steele, P.; Proudman, S.; Minson, R.; Reeves, G.; Lavender, M.; Ng, B.; Mackenzie, M.; Barry, L.; Gruenberger, M.; Huber, C.; Lang, I.; Tilea, I.; Sadushi-Kolici, R.; Löffler-Ragg, J.; Feistmantl, L.-T.; Evrard, P.; Louis, R.; Guiot, J.; Naldi, M.; De Pauw, M.; Mehta, S.; Camacho, R. C.; Tovar, P. P.; Londoño, A.; Campo, F.; Garcia, P.; Lema, C.; Orozco-Levi, M.; Martinez, W.; Gomez, J. E.; Nielsen-Kudsk, J. E.; Mellemkjaer, S.; Anton, L.; Altraja, A.; Vihinen, T.; Vasankari, T.; Sitbon, O.; Cottin, V.; Têtu, L.; Noël-Savina, E.; Shearman, N.; Tayler, S.; Olzik, I.; Kulka, C.; Grimminger, J.; Simon, M.; Nolde, A.; Oqueka, T.; Harbaum, L.; Egenlauf, B.; Ewert, R.; Schulz, C.; Regotta, S.; Kramer, T.; Knoop-Busch, S.; Gerhardt, F.; Konstantinides, S.; Pitsiou, G.; Stanopoulos, I.; Sourla, E.; Mouratoglou, S.; Karvounis, H.; Pappas, A.; Georgopoulos, D.; Fanaridis, M.; Mitrouska, I.; Michalis, L.; Pappas, K.; Kotsia, A.; Gaine, S.; Vizza, C. D.; Manzi, G.; Poscia, R.; Badagliacca, R.; Agostoni, P.; Bruno, N.; Farina, S.; D'Alto, M.; Argiento, P.; Corraera, A.; Di Marco, G. M.; Cresci, C.; Vannucchi, V.; Torricelli, E.; Garcea, A.; Pesci, A.; Sardella, L.; Paciocco, G.; Pane, F.; D'Armini, A. M.; Pin, M.; Grazioli, V.; Massola, G.; Sciortino, A.; Prediletto, R.; Bauleo, C.; Airò, E.; Ndreu, R.; Pavlickova, I.; Lunardi, C.; Mulè, M.; Farruggio, S.; Costa, S.; Galgano, G.; Petrucci, M.; De Luca, A.; Lombardi, F.; Roncon, L.; Conte, L.; Picariello, C.; Wirtz, G.; Alexandre, M.; Vonk-Noordegraaf, A.; Boogaard, H.; Mager, J.; Reesink, H.; van den Toorn, L. M.; Boomars, K.; Andreassen, A. K.; Castro, G.; Tania, G.; Baptista, R.; Marinho, A.; Shiang, T.; Oliveira, A.; Coutinho, D.; Sousa, J.; Loureiro, M. J.; Repolho, D.; Martins Jesus, S. M.; Capinha, M.; Agostinho, J.; Cardoso, T.; Rocha, A.; Espinha, M.; Ivanov, K. I.; Alexeeva, D. E.; Batalina, M. V.; Hegya, D. V.; Zvereva, T. N.; Avdeev, S. N.; Tsareva, N. A.; Galyavich, A. S.; Nikolaevich, B. A.; Filippov, E. V.; Yakovleva, O. E.; Pavlova, O. B.; Skripkina, E. S.; Martynyuk, T. V.; Bukatova, I. F.; Tregubova, A. V.; Platonov, D. Y.; Kolomeytseva, T. M.; Al Dalaan, A.; Abdelsayed, A. A.; Weheba, I.; Saleemi, S.; Sakkijha, H.; Bohacekova, M.; Valkovicova, T.; Farkasova, I.; Quezada, C. A.; Piccari, L.; Blanco, I.; Sebastian, L.; Roman, A.; Lopez, M.; Otero, R.; Elias, T.; Jara, L.; Asencio, I.; Arjona, J. J.; Almagro, R. M.; Cárdenas, S. L.; García, S. A.; Rodríguez, P. V.; Lopez, R.; Garcia, A.; Avilés, F. F.; De La Pava, S.; Yotti, R.; Peñate, G. P.; Marrero, F. L.; Cifrián Martínez, J. M.; Martínez-Meñaca, A.; Alonso, L. P.; Rozas, S. F.; Fernandez, D. I.; Cuesta, V. M.; Söderberg, S.; Bartfay, S.-E.; Rundqvist, B.; Alfetlawi, M.; Wodlin, P.; Schwarz, E.

I.; Speich, R.; Lador, F.; Rochat, T.; Gasche-Soccal, P.; Hsu, C.-H.; Lin, T.-H.; Su, H.-M.; Lai, W.-T.; Chu, C. Y.; Hsu, P.-C.; Voon, W.-C.; Yen, H.-W.; Yih-Jer Wu, J.; Wu, S.-H.; Huang, W.-P.; Fong, M.-C.; Huang, C.-L.; Kuo, P.-H.; Lin, Y.-H.; Lin, J.-L.; Hung, C.-S.; Wu, C.-K.; Sung, S.-H.; Huang, W.-C.; Cheng, C.-C.; Kuo, S.-H.; Wang, W.-H.; Ho, W.-J.; Hsu, T.-S.; Mutlu, B.; Atas, H.; Ongen, G.; Un, Z.; Okumus, G.; Un, Z.; Hant, I.; Corris, P.; Peacock, A.; Church, C.; Toshner, M.; Newnham, M., Riociguat treatment in patients with chronic thromboembolic pulmonary hypertension: Final safety data from the EXPERT registry. *Respiratory Medicine* **2021**, *178*, 106220.

45 Conole, D.; Scott, L. J., Riociguat: First Global Approval. *Drugs* **2013**, *73* (17), 1967-1975.

46 Hanrahan, J. P.; Wakefield, J. D.; Wilson, P. J.; Mihova, M.; Chickering, J. G.; Ruff, D.; Hall, M.; Milne, G. T.; Currie, M. G.; Profy, A. T., A Randomized, Placebo-Controlled, Multiple-Ascending-Dose Study to Assess the Safety, Tolerability, Pharmacokinetics, and Pharmacodynamics of the Soluble Guanylate Cyclase Stimulator Pralicyguat in Healthy Subjects. *Clinical pharmacology in drug development* **2019**, *8* (5), 564-575.

47 Levy, D.; Strassman, A. M., Modulation of Dural Nociceptor Mechanosensitivity by the Nitric Oxide-Cyclic GMP Signaling Cascade. *Journal of Neurophysiology* **2004**, *92* (2), 766-772.

48 Holthusen, H.; Arndt, J. O., Nitric oxide evokes pain at nociceptors of the paravascular tissue and veins in humans. *J Physiol* **1995**, *487* (1), 253-8.

49 Levy, D.; Tal, M.; Höke, A.; Zochodne, D. W., Transient action of the endothelial constitutive nitric oxide synthase (ecNOS) mediates the development of thermal hypersensitivity following peripheral nerve injury. *The European journal of neuroscience* **2000**, *12* (7), 2323-32.

50 Ben Aissa, M.; Tipton, A. F.; Bertels, Z.; Gandhi, R.; Moye, L. S.; Novack, M.; Bennett, B. M.; Wang, Y.; Litosh, V.; Lee, S. H.; Gaisina, I. N.; Thatcher, G. R. J.; Pradhan, A. A., Soluble guanylyl cyclase is a critical regulator of migraine-associated pain. *Cephalalgia* **2017**, *38* (8), 1471-1484.

51 Michimata, T.; Imamura, M.; Mizuma, H.; Murakami, M.; Iriuchijima, T., Sex and age differences in soluble guanylate cyclase activity in human platelets. *Life sciences* **1996**, *58* (5), 415-9.

CHAPTER VII

EFFECTS OF THE PHOSPHODIESTERASE 2 INHIBITOR BI 474121 ON CENTRAL NERVOUS SYSTEM CYCLIC GUANOSINE MONOPHOSPHATE CONCENTRATIONS: TRANSLATIONAL STUDIES

Sebastiaan van Kraaij,^{1,2} Rainer-Georg Goeldner,³ Holger Rosenbrock,³
Geert Jan Groeneveld,^{1,2} Philip Kremer,^{1,2} Jennifer Schaible,³
Janos Zambori,³ Christian Schultheis³

1: Leiden University Medical Center, Leiden, NL

2: Centre for Human Drug Research, Leiden, NL

3: Boehringer Ingelheim Pharma GmbH & Co. KG, Biberach an der Riss, D

Study Highlights

WHAT IS THE CURRENT KNOWLEDGE ON THE TOPIC?

Schizophrenia is characterized by dysfunction in glutamatergic pathways related to N-methyl-D-aspartate (NMDA) receptor hypofunction, providing the rationale for normalization of glutamate-mediated neurotransmission as a treatment for cognitive impairment associated with schizophrenia. Phosphodiesterase 2 (PDE2) inhibitors have been shown to be effective in improving cognitive deficits in animal models.

WHAT QUESTION DID THIS STUDY ADDRESS?

This study assessed the brain penetration of BI 474121 and inhibition of PDE2 through measuring increases in cerebrospinal fluid (CSF) cyclic guanosine monophosphate (cGMP) levels in rats and healthy male participants. The safety of BI 474121 in healthy male participants was also assessed.

WHAT DOES THIS STUDY ADD TO OUR KNOWLEDGE?

BI 474121, a novel PDE2 inhibitor, in clinical development for treatment of cognitive impairment associated with schizophrenia (CIAS), crosses the blood brain barrier and reaches relevant concentrations; BI 474121 inhibits PDE2 in the brain as indicated by elevated cGMP levels in CSF. BI 474121 also has a favourable safety profile.

HOW MIGHT THIS CHANGE CLINICAL PHARMACOLOGY OR TRANSLATIONAL SCIENCE

This study supports cGMP as a translational marker across species to monitor central (i.e., brain-based) and functional target engagement.

Abstract

Phosphodiesterase 2 (PDE2) regulates intracellular cyclic adenosine monophosphate and guanosine monophosphate (cAMP/cGMP) levels, which contribute to processes crucial for learning and memory. BI 474121, a potent PDE2 inhibitor, is in development for the treatment of cognitive impairment associated with schizophrenia. The effects of BI 474121 on cGMP concentrations in rat cerebrospinal fluid (CSF) were assessed to demonstrate central nervous system and functional target engagement. Next, a Phase I study was conducted in healthy participants to assess the pharmacokinetics of BI 474121 in CSF relative to plasma, the pharmacodynamics of BI 474121 by measuring cGMP concentrations in the CSF, and the safety of BI 474121. In rats, BI 474121 was associated with a dose-dependent increase (71% at the highest dose tested [3.0 mg/kg]) in cGMP levels in the CSF relative to vehicle ($p < 0.001$). In healthy participants, the maximum-measured concentration CSF-to-plasma ratio for BI 474121 exposure was similar following single oral doses of BI 474121 at 2.5, 10, 20, or 40 mg (dose-adjusted geometric mean: 8.96% overall). BI 474121 2.5–40 mg administration in healthy participants also increased cGMP levels in CSF (maximum exposure-related change from baseline ratio, BI 474121: 1.44–2.20 vs placebo: 1.26). The most common treatment-emergent adverse event (AE) was mild-to-moderate post-lumbar puncture syndrome, which resolved with standard treatment. No AES of special interest were observed. These findings demonstrate BI 474121 crosses the blood-brain barrier to inhibit PDE2, support cGMP as a translational marker to monitor central nervous system target engagement and promotes further clinical development of BI 474121.

Introduction

Schizophrenia is characterized by glutamatergic dysfunction related to *N*-methyl-D-aspartate (NMDA) receptor hypofunction,¹⁻² which is associated with cognitive deficits.³ Thus, normalization of glutamate-mediated neurotransmission may provide a potential therapeutic target for the treatment of cognitive impairment associated with schizophrenia (CIAS).

Cyclic adenosine monophosphate (cAMP) and cyclic guanosine monophosphate (cGMP) are neuronal second messengers involved in synaptic plasticity and neural network functions important for learning and memory performance.⁴ As phosphodiesterases (PDE), such as PDE2, can regulate these processes by hydrolyzing cAMP and cGMP,⁵ inhibitors of PDE2 may increase neuronal pre-synaptic levels of cAMP and cGMP.⁶ This may in turn lead to a subsequent increase in synaptic function by facilitating glutamate release in brain regions involved in learning and memory, since cGMP is known to increase glutamatergic signaling.⁷ Therefore, PDE2 inhibition may result in a functional potentiation of glutamatergic neurotransmission and NMDA receptor function and thus improve network function and synaptic plasticity. This concept is supported by preclinical findings showing that PDE2 inhibitors are associated with pro-cognitive effects in rodents.⁸⁻¹⁰

BI 474121, a novel PDE2 inhibitor, has been developed for the treatment of CIAS. A previous Phase I study has demonstrated that single doses of BI 474121 (0.25–40 mg) have a favorable safety profile in healthy participants.¹¹ Following on from these findings, the objective of these studies was to firstly assess the effects of BI 474121 on cGMP levels in rat CSF to investigate whether BI 474121 can achieve central and functional target engagement in the brain. Secondly, to translate preclinical findings into humans, a Phase I study was conducted in healthy participants to assess the pharmacokinetics (PK) of BI 474121 in CSF relative to plasma, evaluate the pharmacodynamics (PD) of BI 474121 by measuring cGMP in the CSF and determine the exposure–effect relationship in CSF following BI 474121 administration. The safety of BI 474121 was also assessed.

Methods

PRECLINICAL ANIMALS

Procedures involving animals and their care were performed in conformity with institutional guidelines and European legislation on the use and care of laboratory animals (CEE 86/609 at time of study) and approved by the ethics committee of the responsible regional council. Adult male Wistar rats (CrI:WI[Han], Charles River, Sulzfeld, Germany) weighing 250–300 g on the experimental day were housed in groups of four per cage (33×55×27 cm) with a controlled temperature (22±1 °C) and 12-hour light–dark cycle (lights on at 6 a.m.). Standard rodent lab chow and water were available ad libitum. Before the experiment, rats were allowed to adjust to the new environment for 10 days.

PROCEDURES

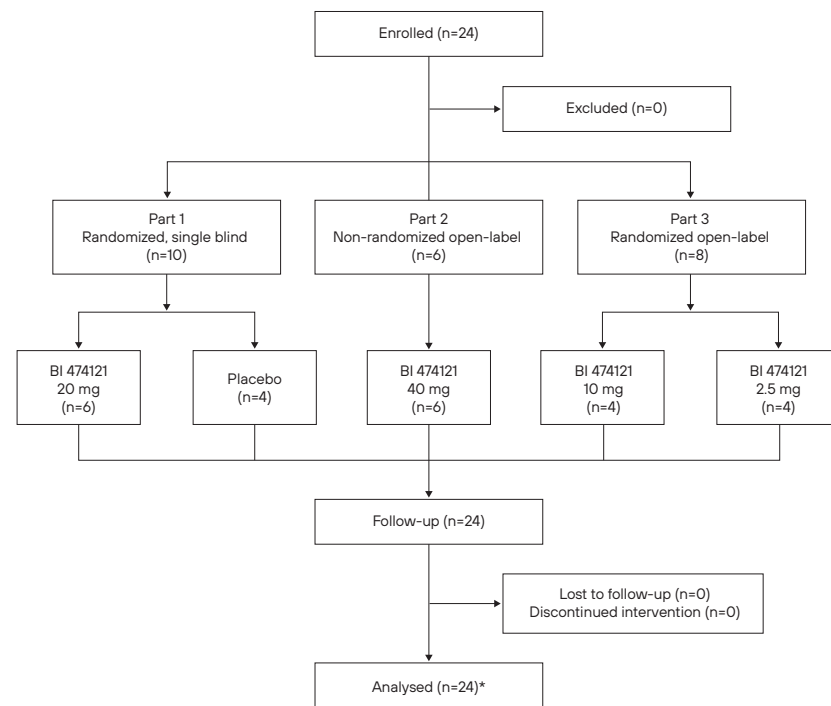
Rats received single oral doses of vehicle (n=8), or BI 474121 0.3 mg/kg (n=8), 1.0 mg/kg (n=8), or 3.0 mg/kg (n=8), with an application volume of 5 mL/kg body weight. After 30 minutes, the animals were fixed in a stereotaxic apparatus under anaesthesia (with subcutaneous inactin 0.85 mL/kg plus ketavet 0.75 mL/kg) and CSF samples (50–100 µL) were collected through the cisterna magna and centrifuged at 10,000 rpm at 4 °C for 5 minutes. The cGMP concentration was determined by cGMP-enzyme-linked immunosorbent assay (ELISA; Enzo Life Sciences Inc., Farmingdale, NY) according to manufacturer's instructions. The BI 474121 levels in CSF probes were determined by high performance liquid chromatography–tandem mass spectrometry (HPLC-MS/MS).

CLINICAL STUDY

The Phase I clinical trial was conducted in three sequential parts with progression dependent on preliminary data analyses (Figure 1). Part 1 was a randomized, placebo-controlled, single-blind study, while Part 2 was a non-randomized study, and Part 3 a randomized open-label study. The trial was conducted at the Centre for Human Drug Research, the Netherlands. Healthy males (N=24) were admitted to the site the day before treatment administration and remained in-house until Day 3. The trial was conducted in compliance with the clinical trial protocol, in accordance with the principles of the Declaration of Helsinki,¹² the International Council for Harmonization Good Clinical Practice,¹³ applicable regulatory requirements, and Boehringer Ingelheim (BI) standard operating procedures. The protocol was approved by the Medical Research Ethics Committee of

the BEBO foundation (Assen, The Netherlands) and prospectively registered in EudraCT (number 2020-002321-28), toetsingonline.nl (CHDR2017, ABR-number 75798), and clinicaltrials.gov (NCT04672954). Participants provided written informed consent prior to enrolment.

FIGURE 1 CONSORT flow diagram of the Phase I clinical study in healthy participants.



*One participant was excluded from PK and PD analysis due to vomiting close to drug administration. PD=pharmacodynamic; PK=pharmacokinetic.

PARTICIPANTS

Participants were healthy male volunteers, >18–≤65 years of age, with a body mass index (BMI) of 18.5–29.9 kg/m². Participants were deemed healthy according to the investigator's assessment based on a complete medical history, physical examination, vital signs (blood pressure and pulse rate), 12-lead electrocardiogram (ECG), and clinical laboratory tests.

Participants were excluded if abnormal findings from these tests were deemed clinically relevant by the investigator, or if evidence of a concomitant disease was identified. Other exclusion criteria included: gastrointestinal, hepatic, renal, respiratory, cardiovascular, metabolic, immunological, or hormonal disorders; diseases of the central nervous system (CNS); other neurological disorders or psychiatric disorders; cholecystectomy or other surgery of the gastrointestinal tract interfering with the PK of the trial medication; history of relevant orthostatic hypotension; fainting spells or blackouts; and chronic or relevant acute infections. Additional exclusion criteria are listed in Supplementary methods.

TREATMENTS

Participants were assigned to four BI 474121 dose levels (2.5, 10, 20, or 40 mg) with drug administered sequentially across all study parts (Figure 1). In Part 1, subjects were randomized in a 3:2 ratio, receiving a single-blind dose of BI 474121 20 mg (n=6) or placebo (n=4). In Part 2, participants received a single, open-label dose of BI 474121 40 mg (n=6). In Part 3, participants were randomized in a 1:1 ratio, receiving a single open-label dose of BI 474121 of either 2.5 mg (n=4) or 10 mg (n=4). All participants received doses in the morning after fasting overnight.

The 20 mg and 40 mg doses were estimated to be supratherapeutic based on the preclinical efficacy data in rats. These doses were chosen to elicit a level of BI 474121 exposure in the CSF anticipated to induce a cGMP increase from baseline to demonstrate functional target engagement in the brain. The 2.5 mg and 10 mg doses were chosen to support the plasma-exposure-to-effect relationship and evaluate the plasma-to-CSF ratio around the projected therapeutic dose. A single-dose administration of BI 474121 was considered sufficient based on the preclinical data in rat CSF, previous experience with cGMP assessment in CSF with a PDE9 inhibitor,¹⁴ and an acceptable adverse event (AE) profile in a single rising dose study.^{11,14} The open-label design in Parts 2 and 3 was not expected to bias results, since the primary and secondary study endpoints are derived from plasma and CSF concentrations of the analytes, and placebo participants from Part 1 served as control.

STUDY ENDPOINTS

PHARMACOKINETICS

The primary PK endpoint was the maximum measured concentration (C_{max}) ratio of BI 474121 in CSF versus plasma. Secondary PK endpoints were the C_{max} and time from dosing to C_{max} of BI 474121 in CSF and plasma (T_{max}). Further

PK endpoints included the areas under the CSF and plasma concentration-time profile from time point 0 to the last measurable time point (AUC_{0-tz}) and AUC from 0 to 24 hours (AUC_{0-24}) for BI 474121.

PHARMACODYNAMICS

The primary PD endpoint was the maximum exposure-related change from baseline of cGMP in the CSF, calculated as a ratio. The secondary PD endpoint was the maximum measured exposure-related cGMP concentration in the CSF (E_{max}). For patients receiving BI 474121, 'exposure-related' refers to measures within 1 hour prior to and 4 hours after attainment of C_{max} in the CSF. For patients treated with placebo, exposure-related measures occurred within 1 hour prior to and 4 hours after the median BI 474121 T_{max} in the CSF of participants treated with 40 mg BI 474121. Additional PD endpoints included the area under the biomarker effect versus time curve from time point 0 to the last quantifiable data point ($AUEC_{0-tz}$) of cGMP in CSF, and time from dosing to E_{max} (T_{max}). The relative change from baseline (ratio) was also assessed for E_{max} , $AUEC_{0-tz}$ and T_{max} .

SAFETY MEASUREMENTS

Safety of BI 474121 was assessed based on AES, vital signs (blood pressure, pulse rate), physical examination, safety laboratory tests, and 12-lead ECG. An AE was defined as any untoward medical occurrence in a trial participant. Drug-related AES were assessed by the investigator to have a possible causal relationship to the trial medication. A serious AE (SAE) was defined as any AE that resulted in death, was immediately life-threatening, required/prolonged hospitalization, resulted in persistent or significant disability or incapacity, was a congenital anomaly/birth defect, or deemed serious for any other reason. AES of special interest were hepatic injury, defined as an elevation of aspartate transaminase (AST) and/or alanine transaminase (ALT) ≥ 3 -fold upper limit of normal (ULN) combined with an elevation of total bilirubin ≥ 2 -fold ULN measured in the same blood sample, or ALT and/or AST elevations ≥ 10 -fold ULN. No concomitant therapy was planned and known inhibitors/inducers of cytochrome P450 3A4 (CYP3A4) activity were avoided during the study due to potential drug-drug interactions. If AES required treatment, symptomatic therapy was allowed.

ASSESSMENTS

CSF was serially collected through a spinal catheter (External Drainage and Monitoring System lumbar catheter set [closed tip, barium impregnated],

Medtronic). On Day 1, pre-dosing samples were taken at 3 time points ≤ 3 hours prior to drug administration. Post-dosing CSF samples were collected at 30-minute intervals for the first 2 hours, 1-hour intervals through 8 hours, 2-hour intervals through 14 hours, and at 24 hours after dosing. Plasma samples were collected prior to drug administration, 15 minutes and 30 minutes after administration, then following the same schedule as post-dosing CSF samples, with additional samples at 24-hour intervals on Days 2–4 (Figure S1). In total, 19 plasma samples (PK analysis) and 17 CSF samples (PK and PD analysis) were collected. BI 474121 CSF and plasma concentrations were determined using a validated LC-MS/MS assay. cGMP CSF concentrations were also analysed using LC-MS/MS, with [$^{15}N_6$] cGMP as an internal standard; samples were subjected to solid phase extraction followed by reversed-phase LC with gradient elution. Detection and quantification were performed by MS/MS using electrospray ionization in the positive ion mode. The lower limit of quantification was defined as 0.10 nmol/L, and the upper limit of quantification as 10.0 nmol/L. LC-MS/MS assays were conducted at Boehringer Ingelheim Pharma GmbH & Co.KG, Drug Metabolism and Pharmacokinetics, Germany.

STATISTICAL ANALYSIS

PRECLINICAL

Quantitative data are presented as mean \pm standard error of the mean (SEM). Comparisons between vehicle and BI 474121-treated groups were performed by one-way analysis of variance (ANOVA) followed by Dunnett's multiple comparisons post hoc analysis. Statistical computations were conducted using GraphPad Prism; $p < 0.05$ was deemed to be statistically significant.

CLINICAL

Statistical analyses were based on the following analysis sets: Treated Set (all participants who were entered/randomized and treated with one dose of study drug); PK Set (participants in the treated set who contributed to ≥ 1 PK primary/secondary endpoint); and PD Set (all evaluable participants from the treated set who provided ≥ 1 pre- and post-dose measure for a PD endpoint). All statistical analyses were performed using SAS (version 9.4, SAS Institute Inc., Cary, NC, USA). Data were reported as descriptive statistics. The primary PK and PD endpoints were assessed using a mixed effects model and an analysis of covariance, respectively. The dose proportionality of BI 474121 was also assessed for C_{max} and AUC_{0-tz} using a Power model (described in Supplementary methods). Further PK and PD endpoints were graphically analysed to determine whether

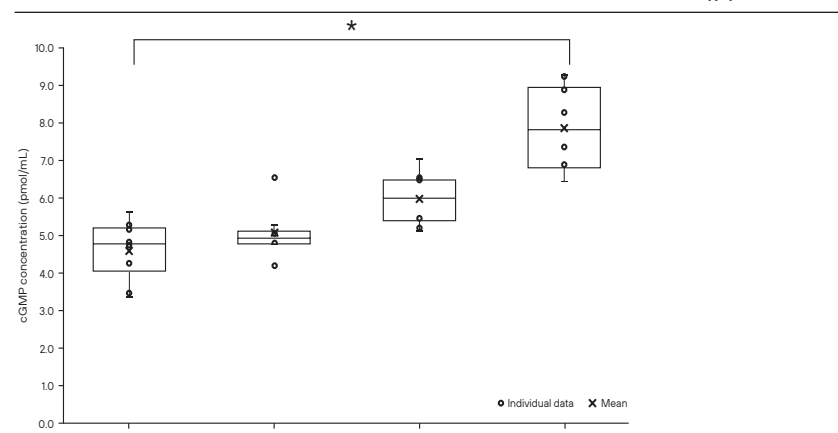
there was a relationship between BI 474121 exposure (C_{\max} and AUC_{0-24} in the CSF) and E_{\max} values of relative change from baseline in cGMP concentration in the CSF.

Results

PRECLINICAL

Single oral administration of BI 474121 induced a dose-dependent increase in CSF cGMP concentrations (Figure 2). The mean cGMP concentration was significantly increased relative to vehicle following administration of BI 474121 3 mg/kg (71% increase, $p < 0.001$). Increases in CSF cGMP levels were also seen with BI 474121 0.3 mg/kg (8%) and 1 mg/kg (30%) relative to vehicle, but increases were not statistically significant. At the time-point of CSF sampling, mean CSF exposure levels of BI 474121 were 1.9 ± 0.4 nM, 7.8 ± 0.8 nM and 27.2 ± 1.6 nM at 0.3, 1, and 3 mg/kg, respectively.

FIGURE 2 CGMP concentrations in the rat CSF after oral treatments with BI 474121.



* $p < 0.001$. CGMP=cyclic guanosine monophosphate; CSF=cerebrospinal fluid.

CLINICAL

STUDY POPULATION

All 24 participants who entered the trial received BI 474121 or placebo and completed the planned observation time (Figure 1). One participant was excluded from the PK and PD analyses due to vomiting close to drug administration. All

participants were healthy males, and most were White ($n=21$). The mean (standard deviation [SD]) age was 30.5 (14.9) years and the mean (SD) BMI was 22.69 (2.35) kg/m^2 . Demographic characteristics were generally similar between the groups, except for age, which ranged from a mean (SD) age of 22.0 (3.2) years in the 10 mg BI 474121 group to 41.5 (24.3) years in the placebo group (Table S1).

PHARMACOKINETICS

After single oral doses of BI 474121, the C_{\max} adjusted geometric mean ratio in CSF to plasma was 8.96% overall and ranged from 7.88% to 9.89% across the individual dose groups (Table 1). Following BI 474121 administration, the CSF and plasma concentrations of BI 474121 increased dose-dependently across the dose range tested. All treatment groups showed similarly shaped CSF and plasma concentration-time profiles, characterized by a rapid absorption phase followed by a disposition phase (Figure 3). The C_{\max} in CSF was markedly lower than in plasma following all doses (Table 1). After reaching C_{\max} , CSF concentrations decreased in parallel with plasma concentrations. The maximum CSF and plasma concentrations were reached at a median T_{\max} of 2.03–4.03 hours and 1.50–4.00 hours across all doses, respectively. The BI 474121 median T_{\max} in CSF was similar to or later than in plasma at the corresponding dose level, except for the 2.5 mg dose group where median T_{\max} in CSF was shorter versus plasma (Table 1). Exposure to BI 474121 in both CSF and plasma also increased in a dose-proportional manner for AUC_{0-tz} (Table 1). Statistical analysis of the dose proportionality of BI 474121 in CSF and plasma showed no substantial deviation from dose proportionality in the exposure parameters of C_{\max} and AUC_{0-tz} (Table S2). Although the 90% CI of the slope (β) did not include 1 for C_{\max} , the upper limit of the 90% CI remained close to 1; for AUC_{0-tz} , the slopes were close to 1 and the 90% CI included 1 for both CSF and plasma (Table S2).

TABLE 1 Summary of BI 474121 PK parameters in CSF and plasma (Pharmacokinetic Set).

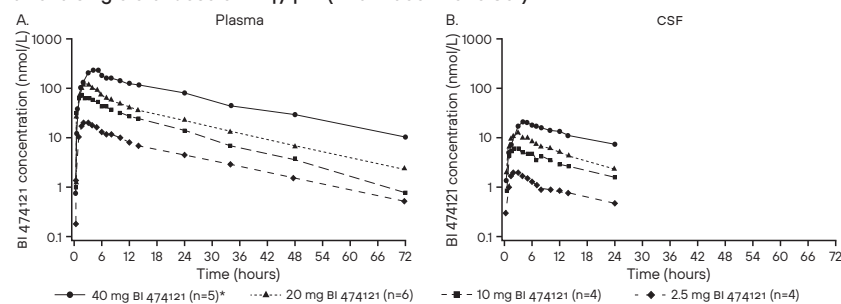
	Overall (N=19)	BI 474121 2.5 mg (n=4)	BI 474121 10 mg (n=4)	BI 474121 20 mg (n=6)	BI 474121 40 mg (n=5)
Comparison of C_{\max} ratio of BI 474121 in CSF to plasma					
C_{\max} adjusted gMean	8.96	9.49	7.88	9.89	8.42
ratio in CSF to plasma, % (90% CI of adjusted G_{mean} ratio) ^{1,2}	(8.37, 9.59)	(8.27, 10.89)	(6.86, 9.04)	(8.84, 11.07)	(7.45, 9.53)

(Continuation Table 1)

	Overall (N=19)	BI 474121 2.5 mg (n=4)	BI 474121 10 mg (n=4)	BI 474121 20 mg (n=6)	BI 474121 40 mg (n=5)
Comparison of C_{max} ratio of BI 474121 in CSF to plasma					
CSF					
C _{max} , nmol/L, G _{mean} (%GCV)	-	2.09 (27.9)	6.87 (25.9)	13.6 (9.17)	23.5 (25.0)
T _{max} , h, median (min-max)	-	2.03 (2.03-4.02)	2.03 (1.02-3.02)	3.02 (2.03-3.07)	4.03 (2.03-5.12)
AUC _{0-tz} , h*nmol/L, G _{mean} (%GCV)	-	22.3 (18.6)	78.3 (18.1)	139 (15.4)	300 (25.9)
AUC ₀₋₂₄ , h*nmol/L, G _{mean} (%GCV)	-	22.2 (18.6)	78.1 (18.0)	138 (15.4)	299 (25.9)
Plasma					
C _{max} , nmol/L, G _{mean} (%GCV)	-	22.0 (30.0)	87.2 (30.3)	137.0 (21.7)	278.0 (13.4)
T _{max} , h, median (min-max)	-	4.00 (1.50-5.02)	1.50 (1.00-3.00)	2.01 (1.00-3.00)	4.00 (1.50-5.08)
AUC _{0-tz} , h*nmol/L, G _{mean} (%GCV)	-	332 (30.4)	1030 (29.2)	1740 (28.7)	4860 (15.1)
AUC ₀₋₂₄ , h*nmol/L, G _{mean} (%GCV)	-	237 (27.7)	820 (26.2)	1280 (24.2)	3210 (11.2)

1. Data were analyzed using a mixed effects model; 2. Intra-individual GCV was the same for all dose groups as it was derived from the same model (GCV was 12.3 % [overall], and 11.1 % [BI474121 2.5-40 mg]). AUC_{0-tz}=area under the concentration-time curve of the analyte in CSF over the time interval from 0 to the last quantifiable data point; C_{max}=maximum measured concentration; CI=confidence interval; CSF=cerebrospinal fluid; GCV=geometric coefficient of variation; G_{mean}=geometric mean; max=maximum; min=minimum; PK=pharmacokinetic; SE=standard error; T_{max}=time to reach C_{max}.

FIGURE 3 Geometric mean BI 474121 concentration-time profiles in (A) CSF and (B) plasma after a single oral dose of BI 474121 (Pharmacokinetic Set).



The concentration-time profiles in CSF and plasma are displayed using a semi-logarithmic scale. CGMP = cyclic guanosine monophosphate; CFB = change from baseline; CSF = cerebrospinal fluid.

PHARMACODYNAMICS

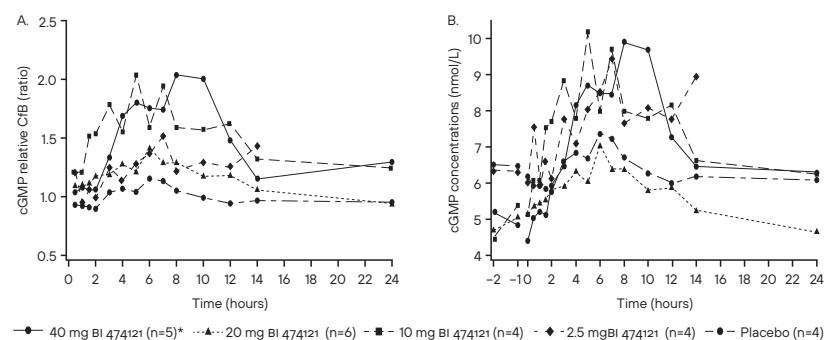
The maximum exposure-related relative change from baseline of CSF cGMP was higher for all BI 474121-treated groups (adjusted GEOMEAN: 1.44-2.20) versus placebo (1.26, Table 2); the most marked change was observed in the 10 mg and 40 mg dose groups. Corrected for placebo, the adjusted geometric mean ratios ranged from 1.14 in the 20 mg dose group to 1.75 in the 40 mg dose group. The relative change from baseline in CSF cGMP ratios showed similar profiles over time for placebo and BI 474121 dose groups, characterized by an increase from the baseline values, peaking at 4-8 hours, followed by a decline (Figure 4A). The increase in cGMP concentration in the placebo group was small and returned to approximately baseline levels by 24 hours. In the BI 474121 dose groups, a more substantial increase was observed for the first 1-8 hours post-treatment followed by a decline to above baseline values (2.5 mg, 10 mg, and 40 mg treatment groups) or a return to approximately baseline values (20 mg treatment group) (Figure 4A). The geometric mean CSF cGMP concentration increased differently across dose groups and throughout the sampling period; the geometric coefficient of variation ranged from 10.0%-87.7% across BI 474121 dose groups) (Figure 4B). A summary of the pharmacodynamic parameters of cGMP in the CSF are reported in Table S3. The cGMP relative changes from baseline E_{max} and AU_{EC0-TZ} were generally higher for the BI 474121-dose groups versus placebo, except for the 2.5 mg (AU_{EC0-TZ}) and 20 mg dose (E_{max} and AU_{EC0-TZ}) groups, but values did not substantially differ between the BI 474121 dose groups overall.

TABLE 2 The maximum exposure-related¹ change from baseline (ratio) of CGMP in CSF following treatment (Pharmacodynamic Set).

	Change from baseline				Comparison vs placebo		
	Adjusted gMean	GSE	90% CI		Ratio	90% CI	
			Lower limit	Upper limit		Lower limit	Upper limit
Placebo (n=4)	1.26	1.24	0.87	1.82	-	-	-
2.5 mg (n=4)	1.62	1.23	1.12	2.33	1.29	0.78	2.13
10 mg (n=4)	2.09	1.23	1.46	2.99	1.66	0.99	2.79
20 mg (n=6)	1.44	1.18	1.07	1.93	1.14	0.71	1.85
40 mg (n=5)	2.20	1.20	1.59	3.04	1.75	1.06	2.89

1. Data were analyzed using an analysis of covariance model. The maximum CGMP change from baseline ratios between the time interval from 1 hour prior to and 4 hours after the individual BI 474121 T_{max}. For participants receiving placebo, the median T_{max} from the 40 mg BI 474121 dose group was used. CI=confidence interval; CGMP=cyclic guanosine monophosphate; CSF=cerebrospinal fluid; GSE=geometric standard error; T_{max}=time to reach C_{max}.

FIGURE 4 Geometric mean effect-time profiles of (A) cGMP relative change from baseline in CSF (ratio) and (B) cGMP concentration after single oral administration of BI 474121 (Pharmacodynamic Set).



*One participant was excluded due to vomiting close to drug intake. CGMP=cyclic guanosine monophosphate; CFB=change from baseline; CSF=cerebrospinal fluid.

PHARMACOKINETIC/PHARMACODYNAMIC RELATIONSHIP

There was no exposure-response relationship between the E_{max} of the relative change from baseline in cGMP concentration in the CSF and either CSF BI 474121 C_{max} (Fig. S2A) or AUC_{0-24} (Fig. S2B) after single oral administration of BI 474121.

SAFETY

Treatment-emergent AEs were reported for all participants treated with BI 474121 or placebo (Table 3). No participants experienced an AE that led to discontinuation of the trial medication, an AE of special interest, or a SAE. The most frequently experienced AEs were post-lumbar syndrome ($n=21$) and musculoskeletal pain ($n=11$). All AEs were mild-to-moderate in intensity.

Investigator-defined drug-related AEs were reported for 10 participants (placebo: $n=1$; 2.5 mg: $n=2$; 10 mg: $n=3$; 20 mg: $n=2$; 40 mg: $n=2$). The most common drug-related AEs were fatigue (2.5 mg: $n=1$; 10 mg: $n=2$), feeling hot (2.5 mg: $n=1$; 10 mg: $n=1$), and headache (placebo: $n=3$; 10 mg: $n=2$; 20 mg: $n=1$).

AEs had resolved by the end of the observation period except for two (tinnitus and post-lumbar puncture syndrome) in one participant. Follow-up activities for this participant indicated that all AEs had resolved following treatment. No clinically relevant abnormalities in laboratory parameters, vital signs, ECGs, and medical examination including the liver enzymes (ALT/AST), or AEs related to these, were reported.

TABLE 3 Treatment-emergent AEs in $\geq 5\%$ participants (total frequency) in any one system organ class (Treated Set).

System organ class/ preferred term, N (%) [*]	Placebo (n=4)	BI 474121 2.5 mg (n=4)	BI 474121 10 mg (n=4)	BI 474121 20 mg (n=6)	BI 474121 40 mg (n=6)	Total
Any AE	4 (100)	4 (100)	4 (100)	6 (100)	6 (100)	24 (100)
Injury, poisoning and procedural complications	3 (75.0)	4 (100)	4 (100)	5 (83.3)	5 (83.3)	21 (87.5)
Post-lumbar puncture syndrome	3 (75.0)	4 (100)	4 (100)	5 (83.3)	5 (83.3)	21 (87.5)
Nervous system disorders	3 (75.0)	2 (50.0)	4 (100)	3 (50.0)	2 (33.3)	14 (58.3)
Headache	3 (75.0)	0	2 (50.0)	1 (16.7)	0	6 (25.0)
Paresthesia	1 (25.0)	1 (25.0)	1 (25.0)	0	2 (33.3)	5 (20.8)
Neuralgia	1 (25.0)	1 (25.0)	1 (25.0)	0	0	3 (12.5)
CSF leakage	1 (25.0)	0	0	1 (16.7)	0	2 (8.3)
Somnolence	0	0	0	1 (16.7)	1 (16.7)	2 (8.3)
Gastrointestinal disorders	1 (25.0)	2 (50.0)	3 (75.0)	1 (16.7)	4 (66.7)	11 (45.8)
Nausea	1 (25.0)	2 (50.0)	1 (25.0)	0	4 (66.7)	8 (33.3)
Vomiting	1 (25.0)	1 (25.0)	2 (50.0)	0	1 (16.7)	5 (20.8)
Musculoskeletal and connective tissue disorders	2 (50.0)	3 (75.0)	2 (50.0)	2 (33.3)	2 (33.3)	11 (45.8)
Musculoskeletal pain	2 (50.0)	3 (75.0)	2 (50.0)	2 (33.3)	2 (33.3)	11 (45.8)
General disorders and administration site conditions	0	2 (50.0)	3 (75.0)	0	3 (50.0)	8 (33.3)
Catheter site pain	0	1 (25.0)	1 (25.0)	0	2 (33.3)	4 (16.7)
Fatigue	0	1 (25.0)	2 (50.0)	0	0	3 (12.5)
Feeling hot	0	1 (25.0)	1 (25.0)	0	0	2 (8.3)
Ear and labyrinth disorders	0	1 (25.0)	0	1 (16.7)	1 (16.7)	3 (12.5)
Tinnitus	0	1 (25.0)	0	0	1 (16.7)	2 (8.3)
Skin and subcutaneous tissue disorders	0	1 (25.0)	1 (25.0)	0	0	2 (8.3)

*Each participant could be counted in more than one category. AE=adverse event.

Discussion

These studies evaluating the effects of BI 474121, a novel PDE2 inhibitor, on cGMP concentrations in rat and human CSF demonstrated that functional target engagement was achieved in both models. In the preclinical study, single oral administration of BI 474121 resulted in a dose-dependent increase in CSF cGMP concentrations. Similarly, CSF cGMP concentrations increased in the clinical study following BI 474121 administration, though without a clear dose-response relationship. Nonetheless, this elevation of CSF cGMP concentrations suggests PDE2 inhibition by BI 474121 in the central nervous system, in humans.

Plasma and CSF concentration profiles in humans showed that BI 474121 was rapidly absorbed and concentrations increased dose-dependently across the dose range tested. The CSF-to-plasma C_{max} ratio remained relatively constant

across the observed dose range, suggesting that distribution of BI 474121 is not altered at higher doses.

Clinical PD data showed that the mean CSF cGMP concentration profiles had similar patterns between placebo and BI 474121 groups, initially increasing from baseline then returning to close to baseline levels within 24 hours. The initial increase in the placebo group indicates a possible circadian effect. A previous study with a PDE9 inhibitor showed a similar increase in the cGMP concentration profile with placebo.¹⁵ Each dose of BI 474121 elicited a significantly greater cGMP mean relative change from baseline than placebo, supporting BI 474121-mediated PDE2 inhibition. Consequently, a treatment-related increase corrected for baseline and placebo was determined. Assessment of downstream biomarkers and CNS functional testing was not conducted in this study, so conclusions regarding potential efficacy cannot be drawn from these data. These preclinical and clinical data indicate that cGMP is a translatable biomarker for PDE2 target functional engagement across species, thereby informing interpretation of cGMP concentrations measured in previous and future studies.^{15–16} Since the results of this study are consistent with preclinical BI 474121 studies, evaluating not only CSF cGMP concentrations, but cGMP levels in brain regions post-mortem (prefrontal cortex, hippocampus, striatum) and CNS functional testing,^{14,17} the results presented here strengthen the use of CSF biomarkers as a proxy for brain function.^{18–19}

The results from the clinical study suggest that BI 474121 has a favourable safety profile, supporting the findings of the single¹¹ and multiple rising dose studies (Schaible et al., unpublished data), with no apparent dose-dependent relationship in the incidence of AES. The most reported AE was post-lumbar puncture syndrome, which may be attributable to use of a large gauge of catheter to reduce risk of occlusion and cessation of CSF flow, which may have occurred with a smaller gauge. This AE was manageable with treatments including bed-rest, paracetamol, caffeine, and blood patch placement. No AES of special interest, or SAES were observed.

Although no PDE inhibitors are currently approved for the treatment of CIAS, the preclinical evidence of PDE modulation enhancing learning and memory is compelling.^{20–21} For example, in conditions of NMDA receptor hypofunction, inhibition of PDE9 may increase cGMP levels by reducing its hydrolysis and improve NMDA receptor signaling.¹⁶ PDE2 is of special interest owing to its high expression levels in forebrain regions important for modulation of emotion and long term memory.²¹

Limitations of this study include the small sample size, the enrolment of males only, and the variability in participant age between dose groups. As PDE expression and cGMP concentrations change with age,²² the variability in age may explain the variability in cGMP concentrations reported in this study. The variability in cGMP levels reduced the ability to detect a difference between groups relative to increased dose level, possibly due to the small sample size. This may be reduced in future studies through increased numbers of participants. Finally, no marker for cognition was included, thus hampering translation to potential clinical efficacy.

CONCLUSION

Although no clear exposure–response relationship was observed in the clinical study, CSF cGMP increased at similar exposure levels in humans and rats. These results demonstrate that BI 474121 crosses the human blood–brain barrier to inhibit PDE2, and measurement of CSF cGMP represents a reliable translational biomarker of central functional target engagement. These observations, with the favourable safety profile, support further clinical development of BI 474121. Further PK/PD modelling may elucidate the mechanistic relationship between BI 474121 and CSF cGMP concentrations and aid selection of future dosing regimens.

SUPPORTING INFORMATION

Additional supporting information may be found in the online version of the article at the publisher's website.

REFERENCES

- 1 Balu, D. T., The NMDA Receptor and Schizophrenia: From Pathophysiology to Treatment. *Adv Pharmacol.* **2016**, *76*, 351-82.
- 2 Liu, J.; Chang, L.; Song, Y.; Li, H.; Wu, Y., The Role of NMDA Receptors in Alzheimer's Disease. *Front. Neurosci.* **2019**, *13*, 43.
- 3 Lakhan, S. E.; Caro, M.; Hadzimichalis, N., NMDA Receptor Activity in Neuropsychiatric Disorders. *Front Psychiatry* **2013**, *4*, 52.
- 4 Duinen, M. V.; Reneerkens, O. A.; Lambrecht, L.; Sambeth, A.; Rutten, B. P.; Os, J. V.; Blokland, A.; Prickaerts, J., Treatment of Cognitive Impairment in Schizophrenia: Potential Value of Phosphodiesterase Inhibitors in Prefrontal Dysfunction. *Curr. Pharm. Des.* **2015**, *21* (26), 3813-28.
- 5 Zhang, C.; Lueptow, L. M.; Zhang, H. T.; O'Donnell, J. M.; Xu, Y., The Role of Phosphodiesterase-2 in Psychiatric and Neurodegenerative Disorders. *Adv Neurobiol* **2017**, *17*, 307-347.
- 6 Fernández-Fernández, D.; Rosenbrock, H.; Kroker, K. S., Inhibition of PDE2A, but not PDE9A, modulates presynaptic short-term plasticity measured by paired-pulse facilitation in the CA1 region of the hippocampus. *Synapse* **2015**, *69* (10), 484-96.
- 7 Neitz, A.; Mergia, E.; Imbrosci, B.; Petrasch-Parwez, E.; Eysel, U. T.; Koesling, D.; Mittmann, T., Postsynaptic NO/cGMP Increases NMDA Receptor Currents via Hyperpolarization-Activated Cyclic Nucleotide-Gated Channels in the Hippocampus. *Cereb. Cortex* **2013**, *24* (7), 1923-1936.
- 8 Ruan, L.; Du, K.; Tao, M.; Shan, C.; Ye, R.; Tang, Y.; Pan, H.; Lv, J.; Zhang, M.; Pan, J., Phosphodiesterase-2 Inhibitor Bay 60-7550 Ameliorates A β -Induced Cognitive and Memory Impairment via Regulation of the HPA Axis. *Front. Cell. Neurosci.* **2019**, *13*.
- 9 Boess, F. G.; Hendrix, M.; van der Staay, F.-J.; Erb, C.; Schreiber, R.; van Staveren, W.; de Vente, J.; Prickaerts, J.; Blokland, A.; Koenig, G., Inhibition of phosphodiesterase 2 increases neuronal cGMP, synaptic plasticity and memory performance. *Neuropharmacology* **2004**, *47* (7), 1081-1092.
- 10 Redrobe, J. P.; Jørgensen, M.; Christoffersen, C. T.; Montezinho, L. P.; Bastlund, J. F.; Carnerup, M.; Bundgaard, C.; Lerdrup, L.; Plath, N., In vitro and in vivo characterisation of Lu AF64280, a novel, brain penetrant phosphodiesterase (PDE) 2A inhibitor: potential relevance to cognitive deficits in schizophrenia. *Psychopharmacology (Berl.)* **2014**, *231* (16), 3151-67.
- 11 Schaible, J.; Goeldner, R. G.; Scholz, A., Safety, tolerability, pharmacokinetics and relative bioavailability of BI 474121 in healthy males – a Phase I study. *Neuroscience Applied* **2022**, *1*, 100272.
- 12 World Medical Association Declaration of Helsinki. <https://www.wma.net/policies-post/wma-declaration-of-helsinki-ethical-principles-for-medical-research-involving-human-subjects/> (accessed May).
- 13 International Conference on Harmonization ICH-E6 Good Clinical Practice. <https://www.ich.org/page/efficacy-guidelines#6-2> (accessed May).
- 14 Schultheis, C.; Gal, P.; van Kraaij, B.; Groeneveld, G. J.; Zambori, J.; Viguerie, L.; Herich, L.; Rosenbrock, H., Effects of the phosphodiesterase 2 inhibitor BI 474121 on central nervous system cyclic guanylyl monophosphate concentrations in rats and humans. *Neuroscience Applied* **2022**, *1*, 100295.
- 15 Boland, K.; Moschetti, V.; Dansirikul, C.; Pichereau, S.; Gheyle, L.; Runge, F.; Zimdahl-Gelling, H.; Sand, M., A phase I, randomized, proof-of-clinical-mechanism study assessing the pharmacokinetics and pharmacodynamics of the oral PDE9A inhibitor BI 409306 in healthy male volunteers. *Hum Psychopharmacol* **2017**, *32* (1), e2569.
- 16 Moschetti, V.; Kim, M.; Sand, M.; Wunderlich, G.; Andersen, G.; Feifel, U.; Jang, I. J.; Timmer, W.; Rosenbrock, H.; Boland, K., The safety, tolerability and pharmacokinetics of BI 409306, a novel and potent PDE9 inhibitor: Overview of three Phase I randomised trials in healthy volunteers. *Eur. Neuropharmacol.* **2018**, *28* (5), 643-655.
- 17 Rosenbrock H; Arban R; Romig H; Hobson S; Schuelert N, Effects of the novel phosphodiesterase-2 inhibitor BI 474121 on rodent auditory event-related potentials biomarkers and cognition tasks related to schizophrenia. In *ECNP*, Vienna, Austria, 2022.
- 18 Rosenbrock, H.; Desch, M.; Kleiner, O.; Dorner-Ciossek, C.; Schmid, B.; Keller, S.; Schlecker, C.; Moschetti, V.; Goetz, S.; Liesenfeld, K. H.; Fillon, G.; Giovannini, R.; Ramael, S.; Wunderlich, G.; Wind, S., Evaluation of Pharmacokinetics and Pharmacodynamics of BI 425809, a Novel GlyT1 Inhibitor: Translational Studies. *Clin. Transl. Sci.* **2018**, *11* (6), 616-623.
- 19 Rosenbrock, H.; Giovannini, R.; Schänzle, G.; Koros, E.; Runge, F.; Fuchs, H.; Marti, A.; Reymann, K. G.; Schröder, U. H.; Fedele, E.; Dorner-Ciossek, C., The Novel Phosphodiesterase 9A Inhibitor BI 409306 Increases Cyclic Guanosine Monophosphate Levels in the Brain, Promotes Synaptic Plasticity, and Enhances Memory Function in Rodents. *J. Pharmacol. Exp. Ther.* **2019**, *371* (3), 633-641.
- 20 Prickaerts, J.; Heckman, P. R. A.; Blokland, A., Investigational phosphodiesterase inhibitors in phase I and phase II clinical trials for Alzheimer's disease. *Expert Opin Invest Drugs* **2017**, *26* (9), 1033-1048.
- 21 Zhang, C.; Lueptow, L. M.; Zhang, H.-T.; O'Donnell, J. M.; Xu, Y., The Role of Phosphodiesterase-2 in Psychiatric and Neurodegenerative Disorders. In *Phosphodiesterases: CNS Functions and Diseases*, 1st ed ed.; Zhang, H.-T.; Xu, Y.; O'Donnell, J. M., Eds. Springer Cham: New York City, NY, 2017; pp 307-347.
- 22 Domek-Łopacińska, K. U.; Strosznajder, J. B., Cyclic GMP and Nitric Oxide Synthase in Aging and Alzheimer's Disease. *Mol. Neurobiol.* **2010**, *41* (2), 129-137.

CHAPTER VIII
GENERAL DISCUSSION

Summary of findings

Nitric oxide, the smallest known signaling molecule produced by mammalian cells¹ is an intracellular and extracellular messenger involved in an extensive array of physiological processes.² First discovered as the mediator of acetylcholine or bradykinin-induced vasodilation and known as 'endothelial-derived relaxing factor',³ the central role of NO in vascular functioning became clear. This initially led to great interest in using drugs affecting the NO system for treatment of cardiovascular disorders. This area of interest later expanded, as it was shown that NO also fulfils functions in the central nervous system and immunological pathways. In the past decades this resulted in investigations on treatments of a wide range of conditions, varying from neurodegenerative diseases to sepsis.⁴⁻⁵ Measurements of NO bioavailability and the effects of NO are vital for the success of early phase clinical trials of compounds targeting it, since early pharmacodynamic biomarkers can guide and enhance further development of drugs.⁶ This thesis explored the use of vascular imaging as a biomarker to measure NO-dependent processes and, by proxy, NO bioavailability. The addition of imaging to the pharmacodynamic measurements performed in clinical trials might be worthwhile due to the advantages of non-invasiveness and the measurement of end organ physiological function as opposed to metabolite or biomarker concentrations.

In the first half of this thesis, potential imaging methods were explored and validated. In **Chapter II**, the effects of a mixed meal tolerance test, a metabolic challenge proven to induce subclinical vascular changes in otherwise healthy volunteers,⁷ were assessed in healthy elderly volunteers with 4 different imaging tools. Laser speckle contrast imaging (LSCI) combined with occlusion – reperfusion and local thermal hyperemia, sidestream darkfield imaging (SDFM) and passive leg movement (PLM) ultrasonography were performed before and after administration of the mixed meal tolerance test and before and after a 12-week treatment regimen of 13 g of dietary fiber, administered once daily. The employed imaging modalities showed high inter- and intraindividual variability, but a change in occlusion – reperfusion measured with LSCI, possibly induced by the mixed meal tolerance test, was detected. This manifested as a distinct pattern of reduced post-occlusive blood flow after consumption of the mixed meal, returning to baseline at the end of the 6-hour measurement period. Further standardization of imaging protocols and use of robust challenges known to affect vascular function may improve the performance of the imaging

techniques that were used, enhancing their ability to detect pharmacodynamic effects of physiological challenges and drugs on the vasculature.

In **Chapter III**, patients diagnosed with mitochondrial disease and matched healthy volunteers underwent imaging assessments as well as assessment of various blood-based biomarkers, including *ex vivo* assessments of mitochondrial function in peripheral blood mononuclear cells. In this study, PLM and flow mediated skin fluorescence detected differences in femoral artery blood flow and reduced nicotinamide adenine dinucleotide (NADH) fluorescence, respectively, when comparing patients and matched volunteers. These results indicate that PLM and FMSF can differentiate between healthy and disordered function of the vasculature, although PLM showed high inter-subject variability, consistent with the variability of this method in Chapter II. In contrast, *ex vivo* assessments of mitochondrial function in peripheral blood mononuclear cells (PBMCS) did not distinguish healthy volunteers and patients. This may be a result of the purifying selection pressure for these cells, as PBMCS with diminished mitochondrial function may have a shorter lifespan in the bloodstream compared to PMBCS with adequate mitochondrial function.⁸ Patients with mitochondrial disease display different levels of disease severity, and not all tissues are similarly affected by the mitochondrial DNA mutations,⁹ probably resulting in the high inter subject variability found in the patients with mitochondrial disease and the failure of several *ex vivo* and *in vivo* assessments to discriminate between healthy and diseased. To combat this problem, usage of a combination of imaging modalities, assays of mitochondrial function and biomarkers in serum or plasma may be advisable in future clinical trials to fully capture the effects of drugs intended to treat this patient population.

Chapter IV investigated the effects of a patch containing titanium dioxide on local skin microcirculation. The hypothesized mode of action of this patch is the absorption of emitted body heat and re-emission as infrared radiation (wavelength between 50 and 1000 μm).¹⁰ This is purported to have health benefits and used in therapeutic modalities such as saunas, heat-emitting lamps and heating garments.¹¹ Using LSCI, SDFM, near infrared spectroscopy, multispectral imaging, and thermography it was shown that the far infrared patch induced a short-lived increase in local skin perfusion, and longer lasting increases in oxygen consumption and skin temperature. The increase in skin temperature may have been the result of mechanical occlusion by the fabric of the patch, but since the increase in skin perfusion did not correlate temporally with the raise in temperature, it more likely was a direct effect of the far infrared radiation

emitted by the patch. Increased oxygen consumption and increased mitochondrial function are possible effects of far-infrared radiation¹²⁻¹³ and hence may also be a result of the titanium dioxide contained in the patch. The study provides a proof-of-concept for the theoretical mode of action of the patch, and thereby evidence that imaging can be used to detect treatment effects of experimental devices on the microcirculation

The second section of this thesis describes clinical trials with compounds affecting the NO-soluble guanylyl cyclase (sGC)-cyclic guanosine monophosphate (cGMP) system. First, **Chapter v** describes the results of a first-in-human trial of zagociguat, an sGC stimulator developed for the treatment of neurodegenerative conditions, showing it to be safe and tolerable in single doses up to 50 mg and multiple doses of up to 15 mg administered once daily. Zagociguat concentrations were also detected in cerebrospinal fluid, making this compound the first in its class to penetrate this compartment in humans, a crucial aspect for the intended treatment indication. Several of the adverse events that occurred with increased frequency in the zagociguat-treated group when compared to placebo in this study, as well as lower blood pressure readings in the zagociguat-treated participants, point to the mechanism of action of zagociguat working as intended. However, central nervous system (CNS) pharmacodynamic tests did not reveal any effects of the compound in the young, healthy population examined in the trial.

The results of a proof-of-concept study in healthy elderly with the same compound, using extensive pharmacodynamic testing, including blood and cerebrospinal fluid biomarkers, a battery of neurocognitive tests, magnetic resonance imaging and PLM, are described in **Chapter vi**. Here, as in the first-in-human trial, blood pressure lowering effects of zagociguat were seen, but pharmacodynamic testing did not reveal any CNS effects of the compound, and the exploratory PLM assessment showed no effects of the drug on systemic NO bioavailability. These results show that even though compounds may be pharmacologically active at the target site, as shown for zagociguat by reduced blood pressure, detection of meaningful pharmacodynamic effects on target organs, i.e. the brain, can be difficult in healthy volunteers who likely have optimal function in the assessed system.

Finally, in **Chapter VII**, the effects of a phosphodiesterase 2 (PDE2) inhibitor on cGMP levels in cerebrospinal fluid were examined. This study confirmed that this PDE inhibitor can reach the cerebral compartment and elevate cGMP by blocking its degradation, although not in a dose-dependent manner.

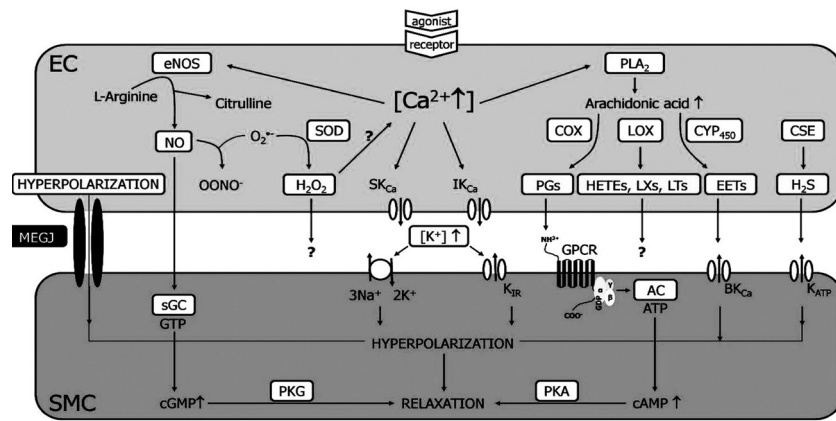
Furthermore, cGMP levels showed a rise-and-fall pattern in both placebo-treated participants as well as participants receiving study drug, confirming the circadian rhythm in cGMP production suggested in earlier studies.¹⁴ PDE inhibitors have been studied for the treatment of central nervous system disease for decades, and this study adds a proof-of-concept for PDE2 inhibition to increase cGMP signaling in the brain.

PATHWAYS INVOLVED IN ENDOTHELIAL FUNCTION

The NO-sGC-cGMP pathway has been extensively discussed in the introduction of this thesis and is the main target of both the therapeutic interventions and imaging methods employed in the described studies. However, endothelial function is a multifactorial physiological process that is influenced by NO-independent pathways and a large variety of intermediary enzymes and messenger molecules, a selection of which is shown in Figure 1.¹⁵ The pathways involved in endothelial function include but are not limited to sensory innervation, cyclo-oxygenase activity, endothelial-derived constrictive factors such as endothelin, thromboxane A₂ and angiotensin II,¹⁶ and endothelium dependent hyperpolarizing factor.¹⁷

Given the multitude of factors involved in endothelial physiology, a multimodal approach to evaluate endothelial function may be advisable. All the components of the endothelial system interact with each other, with both positive and negative feedback loops, regulation by endothelial-derived and systemic factors and cell self-regulation. Therefore, measurement of blood-based biomarkers can be prone to misinterpretation, since, for example, an increase in relaxing factors might be an indicator of healthy endothelial function, or the result of compensatory mechanisms during endothelial dysfunction. Similarly, as discussed in the introduction of this thesis, the actions of NO can be beneficial and detrimental to the endothelium depending on quantity and location. Hence, methodologies that measure the result of the complex interactions within the endothelium, i.e., endothelial function, can provide an intermediary between proximal cell- or blood-based biomarkers and clinical endpoints. The imaging methods employed in the studies in this thesis might achieve this by assessing NO-dependent vasodilation (PLM, LSCI combined with local hyperthermia), general vascular function (LSCI combined with occlusion-reperfusion), density and perfusion of the microcirculation (SDFM), tissue oxygenation and blood flow (NIRS) and metabolic activity (FMSF). In the following section, benefits and drawbacks of each individual imaging method will be discussed.

FIGURE 1 Pathways involved in endothelium-dependent vessel relaxation.



AC=adenylyl cyclase; CAMP=cyclic adenosine monophosphate; CGMP=cyclic guanosine monophosphate; COX=cyclooxygenase; CSE=cystathionine-lyase; CYP450=cytochrome P450 epoxygenase; EC=endothelial cell; eNOS=endothelial nitric oxide synthase; EETS=epoxyeicosatrienoic acids; GPCR=G-protein coupled receptor; HETES=hydroxyeicosatrienoic acids; H2O2=hydrogen peroxide; H2S=hydrogen sulfide; KCA=Ca²⁺-activated potassium channel with small (SKCA), intermediate (IKCA) or big conductance (BKCA); KATP=ATP-sensitive potassium channels; KIR=inwardly rectifying potassium channel; LOX=lipoxygenase; LTS=leukotrienes; LXs=lipoxines; MEGJ=myoendothelial gap junctions; NO=nitric oxide; OONO⁻=peroxynitrite anion; O₂⁻=superoxide anion; PGs=prostaglandins; PKA=protein kinase A; PKG=protein kinase G; PLA2=phospholipase A2; sGC=soluble guanylyl cyclase; SMC=smooth muscle cell; SOD=superoxide dismutase. (Adapted from Schmidt et al.¹⁶)

SYNTHESIS OF FINDINGS BY IMAGING METHOD

The studies contained in this thesis show that imaging can be used to detect effects of both metabolic challenges and pharmacological treatments, and that the possibility to detect no-mediated effects in early phase clinical trials can be increased by including imaging modalities in their design.

LSCI was the imaging method with the largest technical reproducibility, showing low inter- and intrasubject variability in **Chapter II**. LSCI was also able to identify responses elicited by mixed meal challenge tests and 12-week fibre administration (**Chapter II**), measure differences between patients with mitochondrial disease and healthy volunteers (**Chapter III**) and assess the effects of a far-infrared radiation patch (**Chapter IV**). This indicates that LSCI is a valid method to detect expected changes in physiological processes. LSCI might therefore be candidate for inclusion in studies investigating a wide range of

compounds aiming to modulate vascular function. A caveat to widespread application of LSCI is that in its current form, it can only be performed in dedicated centers equipped with the necessary expensive devices, experienced operators, and controlled environments. If those requirements are met, LSCI is a technique with good technical reproducibility, and selected LSCI parameters show biological validity, i.e., response to intervention or discrimination between functional and dysfunctional vascular function.^{18–20} Moreover, LSCI can measure a large range of skin perfusion values, i.e., skin perfusion during complete blood flow occlusion as well as during inflammatory conditions,^{21–22} and can be combined with many local reactivity challenges such as occlusion-reperfusion, local thermal hyperemia and iontophoresis of vasoactive compounds.^{23–24} The combination with these challenges also makes LSCI attractive, since it allows evaluation of different physiological pathways, including cyclooxygenase activity, sensory innervation,²⁵ and the effects of locally administered vasoconstrictors or dilators.²⁶ Although laser doppler flowmetry can achieve similar goals, the advantages of LSCI in this regard are temporal as well as spatial resolution,²⁷ and arguably higher sensitivity.¹⁸ However, the cost of a laser speckle imaging device can be prohibitive, although low-cost LSCI devices show some promise in limited context.²⁸ The LSCI method is very sensitive to influences of temperature and movement of the imaged area, necessitating not only careful instruction of participants in a clinical study, but also dedicated rooms which minimize the possibility of outside interference with measurements. Moreover, LSCI measures blood flow through spatial analysis of changes in speckle pattern, resulting in arbitrary perfusion units instead of units easier to understand in the context of blood flow, e.g., mL/min. The physics of speckle pattern analysis make the translation to clinically useful units challenging,²⁹ and the relation between changes in speckle pattern and physiological blood flow is poorly understood.³⁰ The use of LSCI has remained mainly in carefully controlled clinical trials, although innovations in post-image processing³¹ and machine learning³² show promise for use of LSCI in a clinical setting, for example to identify poorly perfused tissue regions intraoperatively.³³

The PLM technique was employed to assess the effects of a mixed meal challenge (**Chapter II**) determine differences in vascular function between patients with mitochondrial disease and healthy volunteers (**Chapter III**) as well as to measure potential vasodilatory effects of sGC stimulation (**Chapter VI**). PLM could discriminate between healthy volunteers and patients with mitochondrial disease, confirming that PLM can distinguish populations with different

cardiovascular risk factors or characteristics.³⁴⁻³⁷ However, no effects of sGC stimulation or mixed meal administration were detected by PLM, and the technique showed high variability across all studies. The lack of detected treatment effects may be a function of sample size or absence of meaningful macrovascular effects of either sGC stimulation or a mixed meal, but since no positive control was employed in the described studies, this is impossible to ascertain. Alternatively, PLM may not have been able to detect treatment effects due to its operator dependency, a well-known confounder for ultrasonography, particularly when a stable image of a blood vessel with an appropriate insonation angle of 60° during the entire recording is vital.³⁸ Nevertheless, given PLM's clinical relevance and high correlation with NO bioavailability, the technique might still be a worthwhile addition in clinical studies. Based on the studies in this thesis, this is only possible if the method is significantly improved in consistency by performing the procedure with experienced operators adhering to strict guidelines.³⁹

SDFM was used in the assessment of microcirculatory disturbances caused by a mixed meal challenge (**Chapter II**), as well as measurement of differences in sublingual microcirculation between patients and healthy volunteers (**Chapter III**) and effects of a far-infrared emitting patch (**Chapter IV**). SDFM, as a technique to visualize red blood cells and their movement through blood vessels in real time, enables the identification of vessel density and perfusion changes in the microcirculation. SDFM can also be used to calculate glycocalyx thickness, but this requires complicated analyses which were not employed in the studies in this thesis. SDFM has mainly been employed in the study of critically ill subjects such as patients with sepsis,⁴⁰ or undifferentiated patients admitted to the ICU,⁴¹⁻⁴² or patients undergoing various types of surgery,⁴³⁻⁴⁴ since microcirculatory changes are most likely to occur and most evident in these populations. Evidence of microcirculatory changes detected by SDFM has also been found in populations with elevated risk of cardiovascular disease.⁴⁵ However, in the studies in this thesis, SDFM did not detect microcirculatory effects of a mixed meal or a far-infrared patch, nor were differences in sublingual microcirculation found between healthy volunteers and patients with mitochondrial disease. Microcirculatory disturbances are possibly unlikely to occur in the healthy volunteers participating in these trials, a limitation which could be remedied by using a challenge to disturb the microcirculatory perfusion and reveal small potential effects of an intervention. Alternatively, if the proposed mechanism of the studied intervention is to affect angiogenesis

rather than vessel perfusion, e.g., by inhibition of vascular endothelial growth factor,⁴⁶ measurements over a long period of time may be advisable. The studies in this thesis employed neither remedy, which may be an explanation for the negative findings in **Chapter II, III and IV**. In addition, recent developments in the SDFM technique, with novel equipment and analysis software currently available, allow for more in-depth assessments such as automatic measurement of glycocalyx thickness and red blood cell velocity. These innovations were not available or implemented in the described studies.⁴⁷ However, the advantages of SDFM such as minimal participant burden, good reproducibility, in particular when using multiple consecutive measurements,⁴⁸⁻⁴⁹ portability, and ease of use may still make it a worthwhile inclusion in some clinical trials, especially when implemented according to the above recommendations.

NIRS was used in this thesis to assess differences between patients with mitochondrial disease and healthy volunteers in **Chapter III** and to determine the effects of a far-infrared radiation emitting skin patch in **Chapter IV**. In its clinical application, NIRS is a relatively simple technique using the relative concentrations of oxygenated and deoxygenated hemoglobin to derive tissue perfusion and oxygenation.⁵⁰ NIRS has found application in clinical research on a wide range of disorders such as stroke,⁵¹ burns,⁵² central nervous system disorders⁵³⁻⁵⁵ and vascular disease.⁵⁶⁻⁵⁸ The implementation of NIRS varies widely, including measurement of cerebral perfusion and oxygenation,⁵⁹ peripheral oxygen saturation, muscle perfusion and oxygenation, and measurement of mitochondrial oxidative capacity.⁶⁰ The disadvantages of NIRS are similar to other imaging techniques: without a significant challenge to perfusion or oxygenation, NIRS will show optimal tissue saturation indexes for individuals participating in clinical trials. Moreover, to derive a measure of tissue oxygen consumption and hence mitochondrial oxidative capacity as well as to acquire information on vascular function, combination of NIRS with arterial and venous occlusive challenges is necessary.⁶¹⁻⁶² Furthermore, accurate assessment of mitochondrial oxidative capacity may need blood volume corrections,⁶³ which were not employed in the studies in **Chapter III** and **IV**. However, given these limitations, NIRS provides unique information on vascular function vis-à-vis the other imaging modalities used in this thesis: since near-infrared radiation can pass relatively easily through different tissues,⁶⁴ NIRS penetrates skin, underlying muscle and, in the case of cerebral assessments, the skull, thereby providing information on perfusion and oxygenation of deeper tissues. SDFM and LSCI imaging can only assess perfusion and microcirculatory status

in superficial tissues such as the skin or sublingual blood vessels, which creates a niche for NIRS as an imaging endpoint for use in clinical trials evaluating perfusion in deep tissues, without the burdensome use of magnetic resonance imaging or other advanced imaging techniques.

FMSF was solely employed in the study described in **Chapter III**, where significant differences in NADH skin fluorescence between patients with mitochondrial disease and healthy volunteers were found using this unique technique. FMSF uses a different physiological approach to assess vascular function and microcirculation: rather than directly visualizing blood vessels or blood cells, FMSF measures NADH fluorescence, thereby deriving an estimate of the concentration of this compound in the superficial skin cells.⁶⁵ Since NADH is central to many cellular processes, in particular redox metabolism and oxidative phosphorylation, its concentration is directly influenced by the supply of oxygen to the cells, i.e., blood circulation. When combining FMSF with an occlusion-reperfusion challenge, the metabolic shift of skin cells to glycolysis, response to reperfusion, and oscillations in blood flow can be evaluated.⁶⁶⁻⁶⁷ The latter, termed 'flow motion' is of particular interest, since the oscillations in NADH fluorescence reflect movement of blood vessels, i.e., vasomotion, which is critical to vascular homeostasis.⁶⁸ Vasomotion can be differentiated into categories by the frequency of vessel movements through Fourier transformation,⁶⁹ resulting in cardiac, respiratory, neurogenic, myogenic, and endothelial components.⁷⁰⁻⁷¹ The endothelial component can be measured with various imaging methods with sufficient temporal resolution, such as laser doppler flowmetry and FMSF, and may be a useful clinical tool in the assessment of microvascular endothelial function.⁷² FMSF can provide unique physiological information when compared to the other imaging methods investigated in this thesis. Moreover, the FMSF technique is highly standardized and displays good reproducibility and sensitivity to blood flow changes.⁷³ However, since FMSF is a relatively novel technique which necessitates expensive equipment, its use is limited to specialized clinical research centers. In addition, FMSF necessarily must be combined with an occlusion-reperfusion challenge to yield useful information, which may be a significant subject burden especially when repeated measurements are needed. FMSF-derived assessments of vascular function are indirect since no oxygenation or true flow values are measured. This issue is compounded by the fact that, although FMSF does provide some metabolic information, by itself it cannot show a complete picture of the status of cellular respiration, since NAD⁺/NADH ratio is a vital parameter to assess cellular redox

status which cannot be derived from NADH concentrations alone. Combination of FMSF with imaging or biomarkers providing additional information on either blood flow or tissue metabolism is therefore advisable.

RECOMMENDATIONS FOR FUTURE STUDIES

All imaging modalities used in the studies described in this thesis have different benefits and drawbacks. The disadvantages can often be remedied by selecting the methodology to be fit for measuring the intended mechanism of action in tissues that are likely to be affected, by combining pharmacodynamic tests with physiological challenges that disturb homeostasis or create endothelial dysfunction and by incorporating both functional imaging as well as upstream biomarkers in blood or cells in the design of clinical studies. A limitation of the studies described in this thesis is that the employed imaging modalities were not compared to the existing gold standard for endothelial functional measurement, flow mediated dilation (FMD), due to the logistical challenges associated with implementing this technique in the described studies, and only limited data on blood-based biomarkers was collected, specifically in the study described in **Chapter III**. The first half of this thesis thus serves as a pilot for exploring the usefulness of imaging for assessment of endothelial function. The next step in developing these techniques would be to benchmark them against FMD and established biomarkers for endothelial function, such as adhesion molecules and coagulation factors.⁷⁴

When several imaging techniques are combined in the same trial, these can complement each other, providing supportive information and revealing different mechanisms of action. For example, in **Chapter IV**, the combination of both LSCI, NIRS and thermography in the same study revealed that a far-infrared radiating patch does not only increase skin blood flow, but that this is likely not purely due to skin warming, and coincides with an increase in tissue metabolism, thereby providing a credible hypothesis for the mechanism of action of the investigated patch. The combination of an array of imaging methods also revealed differences in both baseline metabolic characteristics as well as NO bioavailability in **Chapter III** of this thesis.

On the other hand, some of the studies in this thesis may have benefited from the inclusion of additional imaging methodology to assess pharmacodynamic effects of the investigated drugs. For example, in **Chapter V**, no functional endothelial testing in the form of imaging was conducted, which may have been missed opportunity, since these could have further supported

potential systemic target engagement in the vascular system. The influence of the sGC stimulator on local and systemic NO bioavailability, as well as general vasodilation, could have been assessed through inclusion of respectively LSCI with local thermal hyperemia, PLM, and LSCI with occlusion-reperfusion. In **Chapter VI**, PLM was included as an exploratory endpoint, but similarly LSCI might have provided more information on upstream or downstream effects in the NO-sGC-cGMP pathway. In this trial the inclusion of a challenge designed to reduce endothelial or vascular function, for example infusion of lipopolysaccharide,⁷⁵ would also have been useful to improve the likelihood of finding pharmacodynamic effects, since detection of treatment effects on the vasculature in individuals without endothelial dysfunction has proven difficult, especially with relatively short treatment regimens. Similar recommendations could be made for the study in **Chapter VII**, although here the most important final common pathway of NO signaling, cGMP, was directly measured in a relevant pharmacokinetic compartment and shown to increase with treatment. The addition of imaging modalities such as LSCI and PLM could have confirmed not only the proof-of-mechanism of PDE-mediated cGMP elevation, but also provide information on whether the induced cGMP elevation caused increased cGMP signaling resulting in improved vascular function.

In conclusion, a variety of imaging methods show some promise to investigate the endothelium, specifically investigations of drugs aiming to influence NO signaling. Obviously, each modality has different requirements and caveats, demanding careful consideration of the study design, technical aspects, sensitivity, variability, and feasibility. The research described in this thesis could aid researchers investigating drugs targeting the NO system to tailor the imaging package exactly to their study objectives. Preferably, this should be combined with circulating markers of endothelial function to establish a coherent picture of both biochemical and functional effects of the investigated drug.

REFERENCES

- Ghaffari, A.; Neil, D. H.; Ardakani, A.; Road, J.; Ghahary, A.; Miller, C. C., A direct nitric oxide gas delivery system for bacterial and mammalian cell cultures. *Nitric Oxide* **2005**, *12* (3), 129-140.
- Tuteja, N.; Chandra, M.; Tuteja, R.; Misra, M. K., Nitric Oxide as a Unique Bioactive Signaling Messenger in Physiology and Pathophysiology. *J Biomed Biotechnol* **2004**, *2004* (4), 227-237.
- Moncada, S.; Palmer, R. M.; Higgs, E. A., The discovery of nitric oxide as the endogenous nitrovasodilator. *Hypertension* **1988**, *12* (4), 365-72.
- Prickaerts, J.; Heckman, P. R. A.; Blokland, A., Investigational phosphodiesterase inhibitors in phase I and phase II clinical trials for Alzheimer's disease. *Expert opinion on investigational drugs* **2017**, *26* (9), 1033-1048.
- Mao, K.; Chen, S.; Chen, M.; Ma, Y.; Wang, Y.; Huang, B.; He, Z.; Zeng, Y.; Hu, Y.; Sun, S.; Li, J.; Wu, X.; Wang, X.; Strober, W.; Chen, C.; Meng, G.; Sun, B., Nitric oxide suppresses NLRP3 inflammasome activation and protects against LPS-induced septic shock. *Cell Research* **2013**, *23* (2), 201-212.
- Cohen, A. F.; Burggraaf, J.; Gerven, J. M. A. v.; Moerland, M.; Groeneveld, G. J., The Use of Biomarkers in Human Pharmacology (Phase I) Studies. *Annual Review of Pharmacology and Toxicology* **2015**, *55* (1), 55-74.
- van den Broek, T. J.; Bakker, G. C. M.; Rubingh, C. M.; Bijlsma, S.; Stroeve, J. H. M.; van Ommen, B.; van Erk, M. J.; Wopereis, S., Ranges of phenotypic flexibility in healthy subjects. *Genes Nutr* **2017**, *12*, 32.
- Walker, M. A.; Lareau, C. A.; Ludwig, L. S.; Karaa, A.; Sankaran, V. G.; Regev, A.; Mootha, V. K., Purifying Selection against Pathogenic Mitochondrial DNA in Human T Cells. *The New England journal of medicine* **2020**, *383* (16), 1556-1563.
- Chinnery, P. F.; Howell, N.; Lightowlers, R. N.; Turnbull, D. M., Molecular pathology of MELAS and MERRF. The relationship between mutation load and clinical phenotypes. *Brain : a journal of neurology* **1997**, *120* (10), 1713-1721.
- Tsai, S. R.; Hamblin, M. R., Biological effects and medical applications of infrared radiation. *Journal of photochemistry and photobiology. B, Biology* **2017**, *170*, 197-207.
- Vatansver, F.; Hamblin, M. R., Far infrared radiation (FIR): its biological effects and medical applications. *Photonics & lasers in medicine* **2012**, *4*, 255-266.
- Lagerwaard, B.; Nieuwenhuizen, A. G.; de Boer, V. C. J.; Keijer, J., In vivo assessment of mitochondrial capacity using NIRS in locomotor muscles of young and elderly males with similar physical activity levels. *GeroScience* **2020**, *42* (1), 299-310.
- Bontemps, B.; Gruet, M.; Verduyssen, F.; Louis, J., Utilisation of far infrared-emitting garments for optimising performance and recovery in sport: Real potential or new fad? A systematic review. *PLoS one* **2021**, *16* (5), e0251282-e0251282.
- Ferreira, G. A.; Golombek, D. A., Rhythmicity of the cGMP-related signal transduction pathway in the mammalian circadian system. *American Journal of Physiology-Regulatory, Integrative and Comparative Physiology* **2001**, *280* (5), R1348-R1355.
- Schmidt, K.; de Wit, C., Endothelium-Derived Hyperpolarizing Factor and Myoendothelial Coupling: The in vivo Perspective. *Frontiers in Physiology* **2020**, *11*.
- Thijssen, D. H.; Rongen, G. A.; Smits, P.; Hopman, M. T., Physical (in)activity and endothelium-derived constricting factors: overlooked adaptations. *J Physiol* **2008**, *586* (2), 319-24.
- Edwards, G.; Félétou, M.; Weston, A. H., Endothelium-derived hyperpolarising factors and associated pathways: a synopsis. *Pflügers Archiv - European Journal of Physiology* **2010**, *459* (6), 863-879.
- Roustit, M.; Millet, C.; Blaise, S.; Dufournet, B.; Cracowski, J. L., Excellent reproducibility of laser speckle contrast imaging to assess skin microvascular reactivity. *Microvasc Res* **2010**, *80* (3), 505-11.
- Rousseau, P.; Mahé, G.; Haj-Yassin, F.; Durand, S.; Humeau, A.; Leftheriotis, G.; Abraham, P., Increasing the 'region of interest' and 'time of interest', both reduce the variability of blood flow measurements using laser speckle contrast imaging. *Microvascular Research* **2011**, *82* (1), 88-91.
- Millet, C.; Roustit, M.; Blaise, S.; Cracowski, J. L., Comparison between laser speckle contrast imaging and laser Doppler imaging to assess skin blood flow in humans. *Microvascular Research* **2011**, *82* (2), 147-151.
- Cordovil, I.; Huguenin, G.; Rosa, G.; Bello, A.; Kohler, O.; de Moraes, R.; Tibirica, E., Evaluation of systemic microvascular endothelial function using laser speckle contrast imaging. *Microvasc Res* **2012**, *83* (3), 376-9.
- Buters, T. P.; Hameeteman, P. W.; Jansen, I. M. E.; van Hindevoort, F. C.; Ten Voorde, W.; Florencia, E.; Osse, M.; de Kam, M. L.; Grievink, H. W.; Schoonakker, M.; Patel, A. A.; Yona, S.; Gilroy, D. W.; Lubberts, E.; Damman, J.; Feiss, G.; Rissmann, R.; Jansen, M. A. A.; Burggraaf, J.; Moerland, M., Intradermal lipopolysaccharide challenge as an acute in vivo inflammatory model in healthy volunteers. *Br J Clin Pharmacol* **2022**, *88* (2), 680-690.
- Cracowski, J. L.; Roustit, M., Current Methods to Assess Human Cutaneous Blood Flow: An Updated Focus on Laser-Based-Techniques. *Microcirculation* **2016**, *23* (5), 337-44.
- Souza, E. G.; De Lorenzo, A.; Huguenin, G.; Oliveira, G. M.; Tibirica, E., Impairment of systemic

- microvascular endothelial and smooth muscle function in individuals with early-onset coronary artery disease: studies with laser speckle contrast imaging. *Coron Artery Dis* **2014**, *25* (1), 23-8.
- 25 Roustit, M.; Cracowski, J. L., Non-invasive assessment of skin microvascular function in humans: an insight into methods. *Microcirculation* **2012**, *19* (1), 47-64.
- 26 Cracowski, J.-L.; Gaillard-Bigot, F.; Cracowski, C.; Sors, C.; Roustit, M.; Millet, C., Involvement of cytochrome epoxygenase metabolites in cutaneous postocclusive hyperemia in humans. *Journal of applied physiology (Bethesda, Md. : 1985)* **2012**, *114*.
- 27 Hodges, G. J.; Klentrou, P.; Cheung, S. S.; Falk, B., Comparison of laser speckle contrast imaging and laser-Doppler fluxmetry in boys and men. *Microvascular Research* **2020**, *128*, 103927.
- 28 Richards, L. M.; Kazmi, S. M.; Davis, J. L.; Olin, K. E.; Dunn, A. K., Low-cost laser speckle contrast imaging of blood flow using a webcam. *Biomed Opt Express* **2013**, *4* (10), 2269-83.
- 29 Briers, D.; Duncan, D. D.; Hirst, E.; Kirkpatrick, S. J.; Larsson, M.; Steenbergen, W.; Stromberg, T.; Thompson, O. B., Laser speckle contrast imaging: theoretical and practical limitations. *Journal of biomedical optics* **2013**, *18* (6), 066018.
- 30 Fredriksson, I.; Hultman, M.; Strömberg, T.; Larsson, M., Machine learning in multiexposure laser speckle contrast imaging can replace conventional laser Doppler flowmetry. *Journal of biomedical optics* **2019**, *24* (1), 1-11.
- 31 Heeman, W.; Steenbergen, W.; van Dam, G.; Boerma, E. C., Clinical applications of laser speckle contrast imaging: a review. *Journal of biomedical optics* **2019**, *24* (8), 1-11.
- 32 Martin, H.; Marcus, L.; Tomas, S.; Ingemar, F., Speed-resolved perfusion imaging using multi-exposure laser speckle contrast imaging and machine learning. *Journal of biomedical optics* **2023**, *28* (3), 036007.
- 33 Wildeboer, A.; Heeman, W.; van der Bilt, A.; Hoff, C.; Calon, J.; Boerma, E. C.; Al-Tajer, M.; Bouvy, N., Laparoscopic Laser Speckle Contrast Imaging Can Visualize Anastomotic Perfusion: A Demonstration in a Porcine Model. *Life (Basel, Switzerland)* **2022**, *12* (8).
- 34 Shields, K. L.; Broxterman, R. M.; Jarrett, C. L.; Bisconti, A. V.; Park, S. H.; Richardson, R. S., The passive leg movement technique for assessing vascular function: defining the distribution of blood flow and the impact of occluding the lower leg. *Exp Physiol* **2019**, *104* (10), 1575-1584.
- 35 Trinity, J. D.; Richardson, R. S., Physiological Impact and Clinical Relevance of Passive Exercise/Movement. *Sports Med* **2019**, *49* (9), 1365-1381.
- 36 Iepsen, U. W.; Munch, G. D.; Rugbjerg, M.; Rinnov, A. R.; Zacho, M.; Mortensen, S. P.; Secher, N. H.; Ringbaek, T.; Pedersen, B. K.; Hellsten, Y.; Lange, P.; Thaning, P., Effect of endurance versus resistance training on quadriceps muscle dysfunction in COPD: a pilot study. *International journal of chronic obstructive pulmonary disease* **2016**, *11*, 2659-2669.
- 37 Witman, M. A.; Ives, S. J.; Trinity, J. D.; Groot, H. J.; Stehlik, J.; Richardson, R. S., Heart failure and movement-induced hemodynamics: partitioning the impact of central and peripheral dysfunction. *Int J Cardiol* **2015**, *178*, 232-8.
- 38 Lew, L. A.; Liu, K. R.; Pyke, K. E., Reliability of the hyperaemic response to passive leg movement in young, healthy women. *Experimental Physiology* **2021**, *106* (9), 2013-2023.
- 39 Gifford, J. R.; Richardson, R. S., CORP: Ultrasound assessment of vascular function with the passive leg movement technique. *J Appl Physiol (1985)* **2017**, *123* (6), 1708-1720.
- 40 Cusack, R.; O'Neill, S.; Martin-Loeches, I., Effects of Fluids on the Sublingual Microcirculation in Sepsis. *J Clin Med* **2022**, *11* (24).
- 41 Huang, W.; Xiang, H.; Hu, C.; Wu, T.; Zhang, D.; Ma, S.; Hu, B.; Li, J., Association of Sublingual Microcirculation Parameters and Capillary Refill Time in the Early Phase of ICU Admission. *Critical care medicine* **2023**.
- 42 Cusack, R.; Leone, M.; Rodriguez, A. H.; Martin-Loeches, I., Endothelial Damage and the Microcirculation in Critical Illness. *Biomedicines* **2022**, *10* (12).
- 43 Zhang, Y.; Jin, L.; Liu, H.; Meng, X.; Ji, F., Ephedrine vs. phenylephrine effect on sublingual microcirculation in elderly patients undergoing laparoscopic rectal cancer surgery. *Frontiers in medicine* **2022**, *9*, 969654.
- 44 Bol, M. E.; Huckriede, J. B.; van de Pas, K. G. H.; Delhaas, T.; Lorusso, R.; Nicolaes, G. A. F.; Sels, J. E. M.; van de Poll, M. C. G., Multimodal measurement of glycocalyx degradation during coronary artery bypass grafting. *Frontiers in medicine* **2022**, *9*, 1045728.
- 45 van der Velden, A. I. M.; van den Berg, B. M.; de Mutsert, R.; van der Vlag, J.; Jukema, J. W.; Rosendaal, F. R.; Rabelink, T. J.; Vink, H., Microvascular differences in individuals with obesity at risk of developing cardiovascular disease. *Obesity (Silver Spring, Md.)* **2021**, *29* (9), 1439-1444.
- 46 Escalante, C. P.; Zalpour, A., Vascular endothelial growth factor inhibitor-induced hypertension: basics for primary care providers. *Cardiol Res Pract* **2011**, *2011*, 816897.
- 47 Eickhoff, M. K.; Winther, S. A.; Hansen, T. W.; Diaz, L. J.; Persson, F.; Rossing, P.; Frimodt-Møller, M., Assessment of the sublingual microcirculation with the GlycoCheck system: Reproducibility and examination conditions. *PLoS One* **2020**, *15* (12), e0243737.
- 48 Bol, M. E.; Beurskens, D. M. H.; Delnoij, T. S. R.; Roekaerts, P.; Reutelingsperger, C. P. M.; Delhaas, T.; van de Poll, M. C. G.; Sels, J. E. M.; Nicolaes, G. A. F., Variability of Microcirculatory Measurements in Critically Ill Patients. *Shock* **2020**, *54* (1), 9-14.
- 49 Bol, M. E.; Broddin, B. E. K.; Delhaas, T.; Sels, J. E. M.; van de Poll, M. C. G., Variability of microcirculatory measurements in healthy volunteers. *Sci Rep* **2022**, *12* (1), 19887.
- 50 Sakudo, A., Near-infrared spectroscopy for medical applications: Current status and future perspectives. *Clinica Chimica Acta* **2016**, *455*, 181-188.
- 51 Pierik, R.; Scheeren, T. W. L.; Erasmus, M. E.; van den Bergh, W. M., Near-infrared spectroscopy and processed electroencephalogram monitoring for predicting peri-operative stroke risk in cardiothoracic surgery: An observational cohort study. *European journal of anaesthesiology* **2023**.
- 52 Kim, Y. H.; Paik, S. H.; Kim, Y.; Yoon, J.; Cho, Y. S.; Kym, D.; Hur, J.; Chun, W.; Kim, B. M.; Kim, B. J., Clinical application of functional near-infrared spectroscopy for burn assessment. *Frontiers in bioengineering and biotechnology* **2023**, *11*, 1127563.
- 53 Liang, J.; Huang, J.; Luo, Z.; Wu, Y.; Zheng, L.; Tang, Z.; Li, W.; Ou, H., Brain network mechanism on cognitive control task in the elderly with brain aging: A functional near infrared spectroscopy study. *Frontiers in human neuroscience* **2023**, *17*, 1154798.
- 54 Hou, M.; Mao, X.; Wei, Y.; Wang, J.; Zhang, Y.; Qi, C.; Song, L.; Wan, Y.; Liu, Z.; Gan, J.; Liu, Z., Pattern of prefrontal cortical activation and network revealed by task-based and resting-state fNIRS in Parkinson's disease's patients with overactive bladder symptoms. *Front Neurosci* **2023**, *17*, 1142741.
- 55 Si, J.; Yang, Y.; Xu, L.; Xu, T.; Liu, H.; Zhang, Y.; Jing, R.; Li, J.; Wang, D.; Wu, S.; He, J., Evaluation of residual cognition in patients with disorders of consciousness based on functional near-infrared spectroscopy. *Neurophotonics* **2023**, *10* (2), 025003.
- 56 Koletsos, N.; Dipla, K.; Triantafyllou, A.; Dolgyras, P.; Aslanidis, S.; Zafeiridis, A.; Galanopoulou, V.; Douma, S.; Gkaliagkousi, E., Depression in systemic lupus erythematosus: A manifestation of microcirculation dysfunction? *Lupus* **2023**, *9612033231167792*.
- 57 Yata, T.; Sano, M.; Inuzuka, K.; Katahashi, K.; Naruse, E.; Kayama, T.; Yamanaka, Y.; Tsuyuki, H.; Endo, Y.; Ishikawa, N.; Takeuchi, H.; Unno, N., Real-Time Assessment of Tissue Oxygen Saturation Using a Novel Oximeter During Revascularization for Acute Limb Ischemia: A Case Report. *Annals of vascular diseases* **2023**, *16* (1), 81-85.
- 58 Kisiel, O.; Siennicka, A. E.; Josiak, K.; Zymliński, R.; Banasiak, W.; Węgrzynowska-Teodorczyk, K., Impact of assisted exercises on skeletal muscle oxygenation levels in men with acutely decompensated heart failure. *Advances in clinical and experimental medicine : official organ Wroclaw Medical University* **2023**, *32* (2), 211-218.
- 59 Milej, D.; He, L.; Abdalmalak, A.; Baker, W. B.; Anazodo, U. C.; Diop, M.; Dolui, S.; Kavuri, V. C.; Pavlosky, W.; Wang, L.; Balu, R.; Detre, J. A.; Amendolia, O.; Quattrone, F.; Kofke, W. A.; Yodh, A. G.; St Lawrence, K., Quantification of cerebral blood flow in adults by contrast-enhanced near-infrared spectroscopy: Validation against MRI. *Journal of cerebral blood flow and metabolism : official journal of the International Society of Cerebral Blood Flow and Metabolism* **2020**, *40* (8), 1672-1684.
- 60 Fennell, C. R. J.; Mauger, A. R.; Hopker, J. G., Reproducibility of NIRS-derived mitochondrial oxidative capacity in highly active older adults. *Experimental gerontology* **2023**, *175*, 112156.
- 61 Gerovasilis, V.; Dimopoulos, S.; Tzani, G.; Anastasiou-Nana, M.; Nanas, S., Utilizing the vascular occlusion technique with NIRS technology. *International Journal of Industrial Ergonomics* **2010**, *40* (2), 218-222.
- 62 Dennis, J. J.; Wiggins, C. C.; Smith, J. R.; Isautier, J. M. J.; Johnson, B. D.; Joyner, M. J.; Cross, T. J., Measurement of muscle blood flow and O₂ uptake via near-infrared spectroscopy using a novel occlusion protocol. *Scientific Reports* **2021**, *11* (1), 918.
- 63 Ryan, T. E.; Erickson, M. L.; Brizendine, J. T.; Young, H.-J.; McCully, K. K., Noninvasive evaluation of skeletal muscle mitochondrial capacity with near-infrared spectroscopy: correcting for blood volume changes. *Journal of Applied Physiology* **2012**, *113* (2), 175-183.
- 64 Wu, S.; Butt, H.-J., Near-infrared photochemistry at interfaces based on upconverting nanoparticles. *Physical Chemistry Chemical Physics* **2017**, *19* (35), 23585-23596.
- 65 Katarzynska, J.; Lipinski, Z.; Cholewinski, T.; Piotrowski, L.; Dworzynski, W.; Urbaniak, M.; Borkowska, A.; Cypryk, K.; Purgal, R.; Marcinek, A.; Gebicki, J., Non-invasive evaluation of microcirculation and metabolic regulation using flow mediated skin fluorescence (FMSF): Technical aspects and methodology. *Review of Scientific Instruments* **2019**, *90* (10), 104104.
- 66 Katarzynska, J.; Cholewinski, T.; Sieron, L.; Marcinek, A.; Gebicki, J., Flowmotion Monitored by Flow Mediated Skin Fluorescence (FMSF): A Tool for Characterization of Microcirculatory Status. *Frontiers in Physiology* **2020**, *11*.
- 67 Marcinek, A.; Katarzynska, J.; Sieron, L.; Skokowski, R.; Zielinski, J.; Gebicki, J., Non-Invasive Assessment of Vascular Circulation Based on Flow Mediated Skin Fluorescence (FMSF) *Biology* [Online], 2023.
- 68 Deanfield, J. E.; Halcox, J. P.; Rabelink, T. J., Endothelial Function and Dysfunction. *Circulation* **2007**, *115* (10), 1285-1295.

- 69 Stefanovska, A.; Bracic, M.; Kvernmo, H. D., Wavelet analysis of oscillations in the peripheral blood circulation measured by laser Doppler technique. *IEEE transactions on bio-medical engineering* **1999**, *46* (10), 1230-9.
- 70 Tikhonova, I. V.; Grinevich, A. A.; Tankanag, A. V.; Safronova, V. G., Skin Microhemodynamics and Mechanisms of Its Regulation in Type 2 Diabetes Mellitus. *Biophysics* **2022**, *67* (4), 647-659.
- 71 Fredriksson, I.; Larsson, M.; Strömberg, T.; Iredahl, F., Vasomotion analysis of speed resolved perfusion, oxygen saturation, red blood cell tissue fraction, and vessel diameter: Novel microvascular perspectives. *Skin research and technology : official journal of International Society for Bioengineering and the Skin (ISBS) [and] International Society for Digital Imaging of Skin (ISDIS) [and] International Society for Skin Imaging (ISSI)* **2022**, *28* (1), 142-152.
- 72 Rossi, M.; Carpi, A.; Galetta, F.; Franzoni, F.; Santoro, G., Skin vasomotion investigation: a useful tool for clinical evaluation of microvascular endothelial function? *Biomedicine & pharmacotherapy = Biomedecine & pharmacotherapie* **2008**, *62* (8), 541-5.
- 73 Hellmann, M.; Tarnawska, M.; Dudziak, M.; Dorniak, K.; Roustit, M.; Cracowski, J. L., Reproducibility of flow mediated skin fluorescence to assess microvascular function. *Microvasc Res* **2017**, *113*, 60-64.
- 74 Leite, A. R.; Borges-Canha, M.; Cardoso, R.; Neves, J. S.; Castro-Ferreira, R.; Leite-Moreira, A., Novel Biomarkers for Evaluation of Endothelial Dysfunction. *Angiology* **2020**, *71* (5), 397-410.
- 75 Bannerman, D. D.; Goldblum, S. E., Mechanisms of bacterial lipopolysaccharide-induced endothelial apoptosis. *American journal of physiology. Lung cellular and molecular physiology* **2003**, *284* (6), L899-914.

CHAPTER IX

SUMMARY IN DUTCH

Dit proefschrift onderzoekt bestaande en nieuwe beeldvormende technieken om de functie of disfunctie van de bloedvaten in de mens te evalueren. Centraal in dit vasculaire systeem staat de functie van het endotheel, een laag cellen die de binnenzijde van alle bloedvaten bedekt. Essentieel voor de functie van dit endotheel is de balans tussen vaatverwijding en vernauwing, die bepaald wordt door een aantal substanties afkomstig uit het endotheel. Een van de belangrijkste stoffen die door het endotheel geproduceerd wordt is stikstofdioxide (NO). NO is een klein molecuul met een zeer korte halfwaardetijd dat voortdurend door nitric oxide synthase (NOS) enzymen geproduceerd wordt, en dat haar effecten voornamelijk via het activeren van het enzym soluble guanylyl cyclase (sGC) uitoefent. Wanneer sGC door NO geactiveerd wordt, zet dit enzym guanosine trifosfaat om in cyclisch guanosine monofosfaat (cyclisch GMP, cGMP). Cyclisch GMP vervult vervolgens diverse rollen als signaal molecuul in de cel, waaronder ontspanning van het gladde spierweefsel dat bloedvaten omhult, resulterend in vaatverwijding. Deze NO-sGC-cGMP cascade wordt in gang gezet door de productie van NO door verschillende isovormen van het NOS-enzym, eNOS, nNOS en iNOS, die respectievelijk primair aanwezig zijn in endotheelcellen, neuronen en witte bloedcellen. De locatie van NO-productie bepaalt mede haar functie, waardoor dit molecuul invloed heeft op een breed scala aan processen in het lichaam. NO afkomstig uit endotheelcellen is met name belangrijk voor de functie van bloedvaten. NO geproduceerd in neuronen speelt een rol bij cognitieve processen en chronische ontsteking in de hersenen. Tot slot maken verschillende celtypen, waaronder witte bloedcellen, grote hoeveelheden NO aan via iNOS als reactie op infectie. NO in deze concentraties heeft celdodende effecten en versterkt de ontstekingsreactie, om op deze manier de verdediging van het lichaam tegen micro-organismen te assisteren.

Vanwege deze breedte van invloed op lichaamsfuncties is het NO-sGC-cGMP systeem een aantrekkelijk doelwit voor (medicamenteuze) interventies ter behandeling van onder andere cardiovasculaire, neurodegeneratieve en immunologische ziekten. Deze interventies pogen de signaaltransductie van NO naar cGMP te versterken door de beschikbaarheid van NO te verhogen, de productie van NO te vergroten, de activiteit van sGC te versterken of de afbraak van cGMP te verminderen. Bekende voorbeelden van interventies op de NO-sGC-cGMP -as zijn nitroglycerine, dat via NO-donatie vaatverwijding bewerkstelligt en gebruikt wordt in de behandeling van pijn op de borst, en sildenafil, een middel dat de afbraak van cGMP door bepaalde enzymen,

zogenoemde fosfodiesterases, remt. De resulterende vaatverwijdende effecten van sildenafil worden ingezet bij behandeling van erectiele disfunctie en pulmonale hypertensie.

Een obstakel bij de ontwikkeling van dergelijke behandelingen is het meten van de farmacodynamische effecten van de onderzochte interventies in vroege fase onderzoek. NO en producten van NO-metabolisme zijn moeilijk te meten omdat ze kortstondig, lokaal en in lage concentraties aanwezig zijn in de bloedsomloop, en het meten van voorlopers of de afbraakproducten van NO zoals arginine, nitriet en nitraat geeft weinig informatie over de stroomafwaartse effecten in de NO-sGC-cGMP cascade. Bovendien geeft het meten van enkele of meerdere biochemische waarden te weinig informatie over de balans van het systeem op weefselniveau door de aanwezigheid van interacties en feedback-mechanismen in dit weefsel.

Dit probleem kan deels ondervangen worden door het gebruik van beeldvormende technieken die de functionele status van de bloedvaten pogen te meten. Voordelen van deze aanpak zijn het non-invasieve karakter van beeldvorming en het feit dat de functie van het doelwit-weefsel, de vasculatuur, als geheel beoordeeld kan worden. Diverse technieken, onder andere gebaseerd op (Doppler) echografie, kernspintomografie (MRI) en plethysmografie (registratie van volumeveranderingen in een ledemaat), zijn in de loop der jaren ontwikkeld om vaatfunctie in kaart te brengen. Deze methodes worden vaak gecombineerd met manoeuvres die bloedvaten activeren om zo vaatverwijding en het evenwicht van het vaatstelsel te beoordelen. In dit proefschrift is een aantal nieuwe technieken onderzocht in studies uitgevoerd in het Centre for Human Drug Research (CHDR) met het doel intra- en interindividuele consistentie, geschiktheid voor evaluatie van NO-afhankelijke processen en de toegevoegde waarde voor klinisch onderzoek met therapeutische interventies te beoordelen.

De beeldvormende modaliteiten die in deze studies zijn onderzocht zijn laser speckle contrast beeldvorming (laser speckle contrast imaging, LSCI), passieve beweging van het onderbeen (passive leg movement, PLM), zijstroom donkerveldmicroscopie (sidestream dark field imaging, SDFM), nabij-infrarood licht spectroscopie (near infrared spectroscopy, NIRS) en stroom-gemedieerde huid fluorescentie (flow mediated skin fluorescence, FMSF).

LSCI is een beeldvormende techniek gebaseerd op het analyseren van veranderingen in 'speckle patroon'. Een typische LSCI-opstelling bestaat uit een laserlichtbron met een camera. Laserlicht wordt op het te-onderzoeken-gebied,

doorgaans de huid, geprojecteerd en de reflectie van dit licht wordt opgevangen door de camera. Niet alle lichtstralen worden perfect gereflecteerd, hetgeen resulteert in een karakteristiek 'speckle patroon', met gebieden van meer en minder intense lichtreflectie, dat wordt opgevangen door de camera. Dit 'speckle patroon' is constant wanneer een onbeweeglijk object wordt bekeken, maar verandert als er minieme beweging is in het onderzochte oppervlak. Wanneer dit de huid betreft, zijn deze minieme bewegingen het gevolg van stroming van rode bloedcellen in de microscopische vaten van de huid. Veranderingen in het 'speckle patroon' kunnen daarom gebruikt worden om de doorbloeding van de microscopische vaten in de huid te meten. Door vervolgens deze meting te combineren met een tweetal manoeuvres die de bloeddoorstroom veranderen kan de mate van reactiviteit van bloedvaten in de huid beoordeeld worden. De eerste handeling bestaat uit het kortstondig afklemmen en weer openstellen van de bloedstroom met een bloeddrukmanchet, ook wel occlusie-reperfusie of post-occlusieve reactieve hyperemie (PORH) genoemd. Een tweede veelgebruikte handeling is het opwarmen van de huid tot 43 °C (local thermal hyperaemia, LTH). Beide interventies induceren een reactieve toename van de doorbloeding, veroorzaakt door verschillende mechanismen, waaronder NO-afhankelijke processen, en kunnen zo gebruikt worden om de functie van microscopische bloedvaten in de huid te onderzoeken.

PLM is een beeldvormende methode waarbij Doppler echografie wordt gebruikt om de snelheid van bloeddorstroom in de liesslagader te meten. Tijdens deze meting wordt het onderbeen van de onderzochte patiënt of deelnemer passief, dat wil zeggen zonder spierspanning van de deelnemer, bewogen. Deze passieve beweging resulteert in vaatverwijding van de vaten in het onderbeen en is meetbaar als een toename in bloedstroomsnelheid in de liesslagader. Uit eerder onderzoek is gebleken dat deze toename in stroomsnelheid voor 70 tot 80 procent afhankelijk is van NO. De techniek kan dus gebruikt worden om de beschikbaarheid van NO in een groot bloedvat zoals de liesslagader te meten.

SDFM is een microscopische techniek waarbij licht met een specifieke golflengte die geabsorbeerd wordt door rode bloedcellen en bloedvaten wordt uitgezonden door een lichtbron en vervolgens wordt opgevangen door een camera geïntegreerd in de microscoop. Dit licht penetreert ongeveer 0,5 mm in menselijk weefsel. Door het SDFM-toestel op weefsel met oppervlakkige bloedvaten zoals de het slijmvlies onder de tong te plaatsen kunnen zo opnames gemaakt

worden waarin bloedvaten en erythrocyten zichtbaar zijn. Hiermee kan de dichtheid van bloedvaten in het weefsel en de beweging van erythrocyten door deze bloedvaten gemeten worden om zo de doorbloeding het weefsel te beoordelen. NIRS benut licht met een golflengte in het nabije infrarode spectrum, dat op verschillende golflengtes wordt geabsorbeerd door hemoglobine. Specifiek absorbeert zuurstofhoudend hemoglobine infrarood licht met een andere golflengte dan hemoglobine dat geen zuurstof bevat. Door het uitgezonden licht op te vangen en te bepalen in welke mate de verschillende golflengtes geabsorbeerd zijn kan de relatieve concentratie van hemoglobine met en zonder zuurstof bepaald worden ('zuurstofsaturatie'), evenals de totale hoeveelheid hemoglobine in het gemeten weefsel. Deze meting kan wederom gecombineerd worden met interventies. In het geval van NIRS betreft dit aderlijke (veneuze) en slagaderlijke (arteriële) occlusie van de bloedstroom. Bij veneuze occlusie wordt een bloeddrukmanchet, geplaatst rond de bovenarm, opgepompt tot een druk tussen de boven- en onderdruk in, waardoor arterieel bloed de arm in kan stromen, maar veneus bloed de arm niet uit kan stromen. Dit resulteert in een toename van de totale hemoglobine concentratie in de arm, waaruit het volume bloed dat de arm instroomt berekend kan worden. Bij arteriële occlusie wordt de bloeddrukmanchet opgepompt tot boven de bovendruk, waardoor het totaal bloedvolume in de arm constant blijft. De afname in zuurstofsaturatie die tijdens deze occlusie gemeten kan worden is een maat voor zuurstofgebruik in het onderzochte weefsel.

FMSF meet de fluorescentie van gereduceerd nicotinamide adenine dinucleotide (NADH) in cellen van de opperhuid. NADH en de geoxideerde versie van nicotinamide adenine dinucleotide (NAD⁺) zijn belangrijke cofactoren in cellulair zuurstofmetabolisme. De ratio tussen NADH en NAD⁺ is daarmee een maat van de metabole balans in de cel en van mitochondriële functie, maar aangezien oxidatief metabolisme afhankelijk is van de toevoer van zuurstof via de microcirculatie ook van vaatfunctie. Door de NADH-fluorescentie meting te combineren met occlusie-reperfusie kan inzicht verkregen worden in de reactie van zowel microscopische bloedvaten als cellulair metabolisme op gebrek aan en overdaad van bloedtoevoer.

De eerste helft van dit proefschrift beschrijft studies waarin de kwaliteit en het nut van deze verschillende beeldvormende technieken is onderzocht. In de tweede helft van het proefschrift worden vervolgens studies met medicamenteuze interventies gericht op het NO-sGC-cGMP systeem besproken.

In **Hoofdstuk 2** wordt de inter- en intra-individuele variabiliteit van LSCI, PLM en SDFM beschreven, evenals het effect van toediening van een vet- eiwit- en suikerrijke maaltijd ('mixed meal challenge') op deze maten van vasculaire functie. In deze studie bleek dat LSCI gecombineerd met PORH en LTH de meest consistentie meetmethode was, waarbij LSCI-PORH tevens een mogelijk negatief effect van de mixed meal challenge op vaatverwijdend vermogen suggereerde, zoals ook in andere studies is beschreven. Zowel SDFM als PLM toonden in deze studie een hoge mate van variabiliteit en konden het uit de literatuur bekende negatieve effect van de 'mixed meal challenge' op de vaatfunctie niet aantonen.

In **Hoofdstuk 3** zijn patiënten met een mitochondriële aandoening en even oude gezonde vrijwilligers van hetzelfde geslacht en met hetzelfde BMI vergeleken met behulp van LSCI, PLM, SDFM, NIRS en FMSF. PLM toonde in deze studie een significant lagere vaatverwijding in de liesslagader bij patiënten vergeleken met gezonde vrijwilligers, terwijl FMSF significant hogere NADH-concentraties in de huid van patiënten mat. De eerste bevinding wijst erop dat PLM slechtere vaatfunctie samenhangend met mitochondriële disfunctie bij patiënten kan detecteren. De tweede bevinding toont aan dat FMSF de verschuiving van cellulaire metabole balans die optreedt als gevolg van disfunctie in cellulair zuurstofmetabolisme bij mitochondriële disfunctie kan meten. In dezelfde studie werden ook *ex vivo* metingen van mitochondriële functie in circulerende perifere mononucleaire bloedcellen verricht, maar deze maten geen verschil tussen patiënten en gezonde vrijwilligers. De studie laat daarmee de toegevoegde waarde van beeldvorming bij onderzoek naar vasculaire en mitochondriële disfunctie zien. De afwezigheid van significante verschillen in LSCI-, SDFM- en NIRS-metingen benadrukken de noodzaak tot verdere verfijning en selectie van de te gebruiken modaliteiten.

Hoofdstuk 4 beschrijft de resultaten van een onderzoek naar de effecten van een pleister die titaniumdioxide bevat op het lokale vaatsysteem. Het hypothetisch werkingsmechanisme van deze pleister is de reflectie van ver-infrarood licht dat uitgezonden wordt door de huid waarop de pleister geplakt is. Dit ver-infrarode licht heeft in eerdere studies positieve effecten gehad op vaatfunctie en gezondheid. Met gebruik van LSCI in combinatie met PORH en LTH, SDFM, NIRS en thermografie werd in deze studie aangetoond dat de pleister een kortstondig vaatverwijdend effect heeft (gemeten met LSCI), een langdurigere toename van zuurstofconsumptie in het onderliggend weefsel veroorzaakt (gemeten met NIRS) en een toename in huidtemperatuur geeft. Zowel

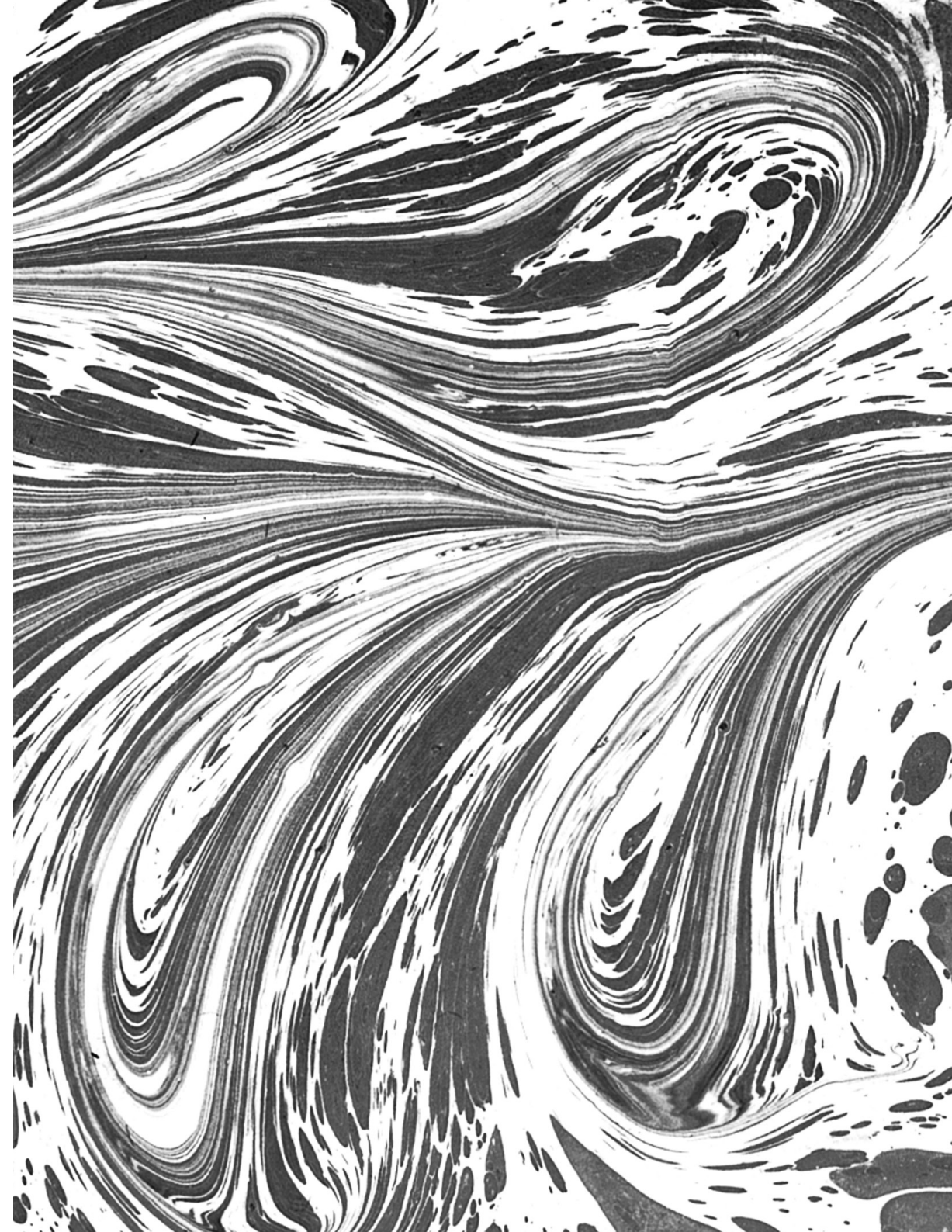
vaatverwijding als toegenomen zuurstofconsumptie zijn effecten die eerder waargenomen zijn als gevolg van therapie met ver-infrarood licht, waarmee deze studie het werkingsmechanisme van de pleister ondersteunt. Met deze studie is ook aangetoond dat LSCI en NIRS effecten van interventies op microscopische vaten kunnen blootleggen.

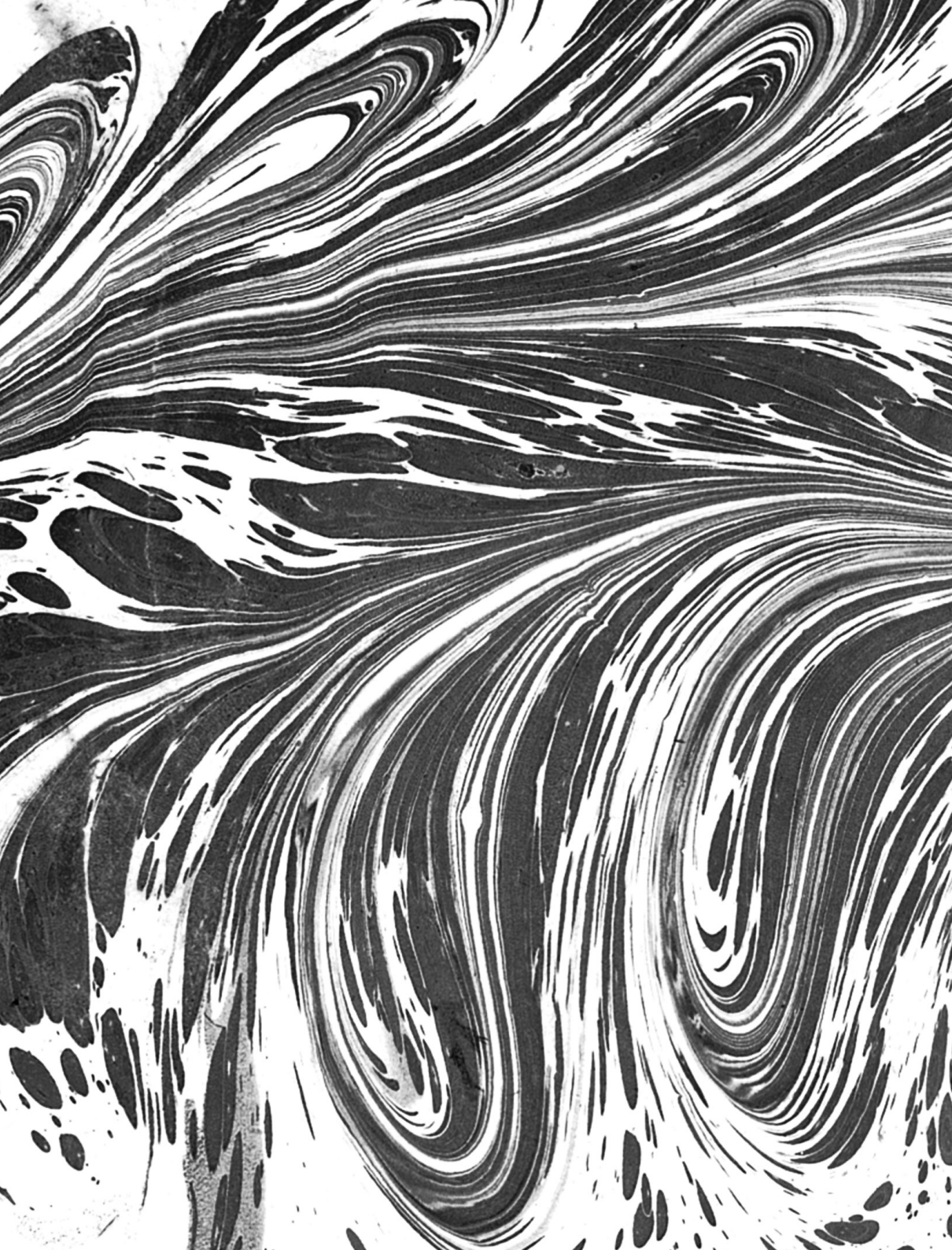
In **Hoofdstuk 5** worden de resultaten van de eerste studie in gezonde vrijwilligers met de sGC-stimulator zagociguat beschreven. Zagociguat wordt ontwikkeld voor de behandeling van neurodegeneratieve aandoeningen, zoals dementie, en ziekten geassocieerd met mitochondriële disfunctie. Zagociguat bleek in deze studie veilig in enkele doseringen tot 50 mg en meerdere doseringen tot 15 mg eenmaal daags gedurende 14 dagen. Tevens werd aangetoond dat het middel de bloed-hersenbarrière kan passeren door het meten van zagociguat concentraties in hersenvocht ('cerebrospinale vloeistof'). De studie liet ook zien dat zagociguat effecten geassocieerd met activatie van NO-sGC-cGMP, zoals een verlaging van de bloeddruk, induceert. Testen gericht op de mogelijke effecten van zagociguat in het centraal zenuwstelsel toonden echter geen veranderingen in diverse cognitieve functies in de onderzochte populatie.

Hoofdstuk 6 beschrijft de vervolgstudie met zagociguat, waarin de effecten van dit middel op cerebrale perfusie en een batterij van neurocognitieve testen werden onderzocht bij gezonde ouderen. In deze studie werd ook onderzocht wat de effecten van zagociguat op PLM waren. Wederom bleek zagociguat veilig in doseringen van 15 mg eenmaal daags gedurende 15 dagen en werden bloeddrukverlagende effecten van de medicatie aangetoond. De studie kon echter geen statistisch significant effect op hersendoorbloeding, neurocognitieve testen of PLM aantonen, mogelijk omdat de onderzochte populatie al optimale functie van de onderzochte systemen heeft, waardoor zagociguat geen verdere verbetering kon bewerkstelligen.

Hierna wordt in **Hoofdstuk 7** het effect van een fosfodiesterase 2 (PDE2) remmer op cGMP concentraties in cerebrospinale vloeistof onderzocht. De studie bevestigt dat deze PDE2 remmer in de cerebrospinale vloeistof terechtkomt en daar een toename van cGMP concentratie veroorzaakt, alhoewel deze toename niet dosisafhankelijk was. Bovendien werd een mogelijk dag- en nachtritme in cGMP concentraties in cerebrospinale vloeistof geobserveerd. De bevindingen van de studie ondersteunen de ontwikkeling van fosfodiesteraseremmers voor de behandeling van aandoeningen van het centraal zenuwstelsel die baat kunnen hebben bij een verhoging van cGMP concentratie in de hersenen.

Tot slot worden in **Hoofdstuk 8** de verschillende beeldvormende technieken en studies kritisch geëvalueerd. Uit de onderzoeken beschreven in de eerste helft van het proefschrift blijkt dat PLM en SDFM hoge variabiliteit vertonen, mogelijk veroorzaakt door zowel natuurlijke als technische factoren, die het vermogen van deze methoden om effecten te meten belemmert. LSCI bleek daarentegen een technisch consistente methode die de effecten van zowel een maaltijd als een therapeutische interventie in de vorm van een pleister kan detecteren. NIRS en FMSF toonden potentie door respectievelijk het effect van een interventie en verschillen tussen gezonde vrijwilligers en patiënten met een mitochondriële aandoening aan te tonen. Alle onderzochte methoden hebben baat bij consistente toepassing door bekwame onderzoekers in gestandaardiseerde omstandigheden, en zijn daarmee het meest geschikt voor toepassing in centra met ervaring met de genoemde technieken. Bovendien zou het waardevol zijn om in vervolgonderzoek deze nieuwe methoden te vergelijken met bestaande vasculaire functionele testen, zoals stroom-gemedieerde verwijding (flow mediated dilation, FMD) en circulerende vasculaire biomarkers in bloed. Daarnaast kan toevoeging van een interventie die het evenwicht van de vaten verstoort nuttig zijn, aangezien zo een verbetering van vaatfunctie in gezonde proefpersonen met (bijna) optimale vaten mogelijk meetbaar wordt. Concluderend stelt dit proefschrift dat beeldvorming kan bijdragen aan de wetenschappelijke waarde van vroege fase klinisch onderzoek met medicatie, mits de gebruikte beeldvormende techniek zorgvuldig is geselecteerd op basis van het hypothetisch werkingsmechanisme van de te onderzoeken interventie, en bij voorkeur wordt gecombineerd met biochemische metingen.





LIST OF PUBLICATIONS

- van Kraaij SJW**, Hamblin MR, Pickering G, Giannokopoulos B, Kechemir H, Heinz M, Igracki-Turudic I, Yavuz Y, Rissmann R, Gal P. A Phase 1 randomized, open-label clinical trial to evaluate the effect of a far-infrared emitting patch on local skin perfusion, microcirculation and oxygenation. *Exp Dermatol.* 2023 Nov 10. doi: 10.1111/exd.14962. Epub ahead of print. PMID: 37950549.
- van Kraaij SJW**, Borghans L, Klaassen ES, Gal P, van der Grond J, Tripp K, Winrow C, Glasser C, Groeneveld GJ. Randomized placebo-controlled crossover study to assess tolerability and pharmacodynamics of zagociguat, a soluble guanylyl cyclase stimulator, in healthy elderly. *Br J Clin Pharmacol.* 2023 Jul 24. doi: 10.1111/bcp.15861. Epub ahead of print. PMID: 37488930.
- van Kraaij SJW**, Pereira DR, Smal B, Summo L, Konkel A, Lossie J, Busjahn A, Grammatopoulos TN, Klaassen E, Fischer R, Schunck WH, Gal P, Moerland M. Identification of peripheral vascular function measures and circulating biomarkers of mitochondrial function in patients with mitochondrial disease. *Clin Transl Sci.* 2023 Jul;16(7):1258-1271. doi: 10.1111/cts.13530. Epub 2023 May 12. PMID: 37177864; PMCID: PMC10339694.
- van Kraaij SJW**, Gal P, Borghans LGJM, Klaassen ES, Dijkstra F, Winrow C, Glasser C, Groeneveld GJ. First-in-human trial to assess safety, tolerability, pharmacokinetics, and pharmacodynamics of zagociguat (CY6463), a CNS-penetrant soluble guanylyl cyclase stimulator. *Clin Transl Sci.* 2023 Aug;16(8):1381-1395. doi: 10.1111/cts.13537. Epub 2023 May 3. PMID: 37118895; PMCID: PMC10432884.
- In 't Veld AE, Grievink HW, van der Plas JL, Eveleens Maarse BC, **van Kraaij SJW**, Woutman TD, Schoonakker M, Klarenbeek NB, de Kam ML, Kamerling IMC, Jansen MAA, Moerland M. Immunosuppression by hydroxychloroquine: mechanistic proof in in vitro experiments but limited systemic activity in a randomized placebo-controlled clinical pharmacology study. *Immunol Res.* 2023 Aug;71(4):617-627. doi: 10.1007/s12026-023-09367-3. Epub 2023 Feb 22. PMID: 36811819; PMCID: PMC9945836.
- Reumkens A, Bakker CM, **van Kraaij SJW**, Winkens B, Raijmakers MT, van Nunen AB, van Deursen CTBM, Masclee AAM. Safety of low-volume PEG-ASC bowel cleansing preparation for colonoscopy: identifying patients at risk for hypokalemia in a prospective cohort study. *Endosc Int Open.* 2021 Aug;9(8):E1198-E1204. doi: 10.1055/a-1478-3361. Epub 2021 Jul 16. PMID: 34447864; PMCID: PMC8383076.

CURRICULUM VITAE

Sebastiaan Jan Wilhelmus van Kraaij was born on the 12th of January 1994 in Nijmegen, The Netherlands. He graduated *cum laude* from secondary school "Sint-Maartenscollege" in Maastricht in 2011 and started studying medicine at Utrecht University. During his study, he joined the student association Unitas Studiosorum Rheno-Traiectina (U.S.R.), where he served several years as secretary of the debate society (A.D.C.) "Forsete Wara". After obtaining his bachelor's degree in 2015, he continued his education with the Master of Science in Medicine at Utrecht University, during which he performed research on renal Xenon-133 washout curves and their implications on the pathophysiology of hypertension, resulting in two poster presentations at international conferences. After graduating *cum laude* as a medical doctor in 2018, he started his professional career as a resident physician at the department of Internal Medicine in the Diakonessenhuis hospital in Utrecht. In 2019, he started working as a research physician at the Centre for Human Drug Research (CHDR). There he also started his PhD track investigating microcirculation under supervision of dr. P. Gal, dr. M. Moerland and prof. dr. J. Burggraaf. The studies contained in this thesis were performed at the CHDR, several in collaboration with different stakeholders in the pharmaceutical field. During his work at CHDR, he also contributed to numerous other clinical studies in the fields of immunology, neurology, and psychiatry. After completion of his PhD thesis, he continued his professional medical career and is currently employed as resident Internal Medicine in the Tergooi Hospital located in Hilversum.

LIST OF ABBREVIATIONS

1H-MRS	Proton magnetic resonance spectroscopy
AC	Adenyl cyclase
ADMA	Asymmetric dimethylarginine
AE_{last}	Amount excreted in urine until last sample, absolute
AE_{last%}	Amount excreted in urine until last sample, percentage of plasma concentration
ALT	Alanine transaminase
ANCOVA	Analysis of covariance
ANOVA	Analysis of variance
APOGC	Haem-free guanylate cyclase
ASL	Arterial spin labelling
AST	Aspartate aminotransferase
ATP	Adenosine triphosphate
AU	Arbitrary units
AUC	Area under the curve
AUC₀₋₂₄	Area under the curve from timepoint 0 to 24 hours
AUC_{0-tz}	Area under the curve from timepoint 0 to the last measurable timepoint
AUC_τ	Area under the curve during 1 dosing interval
AUC_{last}	Area under the curve until the last measurable concentration
AUC_{inf}	Area under the curve extrapolated to infinity
AUEC_{0-tz}	Area under the biomarker curve from time point 0 to the last quantifiable data point
BEBO	Stichting Beoordeling Ethiek Biomedisch Onderzoek
BH₄	Tetrahydrobiopterin
BLQ / BLOQ	Below limit of quantification
BMI	Body mass index
BOLD	Blood-oxygen-level-dependent
BP	Blood pressure
C_{max}	Maximum concentration
C_{trough}	Trough concentration
CAM	Calmodulin
CAMP	Cyclic adenosine monophosphate
CBF	Cerebral blood flow
CFB	Change from baseline
CI	Confidence interval
CIAS	cognitive impairment associated with schizophrenia
CGMP	Cyclic guanosine monophosphate
CL_R	Renal clearance
CL/F	Total clearance
CNS	Central nervous system
CO₂	Carbon dioxide
COVID-19	Coronavirus disease 2019
COX	Cyclooxygenase

CRP	C-reactive protein
CSE	Cystathionine-lyase
CSF	Cerebrospinal fluid
CTNI	Cardiac troponin I
CV	Coefficient of variation
CYP3A4	Cytochrome P450 3A4
CYP450	Cytochrome P450 epoxigenase
DBP	Diastolic blood pressure
DNA	Deoxyribonucleic acid
E_{max}	Maximum exposure-related concentration
EC	Endothelial cell
ECAR	Extracellular acidification rate
ECG	Electrocardiogram
ECLIA	Electrochemiluminescence immunoassay
EETS	Epoxyeicosatrienoic acids
ELISA	Enzyme-linked immunosorbent assay
EMA	European Medicines Agency
ERP	Event-related potential
EU	European Union
FAD	Flavin adenine dinucleotide
FCPP	Carbonyl cyanide-p-trifluoromethoxy-phenylhydrazone
FDA	Food and Drug Administration
FDR	False discovery rate
FI	Food-interaction
FIH	First-in-human
FIR	Far infrared radiation
FMD	Flow mediated dilation
FMN	Flavin mononucleotide
FMRI	Functional magnetic resonance imaging
FMSF	Flow mediated skin fluorescence
GDF-15	Growth/differentiation factor 15
GGT	Gamma-glutamyl transferase
GI	Gastrointestinal
GLP	Good laboratory practice
GPCR	G-protein coupled receptor
H₂O₂	Hydrogen peroxide
H₂S	Hydrogen sulfide
HB	Hemoglobin
HBA1C	Glycated hemoglobin
HED	Human equivalent dose
HETES	Hydroxyeicosatrienoic acids
HNOX	Heme-NO-oxygen binding domain
HV	Healthy volunteer
ICU	Intensive care unit
IL-6	Interleukin 6
JC1	Tetraethylbenzimidazolylcarbocyanine iodide
K2EDTA	Dipotassium ethylenediaminetetraacetic acid
K_{Ca}	Ca ²⁺ -activated potassium channel
KATP	ATP-sensitive potassium channel
KIR	Inwardly rectifying potassium channel

L-ARG	L-arginine
L-CIT	L-citrulline
(HP)LC-MS/MS	(High performance) liquid chromatography with tandem mass spectrometry
LDH	Lactate dehydrogenase
L-NAME	L-nitro-arginine methyl ester
L-NMMA	NG-monomethyl-L-arginine
LOX	Lipoxygenase
LSCI	Laser speckle contrast imaging
LSM	Least squares mean
LTH	Local thermal hyperaemia
LTS	Leukotrienes
LXS	Lipoxines
MAD	Multiple ascending dose
MAX	Maximum
MEDDRA	Medical dictionary for regulatory activities
MEGJ	Myoendothelial gap junctions
MELAS	Mitochondrial encephalopathy, lactic acidosis, and stroke-like episodes
MIN	Minimum
MITOD	Mitochondrial disease
MMP	Mitochondrial membrane potential
MMT	Milner learning maze test
MMTT	Mixed meal tolerance test
MRI	Magnetic resonance imaging
N	Number
NAA	N-acetylaspartate
NAD+	Nicotinamide adenine dinucleotide
NADH	Reduced nicotinamide adenine dinucleotide
NADP	Nicotinamide adenine dinucleotide phosphate
NADPH	Reduced nicotinamide adenine dinucleotide phosphate
NF-L	Neurofilament light polypeptide
NIRS	Near infrared spectroscopy
NMDA	N-methyl-D-aspartate
NO	Nitric oxide
NO₂	Nitric dioxide
NOAEL	No observed adverse event level
NOS	Nitric oxide synthase
NOS1 / INOS	Inducible nitric oxide synthase
NOS2 / NNOS	Neuronal nitric oxide synthase
NOS3 / ENOS	Endothelial nitric oxide synthase
NT-PROBNP	N-terminal prohormone of brain natriuretic peptide
O₂--	Superoxide
OCR	Oxygen consumption rate
OONO-	Peroxyinitrite
OXPHOS	Oxidative phosphorylation
PAT	Peripheral arterial tonometry
PD	Pharmacodynamic
PDE	Phosphodiesterase

PEEG	Pharmaco-electroencephalography
PGS	Prostaglandins
PK	Pharmacokinetic
PKA	Protein kinase A
PKG	Protein kinase G
PLA₂	Phospholipase A2
PLM	Passive leg movement
PMBC	Peripheral blood mononuclear cell
PORH	Post occlusive reactive hyperaemia
PPV	Proportion perfused vessels
PTR	Peak-to-trough ratio
PTX3	Pentraxin 3
PU	Perfusion unit
QD	Once per day
QEEG	Quantitative electroencephalography
R_{csf}	Ratio of cerebrospinal fluid / plasma concentration
R_{csf-free}	Ratio of cerebrospinal fluid / free plasma concentration
R_{AUC}	Accumulation ratio calculated from AUC _τ at steady state and after a single dose
R_{max}	accumulation ratio calculated from C _{max} at steady state and after a single dose
R_{trough}	accumulation ratio calculated from C _{trough} at steady state and after a single dose
ROS	Reactive oxygen species
SAD	Single ascending dose
SAP	Statistical analysis plan
SBP	Systolic blood pressure
SD	Standard deviation
SDFM	Sidestream dark field imaging
SDMA	Symmetric dimethylarginine
SEM	Standard error of the mean
SGC	Soluble guanylyl cyclase (<i>syn.:</i> soluble guanylate cyclase)
SMC	Smooth muscle cell
SOD	Superoxide dismutase
SST	Serum separator tube
T_{1/2}	Elimination half life
T_{1/2,eff}	Effective half life based on accumulation
T_{max}	Time to maximum concentration
TEAE	Treatment emergent adverse event
UB	Ubiquitin
ULN	Upper limit of normal
VAS	Visual analogue scale
VCAM-1	Vascular cell adhesion molecule 1
VSMC	Vascular smooth muscle cell
VVLT	Visual verbal learning test

ACKNOWLEDGEMENTS

This thesis could not have been written without the help, feedback, and support of countless people around me.

First, I would like to thank the participants in the scientific studies described in this thesis, as they form the bedrock of all clinical trials. Without their willingness to be at the forefront of pharmacological research, none of the techniques tested in this thesis would have existed.

I would like to thank my promotor, professor Koos Burggraaf, for his constructive feedback and guidance during the PhD process, which has helped me to impart a coherent scientific narrative to the reader of this thesis.

Dr Gal, dear Pim, you have been my mentor at CHDR, *really* introduced me to scientific thinking, and guided me through countless aspects of research, writing, and life. For your support and contributions to this thesis, I cannot thank you enough.

Dr Moerland, dear Matthijs, as a thesis advisor you have aided my work at CHDR tremendously. I have always enjoyed working with you as a team leader, and appreciated how you looked out for me and others in your team.

I would also like to express my gratitude and appreciation to professor Geert Jan Groeneveld for supervising and guiding me on multiple chapters in this thesis. Your keen observations and feedback I have taken with me in all subsequent writing and thinking

A thank you to professor Robert Rissmann as well, for your help with Chapter IV. Blood vessels meet skin everywhere, and our collaboration felt equally natural.

A special thank you to all my direct colleagues at the immuno-cardiovascular group, the researchers of other therapeutic areas and all other hard workers of CHDR. Jointly, you keep CHDR running and provided indispensable contribution to the research described in this thesis.

I want to thank my rock-solid friends in Utrecht, Max, Joep and Naud, for being there for me, providing much needed relief of stress and thousands of hours of splendid conversation, card- and board gaming and general shenanigans.

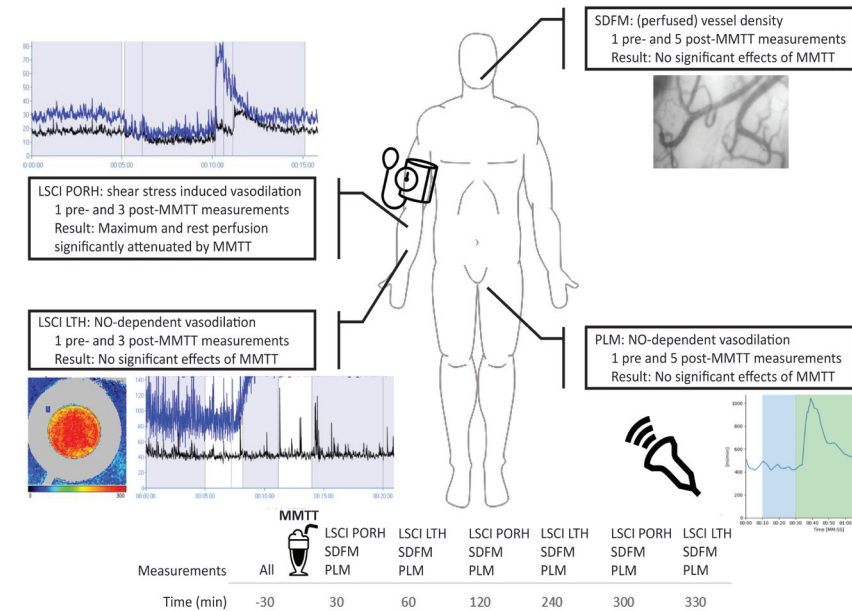
Also, a thank you to the lads, Mick, Jacob, Pedram, Jelmer, Kieran, Christiaan, Pieter. The ever-expanding MTG crew especially has a warm place in my heart. My gratitude goes out specifically to Mick and my brother Vincent, for taking the solemn responsibility of being paranymphs.

Mom, dad, Tom, Vincent, Joris: thank you for 30 years of love and support, and unwittingly contributing a lot to my drive to complete this work. A lot of thanks also to my in-laws, Pashtoon, Zhala, Farshad, Alben and Tristan, for your unwavering support.

To my wife, Krishma, the love of my life: I think little needs to be written, since all has been said. Thank you for always sticking by me and supporting me more than I thought humanly possible.

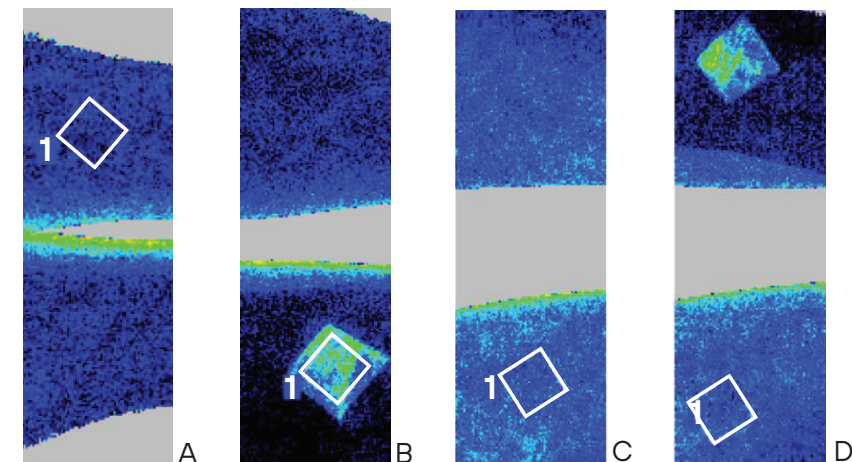
And finally, to the little voice that rose recently in my family: Kianush, you light up my life.

CH.2 / F.1 Overview of employed imaging techniques and timepoints of assessments pre- and post-MMTT administration.



LSCI=laser speckle contrast imaging;
LTH=local thermal hyperaemia; min=minutes;
MMTT=mixed meal tolerance test; NO=nitric oxide; PLM=passive leg movement; PORH=post occlusive reactive hyperaemia;
SDFM=side-stream dark field microscopy.

CH.4 / F.4 Representative LSCI images of baseline flow before and after patch application for subject 4 (A, B) and 6 (C, D).



The window in the patch through which measurements were performed is shown in picture B and D (area marked with '1' in picture B). LSCI=laser speckle contrast imaging.

